



Universitat Autònoma de Barcelona

ADVERTIMENT. L'accés als continguts d'aquesta tesi queda condicionat a l'acceptació de les condicions d'ús establertes per la següent llicència Creative Commons:  http://cat.creativecommons.org/?page_id=184

ADVERTENCIA. El acceso a los contenidos de esta tesis queda condicionado a la aceptación de las condiciones de uso establecidas por la siguiente licencia Creative Commons:  <http://es.creativecommons.org/blog/licencias/>

WARNING. The access to the contents of this doctoral thesis it is limited to the acceptance of the use conditions set by the following Creative Commons license:  <https://creativecommons.org/licenses/?lang=en>



Effective field theories for heavy quarkonia and hydrogen-like bound states

A dissertation by

Clara Peset Martín

aimed at the achievement of

Ph.D. in physics

granted by

Departament de Física
Universitat Autònoma de Barcelona

March 16, 2016

Supervised by:

Prof. Antonio Miguel Pineda Ruíz

A mis queridísimos padres
que me han enseñado a ser valiente.

*Nothing in life is to be feared,
it is only to be understood.
Now is the time to understand more,
so that we may fear less.*

Marie Skłodowska Curie

Acknowledgements

First of all, I would like to express my deepest gratitude to Antonio Pineda. He took me in from the beginning and it has been a privilege and a pleasure to learn from him. I just hope I got to grab some of your deep understanding and your thoroughness in the management of physics, which I so much admire.

Special thanks to Yuval Grossman, for making it possible for me to spend some amazing months in Cornell, and for teaching me everything I know about neutrinos and SUSY. And to Maximilian Stahlhofen, with whom sharing dinners and ideas is always enjoying. It has been a pleasure collaborating with both you.

Son muchas las personas que me han apoyado estos años y a las que quiero dar las gracias:

A mi madre y a mi padre, que me han enseñado a perseverar, a disfrutar y a superar la frustración. Me habéis apoyado y cuidado y rodeado de vuestro cariño, sin vosotros no hubiera sido posible. Nunca estaré suficientemente agradecida.

A Isa, cuyos consejos sobre la carrera científica me han traído hasta aquí. Eres mi hermana preferida.

A Javi... sé que prometí no hacer esto, pero tengo que decir que conocerte es la mejor consecuencia de esta tesis. Muchísimas gracias por aguantarme estas semanas, por leer mi introducción 100 veces, y por todo lo que me has ayudado estos años. Eres mi motivación y mi inspiración para hacer física.

A mi tío Carlos, por todos los emails de ciencia actual, tu interés hace que todo sea más emocionante. Gracias por tus consejos vitales y por leerte todos mis artículos (e incluso preguntarme!), es un esfuerzo que valoro. A mi tía Susa, por todas las velas a san Pancrancio y por acercarme a Marie Curie. A mi tía postiza, Ananita, por su apoyo incondicional. Y a toda mi familia, con la que siempre puedo contar. Un especial recuerdo a mis abuelos, a los que me encantaría poder enseñar este trabajo.

A todos mis compañeros y colegas del IFAE que han compartido conmigo el día a día de esta tesis: a todos los seniors que me han hecho sentir como en casa y a los estudiantes que están y que se han ido: a Diogo, Marc M., Thibaud, Mateo, Matteo, Sergi, Ke-Yang, Marc R., Oriol, Joan Antoni, Joan, Mariona... Y un agradecimiento especial a mis hermanos de familia arcoiris, Basti y Alvise, que me enseñaron a disfrutar Gracia.

Y a todos los amigos que han estado cerca apoyándome estos años: a Moli quien ha recorrido todo el camino conmigo, a Pove y a Anna que me ayudan a tener estilo hasta en la tesis y siempre me han cuidado. A Camille, mi gabacha preferida. A Mont, Javi y Garo con quienes he compartido mucho más que el master. A todos los que han vivido conmigo aguantándome y haciéndome reír: Nachete, Andrés, Cisco, Naima, Alex y los varios escritores de tesis del IFAE. A Gabriel y Lorena por todos los planes para hacernos ricos. A Ana, mi querida amiga y compañera

de las desesperaciones del camino del doctorante. A Juancar por esos tases que hacen los días más ligeros. A Ali y a Cris, por hacer Barcelona más divetido. Y a mis amigos que están lejos, Ana, Bea, Merchán, Javi y Hector, porque aún así os siento cerca.

Thanks to everybody at Cornell, who welcomed me and made my stay so nice that I even forgot about the cold: Csaba, Yuval, Maxim, Liam, Flip, Paul, Marco, Cody, Julia, Bibushan, Nick, Alisha...

My sincere gratitude to the Universitat Autònoma de Barcelona PIF fellowship program PR-404-01-2/E2010, for supporting the development of this thesis.

And now for something completely different...

Monty Python

Abstract

In this dissertation, we concentrate on the physics of weakly bound states made of two heavy fermions with different masses. Their description is performed in the framework of effective field theorys (EFTs), specifically pNRQED and pNRQCD. We compute the potentials up to next-to-next-to-next-to-leading order (N³LO) for two systems: hydrogen-like atoms and heavy quarkonia. We apply our results to the extraction of some associated energy levels.

In the first part of this thesis, we obtain a model independent expression for the muonic hydrogen Lamb shift. This expression includes the leading logarithmic $\mathcal{O}(m_\mu\alpha^6)$ terms, as well as the leading $\mathcal{O}(m_\mu\alpha^5\frac{m_\mu^2}{\Lambda_{\text{QCD}}^2})$ hadronic effects. Most remarkably, our analysis include the determination of the spin-dependent and spin-independent structure functions of the forward virtual-photon Compton tensor of the proton to $\mathcal{O}(p^3)$, using HBET and including the Delta particle. Using these results we obtain the leading hadronic contributions to the Wilson coefficients of the lepton-proton four fermion operators in NRQED. The spin-independent coefficient yields a pure prediction for the two-photon exchange contribution to the muonic hydrogen Lamb shift, which is the main source of uncertainty in our computation. The use of EFTs crucially helps us organizing the computation, in such a way that we can clearly address the parametric accuracy of our result. Furthermore, we review in the context of NRQED all the contributions to the energy shift of order α^5 , as well as those that scale like $\alpha^6 \times \text{logarithms}$. With our final determination of the Lamb shift, we obtain the proton charge radius in a model independent way. The value we obtain is 6.8σ away from the CODATA value.

In the second part of this thesis, we determine the $1/m$ and $1/m^2$ spin-independent heavy quarkonium potentials in the unequal mass case with $\mathcal{O}(\alpha^3)$ and $\mathcal{O}(\alpha^2)$ accuracy, respectively. We discuss in detail different methods to calculate such potentials, and explicitly show the equivalence among them. In particular we obtain, for the first time, the manifestly gauge invariant $1/m$ and $1/m^2$ potentials in terms of Wilson loops with next-to-leading order (NLO) precision. As an application of our results we derive the theoretical expression for the B_c spectrum in the weak-coupling limit to N³LO.

List of published works

REFEREED ARTICLES

- i. **Potential NRQCD and the B_c spectrum at $N^3\text{LO}$**
C. Peset, A. Pineda, M. Stahlhofen
JHEP to be published, arXiv:1511.08210 [hep-ph]
- ii. **The Lamb shift in muonic hydrogen and the proton radius from effective field theories**
C. Peset, A. Pineda
Eur. Phys. J. A **51** (2015) 12, 156, arXiv:1508.01948 [hep-ph]
- iii. **The two-photon exchange contribution to muonic hydrogen from chiral perturbation theory**
C. Peset, A. Pineda
Nucl. Phys. B **887** (2014) 69-111 arXiv:1406.4524 [hep-ph]
- iv. **Model-independent determination of the Lamb shift in muonic hydrogen and the proton radius**
C. Peset, A. Pineda
Eur. Phys. J. A **51** (2015) 32, arXiv:1403.3408 [hep-ph]
- v. **Neutrino masses in RPV models with two pairs of Higgs doublets**
Y. Grossman, C. Peset
JHEP 1404 (2014) 033, arXiv:1401.1818 [hep-ph]

CONFERENCE PROCEEDINGS

- i. **The hadronic corrections to muonic hydrogen Lamb shift from ChPT and the proton radius**
C. Peset, QCHS XI, Saint Petersburg (RUSSIA)
AIP Conf. Proc. **1701** (2016) 040017, doi:10.1063/1.4938634
- ii. **The muonic hydrogen Lamb shift and the proton radius**
C. Peset, QCD 14, Montpellier (FRANCE)
Nucl. Part. Phys. Proc. **258-259** (2015) 231 arXiv:1411.3931 [hep-ph]

Contents

Acknowledgements	v
Abstract	vii
List of published works	ix
Abbreviations	xv
I Introduction	1
II Muonic hydrogen	11
1 Introduction	13
2 Effective field theories	17
2.1 HBET	17
2.2 NRQED(μp)	19
2.3 NRQED(e)	24
2.4 pNRQED	24
3 Matching HBET to NRQED	27
3.1 The forward virtual Compton tensor	27
3.2 Computation of $T_{\text{Born}}^{\mu\nu}$	28
3.3 Computation of $T_{\text{pol}}^{\mu\nu}$	32
3.4 Spin-independent matching: c_3	36
3.4.1 $c_{3,\text{Born}}$ and Zemach moments	36
3.4.2 $c_{3,\text{pol}}$, the polarizability term	40
3.5 Spin-dependent matching: c_4	43
4 Matching NRQED to pNRQED	47
4.1 The static potential: $V^{(0)}$	47
4.2 The potential beyond the static limit	50
4.3 The potential in position space	51

5	The muonic hydrogen Lamb shift and the proton radius	57
5.1	Corrections from the static potential: $V^{(0)}$	59
5.1.1	One-loop Vacuum Polarization: $\delta E_L^{V_{\text{VP}}^{(0,2)}} \sim \mathcal{O}(m_\mu \alpha^3)$	59
5.1.2	Two-loop Vacuum Polarization: $\delta E_L^{V_{\text{VP}}^{(0,3)}} \sim \mathcal{O}(m_r \alpha^4)$	60
5.1.3	Double Vacuum Polarization: $\delta E_L^{V_{\text{VP}}^{(0,2)} \times V_{\text{VP}}^{(0,2)}} \sim \mathcal{O}(m_r \alpha^4)$	60
5.1.4	Static potential (vacuum polarization): $\delta E_L \sim \mathcal{O}(m_r \alpha^5)$	60
5.1.5	Static potential (light-by-light): $\delta E_L^{V_{\text{LbL}}^{(0,4)}} \sim \mathcal{O}(m_r \alpha^5)$	61
5.2	Corrections from the $1/m_\mu$ potentials without vacuum polarization	61
5.2.1	Relativistic corrections: $\delta E_L \sim \mathcal{O}(m_r \alpha^4)$	62
5.2.2	Relativistic corrections: $\delta E_L \sim \mathcal{O}(m_r \alpha^5)$	63
5.3	Ultrasoft effects: $\delta E_L \sim \mathcal{O}(m_r \alpha^5)$	64
5.4	$1/m_\mu^2$ hadronic corrections: $\delta E_L \sim \mathcal{O}(m_r \alpha^5)$	66
5.5	$1/m_\mu^2$ electron VP corrections: $\delta E_L \sim \mathcal{O}(m_r \alpha^5)$	69
5.6	$\mathcal{O}(m_r \alpha^6 \times \ln)$ effects	70
5.7	The proton radius	72
6	Conclusions	75
III	Heavy quarkonium: the B_c system	79
7	Introduction	81
8	Effective field theories: Matching NRQCD to pNRQCD	85
8.1	NRQCD	85
8.2	pNRQCD: the potentials	87
8.2.1	Potentials in momentum space	89
8.2.2	The \mathbf{L}^2 operator and potentials in D dimensions	90
8.2.3	Position versus momentum space	90
8.3	Field redefinitions	92
9	Determination of the potential for unequal masses	95
9.1	The $\mathcal{O}(\alpha_s^2/m^2)$ potential: matching with Green functions	95
9.1.1	Off-shell matching: Coulomb gauge	96
9.1.2	Off-shell matching: Feynman gauge	97
9.1.3	On-shell matching	98
9.2	The $\mathcal{O}(\alpha_s^2/m^2)$ potential: matching with Wilson loops	99
9.2.1	The quasi-static energy and general formulas	99
9.2.2	Results in perturbation theory: the $\mathcal{O}(\alpha_s^2/m^2)$ potential	104
9.3	Determination of the $\mathcal{O}(\alpha_s^3/m)$ potential for unequal masses	111
9.4	Renormalized potentials	116
9.5	Static and spin-dependent potentials	119
9.6	Poincaré invariance constraints	121

10 The B_c mass to N^3LO	123
10.1 The ultrasoft energy correction	123
10.2 Energy correction associated with the static potential	123
10.3 Energy correction associated with the relativistic potentials	124
10.4 The $\mathcal{O}(m\alpha_s^5)$ spectrum for unequal masses	127
11 Conclusions	129
IV Final Remarks	131
A Parameters and functions	137
A.1 QCD-related parameters	137
A.2 \overline{MS} renormalized NRQCD Wilson coefficients	138
A.3 Finite Sums for the spectrum computation	138
A.4 List of transformations from momentum to position space	140
B Feynman rules	141
B.1 Feynman rules for HBET	141
B.2 Feynman rules for NRQCD	142
B.3 Feynman rules for the matching with Wilson loops	144
C Master integrals	147
C.1 Master integrals in HBET	147
C.2 Master integrals for NRQCD in the Coulomb gauge	148
D HBET amplitudes	151
D.1 Pion loops	151
D.2 Pion loops which include a Δ excitation	155
E Muonium spectrum	161
F Off-shell NRQCD amplitudes for the $\mathcal{O}(\alpha^2/m^2)$ potential	163
G The NRQCD potential	169
G.1 The NRQCD potential in position space	169
G.2 The static potential in momentum space	170
G.3 The renormalized potential in momentum space	171
H Expectation values	175
H.1 List of expectation values of single potential insertions	175
H.2 List of expectation values of double potential insertions	177
Bibliography	179

List of abbreviations

ChPT	chiral perturbation theory
CG	Coulomb gauge
EFT	effective field theory
EOM	equation of motion
FG	Feynman gauge
FVCT	forward virtual Compton tensor
HBChPT	heavy baryon chiral perturbation theory
HBET	heavy baryon effective theory
HQET	heavy quark effective theory
LHC	Large Hadron Collider
MS	minimal subtraction
NLO	next-to-leading order
NNLO	next-to-next-to-leading order
N³LO	next-to-next-to-next-to-leading order
NR	non-relativistic
NREFT	non-relativistic effective field theory
NRQED	non-relativistic QED
NRQCD	non-relativistic QCD
pNRQED	potential NRQED
pNRQCD	potential NRQCD
QED	quantum electrodynamics
QCD	quantum chromodynamics
TPE	two photon exchange

Contents

vNRQCD velocity NRQCD

VP vacuum polarization

Part I

Introduction

Introduction

The Standard Model of particle physics found experimental completion in 2012 with the discovery of the Higgs boson at the Large Hadron Collider (LHC). This spectacularly successful theory, based entirely on gauge and local space-time symmetries, describes *most* of the physical processes taking place in our universe, between the tiniest Planck length and the vastness of our observable cosmos. Nevertheless, it has some limitations. In this dissertation we focus on those shortcomings related to the description of the strong interactions among quarks and gluons, i.e. quantum chromodynamics (QCD).

The existence of quarks was predicted theoretically by Gell-Mann and Zweig in 1964 [1, 2] and confirmed experimentally at SLAC in 1968. QCD was definitely established in 1973 after the discovery of asymptotic freedom by Gross and Wilczek [3], and by Politzer [4] in the same year. The dynamics of quarks and gluons is described by the QCD Lagrangian. In the massless quark and classical limit this Lagrangian is scale invariant, and so its interactions are only dictated by the dimensionless parameter α_s , the strong coupling constant. This conformal symmetry of the classical theory is anomalously broken upon quantization, thereby setting up a mass scale, namely Λ_{QCD} . In other words, at the quantum level the dimensionless coupling constant runs with the energy, being Λ_{QCD} the renormalization group scale at which the coupling constant diverges. Such a trade of a coupling constant by a mass scale is known as dimensional transmutation. The strong coupling constant, unlike the electromagnetic one, decreases as the energy increases. This means that particles which interact weakly at very high energies, do so very strongly at low energies. As a result, on the one hand, in the high energy regime the theory is fully described perturbatively, leading to very successful and accurate predictions. On the other hand, the theory is non-perturbative at low energies, and so the challenging need for appropriate methods and models to describe physical processes arises. The physics that at high energies is described by quarks and gluons, is described by hadrons at low energies. This implies that in the transition a process of confinement must occur¹ and, as a result, no single quark or gluon can be directly observed in Nature. In fact, we can only find them bounded in hadrons: baryons, such as the proton, and mesons.

In order to overcome these limitations different approaches have been developed. On the computational side, lattice gauge theory has proven to be an extremely useful tool to determine some of the QCD parameters and observables, having provided estimates for quark masses, decay widths, or even the strong coupling constant among others. In fact, the realm of applicability of lattice theories is far larger than QCD, being useful in the description of any generic gauge theory. On the analytical side, great success has been achieved by developing effective field theories (EFTs) that are specifically dedicated to describing an interval of the energy range

¹However, confinement has not yet been analytically proven. This is the challenge of the problem “Yang-Mills existence and mass gap”. Solving it will earn the fortunate researcher one of the Millennium prizes.

in which a particular dynamics of the strong sector dominates. Well-known and very relevant examples of these theories are chiral perturbation theory (ChPT) [5, 6], heavy baryon effective theory (HBET) [7, 8], heavy baryon effective theory in the large- N_c limit [9], heavy quark effective theory (HQET) [10–13], non-relativistic QCD (NRQCD) [14] or potential NRQCD (pNRQCD) [15]. Throughout this work we make an extensive use of the EFT framework in order to describe the physics of non-relativistic (NR) bound states. Let us now briefly introduce the two physical systems under study in this dissertation: hydrogen-like atoms and heavy quarkonia.

The existence of baryons was established in the beginning of the 20th Century (long before the discovery of QCD) with the discovery of the proton by Rutherford. The proton is the most stable baryon in the Universe ($\tau_p > 10^{34}$ years), and it is essential to the existence of the world as we know it, being the main constituent of visible matter. Due to its composite nature, one of the principal features characterising the proton is its size. The interaction of protons and electrons has been primal to measure the proton charge radius. It was first measured by Hofstadter and collaborators in the 1950s via elastic electron scattering [16]. Most recently the electron scattering experiment in Mainz measured a new set of data points at low momentum [17]. The CODATA 2010 value for the proton radius [18] is based both on ep -scattering measurements and determinations from hydrogen spectroscopy. Hydrogen arises from the bound state of a proton and an electron and it is the most abundant element in the universe, making up 75% of normal matter. It is essential to the existence of life. Without hydrogen the Sun would not give us heat or light, and water, crucial to any kind living system, would not exist. The spectroscopy lines of hydrogen were discovered by Lyman in 1906 [19] and during the last century a large number of the hydrogen spectral transitions have been measured in different experiments all around the world. Similar hydrogen-like bound states, such as muonic hydrogen are the perfect place to obtain precise measurements of hadronic effects. This is so because the probability of a lepton being within the size of the proton grows cubically with the mass, i.e. heavier leptons are more susceptible to finite size effects. In 2010, for the first time, the muonic hydrogen Lamb shift was measured at PSI [20]. In particular, they measured the Lamb shift (the 2S-2P transition), which allows for a precise determination of the value of the proton radius. Surprisingly for the scientific community, this measurement is $\sim 7\sigma$ away from the CODATA value. This puzzle is one of the main reasons driving us to study the model independent prediction of the proton radius that the implementation of an EFT framework provides.

Heavy quarkonium physics found its first experimental evidence when in 1974 the very narrow resonance J/Ψ (charmonium) was first measured simultaneously at SLAC and Brookhaven National Laboratory [21, 22]. It was concluded that this resonance was a bound state of a quark much heavier than any other known at the moment: it was the discovery of the charm quark. A few years later, in 1977 the Υ resonance (bottomium) was found in Fermilab [23], leading to the discovery of the bottom quark. It took perseverance to finally discover the long expected partner of the bottom quark, the top quark, which was first measured 18 years later, in 1995, at Fermilab [24]. The main differential characteristic of the top quark is the impossibility to create toponium states. This is due to the top quark's fast decay rate, mediated by the weak interactions. Ever since the beginning of these discoveries, there have been extensive investigations and further discoveries of heavy quarkonium states. On the experimental side, quarkonium factories have been able to measure several types of spectra and decays. Among the most relevant experiments are BaBar at SLAC, Belle at KEK, CLEO-III and CLEO-c at CESR, CDF and $D\bar{A}\bar{Y}$ at Fermilab, and BESII and BESIII at IHEP, and LHC at CERN (in the short term future, the PANDA experiment at FAIR will use proton-antiproton collisions to study the strong interaction). These experiments have measured different states of charmonium and bottomium

but also other mesons such as B -mesons (among which the B_c is an example of heavy quarkonium with different heavy masses) or D -mesons, and even more exotic states such as the X(3872). There is room for a lot of theoretical improvements in this area (current reviews on the matter can be found in Refs. [25–27]), and this dissertation constitutes a significant contribution in this direction.

In the first part of this work, we study those systems composed by a lepton and a proton which are weakly bounded by the electromagnetic force, such as hydrogen and specially muonic hydrogen. Hadronic information is encoded in the interaction of the baryon and the lepton it is bounded to, when one takes into account the effects of the hadron's finite size. Therefore, they are a good place to learn about the physics inside hadrons upon comparison with experimental measurements. The physics of systems composed by a heavy quark and a heavy antiquark with different masses weakly bounded by QCD, i.e. heavy quarkonium, comprises the second part of this dissertation. Its description in terms of EFTs is a powerful tool to perform QCD computations, which allows us to obtain important information on observables such as heavy quark masses, the strong coupling constant, etc. These determinations help us overcome our limitations in dealing with low energy QCD. The two systems at hand are in fact very similar in their EFT description. In both cases, an expansion in the inverse of the masses of the heavy quarks and their coupling constant α/α_s is a good perturbative approach, therefore allowing for a well-defined theoretical description of the system. The main difference between the two is the different gauge symmetry structures of their interactions: U(1) in quantum electrodynamics (QED) vs. SU(3) in QCD. However, by explicitly keeping track of the Casimir coefficients of the non-Abelian theory (QCD) in the computations, one can easily recover the Abelian case (QED) for point-like particles. Besides, hadronic corrections that arise in the QED case when coping with the finite size baryons do not happen in QCD. This mismatching arises from the different nature of the theories at scales of the order of the heavy masses i.e. HBET vs. QCD.

Effective field theories for baryons

The development of quantum field theories for baryons at low energies is closely related to the chiral symmetry that the QCD Lagrangian exhibits when the three lightest flavors of quarks (up, down and strange) are considered in the massless limit. Since the actual mass of these quarks is much smaller than Λ_{QCD} , this allows for a good expansion parameter and, thus, a perturbative theory. In this energy range (below 1 GeV) the heavy quark flavors (bottom, charm and top) play no significant role due to their large masses. Therefore, the chiral QCD Lagrangian exhibits an approximate $SU(3)_L \times SU(3)_R \times U(1)_{L+R}$ chiral symmetry which is spontaneously broken to a $SU(3)_{L+R} \times U(1)_{L+R}$ vector symmetry (flavor symmetry). The effects of the symmetry breaking become important at energies below Λ_{QCD} , which is where hadrons become the appropriate degrees of freedom. Associated with the spontaneously broken generators of the chiral symmetry, eight Goldstone bosons arise, which in the case at hand are the octet of the lowest pseudoscalar mesons: the three pions, the four kaons and the eta. However, we know for a fact that these quarks and mesons are not actually massless. In fact, the chiral symmetries are explicitly broken, e.g. due to non-zero quark masses, and consequently, masses for the Goldstone bosons are generated.

This rationale gives rise to an effective Lagrangian at tree level that describes the physics of mesons and baryons at low energies. It was in 1979 that, for the first time, Weinberg took this Lagrangian beyond the tree level [5], which can be naturally done as long as the energy of the

process is smaller than the chiral breaking scale ($\sim \Lambda_{\text{QCD}}$). This provides a power counting for the chiral Lagrangian in powers of E/Λ_{QCD} . Shortly after, in the 1980's a systematic study of the Lagrangian beyond tree level was performed by Gasser and Leutwyler [6], extending it to $\text{SU}(3)$ and expressing it in terms of the Goldstone matrix field containing the octet of pseudoscalars. This is known today as ChPT and it is organised as an expansion in the derivatives of the fields p , i.e. it is equipped with a well-defined power counting.

Much as baryons were known long before quarks, historically its description in terms of fields has been problematic. The main reason for this is that their mass is comparable to the hadronisation scale Λ_{QCD} (in the case of nucleons $m_N \sim 1 \text{ GeV}$), reaching the limit where the chiral expansion ceases to be valid. This fact gives rise to the question of whether their physics can be described in a perturbative manner. The introduction of baryons in the chiral Lagrangian was proposed by Weinberg in 1968 [28]. However, power counting rules remained problematic until the inclusion of the heavy mass methods, which overcome the issue by going to the NR limit. This idea was first carried out for the pion-nucleon sector in the 1990's by Jenkins and Manohar in [7] and by Bernard et al. [8], and has since then been extensively developed in what is today known as heavy baryon chiral perturbation theory (HBChPT).² This theory provides a consistent power counting in terms of the small velocity of the heavy baryon hence allowing for extensive calculations. A concern that remains, however, is that of finding the appropriate way of handling the baryon resonances. In general, these states are heavier than the nucleon, and so their contribution could be included simply by integrating them out from the Lagrangian, in such a way that their effect would be subleading. A different approach, though, should be adopted with the Delta particle ($\Delta(1232)$), which is only $\sim 300 \text{ MeV}$ away from the nucleon mass and couples strongly to the pion-nucleon sector. On top of this, an outcome of applying large- N_c rationale to baryons, is that the proton and the Delta particle become degenerate in mass. Even though for $N_c = 3$ the $1/N_c$ expansion is not optimal, the former argument may signal that the Delta particle represents the largest resonant contribution and thus should be taken into account. A HBET Lagrangian that includes the interaction of pions, the proton, and the Delta was developed by Jenkins and Manohar in 1991 [29] and by Hemmert et al. [30] in 1996 in a chiral context (see also [31]). It was studied within a large- N_c ideology by Dashen and Manohar in 1993 [32]. In this work we make use of these EFTs.

Effective field theories for NR bound states

A NR bound state is a system where a particle is subject to a potential in such a way that it has a tendency to remain (in time) quasi-localised (in space). The interaction of the potential happens an infinite number of times, which in fact is what causes the system to be bounded. In this way, the physics describing the bound state is clearly non-perturbative, as it requires summing up an infinite series. This is compactly achieved by solving exactly the Schrödinger equation for a given potential. However, through the application of EFT mechanisms, we can find the potential up to some order in the velocity expansion and safely assume that the rest of the contribution will be small. Here we will give some details on how this approach is taken. Both (muonic) hydrogen and heavy quarkonium systems admit a description in terms of EFTs for NR bound states.

In a classical system interacting through electromagnetism, the potential giving rise to the bound state is the well-known Coulomb potential. Upon quantization, electromagnetism becomes

²In fact, the name HBET is sometimes used to refer to HBChPT. We will use them indistinctly throughout this text.

the well-known QED. However, incorporating quantum effects to the Coulomb potential is not straightforward. The first attempt to address this issue was the Bethe-Salpeter equation [33], presented in 1951. This equation describes bound states of a two-body quantum field system in a relativistically covariant formalism. However, it turned out that the equation cannot be exactly solved in a general case, and in the cases where the solution can be exactly found, it turned out to be problematic [34]. In other words, provided it can be achieved, solving this equation for a physical system requires considerable effort. It consequently fails to provide a systematic approach to the bound state problem. This motivated extensive effort of the community to bypass this difficulty. The answer laid, once again, in the application of EFTs to take away the irrelevant information hence simplifying the treatment of the relevant one.

The main point to consider is that the heavy constituents in a bound state barely move with respect to each other, and thus are naturally NR systems. The problem was then how to incorporate the relativistic quantum corrections into this NR system. It was in 1986 that a NR effective Lagrangian was first proposed by Caswell and Lepage [14]. This theory is today known as non-relativistic QED (NRQED)/NRQCD. The success of this approach lays on its improvement on the computational side, where, having disposed of the irrelevant information, the effort needed to describe the system is heavily reduced.

Let us now explain the different approaches taken to describe the physics of a bound state, depending on the characteristics of the system. First, we consider the case where the bound state has one heavy (m_h) and one light constituents (m_l). In terms of the scales of the system, we may regard the heavy fermion as a static source with the energy scale hierarchy $m_h \gg m_l, |\mathbf{p}_l|, E_l$, where $|\mathbf{p}_l|$ and E_l are the momentum and energy of the light fermion respectively. The light fermion is still a relativistic degree of freedom, fulfilling the linear dispersion relation and therefore $E_l \sim |\mathbf{p}_l|$. Moreover, the typical energy and momentum transferred within the bound state will be of the same order as those of the light fermion, $E \sim |\mathbf{p}| \sim E_l \sim |\mathbf{p}_l|$, as this is the scale of the energy/momentum exchange between the heavy and the light fermions. In other words, the momentum of the heavy particle (at the lowest order) can be split into a large component proportional to its mass and a small component, i.e. $p^\mu = mv^\mu + k^\mu$ where $k^2 \ll m^2$. This consideration leads to the aforementioned leading order HBET/HQET Lagrangians. This is the appropriate approach to describe systems such as the D -mesons. Moreover, we have that $E \sim |\mathbf{p}| \sim \Lambda_{\text{QCD}}$ and therefore the counting in HQET is provided by one single scale Λ_{QCD} . In the case of QED, we could apply it to systems with atomic number Z big enough such that $Z\alpha \sim 1$. Then any number of e^+e^- pairs could be created, giving rise to non-perturbative physics, similar to the case of the D -meson.

Now let us move on to the case where we have two heavy fermions of masses m_1 and m_2 in the bound state. The physics of this system is more complicated as well as more interesting, since it allows for different scale configurations. It is in this case in which this work is focused. The NR nature of this situation is described by the relation

$$m_1 \sim m_2 \gg |\mathbf{p}| \gg E. \quad (1)$$

This correspondence establishes the scale hierarchy which allows for the use of EFTs in all their glory. We can successively integrate out the higher scales obtaining an EFT for each energy range.

The largest scale is known as the **hard scale** and it is set by the masses of the heavy fermions, as well as by the reduced and total masses of the bound state, which read

$$m_r = \frac{m_1 m_2}{m_1 + m_2}, \quad M = m_1 + m_2, \quad (2)$$

respectively. This scale plays no dynamical role in the EFT and therefore it is integrated out. It appears only through fluctuations, i.e. an expansion in the inverse of the mass can be carried out. However, it does have a role in the power counting since momentum and energy depend on the reduced mass m_r . Corrections due to the hard scale are encoded in the Wilson coefficients. The **soft scale** is set by the typical momentum of the bound state $\mathbf{p} \sim m_r v$. Finally, the **ultrasoft** scale is given by the typical binding energy in the bound state $E \sim m_r v^2$. The already established fact that the velocity v is small yields a wide separation among these three scales, as well as it provides a good expansion parameter.

In the case of QED, the only expansion parameter that we have is the fine-structure coupling constant α , which is of the order of the velocity $v \sim \alpha$. Therefore, it can be successfully approached perturbatively, and an expansion in terms of the coupling constant and the inverse of the mass is carried out. Within these systems, depending on the relation among the masses, we can distinguish two cases. We may contemplate the case where the masses are similar $m_1 \sim m_2 \sim m_r$ such as in positronium and dimuonium, but also the case where they are different in size, $m_1 \gg m_2 \sim m_r$, but still both particles are considered NR. This is the case of hydrogen and also muonic hydrogen, to which we devote the first part of this thesis. In these systems, keeping the full dependence on the masses allows for an increase in the precision of the computations. As a first approximation these systems can be regarded as a quasi-static source interacting with a NR particle.

When we are dealing with QED-like bound states, the system can be completely described in terms of the scale $m_r \alpha^n$. However, when the system is bounded by QCD, in addition to the equivalent scale $m_r \alpha_s^n(\nu)$, we have to consider the scale of $\Lambda_{\text{QCD}} \sim \nu e^{-2\pi/(\beta_0 \alpha_s(\nu))}$. In order to stay in the NR limit, only the relation $m_r \gg \Lambda_{\text{QCD}}$ needs to hold. However energy/momentum can relate differently to Λ_{QCD} . Note that configurations where Λ_{QCD} is a large scale will be controlled by non-perturbative physics and the EFT will not provide important predictions. However, we will focus on states where this is not the case and the non-perturbative physics is negligible or encoded in small corrections. In this case the EFT may give important information about the size and characteristics of these corrections, making this an ideal system in which to study QCD.

Now let us examine the case where $|\mathbf{p}| \gg E \sim \Lambda_{\text{QCD}}$. This case can still be considered as mainly perturbative and non-perturbative effects will be regarded as corrections. However, due to our little understanding, these corrections need some modelling. They are non-local and therefore difficult to assess. We will not further study this interesting field in this thesis.

Finally, we can also consider the case where $|\mathbf{p}| \gg E \gg \Lambda_{\text{QCD}}$. i.e. the weak coupling regime. In this case the strong coupling constant will be small, as it has to be taken at scales larger than Λ_{QCD} , and therefore, it can be compared to the velocity, $\alpha_s \sim v$. This provides a good perturbative approach, at least for the lowest levels of the spectrum since the momentum and energy can be parametrized as

$$|\mathbf{p}| \sim m_r \frac{\alpha_s}{n}, \quad E \sim m_r \frac{\alpha_s^2}{n^2}. \quad (3)$$

In this case we can obtain in a perturbative fashion precise determinations of the heavy quark masses and the strong coupling constant. Non-perturbative corrections in this case would be in the form of local condensates, and are beyond the accuracy we consider.

Once the dynamical situation of the system is established we shall proceed to finding the most suitable EFT to describe our bound states. In fact, we are most interested in determining the potential, which will allow us to obtain the bound state by solving the Schrödinger equation. For states involving QCD we focus on the more general case where $m_r v \gg \Lambda_{\text{QCD}}$.

We start from a theory containing the physics at all scales, in particular up to the hard scale: this would be QED/QCD (for finite size hadronic effects in QED-like systems we will instead consider this theory to be HBET). Since the chief energy range characterising the system is much smaller than the hard and soft scales, we may integrate them out. By means of this procedure the effects of large scales are encoded in higher order terms in the Lagrangian and the Wilson coefficients. When we integrate out the hard scale we obtain the theory of NRQED/NRQCD. The Lagrangian is obtained as an expansion in the (inverse of the) masses, as well as in the small coupling constant. The Wilson coefficients are determined via a matching procedure between these theories and QED/QCD. As we already mentioned, the power counting in this theory is fully controlled by the small parameter v . Not only all the symmetries of the full theory are inherited by the effective Lagrangian, new ones can arise in the low energy theory. The latter is the case of the spin symmetry of the NRQED/NRQCD Lagrangian. An example of the former is the inherited non-linearly realized Poincaré/reparametrization invariance.

At this point, however, there are still terms in the Lagrangian where different scales are mixed, therefore complicating the determination of a well-defined potential. This is solved by integrating out the soft scale which in fact is the natural thing to do in the systems we are discussing. We are then left with an EFT for ultrasoft photons/gluons known as potential-NRQED/NRQCD (pNRQED/pNRQCD). This effective Lagrangian was first presented by Pineda and Soto [15] in 1998. Since then it has been established as the most suitable theory to perform computations in bound states both for QED and QCD. The Lagrangian in this theory can be written in terms of a Schrödinger-like potential plus a term for the interactions of ultrasoft photons. The potential is written as an expansion in inverse powers of the mass and the coupling constant, rendering an explicit power counting. As commonly done in the literature, throughout this text we will frequently refer to the different (well-defined) terms at different orders in the $1/m$ or v expansion of the potential as the “potentials”. We shall distinguish between two kinds of pNRQCD. When we are working at energies such that $mv^2 \sim \Lambda_{\text{QCD}}$, then we talk about weakly coupled pNRQCD, and the matching to NRQCD can be performed perturbatively. The other case arises when $mv \sim \Lambda_{\text{QCD}}$, then we refer to strongly coupled pNRQCD, and the matching is to be carried out non-perturbatively (as now the soft scale is already non-perturbative). In this work we will focus in weakly coupled pNRQCD. Note that this is not a problem for potential NRQED (pNRQED), where the matching to NRQED is always carried out perturbatively.

In the weak-coupling limit, the EFT can be summarized schematically by

$$\left. \begin{aligned} & \left(i\partial_0 - \frac{\mathbf{p}^2}{2m_r} - V^{(0)}(r) \right) \phi(\mathbf{r}) = 0 \\ & + \text{corrections to the potential} \\ & + \text{interaction with other low-energy degrees of freedom} \end{aligned} \right\} \text{pNRQCD/pNRQED.} \quad (4)$$

The matching of pNRQCD to NRQCD is performed by equating Green functions, which in practice may be done in several ways, producing different potentials for different matching schemes (which will nevertheless yield the same physical results). We will further extend on this in the second part of this thesis. Some remarks, however, are to be noted in advance. The matching is always performed by equating Green functions. However we will use three different kinds of Green functions: truncated on-shell Green functions (i.e. S-matrix elements) for the on-shell matching scheme, truncated off-shell Green functions for the off-shell matching scheme and off-shell gauge independent Green functions for the matching with Wilson loops. The latter scheme is of special interest to us. A Wilson loop is defined as a gauge-invariant observable obtained from the holonomy of the gauge connection around a given loop. Formulae for the different potentials in

terms of Wilson loops have been known for a long time. It was used for the first time to describe the static potential between quarks by in 1977 [35], in the context of lattice gauge theory. This formula has been established as the way to compute this potential, which has been done now up to three loops Refs. [36–41]. The formulation was then translated to the language of pNRQCD in 2000 by Brambilla, Pineda, Soto and Vairo [42, 43], who computed the formula for the $1/m$ and then $1/m^2$ potentials. The most interesting feature of these formulae is that they are valid both in the perturbative regime at short distances and the non-perturbative regime at long distances. We devote a considerable fragment of the second part of the thesis to extend on how to perform this computation in the perturbative regime.

In summary, this thesis is divided into two main parts. In Part II, we focus on the study the muonic hydrogen system, and, in particular, on the hadronic contributions to the Lamb shift coming from the two photon exchange (TPE). Gathering the results of our investigation we are able to theoretically compute the $n=2$ Lamb shift with accuracy $\mathcal{O}(m_\mu\alpha^6 \ln \alpha, m_\mu\alpha^5 \frac{m_\mu^2}{m_p^2})$, and upon comparison with its experimental value, we determine the value of the proton radius. In Part III, we concentrate on the analysis of heavy quarkonium systems with different masses. We compute the next-to-next-to-next-to-leading order (N³LO) potential with different matching schemes and find the relation among them. We use our results to compute the B_c spectrum up to $\mathcal{O}(m_r\alpha_s^5)$. We devote Part IV to providing a summary and some final remarks on the work carried out and future related lines of research.

Part II

Muonic hydrogen

Chapter 1

Introduction

In the first part of this thesis we focus on the development of the abelian effective theory pNRQED applied to (muonic) hydrogen. We will use it to comprehensively analyse the theoretical prediction of the Lamb shift in muonic hydrogen, and the associated determination of the proton radius. The use of EFTs allows us to relate the proton radius with well-defined objects in quantum field theory, eliminating unnecessary model dependence. We obtain the potentials that allow us to find an expression for the muonic hydrogen Lamb shift that includes the leading logarithmic $\mathcal{O}(m_\mu\alpha^6)$ terms, as well as the leading $\mathcal{O}(m_\mu\alpha^5\frac{m_\mu^2}{m_p^2})$ hadronic effects. This part of the thesis is based in the work published in Refs. [44–46] by the author.

The Lamb shift in muonic hydrogen has been measured at PSI, Refs. [20, 47], obtaining

$$E(2P_{3/2}) - E(2S_{1/2}) \equiv \Delta E_L^{\text{exp}} = 202.3706(23) \text{ meV}. \quad (1.1)$$

By comparing this measurement to its theoretical prediction, the proton radius (more precisely, the root mean square of the electric proton radius), was determined: $r_p \equiv \sqrt{\langle r_p^2 \rangle} = 0.84087(39)$ fm. This result has led to a lot of controversy as it is 7.1σ away from the 2012 CODATA value, $r_p = 0.8775(51)$ fm, Ref. [18] (see Refs. [48, 49] for reviews on the proton radius puzzle). The latter value is an average of determinations coming from hydrogen spectroscopy and electron-proton scattering¹.

In order to assess the significance of the discrepancy, it is of fundamental importance to perform the computation of the Lamb shift in muonic hydrogen (in particular of its errors) in a model independent way.

In this respect, the use of EFTs is specially useful. They help organizing the computation by providing power counting rules that assess the importance of the different contributions. This becomes increasingly necessary as higher order effects are included. Even more important, these power counting rules allow to parametrically control the size of the higher order non-computed terms and, thus, give a reliable and model-independent estimate of the error (which is of the size of such terms).

The EFT approach is specially convenient in the case of NR bound states where the relevant scales are naturally well-separated. They are: the hard scale or reduced mass (m_r), the soft

¹The determination from ep scattering data, however, has been challenged in Refs. [50, 51], and its exclusion would certainly diminish this tension. Further experiments and theoretical analyses of the ep scattering are being carried out in order to clarify this issue. See Refs. [52–56].

scale or typical momentum ($\mathbf{p} \sim m_r v \sim m_r \alpha$) and the ultrasoft scale or typical binding energy ($E \sim m_r v^2 \sim m_r \alpha^2$), where $v(\sim \alpha)$ is the typical velocity of the particles in the bound state. This allows us to systematically integrate out the large scales until we find an EFT suitable for the setting of our problem.

In the case of muonic hydrogen the EFT organization is specially useful, as its dynamics is characterized by several scales:

$$m_p \sim m_\rho, \quad m_\mu \sim m_\pi \sim m_r \equiv \frac{m_\mu m_p}{m_p + m_\mu}, \quad m_r \alpha \sim m_e.$$

By considering ratios between them, the main expansion parameters are obtained:

$$\frac{m_\pi}{m_p} \sim \frac{m_\mu}{m_p} \approx \frac{1}{9}, \quad \frac{m_e}{m_r} \sim \frac{m_r \alpha}{m_r} \sim \frac{m_r \alpha^2}{m_r \alpha} \sim \alpha \approx \frac{1}{137}. \quad (1.2)$$

In our approach we combine the use of HBET, Refs. [7,8], NRQED, Ref. [14] and, specially, pNRQED, Refs. [15,57,58]. Partial results following this approach can be found in Refs. [59–62], and the complete results are presented in [44–46].

Since pNRQED describes degrees of freedom with $E \sim m_\mu \alpha^2$, any other degree of freedom with larger energy is integrated out. This implies treating the proton and muon in a NR fashion and integrating out pions and Delta particles. This is the step of going from HBChPT to NRQED. By integrating out the scale $m_\mu \alpha$, pNRQED is obtained and the potentials appear. Schematically the path followed is ($\Delta \equiv m_\Delta - m_p$):

$$\text{HBChPT} \xrightarrow{(m_\pi/\mu, \Delta)} \text{NRQED} \xrightarrow{(m_\mu \alpha)} \text{pNRQED}.$$

Following this program, we start by setting the Lagrangians of the EFTs of our interest: HBChPT, NRQED and pNRQED in Chapter 2. By exploiting the symmetries of our system, we determine these Lagrangians that will produce contributions to the computation up to the order of our interest. The Wilson coefficients in the HBChPT Lagrangian are typically fixed by comparison to experimental data. In particular, those corresponding to the lowest order Lagrangian and of which we make use in our computation (F_π , g_A , $g_{\pi N \Delta}$ and b_{1F}) are already well-known. For the point-like NRQED Lagrangian, we are able to compute all of its Wilson coefficients analytically in terms of the parameters of the higher energy theory QED and the matching energy scale. This is so because we have full control on the behavior of the full theory (QED) at all energies. Therefore the challenge lays in the computation of the hadronic part of these Wilson coefficients.

In Chapter 3, a detailed explanation of the matching computation between HBChPT and NRQED is given. The hadronic contribution to the Lamb shift in muonic hydrogen is obtained through this matching procedure. It includes the contribution of the TPE, which is of utmost interest to us as it corresponds to the main source of uncertainty in our computation. The computation of the TPE needs of the determination of the forward virtual Compton tensor (FVCT). The spin-dependent and spin-independent structure functions of the FVCT of the proton, $T^{\mu\nu}$, carry important information about the QCD dynamics. They test the Euclidean region of the theory since $Q^2 \equiv -q^2 > 0$. For $Q^2 \sim m_\pi^2 \neq 0$, the behavior of $T^{\mu\nu}$ is determined by the chiral theory, and can be obtained within a chiral expansion using HBChPT. If one works within a large- N_c ideology (where N_c is the number of colours) the Delta particle should be incorporated in the HBET Lagrangian, Ref. [32] (see also Refs. [30,31]). This produces a

double expansion in $\sim m_\pi/m_\rho$ and $\sim \Delta/m_\rho$. Note that this creates a new expansion parameter $m_\pi/\Delta \sim 1/2$, and therefore the associated corrections will be incorporated in our computation together with the pure chiral result.

Within this framework we compute the spin-dependent and spin-independent structure functions of the FVCT of the proton to $\mathcal{O}(p^3)$ in HBChPT including the Delta particle. The tensor $T^{\mu\nu}$ cannot be directly related to cross sections obtained at fixed energies, as it tests the Euclidean regime. Nevertheless, it is possible to obtain it (up to eventual subtractions) from experiment through dispersion relations, i.e., through specifically weighted averages of measured cross sections over all energies. Possible constructions are the so-called generalized sum rules, which, for large energies, can be related with the deep inelastic sum rules. These have been studied in Ref. [63] for the spin-dependent case and briefly discussed in Ref. [61] for the spin-independent case. This constitutes an interesting new line of research, since we could use the results of our study to develop generalized sum rules for the spin-independent part of $T^{\mu\nu}$ analogous to those obtained in Ref. [63] for the spin-dependent part.

The tensor $T^{\mu\nu}$ appears in the matching computation between HBChPT and NRQED that determines $c_3^{pl_i}$ and $c_4^{pl_i}$ ($l_i = e$ or μ), the Wilson coefficients of the lepton-proton four-fermion operators in the NRQED Lagrangian. At the scales at which we perform the matching, $T^{\mu\nu}$ is fixed by its chiral structure. This is our main motivation for its computation. As soon as hadronic effects start to become important in atomic physics, the Wilson coefficients $c_3^{pl_i}$ and $c_4^{pl_i}$ play a major role. They appear in the hyperfine splitting (spin-dependent) and Lamb shift (spin-independent) in hydrogen and muonic hydrogen (see Refs. [44–46, 59–61]). Therefore, their determination allows us to relate the energy shifts obtained in hydrogen and muonic hydrogen. Even more important, these Wilson coefficients are often responsible for most of the theoretical uncertainty in these splittings, as happens for the Lamb shift in muonic hydrogen. The necessity to improve our knowledge of the (spin-independent) lepton-proton four-fermion Wilson coefficient has led us to compute this quantity in HBChPT including the Delta particle. Fortunately enough, this object is chiral enhanced. Therefore, the $\mathcal{O}(p^3)$ chiral computation yields a pure prediction (without the need of new counterterms) of $\delta E_{L,\text{TPE}}$, the (hadronic) TPE contribution to the muonic hydrogen Lamb shift: $\Delta E_L = E(2P_{3/2}) - E(2S_{1/2})$. Note that, since $m_\mu/m_\pi \sim 1$, we keep the complete m_μ/m_π dependence in such predictions.

We profit this analysis to revisit the distinction between Born and non-Born terms of $T^{\mu\nu}$ and $\delta E_{L,\text{TPE}}$. Such distinction is translated into the so-called Born (or Zemach) and polarizability corrections to the Wilson coefficients (names also used for the associated contributions to the energy shifts: hyperfine or Lamb shift). For the spin-independent case we have a good analytic control and can also compute the charge moments, $\langle r^n \rangle$, and the Zemach, $\langle r^n \rangle_{(2)}$, moments, for $n \geq 3$, since they are dominated by the chiral theory. The polarizability correction of ΔE_{TPE} is also usually split into the so-called inelastic and subtraction terms. We will also discuss what HBChPT has to say in this respect.

In Chapter 4, we give the details of the matching of NRQED to pNRQED. In this way, all the information associated to scales higher than the ultrasoft scale that will allow us to compute the spectrum, is encoded in potentials. Hence we need to find all the potentials that contribute to the order of interest. Our main goal is the reorganization of all the contributions within the EFT framework, since most of these computations were previously known. However, we add some new analytical information to some of the potentials. We compute the relativistic corrections in dimensional regularization and we express them in terms of the NRQED Wilson coefficients, which contain information of higher order effects. On top of this, we have made some effort to

present the result assuming an arbitrary charge for the muon and proton, so that the results can be of use in a more general situation, in particular for other muonic atoms. The expressions of the potentials we found would be equal for light muonic atoms after appropriately eliminating the effects of the hadronic scales from the NRQED Wilson coefficients. We also expect that the analysis presented here will set the basis for higher order computations using EFTs.

In Chapter 5 we compute the energy shifts that the pNRQED potentials and the ultrasoft photons yield. Gathering these results together we compute the $n = 2$ Lamb shift with accuracy $\mathcal{O}(m_\mu \alpha^6 \ln \alpha, m_\mu \alpha^5 \frac{m_\mu^2}{m_p^2})$. This allow us, by comparing to the experimental measurement in Eq. (1.1), to obtain a model independent prediction of the proton radius. On top of this, the parametric control of the uncertainties allows us to obtain a model independent estimate of the error, which is dominated by hadronic effects.

Chapter 2

Effective field theories

In this chapter, we will present the main building blocks of the HBET, NRQED and pNRQED Lagrangians needed for our analysis.

2.1 HBET

Our starting point is the SU(2) version of HBET coupled to leptons where the Delta particle is kept as an explicit degree of freedom. The degrees of freedom of this theory are the proton, neutron and Delta, for which the NR approximation can be taken, and pions, leptons (muons and electrons) and photons, which will be taken relativistic. This theory has a cut-off $\mu \ll m_p, m_\rho$, which is much larger than any other scale in the problem. The Lagrangian can be split in several sectors. Nevertheless, the fact that some particles will only enter through loops, since only some specific final states are wanted, simplifies the problem. The Lagrangian can be written as an expansion in e and $1/m_p$ and can be structured as follows

$$\mathcal{L}_{HBET} = \mathcal{L}_\gamma + \mathcal{L}_l + \mathcal{L}_\pi + \mathcal{L}_{l\pi} + \mathcal{L}_{(N,\Delta)} + \mathcal{L}_{(N,\Delta)l} + \mathcal{L}_{(N,\Delta)\pi} + \mathcal{L}_{(N,\Delta)l\pi}, \quad (2.1)$$

representing the different sectors of the theory. In particular, the Δ stands for the Delta particle: the spin 3/2 baryon multiplet (we also use $\Delta = m_\Delta - m_p$, the specific meaning in each case should be clear from the context).

The photonic HBET Lagrangian reads (the first corrections to this expression scale like α^2/m_p^4)

$$\mathcal{L}_\gamma = -\frac{1}{4}F^{\mu\nu}F_{\mu\nu} + \left(\frac{d_{2,R}}{m_p^2} + \frac{d_2^{(\tau)}}{m_\tau^2} \right) F_{\mu\nu}D^2F^{\mu\nu}, \quad (2.2)$$

where $d_{2,R}$ stands for the hadronic contribution.

The leptonic sector can be approximated to ($iD_\mu = i\partial_\mu - eA_\mu$)

$$\mathcal{L}_l = \sum_i \bar{l}_i (i\not{D} - m_{l_i}) l_i, \quad (2.3)$$

where $l_i = e, \mu$.

The Lagrangian of a heavy baryon at $\mathcal{O}(1/m_p^2)$ coupled to electromagnetism reads

$$\mathcal{L}_N = N_p^\dagger \left\{ iD_0 + \frac{\mathbf{D}_p^2}{2m_p} + \frac{\mathbf{D}_p^4}{8m_p^3} - e \frac{c_F^{(p)}}{2m_p} \boldsymbol{\sigma} \cdot \mathbf{B} \right. \\ \left. - e \frac{c_D^{(p)}}{8m_p^2} [\boldsymbol{\nabla} \cdot \mathbf{E}] - ie \frac{c_S^{(p)}}{8m_p^2} \boldsymbol{\sigma} \cdot (\mathbf{D}_p \times \mathbf{E} - \mathbf{E} \times \mathbf{D}_p) \right\} N_p, \quad (2.4)$$

where $iD_p^0 = i\partial_0 + Z_p e A^0$, $i\mathbf{D}_p = i\boldsymbol{\nabla} - Z_p e \mathbf{A}$. For the proton $Z_p = 1$ (for the neutron all indices $p \rightarrow n$ and $Z_n = 0$).

The hadronic interactions are organized according to their chiral counting. Since a single chiral loop already produces a factor $1/(4\pi F_0)^2 \sim 1/m_p^2$, we only need the free-particle pionic Lagrangian:

$$\mathcal{L}_\pi = \left[(\partial_\mu - ieA^\mu)\pi^+ \right] \left[(\partial^\mu + ieA^\mu)\pi^- \right] - m_\pi^2 \pi^+ \pi^- + \frac{1}{2} (\partial_\mu \pi^0)(\partial^\mu \pi^0) - \frac{1}{2} m_\pi^2 \pi^0 \pi^0. \quad (2.5)$$

We need not account for pion self-interactions, and the pion-baryon interactions are only needed at $\mathcal{O}(m_\pi)$, which is the leading order and reads (Refs. [64, 65]):

$$\mathcal{L}_{(N,\Delta)\pi} = \bar{N} (iv \cdot \Gamma + g_{A\pi} \cdot S) N - \bar{T}_a^\mu (iv \cdot D^{ab} - \Delta \delta^{ab}) T_{\mu b} + g_{\pi N \Delta} \left(\bar{T}_a^\mu w_\mu^a N + h.c. \right), \quad (2.6)$$

where T_a^μ stands for the Rarita-Schwinger spin 3/2 field, N for the nucleon 1/2 isospin multiplet and $S_\mu = \frac{i}{2} \gamma_5 \sigma_{\mu\nu} v^\nu$ is the spin operator (where we will take $v_\mu = (1, \mathbf{0})$).

The only relevant $1/m_p$ interaction mixing the Delta and the nucleon in our case is the $p\text{-}\Delta^+\text{-}\gamma$ term reading

$$\mathcal{L}_{(N,\Delta)} = \frac{ib_{1,F}}{2m_p} \left(\bar{T}_a^\mu S_\nu \frac{1}{2} Tr [f_+^{\nu\mu} \tau^a] N + h.c. \right). \quad (2.7)$$

The previous equations make use of the definitions:

$$\begin{aligned} D_\mu^{ij} &= \left(\partial_\mu \delta^{ij} + \Gamma_\mu^{ij} \right), \\ \Gamma_\mu^{ij} &= \Gamma_\mu \delta^{ij} - \frac{i}{2} \epsilon^{ijk} Tr [\tau^k \Gamma_\mu], \\ \Gamma_\mu &= \frac{1}{2} [u^\dagger, \partial_\mu u] - \frac{i}{2} u^\dagger (\mathbf{v}_\mu + \mathbf{a}_\mu) u - \frac{i}{2} u (\mathbf{v}_\mu - \mathbf{a}_\mu) u^\dagger, \\ f_{\mu\nu}^\pm &= u^\dagger F_{\mu\nu}^R u \pm u F_{\mu\nu}^L u^\dagger \equiv \tau^i f_{\pm\mu\nu}^i, \\ F_{\mu\nu}^X &= \partial_\mu F_\nu^X - \partial_\nu F_\mu^X - i [F_\mu^X, F_\nu^X]; \quad X = L, R, \\ F_\mu^R &= \mathbf{v}_\mu + \mathbf{a}_\mu, \quad F_\mu^L = \mathbf{v}_\mu - \mathbf{a}_\mu, \\ u_\mu^{ij} &= u_\mu \delta^{ij} - i \epsilon^{ijk} w_\mu^k, \\ w_\mu^i &= \frac{1}{2} Tr [\tau^i u_\mu] = -\frac{1}{F_\pi} \partial_\mu \pi^a - \frac{e}{F_\pi} A_\mu \epsilon^{a3b} \pi^b + \dots, \\ u_\mu &= iu^\dagger \nabla_\mu U u^\dagger, \\ \nabla_\mu U &= \partial_\mu U - iF_\mu^R U + iU F_\mu^L, \\ U &= u^2 = \exp \left(\frac{i}{F_\pi} \tilde{\tau} \cdot \tilde{\pi} \right), \end{aligned} \quad (2.8)$$

where \mathbf{v}_μ , \mathbf{a}_μ denote external vector, axial-vector fields and are the only external sources possible at this order.

The baryon-lepton Lagrangian provides new terms that are not usually considered in HBET. The relevant term in our case is the interaction between the leptons and the nucleons (actually only the proton):

$$\mathcal{L}_{(N,\Delta)l} = \frac{1}{m_p^2} \sum_i c_{3,R}^{pl_i} \bar{N}_p \gamma^0 N_p \bar{l}_i \gamma_0 l_i + \frac{1}{m_p^2} \sum_i c_{4,R}^{pl_i} \bar{N}_p \gamma^j \gamma_5 N_p \bar{l}_i \gamma_j \gamma_5 l_i. \quad (2.9)$$

The above matching coefficients fulfil $c_{3,R}^{pl_i} = c_{3,R}^p$ and $c_{4,R}^{pl_i} = c_{4,R}^p$ up to terms suppressed by m_{l_i}/m_p , which will be sufficient for our purposes.

Let us note that with the conventions above, N_p is the field of the proton (understood as a particle) with positive charge if l_i represents the leptons (understood as particles) with negative charge.

This finishes all the needed terms for the computation of the Lamb shift up to the order of our interest, since the other sectors of the Lagrangian would give subleading contributions.

2.2 NRQED(μp)

In the muon-proton sector, by integrating out the $m_\pi \sim m_\mu$ and Δ scales, an EFT for muons, protons and photons appears. In principle, we should also consider neutrons but they play no role at the precision we aim. The effective theory corresponds to a hard cut-off $\nu \ll m_\pi$ and therefore pions and Deltas have been integrated out. The Lagrangian is equal to the previous case but with neither pions nor Deltas, and with the following modifications: $\mathcal{L}_l \rightarrow \mathcal{L}_e + \mathcal{L}_\mu^{(\text{NR})}$ and $\mathcal{L}_{(N,\Delta)l} \rightarrow \mathcal{L}_{Ne} + \mathcal{L}_{N\mu}^{(\text{NR})}$, where it is made explicit that the muon has become NR. Any further difference goes into the Wilson coefficients, in particular, into the Wilson coefficients of the baryon-lepton operators.

The effective Lagrangian reads

$$\mathcal{L}_{\text{NRQED}(\mu)} = \mathcal{L}_\gamma + \mathcal{L}_e + \mathcal{L}_\mu^{(\text{NR})} + \mathcal{L}_N + \mathcal{L}_{Ne} + \mathcal{L}_{N\mu}^{(\text{NR})}. \quad (2.10)$$

The pure photon sector is approximated by the following Lagrangian

$$\mathcal{L}_\gamma = -\frac{1}{4} F^{\mu\nu} F_{\mu\nu} + \left(\frac{d_2^{(\mu)}}{m_\mu^2} + \frac{d_2}{m_p^2} + \frac{d_2^{(\tau)}}{m_\tau^2} \right) F_{\mu\nu} D^2 F^{\mu\nu}, \quad (2.11)$$

$d_2^{(\mu)}$ and $d_2^{(\tau)}$ are generated by the vacuum polarization (VP) loops with only muons and taus respectively. Note that, in comparison to Eq. (2.2), there is here an extra contribution from the VP loop with muons, which are now NR. At $\mathcal{O}(\alpha)$ they read

$$d_2^{(\mu)} = \frac{Z_\mu^2 \alpha}{60\pi} + \mathcal{O}(\alpha^2), \quad d_2^{(\tau)} = \frac{\alpha}{60\pi} + \mathcal{O}(\alpha^2). \quad (2.12)$$

The hadronic effects of the VP are encoded in d_2 , which is the NR version of $d_{2,R}$ in Eq. (2.2):

$$d_2 = \frac{m_p^2}{4} \Pi'_h(0) = \frac{Z_p^2 \alpha}{60\pi} + d_2^{\text{had}} + \mathcal{O}(\alpha^2). \quad (2.13)$$

We define $\Pi'_h(0)$ as the derivative of the hadronic VP (such that $\Pi_h(-\mathbf{k}^2) = -\mathbf{k}^2 \Pi'_h(0) + \dots$). The experimental figure for the total hadronic contribution reads $\Pi'_h \simeq 9.3 \times 10^{-3} \text{ GeV}^{-2}$, Ref. [66]. Following standard practice, we have singled out the contribution due to the one loop VP of a point-like proton in the second equality of Eq. (2.13). Note though that d_2^{had} is still of order α .

The electron sector reads ($iD_\mu = i\partial_\mu - eA_\mu$)

$$\mathcal{L}_e = \bar{l}_e (i\not{D} - m_{l_e}) l_e. \quad (2.14)$$

We do not include the term

$$- \frac{eg_{l_e}}{m_\mu} \bar{l}_e \sigma_{\nu\lambda} l_e F^{\nu\lambda}, \quad (2.15)$$

since the coefficient g_{l_e} is suppressed by powers of α and the mass of the lepton. Therefore, it would give contributions beyond the accuracy we aim. In any case, any eventual contribution would be absorbed in a low energy constant.

The muonic sector reads

$$\begin{aligned} \mathcal{L}_\mu^{(\text{NR})} = & l_\mu^\dagger \left\{ iD_\mu^0 + \frac{\mathbf{D}_\mu^2}{2m_\mu} + \frac{\mathbf{D}_\mu^4}{8m_\mu^3} + e \frac{c_F^{(\mu)}}{2m_\mu} \boldsymbol{\sigma} \cdot \mathbf{B} \right. \\ & \left. + e \frac{c_D^{(\mu)}}{8m_\mu^2} [\boldsymbol{\nabla} \cdot \mathbf{E}] + ie \frac{c_S^{(\mu)}}{8m_\mu^2} \boldsymbol{\sigma} \cdot (\mathbf{D}_\mu \times \mathbf{E} - \mathbf{E} \times \mathbf{D}_\mu) \right\} l_\mu, \end{aligned} \quad (2.16)$$

with the following definitions: $iD_\mu^0 = i\partial_0 - Z_\mu eA^0$, $i\mathbf{D}_\mu = i\boldsymbol{\nabla} + Z_\mu e\mathbf{A}$ and $Z_\mu = 1$. The Wilson coefficients can be computed order by order in α . They read (where we have used the fact that $c_S^{(\mu)} = 2c_F^{(\mu)} - Z_\mu$, Ref. [67])

$$c_F^{(\mu)} = Z_\mu \left(1 + \frac{Z_\mu^2 \alpha}{2\pi} + \mathcal{O}(\alpha^2) \right), \quad (2.17)$$

$$c_S^{(\mu)} = Z_\mu \left(1 + \frac{Z_\mu^2 \alpha}{\pi} + \mathcal{O}(\alpha^2) \right). \quad (2.18)$$

Taking the values of the form factors for the muon-electron difference computed in Ref. [68] and those for the electron computed in Ref. [69], we can deduce the following expression for the $c_{D,\overline{\text{MS}}}^{(\mu)}(\nu)$ Wilson coefficient¹:

$$\begin{aligned} c_{D,\overline{\text{MS}}}^{(\mu)}(\nu) = & Z_\mu \left(1 + \frac{4\alpha}{3\pi} Z_\mu^2 \ln \left(\frac{m_\mu^2}{\nu^2} \right) \right. \\ & + \left(\frac{\alpha}{\pi} \right)^2 Z_\mu^2 \left\{ Z_\mu^2 \left[\frac{\pi^2}{6} \left(18 \ln(2) - \frac{40}{9} \right) - \frac{1523}{324} - \frac{9}{2} \zeta(3) \right] \right. \\ & + \frac{8}{9} \ln^2 \left(\frac{m_\mu}{m_e} \right) - \frac{40}{27} \ln \left(\frac{m_\mu}{m_e} \right) + \frac{85}{81} + \frac{4\pi^2}{27} + \mathcal{O} \left(\frac{m_e}{m_\mu} \right) \left. \right\} \\ & \left. + \mathcal{O}(\alpha^3) \right). \end{aligned} \quad (2.19)$$

¹In NRQED(μp), the electron has not been integrated out, therefore Eq. (2.19) is not the $c_D^{(\mu)}$ Wilson coefficient of NRQED(μp). It is the $c_D^{(\mu)}$ that will show up after lowering the muon energy cut-off below the electron mass in pNRQED. Still we choose to present it here as otherwise we would be forced to do an extra intermediate matching computation that is unnecessary to obtain the final result. Since we have integrated out the electron, note also that $\alpha = 1/137.14\dots$ in this equation, i.e. any running associated to the electron is written explicitly in Eq. (2.19).

Note that written in this way one can easily identify the $\mathcal{O}(\alpha_s^2)$ color structures C_F^2 and $C_F T_F n_l$ (for the case of n_l massive quarks): the second line in Eq. (2.19) would correspond to the C_F^2 term and the third line to the $C_F T_F n_l$ one. In this way we could obtain the analogous Wilson coefficient c_D in QCD.

For the Lamb shift computation we perform here we only need $c_D^{(\mu)}$ with $\mathcal{O}(\alpha^2 \times \ln)$ accuracy. We also include the finite piece for completeness but neglect $\mathcal{O}(m_e/m_\mu)$ terms. Note that analogous $\mathcal{O}(\alpha^2)$ terms (changing m_μ by m_p and either keeping m_e or changing it by m_μ) would exist for $c_D^{(p)}$ if computing the Wilson coefficient as if the proton were point-like at the m_p scale. Even if these effects are small, they should be taken into account for eventual comparisons with lattice where typically only the hadronic correction is computed.

For the proton sector we have the same Lagrangian as Eq. (2.4). The proton Wilson coefficients are hadronic, non-perturbative quantities. In some cases they can be directly related with low energy constants, for instance with the anomalous magnetic moment of the proton $\kappa_p = 1.792847356(23)$, Ref. [70]:

$$c_F^{(p)} = Z_p + \kappa_p = Z_p + \kappa_p^{\text{had}} + \frac{Z_p^3 \alpha}{2\pi} + \mathcal{O}(\alpha^2), \quad (2.20)$$

$$c_S^{(p)} = Z_p + 2\kappa_p = Z_p + 2\kappa_p^{\text{had}} + \frac{Z_p^3 \alpha}{\pi} + \mathcal{O}(\alpha^2). \quad (2.21)$$

Note that κ_p includes $\mathcal{O}(\alpha)$ effects. In principle, this is also so for κ_p^{had} , to which we have subtracted the proton-associated point-like contribution to the anomalous magnetic moment (note that the point-like result is a bad approximation for $c_F^{(p)}$, even though it gives the right order of magnitude). The case of $c_D^{(p)}$ is more complicated (a more detailed discussion can be found in Ref. [60]). It can be written in the following way in terms of the electromagnetic current form factors at zero momentum (where $F_1(0) = Z_p$):

$$c_D^{(p)} = Z_p + 2F_2(0) + 8F_1'(0) = Z_p + 8m_p^2 \left. \frac{dG_{p,E}(q^2)}{dq^2} \right|_{q^2=0}. \quad (2.22)$$

This object is infrared divergent, which makes it scale and scheme dependent. This is not a problem from the EFT point of view but makes the definition of the proton radius ambiguous. The standard practice is to make explicit the proton-associated point-like contributions to the computation. In practice this means that one uses the following definition for the proton radius

$$c_{D,\overline{\text{MS}}}^{(p)}(\nu) \equiv Z_p + \frac{4}{3} \frac{Z_p^3 \alpha}{\pi} \ln \left(\frac{m_p^2}{\nu^2} \right) + \frac{4}{3} r_p^2 m_p^2 + \mathcal{O}(\alpha^2). \quad (2.23)$$

In other words (up to $\mathcal{O}(\alpha^2)$ corrections)

$$c_{D,\overline{\text{MS}}}^{(p)}(m_p) - Z_p \equiv \frac{4}{3} r_p^2 m_p^2. \quad (2.24)$$

Note that r_p includes $\mathcal{O}(\alpha)$ terms in its definition. This should be kept in mind when comparing with lattice determinations. Note also that it is not natural to set $\nu = m_p$, or, in other words, to assume that the proton is point-like up to (and beyond) the scales of the proton mass; $\frac{4}{3} r_p^2 m_p^2 \simeq 21.3$, to be compared with "1" for a point-like particle. This illustrates that the point-like result does not even give the right order of magnitude of c_D .

The Lagrangian \mathcal{L}_{Ne} refers to the four-fermion operator made of nucleons and (relativistic) electrons. It corresponds to the Lagrangian in Eq. (2.9), for the electron case only. Note that this Lagrangian is only meaningful in the case of muonic hydrogen, as in the case of hydrogen the electron would not be relativistic. It will not contribute to the spectrum at $\mathcal{O}(m_r\alpha^5)$, therefore we will not consider it any further. For a detailed discussion see Ref. [59].

Finally, we consider the four-fermion operators ²:

$$\mathcal{L}_{N\mu}^{\text{NR}} = \frac{c_3}{m_p^2} N_p^\dagger N_p l_\mu^\dagger l_\mu - \frac{c_4}{m_p^2} N_p^\dagger \boldsymbol{\sigma} N_p l_\mu^\dagger \boldsymbol{\sigma} l_\mu. \quad (2.25)$$

Our main interest in the next two chapters will be the determination of c_3 and c_4 by performing the matching from HBET to NRQED. At $\mathcal{O}(\alpha^2)$, we symbolically represent this matching as in Fig. 2.1.

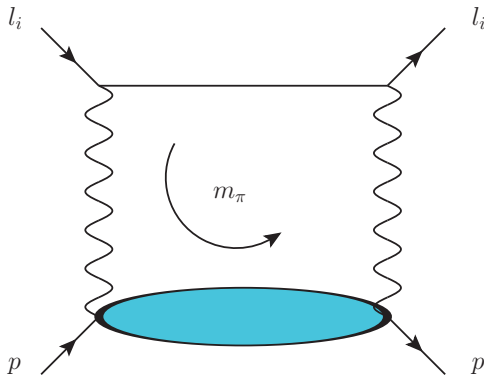


Figure 2.1: *Symbolic representation of the matching between HBET and NRQED for $c_3^{pl_i}$ and $c_4^{pl_i}$. The bubble represents the hadronic corrections.*

Again in this case it is common practice to single-out the proton-associated point-like contribution. Note that this assumes that one can treat the proton as point-like at energies of the order of the proton mass. We have already seen that this is a bad approximation for c_D and other Wilson coefficients. Nevertheless, we keep this procedure for the sake of comparison. Therefore,

$$c_3 \equiv c_{3,\text{R}} + c_{3,\text{point-like}} + c_3^{\text{had}} + \mathcal{O}(\alpha^3), \quad (2.26)$$

$$c_4 \equiv c_{4,\text{R}} + c_{4,\text{point-like}} + c_4^{\text{had}} + \mathcal{O}(\alpha^3). \quad (2.27)$$

Note that $c_{3/4,\text{R}}$ is suppressed by an extra factor m_μ/m_p , i.e. $c_{3/4,\text{R}} \sim \alpha^2 m_\mu/m_p$. This goes beyond the aimed accuracy of our calculation and so we neglect $c_{3/4,\text{R}}$. The point-like Wilson

²Note that we have renamed $c_{3/4}^{pl_\mu} \rightarrow c_{3/4}$ here and throughout the text for muonic hydrogen. Furthermore, in Ref. [59] $c_{3/4} \rightarrow c_{3/4,\text{NR}}^{pl_\mu}$. We eliminate some indices to lighten the notation.

coefficients read as follows ³:

$$c_{3,\text{point-like}} \equiv -\frac{m_p}{m_\mu} d_s(\nu) = \frac{m_p}{m_\mu} \frac{Z^2 \alpha^2}{m_\mu^2 - m_p^2} \left[m_\mu^2 \left(\ln \frac{m_p^2}{\nu^2} + \frac{1}{3} \right) - m_p^2 \left(\ln \frac{m_\mu^2}{\nu^2} + \frac{1}{3} \right) \right], \quad (2.30)$$

$$c_{4,\text{point-like}} \equiv -\frac{m_p}{m_\mu} d_v = -\frac{Z^2 \alpha^2 m_p^2}{m_\mu^2 - m_p^2} \ln \frac{m_\mu^2}{m_p^2}. \quad (2.31)$$

The expression of d_s should be understood in the $\overline{\text{MS}}$ scheme, d_v , on the other hand, is finite. The Wilson coefficient d_s was computed in Ref. [71] and d_v in Ref. [14].

c_3^{had} encodes the hadronic effects of pions and the Delta to $\mathcal{O}(\alpha^2)$ in the spin-independent four-fermion Wilson coefficient. At $\mathcal{O}(\alpha^2)$ it is generated by the two-photon exchange contribution. Since c_3^{had} depends linearly on the muon mass, it is dominated by the infrared dynamics and diverges linearly in the chiral limit. This produces an extra m_μ/m_π suppression with respect to its natural size, and allows us to compute the leading pure-chiral and Delta-related effects in a model independent way. The detailed matching computation between HBET and NRQED will be carried out in Chapter 3 (partial results can be found in Refs. [60, 61], and in Ref. [72] in the context of relativistic baryon effective theory). We quote here the result we get for ease of reference,

$$\begin{aligned} c_3^{\text{had}} &\sim \alpha^2 \frac{m_\mu}{m_\pi} \left[1 + \# \frac{m_\pi}{\Delta} + \dots \right] + \mathcal{O} \left(\alpha^2 \frac{m_\mu}{\Lambda_{\text{QCD}}} \right) \\ &= \alpha^2 \frac{m_\mu}{m_\pi} \begin{cases} 47.2(23.6) & (\pi), \\ 56.7(20.6) & (\pi + \Delta), \end{cases} \end{aligned} \quad (2.32)$$

where the upper and lower numbers refer to the matching computation with only pions, or with pions and the Delta particle, respectively. For comparison, the value $c_3^{\text{had}} = \alpha^2 \frac{m_\mu}{m_\pi} 54.4(3.3)$, which follows from the analysis in Ref. [73], was used in Ref. [20].

c_4^{had} encodes the hadronic effects of pions and the Delta to $\mathcal{O}(\alpha^2)$ in the spin-dependent four-fermion Wilson coefficients. As in the previous case, this coefficient diverges in the chiral limit. Nevertheless, it only does so logarithmically (unlike in the previous case, where the divergence was linear). Such computation can be found in Ref. [59]. Still it is possible to determine c_4^{had} from the analogous one of the proton-electron four-fermion operator determined in Ref. [59]. Again, we leave the details of the matching for Chapter 3, but quote here the result:

$$c_4^{\text{had}} \simeq -46\alpha^2. \quad (2.33)$$

³In this expression we have computed the loop with the proton being relativistic to follow common practice. Nevertheless, this assumes that one can consider the proton to be point-like at the scales of the proton mass. To stick to an standard EFT approach one should consider the proton to be NR. Then one would obtain

$$c_{3,\text{point-like}}^{p_i} = Z^2 \alpha^2 \frac{m_p}{m_{l_i}} \left(\ln \frac{m_{l_i}^2}{\nu^2} + \frac{1}{3} \right), \quad (2.28)$$

$$c_{4,\text{point-like}}^{p_i} = \left(1 - \frac{\kappa_p^2}{4} \right) Z^2 \alpha^2 \ln \frac{m_{l_i}^2}{\nu^2}. \quad (2.29)$$

The difference between both results is of the order of $c_{3/4,\text{R}}$, and gets absorbed into this coefficient (which we do not know anyhow). Therefore, the value of $c_{3/4}^{p_i}$, will be the same no matter the prescription used. In practice there could be some difference due to truncation, but always of the order of the error of our computation.

2.3 NRQED(e)

If we focus in the electron-proton sector, things go quite as in the previous section. After integrating out scales of $\mathcal{O}(m_\pi, \Delta)$, an EFT for electrons coupled to protons (and photons) appears. This effective theory has a cut-off $\nu \ll m_\pi$ and pions, Deltas and muons have been integrated out, but the electron is still relativistic. After integrating out scales of $\mathcal{O}(m_e)$ in the electron-proton sector, we still have an EFT for electrons coupled to protons and photons. Nevertheless, now the electrons are NR. The Lagrangian is quite similar to the one in Sec. 2.2 but without a light fermion and with the replacement $\mu \rightarrow e$. It reads

$$\mathcal{L}_{NRQED(e)} = \mathcal{L}_\gamma + \mathcal{L}_e^{(NR)} + \mathcal{L}_N + \mathcal{L}_{Ne}^{(NR)}. \quad (2.34)$$

We will perform the matching to this theory directly from HBET. At $\mathcal{O}(\alpha^2)$ this matching can be symbolically represented by the same figure as in the case of the muon, namely Fig. 2.1.

2.4 pNRQED

After integrating out scales of $\mathcal{O}(m_\mu \alpha \sim m_e)$, the resulting effective theory is pNRQED Ref. [15]. This EFT naturally gives a Schrödinger-like formulation of the bound-state problem but still keeping the quantum field theory nature of the interaction with ultrasoft photons, as well as keeping the information due to high energy modes (of a quantum field theory nature) in the Wilson coefficients of the theory. pNRQED has been applied to hydrogen Ref. [57], positronium Ref. [58] and muonic hydrogen Refs. [59, 60] providing with much of the information we need for our computation. In particular in the last reference the explicit form of the Lagrangian up to $\mathcal{O}(m_r \alpha^5)$ was presented. This is:

$$\begin{aligned} L_{\text{pNRQED}} = \int d^3\mathbf{x} d^3\mathbf{X} S^\dagger(\mathbf{x}, \mathbf{X}, t) & \left\{ i\partial_0 - \frac{\mathbf{p}^2}{2m_r} + \frac{\mathbf{p}^4}{8m_\mu^3} + \frac{\mathbf{p}^4}{8m_p^3} - \frac{\mathbf{P}^2}{2M} \right. \\ & \left. - V(\mathbf{x}, \mathbf{p}, \boldsymbol{\sigma}_1, \boldsymbol{\sigma}_2) + e \left(\frac{Z_\mu m_p + Z_p m_\mu}{m_p + m_\mu} \right) \mathbf{x} \cdot \mathbf{E}(\mathbf{X}, t) \right\} S(\mathbf{x}, \mathbf{X}, t) - \int d^3\mathbf{X} \frac{1}{4} F_{\mu\nu} F^{\mu\nu}, \end{aligned} \quad (2.35)$$

where $M = m_\mu + m_p$, $m_r = \frac{m_\mu m_p}{m_\mu + m_p}$, \mathbf{x} and \mathbf{X} , and \mathbf{p} and \mathbf{P} are the relative and center of mass coordinate and momentum respectively.

V can be written as an expansion in $1/m_\mu$, $1/m_p$, α , ... We will assume $1/r \sim m_e$ (which is realistic for the case at hand) and that $m_\mu \ll m_p$. We then organize the potential as an expansion in $1/m_\mu$:

$$V(\mathbf{x}, \mathbf{p}, \boldsymbol{\sigma}_1, \boldsymbol{\sigma}_2) = V^{(0)}(r) + V^{(1)}(r) + V^{(2)}(r) + \dots, \quad (2.36)$$

where

$$V^{(n)} \propto \frac{1}{m_\mu^n}. \quad (2.37)$$

We will also make the expansion in powers of α explicit. This means that

$$V^{(n,r)} \propto \frac{1}{m_\mu^n} \alpha^r. \quad (2.38)$$

$V^{(0,1)} = -\frac{Z\alpha}{r}$ has to be included exactly in the leading order Hamiltonian to yield the leading order solution to the bound-state problem:

$$h = \frac{\mathbf{p}^2}{2m_r} - \frac{Z\alpha}{r}. \quad (2.39)$$

Thus, the contribution to the energy of a given potential is

$$\langle V^{(n,r)} \rangle \sim m_\mu \alpha^{1+n+r}$$

up to large logarithms or potential suppression factors due to powers of $1/m_p$. Iterations of the potential are dealt with using standard quantum mechanics perturbation theory producing corrections such as:

$$\langle V^{(n,r)} \dots V^{(m,s)} \rangle \sim m_\mu \alpha^{1+n+r+(1+m+s-2)} \quad (2.40)$$

and alike. Therefore, in order to reach the desired $\mathcal{O}(m\alpha^5)$ accuracy, $V^{(0)}$ has to be computed up to $\mathcal{O}(\alpha^4)$, $V^{(1)}$ up to $\mathcal{O}(\alpha^3)$, $V^{(2)}$ up to $\mathcal{O}(\alpha^2)$ and $V^{(3)}$ up to $\mathcal{O}(\alpha)$.

Chapter 3

Matching HBET to NRQED

In this chapter we will perform in detail the computation of the NRQED(μp) coefficients c_3 and c_4 . We focus on their hadronic contributions which we find by matching to HBET an EFT where the muons and pions are still relativistic. These hadronic Wilson coefficients are related to the FVCT, which we compute in HBET by splitting it in two contributions: Born and polarizability. We start by computing the Born tensor, which was already known and which we can use to compute different Zemach momenta. Then we compute analytically the polarizability tensor. With both results together we compute both c_3 and c_4 . We compare these results to previous results in the literature.

3.1 The forward virtual Compton tensor

The electromagnetic current reads $J^\mu = \sum_i Q_i \bar{q}_i \gamma^\mu q_i$, where $i = u, d$ (we will not consider the strange quark in this work) and Q_i is the quark charge. The form factors (which we will understand as pure hadronic quantities, i.e. without electromagnetic corrections) are then defined by the following equation:

$$\langle p', s | J^\mu | p, s \rangle = \bar{u}(p') \left[F_1(q^2) \gamma^\mu + i F_2(q^2) \frac{\sigma^{\mu\nu} q_\nu}{2M_p} \right] u(p), \quad (3.1)$$

where $q = p' - p$ and F_1, F_2 are the Dirac and Pauli form factors, respectively. The states are normalized in the following (standard relativistic) way:

$$\langle p', \lambda' | p, \lambda \rangle = (2\pi)^3 2p^0 \delta^3(\mathbf{p}' - \mathbf{p}) \delta_{\lambda'\lambda}, \quad (3.2)$$

and

$$u(p, s) \bar{u}(p, s) = (\not{p} + M_p) \frac{1 + \gamma_5 \not{s}}{2}, \quad (3.3)$$

where s is an arbitrary spin four-vector obeying $s^2 = -1$ and $p \cdot s = 0$.

More suitable for a NR analysis are the Sachs form factors:

$$G_E(q^2) = F_1(q^2) + \frac{q^2}{4M_p^2} F_2(q^2), \quad G_M(q^2) = F_1(q^2) + F_2(q^2). \quad (3.4)$$

Nevertheless, the main object of interest of our work here is the FVCT,

$$T^{\mu\nu} = i \int d^4x e^{iq \cdot x} \langle p, s | T \{ J^\mu(x) J^\nu(0) \} | p, s \rangle, \quad (3.5)$$

which has the following structure ($\rho = q \cdot p / m_p \equiv v \cdot q$, although we will usually work in the rest frame where $\rho = q^0$):

$$\begin{aligned} T^{\mu\nu} = & \left(-g^{\mu\nu} + \frac{q^\mu q^\nu}{q^2} \right) S_1(\rho, q^2) + \frac{1}{m_p^2} \left(p^\mu - \frac{m_p \rho}{q^2} q^\mu \right) \left(p^\nu - \frac{m_p \rho}{q^2} q^\nu \right) S_2(\rho, q^2) \\ & - \frac{i}{m_p} \epsilon^{\mu\nu\rho\sigma} q_\rho s_\sigma A_1(\rho, q^2) - \frac{i}{m_p^3} \epsilon^{\mu\nu\rho\sigma} q_\rho ((m_p \rho) s_\sigma - (q \cdot s) p_\sigma) A_2(\rho, q^2) \equiv T_S^{\mu\nu} + T_A^{\mu\nu}. \end{aligned} \quad (3.6)$$

It depends on four scalar functions, which we call structure functions. We split the tensor into two pieces, namely $T_S^{\mu\nu}$ and $T_A^{\mu\nu}$. The tensor $T_S^{\mu\nu} = T_S^{\nu\mu}$ is symmetric and spin-independent and it corresponds to the first two terms of Eq. (3.6). The tensor $T_A^{\mu\nu} = -T_A^{\nu\mu}$ is the antisymmetric and spin-dependent and corresponds to the and the last two terms of Eq. (3.6). We have computed this tensor at $\mathcal{O}(p^3)$ in HBChPT. The diagrams that contribute are listed in Figs. 3.1, 3.2 and 3.3 (without closing the loop with the muon, i.e. without the muon line). Note that the tensor arises when the loop with the muon is not closed. The first figure refers to diagrams without Delta contributions (pure chiral), the second to the tree-level Delta contribution, and the last to one-loop chiral diagrams involving the Delta particle. Expressions in $D = 4 + 2\epsilon$ and four dimensions for each diagram can be found in Appendix D.2. Summing them up we can reconstruct the tensor structure of $T^{\mu\nu}$ (in other words, check gauge invariance). In principle, more diagrams, besides those drawn should be considered but they do not contribute to the structure functions at the order we aim in this work.

It is also common to split $T^{\mu\nu}$ into two components, which we label "Born" and "pol" (i.e. polarizability):

$$T^{\mu\nu} = T_{\text{Born}}^{\mu\nu} + T_{\text{pol}}^{\mu\nu}. \quad (3.7)$$

3.2 Computation of $T_{\text{Born}}^{\mu\nu}$

The Born term (also referred to as Zemach term in the literature) is defined as the contribution coming from the intermediate state being the proton (somewhat the elastic contribution). The associated structure functions can be written in terms of the form factors. They read (or, rather, they are defined as)

$$S_1^{\text{Born}}(\rho, q^2) \equiv -2F_1^2(q^2) - \frac{2(q^2)^2 G_M^2(q^2)}{(2m_p \rho)^2 - (q^2)^2}, \quad (3.8)$$

$$S_2^{\text{Born}}(\rho, q^2) \equiv 2 \frac{4m_p^2 q^2 F_1^2(q^2) - (q^2)^2 F_2^2(q^2)}{(2m_p \rho)^2 - (q^2)^2}, \quad (3.9)$$

$$A_1^{\text{Born}}(\rho, q^2) \equiv -F_2^2(q^2) + \frac{4m_p^2 q^2 F_1(q^2) G_M(q^2)}{(2m_p \rho)^2 - (q^2)^2}, \quad (3.10)$$

$$A_2^{\text{Born}}(\rho, q^2) \equiv \frac{4m_p^3 \rho F_2(q^2) G_M(q^2)}{(2m_p \rho)^2 - (q^2)^2}. \quad (3.11)$$

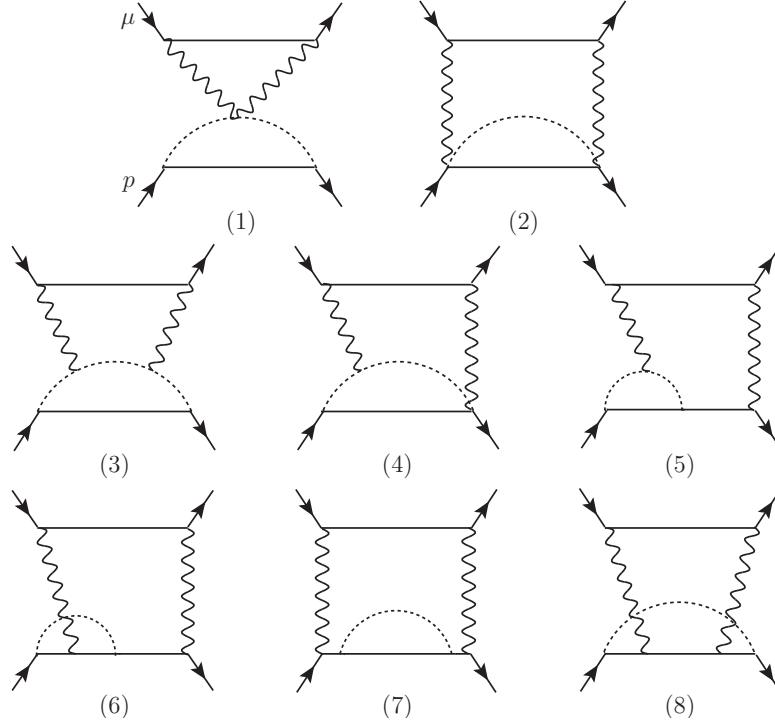


Figure 3.1: Two-loop TPE diagrams with an internal pion (dashed line) loop contributing to c_3 and c_4 . Crossed diagrams and those obtained through permutations are implicit.

From these expressions one could easily single out the point-like contributions. The remaining contributions, with the one-loop accuracy of our chiral computation, are encoded in the following expression (we split $G_{E,M}$ into pieces according to its chiral counting: $G_{E,M}^{(n)} \sim 1/m_p^n \sim 1/\Lambda_\chi^n$):

$$T_{\text{Born}}^{\mu\nu} = i\pi\delta(v \cdot q) \quad (3.12)$$

$$\times \text{Tr} \left[u\bar{u} \left(-4p_+ G_E^{(0)} G_E^{(2)} v^\mu v^\nu + \frac{2}{m_p} G_E^{(0)} G_M^{(1)} \left(v^\mu p_+ [s^\nu, s^{\rho'}] q_{\rho'} p_+ - v^\nu p_+ [s^\mu, s^{\rho'}] q_{\rho'} p_+ \right) \right) \right],$$

where $p_+ = \frac{1+v \cdot \gamma}{2}$. Note that $T_{\text{Born}}^{\mu\nu}$ is proportional to $\delta(v \cdot q)$ and $G_E^{(0)} = 1$. The expressions for $G_E^{(2)}$, $G_M^{(1)}$ were computed in Refs. [8, 74, 75]. They read:

$$G_E^{(2)}(q^2) = q^2 \frac{\langle r^2 \rangle}{6} + \frac{1}{(4\pi F_\pi)^2} \left(q^2 \left(\frac{1}{12} + \frac{g_A^2}{4} - \frac{2g_{\pi N\Delta}^2}{9} \right) \right. \\ \left. - \frac{4}{3} g_{\pi N\Delta}^2 \Delta \left(\frac{5}{9} \frac{q^2}{\sqrt{\Delta^2 - m_\pi^2}} + 4\sqrt{\Delta^2 - m_\pi^2} \right) \ln \mathcal{R}(m_\pi^2) \right) \\ + \frac{1}{(4\pi F_\pi)^2} \int_0^1 dx \left\{ \left[m_\pi^2 \left(\frac{1}{2} + \frac{3}{2} g_A^2 - \frac{4}{3} g_{\pi N\Delta}^2 \right) + \Delta^2 \frac{8}{3} g_{\pi N\Delta}^2 \right. \right. \\ \left. \left. + \left(\frac{1}{2} + \frac{5}{2} g_A^2 - \frac{20}{9} g_{\pi N\Delta}^2 \right) q^2 (-1+x)x \right] \ln \left(\frac{\tilde{m}^2}{m_\pi^2} \right) \right. \\ \left. + \frac{16}{3} g_{\pi N\Delta}^2 \frac{\Delta}{\sqrt{\Delta^2 - \tilde{m}^2}} \left(\frac{4}{3} q^2 x(1-x) + \Delta^2 - m_\pi^2 \right) \ln \mathcal{R}(\tilde{m}^2) \right\}, \quad (3.13)$$

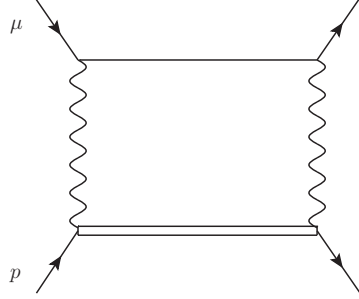


Figure 3.2: One-loop TPE diagram with an internal Delta particle (double line) contributing to c_3 and c_4 . Crossed diagram is implicit.

where (the coefficients \tilde{B}_1 and B_{10} are counterterms of the HBET Lagrangian from [75])

$$\begin{aligned} \langle r^2 \rangle &= -6 \frac{dG_E(-\mathbf{q}^2)}{d(\mathbf{q}^2)} \Big|_{\mathbf{q}^2=0} = \frac{3(\kappa_s + \kappa_v)}{4m_p^2} - \frac{1}{(4\pi F_\pi)^2} \left(\frac{1}{2} + 12\tilde{B}_1 + 6B_{10} + \frac{7}{2}g_A^2 - \frac{104}{27}g_{\pi N\Delta}^2 \right. \\ &\quad \left. - \frac{40}{9}g_{\pi N\Delta}^2 \frac{\Delta}{\sqrt{\Delta^2 - m_\pi^2}} \ln(\mathcal{R}(m_\pi^2)) + \left(1 + 5g_A^2 - \frac{40}{9}g_{\pi N\Delta}^2 \right) \ln\left(\frac{m_\pi}{\lambda}\right) \right), \end{aligned} \quad (3.14)$$

and

$$\begin{aligned} G_M^{(1)}(q^2) &= -g_A^2 \frac{4\pi m_p}{(4\pi F_\pi)^2} \int_0^1 dx \left\{ \sqrt{\tilde{m}^2} - m_\pi \right\} \\ &\quad + \frac{32}{9}g_{\pi N\Delta}^2 \frac{m_p \Delta}{(4\pi F_\pi)^2} \int_0^1 dx \left\{ \frac{1}{2} \ln\left(\frac{\tilde{m}^2}{4\Delta^2}\right) - \ln\left(\frac{m_\pi}{2\Delta}\right) \right. \\ &\quad \left. + \frac{\sqrt{\Delta^2 - \tilde{m}^2}}{\Delta} \ln \mathcal{R}(\tilde{m}^2) - \frac{\sqrt{\Delta^2 - m_\pi^2}}{\Delta} \ln \mathcal{R}(m_\pi^2) \right\}, \end{aligned} \quad (3.15)$$

with

$$\mathcal{R}(m^2) = \frac{\Delta}{m} + \sqrt{\frac{\Delta^2}{m^2} - 1}, \quad \tilde{m}^2 = m_\pi^2 - q^2 x(1-x). \quad (3.16)$$

For the spin-dependent case, the only contribution is the term proportional to $G_M^{(1)}$, which comes from the A_1^{Born} term (this is the only term that contributes to the Born piece of the hyperfine splitting). For the spin-independent case we only need $G_E^{(2)}$.

Eq. (3.12) comes from diagrams (5) and (6) in Figs. 3.1 and 3.3 after properly subtracting the subdivergences.

Following common practice we define the electromagnetic charge density as

$$\rho_e(r) \equiv \int \frac{d^3k}{(2\pi)^3} e^{i\mathbf{k}\cdot\mathbf{r}} G_E(-\mathbf{k}^2). \quad (3.17)$$

The inverse of its Fourier transform allows us to obtain the even powers of the moments of the charge distribution of the proton,

$$G_E(-\mathbf{k}^2) = \sum_{n=0}^{\infty} \frac{(-1)^n}{(2n+1)!} \mathbf{k}^{2n} \int_0^\infty dr (4\pi) r^{2n} \rho_e(r) = \sum_{n=0}^{\infty} \frac{(-1)^n}{(2n+1)!} \mathbf{k}^{2n} \langle r^{2n} \rangle. \quad (3.18)$$

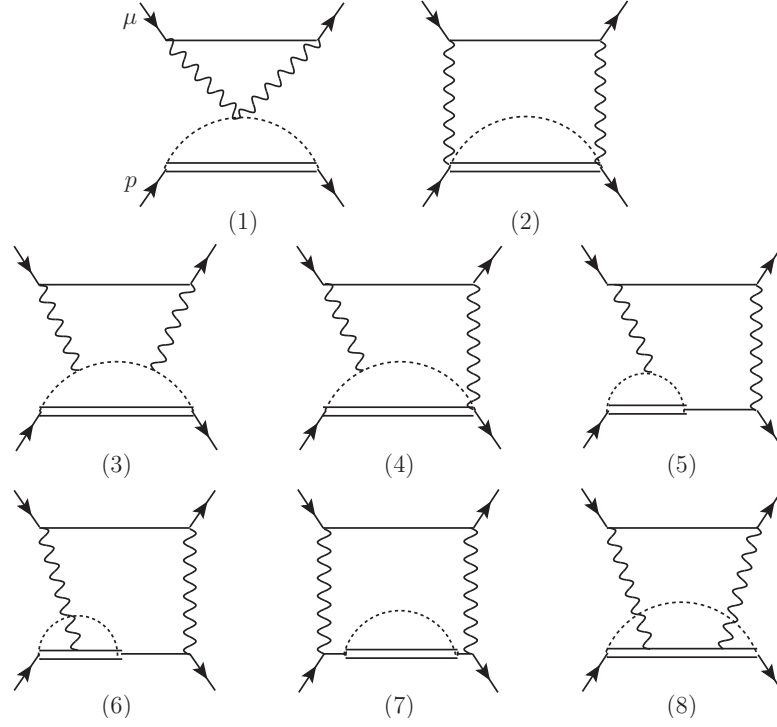


Figure 3.3: Two-loop TPE diagrams with an internal pion and Delta loop contributing to c_3 and c_4 . Crossed diagrams and those obtained through permutations are implicit.

By Taylor expanding Eq. (3.13) we obtain (for $k > 1$)

$$\begin{aligned}
 \langle r^{2k} \rangle &= \frac{m_\pi^{2-2k}}{32F_\pi^2\pi^2} \left(1 + g_A^2(3 + 2k)\right) k(k-1)\Gamma(k-1)^2 \tag{3.19} \\
 &+ \frac{m_\pi^{2-2k}g_{\pi N\Delta}^2}{36F_\pi^2\pi^2y^2} \left\{ k \left(\frac{(3+2k)}{1-k}y^2 - 6 \right) \Gamma(k)^2 + \ln(2) \frac{(-1)^{k+1}4^{1-k}(3+2k)(2k)!}{(2k-1)} y^{2k} \frac{\sqrt{1-y^2}}{(1-y^2)^k} \right\} \\
 &+ \frac{m_\pi^{2-2k}g_{\pi N\Delta}^2(k!)^2}{18F_\pi^2\pi^2} y^{-4+2k} (1-y^2)^{\frac{1}{2}-k} \left\{ -3(y^2-1) \binom{-1/2}{k-1} {}_3F_2 \left(1, 1, 1-k; 2, \frac{3}{2}-k; 1-\frac{1}{y^2} \right) \right. \\
 &- 4(y^2-1) \binom{-1/2}{k-2} {}_3F_2 \left(1, 1, 2-k; 2, \frac{5}{2}-k; 1-\frac{1}{y^2} \right) - y^2 \ln(y^2) \left(4 \binom{-1/2}{k-1} + 3 \binom{-1/2}{k} \right) \left. \right\} \\
 &- \frac{m_\pi^{2-2k}g_{\pi N\Delta}^2}{9F_\pi^2\pi^2} \frac{(y^2-1)^k}{y^2(1-y^2)^{\frac{1}{2}+k}} (k!)^2 \sum_{r=1}^{\infty} \frac{(2r)!}{2^{2r+1}r!(r!)^2} y^{2r} \\
 &\times \left[(3+y^2) \binom{r}{k} {}_2F_1 \left(-k, \frac{1}{2}, 1-k+r, \frac{y^2}{y^2-1} \right) \right. \\
 &\left. - 4y^2 \binom{1+r}{k} {}_2F_1 \left(-k, \frac{1}{2}, 2-k+r, \frac{y^2}{y^2-1} \right) \right],
 \end{aligned}$$

where $y \equiv \frac{m_\pi}{\Delta}$, and $\Gamma(n)$ is the Euler Γ function.

The odd powers are obtained (defined) through the relation:

$$\langle r^{2k+1} \rangle = \frac{\pi^{3/2} \Gamma[2+k]}{\Gamma[-1/2-k]} 2^{4+2k} \int \frac{d^3 q}{(2\pi)^3} \frac{1}{\mathbf{q}^{2(2+k)}} \left[G_E(-\mathbf{q}^2) - \sum_{n=0}^k \frac{\mathbf{q}^{2n}}{n!} \left(\frac{d}{d\mathbf{q}^2} \right)^n G_E(-\mathbf{q}^2) \Big|_{\mathbf{q}^2=0} \right]. \quad (3.20)$$

An analytic expression of this quantity is relegated to Eq. (3.55). Note that, by using dimensional regularization, we can eliminate all the terms proportional to integer even powers of \mathbf{q}^2 in this expression. For $k > 1$, this integral is dominated by the chiral result and can be approximated by

$$\langle r^{2k+1} \rangle \simeq \frac{\pi^{3/2} \Gamma[2+k]}{\Gamma[-1/2-k]} 2^{4+2k} \int \frac{d^{D-1} q}{(2\pi)^{D-1}} \frac{1}{\mathbf{q}^{2(2+k)}} G_E^{(2)}(-\mathbf{q}^2). \quad (3.21)$$

Finally, let us note that, by construction, both $T_{\text{Born}}^{\mu\nu}$ and $T_{\text{pol}}^{\mu\nu}$ comply with current conservation. The separation (definition) of the Born and polarizability terms is in general ambiguous, see, for instance, the discussion in Refs. [76,77]. In our case, as far as we give an explicit definition for $T_{\text{Born}}^{\mu\nu}$, this ambiguity disappears. In what follows we consider the computation of $T_{\text{pol}}^{\mu\nu}$.

3.3 Computation of $T_{\text{pol}}^{\mu\nu}$

We split each $S_i^{\text{pol}}/A_i^{\text{pol}}$ in the following way:

$$S_i^{\text{pol}} = S_{i,\pi}^{\text{pol}} + S_{i,\Delta}^{\text{pol}} + S_{i,\pi\Delta}^{\text{pol}}, \quad A_i^{\text{pol}} = A_{i,\pi}^{\text{pol}} + A_{i,\Delta}^{\text{pol}} + A_{i,\pi\Delta}^{\text{pol}}. \quad (3.22)$$

$S_{i,\pi}^{\text{pol}}$ and $A_{i,\pi}^{\text{pol}}$ encode the contributions only due to pions. They are produced by the diagrams listed in Fig. 3.1, which we compute using the Feynman rules in Appendix B.1. Summing them up we can reconstruct the tensor structure of $T^{\mu\nu}$. In D -dimensions the structure functions read

$$\begin{aligned} S_{1,\pi}^{\text{pol}}(q^2, q_0) &= -\frac{g_A^2}{F_\pi^2} m_p \left(m_\pi^2 J'_0(0, m_\pi^2) + J_0(0, m_\pi^2) - J_0(q_0, m_\pi^2) \right. \\ &\quad \left. + 4 \int_0^1 dx \left\{ (2x-1) J'_2(q_0 x, \tilde{m}^2) - (1-x) (\tilde{m}^2 + (q^2 - 2q_0^2)x^2) J''_2(q_0 x, \tilde{m}^2) \right\} \right) \\ &\quad + (q_0 \rightarrow -q_0), \end{aligned} \quad (3.23)$$

$$\begin{aligned} S_{2,\pi}^{\text{pol}}(q^2, q_0) &= \frac{g_A^2}{F_\pi^2} m_p m_\pi \frac{q^2}{q_0^2} \left(J_0(0, m_\pi^2) + m_\pi^2 J'_0(0, m_\pi^2) - J_0(q_0, m_\pi^2) \right. \\ &\quad \left. + \int_0^1 dx \left\{ q^2 \mathbf{q}^2 (1-2x)^2 (1-x)x^2 J''_0(q_0 x, \tilde{m}^2) + 2q^2 (2x-1)x J'_0(q_0 x, \tilde{m}^2) \right. \right. \\ &\quad \left. \left. - (1-x) \left(4(\tilde{m}^2 - 2q_0^2 x^2) + q^2 (4x^2 + (2x-1)(1+6x+d(2x-1))) \right) J''_2(q_0 x, \tilde{m}^2) \right. \right. \\ &\quad \left. \left. + 4(2x-1) J'_2(q_0 x, \tilde{m}^2) \right\} \right) + (q_0 \rightarrow -q_0), \end{aligned} \quad (3.24)$$

$$\begin{aligned} A_{1,\pi}^{\text{pol}}(q^2, q_0) &= -2 \frac{g_A^2}{F_\pi^2} m_p^2 \int_0^1 dx \left\{ \frac{1}{q_0} J'_2(q_0 x, \tilde{m}^2) + q_0 x^2 J'_0(q_0 x, \tilde{m}^2) + x \mathcal{D}_\pi(\tilde{m}^2) \right\} \\ &\quad + (q_0 \rightarrow -q_0), \end{aligned} \quad (3.25)$$

$$A_{2,\pi}^{\text{pol}}(q^2, q_0) = \frac{g_A^2}{F_\pi^2} m_p^3 \int_0^1 dx x(2x-1) J'_0(q_0 x, \tilde{m}^2) - (q_0 \rightarrow -q_0), \quad (3.26)$$

where the loop functions J_i have been defined in D -dimensions in Appendix C.1.

These structure functions reduce to the following expressions in $D = 4$:

$$S_{1,\pi}^{\text{pol}}(q^2, q_0) = \frac{1}{\pi} \left(\frac{g_A}{2F_\pi} \right)^2 m_p m_\pi \left\{ \frac{3}{2} + \frac{m_\pi^2}{\mathbf{q}^2} - \left(1 + \frac{m_\pi^2}{\mathbf{q}^2} \right) \sqrt{1-z} - \frac{1}{2} \sqrt{\frac{m_\pi^2}{\mathbf{q}^2}} \left(2 + \frac{q^2}{\mathbf{q}^2} \right) \mathcal{I}_1(m_\pi^2, q^0, q^2) \right\}, \quad (3.27)$$

$$S_{2,\pi}^{\text{pol}}(q^2, q_0) = \frac{1}{\pi} \left(\frac{g_A}{2F_\pi} \right)^2 m_p m_\pi \frac{q^2}{\mathbf{q}^2} \left\{ - \left(\frac{3}{2} + \left(\frac{1}{2} + \frac{m_\pi^2}{q^2} + \frac{m_\pi^2}{(q^0)^2} \right) \frac{q^2}{\mathbf{q}^2} \right) - \frac{(q^0)^2 q^2}{4m_\pi^2 \mathbf{q}^2 + (q^2)^2} \left(\frac{m_\pi^2}{\mathbf{q}^2} - \frac{q^2}{2\mathbf{q}^2} \right) + \frac{m_\pi^2}{\mathbf{q}^2} \left(2 - \frac{\mathbf{q}^2}{(q^0)^2} (1-z) + \frac{q^2 (q^0)^2}{4m_\pi^2 \mathbf{q}^2 + (q^2)^2} \right) \sqrt{1-z} + \frac{1}{2} \sqrt{\frac{m_\pi^2}{\mathbf{q}^2}} \left(2 + 3 \frac{q^2}{\mathbf{q}^2} + \frac{q^2}{m_\pi^2} \right) \mathcal{I}_1(m_\pi^2, q^0, q^2) \right\}, \quad (3.28)$$

$$A_{1,\pi}^{\text{pol}}(q^2, q_0) = -\frac{1}{2\pi^2} \frac{g_A^2}{F_\pi^2} m_p^2 \int_0^1 dx \frac{\sqrt{\tilde{m}^2}}{q_0} \left(\frac{q_0 x}{\sqrt{\tilde{m}^2}} - \left(1 - \frac{q_0^2 x^2}{\tilde{m}^2} \right)^{-1/2} \sin^{-1} \left(\frac{q_0 x}{\sqrt{\tilde{m}^2}} \right) \right), \quad (3.29)$$

$$A_{2,\pi}^{\text{pol}}(q^2, q_0) = -\frac{1}{4\pi^2} \frac{g_A^2}{F_\pi^2} m_p^3 \int_0^1 dx \frac{x(2x-1)}{\sqrt{\tilde{m}^2}} \left(1 - \frac{q_0^2 x^2}{\tilde{m}^2} \right)^{-1/2} \sin^{-1} \left(\frac{q_0 x}{\sqrt{\tilde{m}^2}} \right), \quad (3.30)$$

where

$$z = \frac{q_0^2}{m_\pi^2}, \quad (3.31)$$

and

$$\begin{aligned} \mathcal{I}_1(m_\pi^2, q^0, q^2) &= \int_0^1 dx \frac{1}{\sqrt{\frac{m_\pi^2}{\mathbf{q}^2} - \frac{q^2}{\mathbf{q}^2} x - x^2}} \\ &= -\arctan \left(\frac{q^2}{2m_\pi |\mathbf{q}|} \right) + \arctan \left(\frac{2\mathbf{q}^2 + q^2}{2|\mathbf{q}| \sqrt{m_\pi^2 - q_0^2}} \right) \\ &= i \ln \left(\frac{2im_\pi |\mathbf{q}| - q^2}{2i|\mathbf{q}| \sqrt{m_\pi^2 - q_0^2} + q^2 - 2q_0^2} \right). \end{aligned} \quad (3.32)$$

Note that in order to find a finite result we have subtracted the usual $\overline{\text{MS}}$ factor as defined in Eq. (C.8). For $D = 4$ we can compare with previous results in the literature. $S_{1,\pi}^{\text{pol}}$ and $S_{2,\pi}^{\text{pol}}$ were originally computed in Ref. [61]. We agree with those results, which were obtained with different methods, either by dispersion relations or through a diagrammatic computation assuming gauge invariance. In the case of real photons (for $q^2 = 0$ in the Coulomb gauge (CG)) we recover the results of Ref. [8]. $S_{1,\pi}^{\text{pol}}$ has also been checked in the limit $q_0 \rightarrow 0$ in Ref. [73], and $S_{1/2,\pi}^{\text{pol}}$ for all q_0 and q^2 in Ref. [72].

The spin-dependent structure functions, $A_{1,\pi}^{\text{pol}}$ and $A_{2,\pi}^{\text{pol}}$, agree with the ones given in Eqs. (30) and (34) of Ref. [63], up to a normalization factor. They follow from summing up all the contributions of the diagrams in Fig. 3.1 that have an antisymmetric contribution, i.e. diagrams (2), (4) and (5).

We now move to contributions involving Delta particles. We first consider tree-level Delta mediated contributions. The corresponding diagram is pictured in Fig. 3.2, and the associated contributions read:

$$S_{1,\Delta}^{\text{pol}}(q^2, q_0) = -\frac{4}{9} \frac{b_{1F}^2}{m_p^2} m_p \frac{\Delta \mathbf{q}^2}{q_0^2 - \Delta^2 + i\eta}, \quad (3.33)$$

$$S_{2,\Delta}^{\text{pol}}(q^2, q_0) = \frac{4}{9} \frac{b_{1F}^2}{m_p^2} m_p \frac{\Delta q^2}{q_0^2 - \Delta^2 + i\eta}, \quad (3.34)$$

$$A_{1,\Delta}^{\text{pol}}(q^2, q_0) = \frac{4b_{1F}^2}{9m_p^2} m_p^2 \frac{q_0^2}{q_0^2 - \Delta^2 + i\eta}, \quad (3.35)$$

$$A_{2,\Delta}^{\text{pol}}(q^2, q_0) = -\frac{4b_{1F}^2}{9m_p^2} m_p^3 \frac{q_0}{q_0^2 - \Delta^2 + i\eta}. \quad (3.36)$$

We have checked that Eq. (3.33) agrees with Ref. [61] and, in the limit $q_0 \rightarrow 0$, with the leading order expression of Ref. [73] up to normalization. Eq. (3.34) differs from the expression obtained in Ref. [61] using dispersion relations by a local term, i.e. the expression in Ref. [61] is only valid in a logarithmic approach (taking the limit $m_l \ll \Delta$). For the spin-dependent terms we are in agreement with Ref. [63], as we would expect since they are computed in the same way.

The last set of diagrams that we consider are those with one internal chiral loop and virtual Delta particles. They are drawn in Fig. 3.3 producing the following D -dimensional expressions for the structure functions:

$$\begin{aligned} S_{1,\pi\Delta}^{\text{pol}}(q^2, q_0) &= -\frac{32}{3} \frac{D-2}{D-1} m_p \left(\frac{g_{\pi N\Delta}}{F_\pi} \right)^2 \left(\frac{1}{4} (D-1) J_2'(-\Delta, m_\pi^2) - \frac{1}{4} J_0(q_0 - \Delta, m_\pi^2) \right. \\ &\quad - \int_0^1 dx \left\{ (1-x) \left(-\Delta^2 + \tilde{m}^2 + q^2 x^2 + 2q_0 x(\Delta - q_0 x) \right) J_2''(q_0 x - \Delta, \tilde{m}^2) \right. \\ &\quad \left. \left. + \frac{\Delta}{D} (1-x) \left(\tilde{m}^2 \mathcal{D}_\pi''(\tilde{m}^2) + 2\mathcal{D}_\pi'(\tilde{m}^2) \right) + (2x-1) J_2'(q_0 x - \Delta, \tilde{m}^2) \right\} \right) \\ &\quad + (q_0 \rightarrow -q_0), \end{aligned} \quad (3.37)$$

$$\begin{aligned} S_{2,\pi\Delta}^{\text{pol}}(q^2, q_0) &= -\frac{8}{3} \frac{D-2}{D-1} m_p \frac{q^2}{q_0^2} \left(\frac{g_{\pi N\Delta}}{F_\pi} \right)^2 \left(J_0(q_0 - \Delta, m_\pi^2) - (D-1) J_2'(-\Delta, m_\pi^2) \right. \\ &\quad + \int_0^1 dx \left\{ (1-x) J_2''(q_0 x - \Delta, \tilde{m}^2) \left(q^2 \left(D(1-2x)^2 - 4x(1-4x) - 1 \right) \right. \right. \\ &\quad \left. \left. + 4\tilde{m}^2 - 4 \left(\Delta^2 + 2q_0 x(q_0 x - \Delta) \right) \right) + 2q^2 x(1-2x) J_0'(q_0 x - \Delta, \tilde{m}^2) \right. \\ &\quad \left. + q^2 \mathbf{q}^2 (1-x)x^2(2x-1)(1-2x) J_0''(q_0 x - \Delta, \tilde{m}^2) \right. \\ &\quad \left. - 4(2x-1) J_2'(q_0 x - \Delta, \tilde{m}^2) + \frac{4\Delta}{D} (1-x) \left(\tilde{m}^2 \mathcal{D}_\pi''(\tilde{m}^2) + 2\mathcal{D}_\pi'(\tilde{m}^2) \right) \right\} \right) \\ &\quad + (q_0 \rightarrow -q_0), \end{aligned} \quad (3.38)$$

$$A_{1,\pi\Delta}^{\text{pol}}(q^2, q_0) = -\left(\frac{g_{\pi N\Delta}}{F_\pi} \right)^2 m_p^2 \frac{16}{3(D-1)} \int_0^1 dx \left\{ x(\Delta + q_0 x) J_0'(-q_0 x - \Delta, \tilde{m}^2) \right.$$

$$- x \mathcal{D}'_{\pi}(\tilde{m}^2) \frac{1}{q_0} J'_2(-q_0 x - \Delta, \tilde{m}^2) \Big\} + (q_0 \rightarrow -q_0), \quad (3.39)$$

$$A_{2,\pi\Delta}^{\text{pol}}(q^2, q_0) = - \left(\frac{g_{\pi N\Delta}}{F_{\pi}} \right)^2 m_p^3 \frac{8}{3(D-1)} \int_0^1 dx x(1-2x) J'_0(-q_0 x - \Delta, \tilde{m}^2) - (q_0 \rightarrow -q_0). \quad (3.40)$$

The results for $D = 4$ dimensions are:

$$S_{1,\pi\Delta}^{\text{pol}}(q^2, q_0) = - \frac{4}{9\pi^2} \frac{g_{\pi N\Delta}^2}{F_{\pi}^2} m_p m_{\pi} \left[3\mathcal{Z}\left(\frac{\Delta}{m_{\pi}}\right) - \mathcal{Z}\left(\frac{\Delta - q_0}{m_{\pi}}\right) - \mathcal{Z}\left(\frac{\Delta + q_0}{m_{\pi}}\right) + \int_0^1 dx \left\{ \frac{\Delta}{m_{\pi}} (5x - 3) \ln\left(\frac{\tilde{m}^2}{m_{\pi}^2}\right) + \sqrt{\frac{\tilde{m}^2}{m_{\pi}^2}} \left(\left(5x - 3 + \frac{\mathbf{q}^2(1-x)x^2}{\tilde{m}^2 - (\Delta + q_0 x)^2} \right) \mathcal{Z}\left(\frac{\Delta + q_0 x}{\sqrt{\tilde{m}^2}}\right) + \left(5x - 3 + \frac{\mathbf{q}^2(1-x)x^2}{\tilde{m}^2 - (\Delta - q_0 x)^2} \right) \mathcal{Z}\left(\frac{\Delta - q_0 x}{\sqrt{\tilde{m}^2}}\right) \right) \right] \right], \quad (3.41)$$

$$S_{2,\pi\Delta}^{\text{pol}}(q^2, q_0) = - \frac{4}{9\pi^2} \frac{g_{\pi N\Delta}^2}{F_{\pi}^2} m_p m_{\pi} \frac{q^2}{q_0^2} \left[-3\mathcal{Z}\left(\frac{\Delta}{m_{\pi}}\right) + \mathcal{Z}\left(\frac{\Delta - q_0}{m_{\pi}}\right) + \mathcal{Z}\left(\frac{\Delta + q_0}{m_{\pi}}\right) + \int_0^1 dx \left\{ \frac{\Delta}{m_{\pi}} (3x - 5) \ln\left(\frac{\tilde{m}^2}{m_{\pi}^2}\right) + \frac{1}{4} \sqrt{\frac{\tilde{m}^2}{m_{\pi}^2}} \mathcal{Z}\left(\frac{\Delta + q_0 x}{\sqrt{\tilde{m}^2}}\right) \left(4(3 - 5x) + \frac{(3 - 7x)(1 - 2x)^2 q^2 - 4\mathbf{q}^2 x^2}{\tilde{m}^2 - (\Delta + q_0 x)^2} + \frac{q^2 \mathbf{q}^2 (1 - x)x^2 (1 - 2x)^2}{(\tilde{m}^2 - (\Delta + q_0 x)^2)^2} \right) + \frac{1}{4} \sqrt{\frac{\tilde{m}^2}{m_{\pi}^2}} \mathcal{Z}\left(\frac{\Delta - q_0 x}{\sqrt{\tilde{m}^2}}\right) \left(4(3 - 5x) + \frac{(3 - 7x)(1 - 2x)^2 q^2 - 4\mathbf{q}^2 x^2}{\tilde{m}^2 - (\Delta - q_0 x)^2} + \frac{q^2 \mathbf{q}^2 (1 - x)x^2 (1 - 2x)^2}{(\tilde{m}^2 - (\Delta - q_0 x)^2)^2} \right) + \frac{q^2 \mathbf{q}^2}{4\tilde{m}^2} (1 - 2x)^2 (1 - x)x^2 \right. \right. \\ \left. \left. \left(\frac{\Delta + q_0 x}{m_{\pi}(\tilde{m}^2 - (\Delta + q_0 x)^2)} + \frac{\Delta - q_0 x}{m_{\pi}(\tilde{m}^2 - (\Delta - q_0 x)^2)} \right) \right\} \right], \quad (3.42)$$

$$A_{1,\pi\Delta}^{\text{pol}}(q^2, q_0) = \frac{2}{9\pi^2} \frac{g_{\pi N\Delta}^2}{F_{\pi}^2} m_p^2 \left(1 - \int_0^1 dx \sqrt{\tilde{m}^2} \left\{ \left(-\frac{1}{q_0} + \frac{x(\Delta - q_0 x)}{\tilde{m}^2 - (\Delta - q_0 x)^2} \right) \mathcal{Z}\left(\frac{\Delta - q_0 x}{\sqrt{\tilde{m}^2}}\right) + \left(\frac{1}{q_0} + \frac{x(\Delta + q_0 x)}{\tilde{m}^2 - (\Delta + q_0 x)^2} \right) \mathcal{Z}\left(\frac{\Delta + q_0 x}{\sqrt{\tilde{m}^2}}\right) \right\} \right), \quad (3.43)$$

$$A_{2,\pi\Delta}^{\text{pol}}(q^2, q_0) = \frac{1}{9\pi^2} \frac{g_{\pi N\Delta}^2}{F_{\pi}^2} m_p^3 \int_0^1 dx x(1-2x) \sqrt{\tilde{m}^2} \left\{ \frac{\mathcal{Z}\left(\frac{\Delta - q_0 x}{\sqrt{\tilde{m}^2}}\right)}{\tilde{m}^2 - (\Delta - q_0 x)^2} - \frac{\mathcal{Z}\left(\frac{\Delta + q_0 x}{\sqrt{\tilde{m}^2}}\right)}{\tilde{m}^2 - (\Delta + q_0 x)^2} \right\}, \quad (3.44)$$

where we have defined \mathcal{Z} as

$$\mathcal{Z}(x) \equiv \sqrt{x^2 - 1} \ln(\sqrt{x^2 - 1} + x). \quad (3.45)$$

The $D = 4$ expressions for $S_{1,\pi\Delta}^{\text{pol}}$ and $S_{2,\pi\Delta}^{\text{pol}}$ agree with Eqs. (51) in Ref. [65] for the case of real photons, i.e. $q^2 = 0$ and in the CG.

Summing up all the contributions of the diagrams in Fig. 3.3 that have an antisymmetric contribution, i.e. diagrams (2), (4) and (5), we get the spin-dependent part that agrees with Eqs. (33) and (36) in Ref. [63], up to a normalization factor.

In all expressions we use principal value prescriptions, the Dirac delta contributions associated to the propagators have gone into the Born term. Nevertheless, from the point of view of the effective theory this splitting between the polarizability and Born term is quite arbitrary.

3.4 Spin-independent matching: c_3

The matching between HBET and NRQED can be performed in a generic expansion in $1/m_p$, $1/m_\mu$ and α . We have two sorts of loops: chiral and electromagnetic. The former are always associated to $1/(4\pi F_0)^2$ factors, whereas the latter are always suppressed by α factors. Any scale left to get the dimensions right scales with m_π or Δ . In our case we are only concerned with obtaining the matching coefficients of the lepton-baryon operators of NRQCD with $\mathcal{O}\left(\alpha^2 \times \left(\frac{m_{l_i}}{m_\pi}, \frac{m_{l_i}}{\Delta}\right)\right)$ accuracy.

At $\mathcal{O}(\alpha^2)$, the contribution to $c_3^{pl_i}$ (see Fig. 2.1) from matching HBET to NRQED can be written in a compact way in terms of the structure functions of the FVCT. It reads (Ref. [78])

$$c_3^{pl_i} = -e^4 m_p m_{l_i} \int \frac{d^4 k_E}{(2\pi)^4} \frac{1}{k_E^4} \frac{1}{k_E^4 + 4m_\mu^2 k_{0,E}^2} \times \left\{ (3k_{0,E}^2 + \mathbf{k}^2) S_1(ik_{0,E}, -k_E^2) - \mathbf{k}^2 S_2(ik_{0,E}, -k_E^2) \right\} + \mathcal{O}(\alpha^3). \quad (3.46)$$

This result keeps the complete dependence on the lepton mass m_{l_i} and so it is valid both for NRQED(μp) and NRQED(ep). In what follows, we will assume that we are doing the matching to NRQED(μp). Therefore, we keep the whole dependence on m_μ/m_π since they are similar in size. In order to recover the coefficient $c_3^{pl_i}$ from our computation one would just replace $m_\mu \rightarrow m_{l_i}$. The NRQED(ep) case can then be derived by expanding m_e versus m_π . This contribution is usually organized as in Eq. (2.26), and so we do. From now on we will focus in obtaining the hadronic part of the coefficient, which we split, as is customary, in:

$$c_3^{\text{had}} = c_{3,\text{Born}} + c_{3,\text{pol}}. \quad (3.47)$$

We compute each of these terms separately.

3.4.1 $c_{3,\text{Born}}$ and Zemach moments

The first term in Eq. (3.47) is generated by the spin-independent Born contribution to $T^{\mu\nu}$ in Eq. (3.12). We symbolically picture it for a given lepton in Fig. 3.4. At leading order in the NR expansion it reads¹

$$c_{3,\text{Born}} = 4(4\pi\alpha)^2 m_p^2 m_\mu \int \frac{d^{D-1}q}{(2\pi)^{D-1}} \frac{1}{q^6} G_E^{(0)} G_E^{(2)}(-\mathbf{q}^2). \quad (3.48)$$

Note again that the exact dependence on m_μ is kept at leading order in the NR expansion and so this result holds for NRQED($l_i p$). The linear dependence in the lepton mass makes this

¹In Ref. [60] this object is named $c_{3,\text{Zemach}}^{pl_i}$.

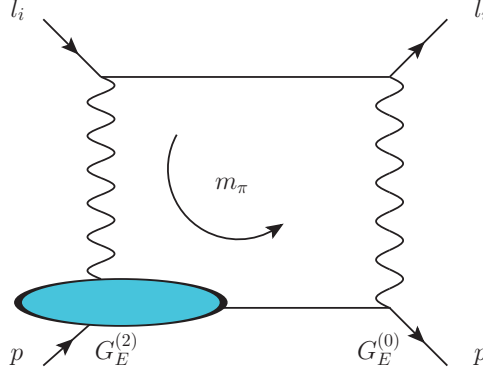


Figure 3.4: *Symbolic representation (plus permutations) of the Zemach correction in Eq. (3.48).*

contribution much smaller for the case of hydrogen. $G_E^{(0)} = 1$. We take the expression for $G_E^{(2)}$ from Eq. (3.13). The use of EFTs and dimensional regularization is a strong simplification, which we have already used when writing Eq. (3.48). This guarantees that only low energy modes contribute to the integral, and that we only need the non-analytic behavior of $G_E^{(2)}$ in q^2 around m_π and Δ . In other words, even though some point-like contributions are still encoded in $G_E^{(2)}$, they do not contribute to the integral. The analytical behavior in q^2 produces scaleless integrals, which are zero in dimensional regularization. This is a reflection of the factorization of the different scales. Therefore, we do not need to introduce the point-like interactions to regulate the infrared divergences of the integrals at zero momentum, as it is done if trying to compute this object directly from the experimental data. We will come back to this issue when we discuss the Zemach moments.

The computation of $c_{3,\text{Born}}$ was made in Ref. [60]. Here we give a simplified expression:

$$c_{3,\text{Born}} = 2(\pi\alpha)^2 \left(\frac{m_p}{4\pi F_0}\right)^2 \frac{m_\mu}{m_\pi} \left\{ \frac{3}{4}g_A^2 + \frac{1}{8} + \frac{32}{9}\pi g_{\pi N\Delta}^2 \frac{m_\pi^2}{\Delta^2 - m_\pi^2} \right. \\ \left. + \frac{2}{\pi}g_{\pi N\Delta}^2 \frac{m_\pi}{\Delta} \sum_{r=0}^{\infty} \frac{(-1)^r \Gamma(-3/2)}{\Gamma(r+1)\Gamma(-3/2-r)} \left\{ B_{6+2r} - \frac{2(r+2)}{3+2r} B_{4+2r} \right\} \left(\frac{m_\pi}{\Delta}\right)^{2r} \right\}, \quad (3.49)$$

where the first line is due to scales of $\mathcal{O}(m_\pi)$ and the terms proportional to B_n are due to scales of $\mathcal{O}(\Delta)$, where (this corrects Eq. (61) of Ref. [60])

$$B_n \equiv \int_0^\infty dt \frac{t^{2-n}}{1-t^2} \times \begin{cases} \sqrt{1-t^2} \ln \left[\frac{1}{t} + \sqrt{\frac{1}{t^2} - 1} \right] & \text{if } t < 1 \\ -\sqrt{t^2-1} \arccos\left[\frac{1}{t}\right] & \text{if } t > 1 \end{cases} \quad (3.50) \\ = -\frac{\sqrt{\pi} \left(S_1\left(\frac{1}{2} - \frac{n}{2}\right) - S_1\left(1 - \frac{n}{2}\right) \right) \Gamma\left(\frac{3}{2} - \frac{n}{2}\right)}{4\Gamma\left(2 - \frac{n}{2}\right)} \\ + 2^{1-n} \pi \frac{\Gamma(n-2)}{\Gamma^2\left(\frac{n}{2}\right)} {}_3F_2\left(\frac{1}{2}, \frac{n-2}{2}, \frac{n-1}{2}; \frac{n}{2}, \frac{n}{2}; 1\right) \\ + \frac{2^{\frac{5}{2}-\frac{n}{2}} {}_3F_2\left(\frac{3}{2} - \frac{n}{2}, \frac{3}{2} - \frac{n}{2}, \frac{n}{2} + \frac{1}{2}; \frac{5}{2} - \frac{n}{2}, \frac{5}{2} - \frac{n}{2}; \frac{1}{2}\right)}{(n-3)^2}$$

$$\begin{aligned}
 & - \frac{2^{\frac{3}{2}-\frac{n}{2}} {}_3F_2\left(\frac{5}{2}-\frac{n}{2}, \frac{5}{2}-\frac{n}{2}, \frac{n}{2}+\frac{1}{2}; \frac{7}{2}-\frac{n}{2}, \frac{7}{2}-\frac{n}{2}; \frac{1}{2}\right)}{(n-5)^2} \\
 & + \frac{\pi^{3/2} \sec\left(\frac{\pi n}{2}\right) \left((n-2)S_1(1-n) + (2-n)S_1\left(\frac{1}{2}-\frac{n}{2}\right) + n(-\ln(2)) - 1 + \ln(4)\right)}{(n-2)\Gamma\left(2-\frac{n}{2}\right)\Gamma\left(\frac{n-1}{2}\right)},
 \end{aligned}$$

where $S_1(n)$ is the n harmonic number as defined in Appendix A.

Eq. (3.49) encapsulates all the non-analytic dependence in the light quark masses and in the splitting between the nucleon and the Delta mass (proportional to powers of $1/N_c$ in the large N_c limit) of $c_{3,\text{Born}}$. This expression is the leading contribution to the Zemach term in the chiral counting (supplemented with a large N_c counting). This is a model independent result. Other contributions to the Zemach term are suppressed in the chiral counting.

$c_{3,\text{Born}}$ can be related with (one of) the Zemach moments:

$$\langle r^m \rangle_{(2)} \equiv \int d^3r r^m \int d^3z \rho_e(|\mathbf{z}-\mathbf{r}|) \rho_e(z). \quad (3.51)$$

The Zemach moments can be determined in a similar way as the moments of the charge distribution of the proton. For even powers we have the relation²

$$G_E^2(-\mathbf{k}^2) = \sum_{n=0}^{\infty} \frac{(-1)^n}{(2n+1)!} \mathbf{k}^{2n} \langle r^{2n} \rangle_{(2)}. \quad (3.52)$$

The odd powers are obtained (defined) through the relation:

$$\langle r^{2k+1} \rangle_{(2)} = \frac{\pi^{3/2} \Gamma(2+k)}{\Gamma(-1/2-k)} 2^{4+2k} \int \frac{d^3q}{(2\pi)^3} \frac{1}{\mathbf{q}^{2(2+k)}} \left[G_E^2(-\mathbf{q}^2) - \sum_{n=0}^k \frac{\mathbf{q}^{2n}}{n!} \left(\frac{d}{d\mathbf{q}^2} \right)^n G_E^2(-\mathbf{q}^2) \Big|_{\mathbf{q}^2=0} \right]. \quad (3.53)$$

Again, using dimensional regularization, we can eliminate all the terms proportional to integer even powers of \mathbf{q}^2 in this expression. For $k \geq 1$ this integral is dominated by the chiral result and can be approximated by

$$\langle r^{2k+1} \rangle_{(2)} \simeq 2 \times \frac{\pi^{3/2} \Gamma(2+k)}{\Gamma(-1/2-k)} 2^{4+2k} \int \frac{d^{D-1}q}{(2\pi)^{D-1}} \frac{1}{\mathbf{q}^{2(2+k)}} G_E^{(2)}(-\mathbf{q}^2) \simeq 2 \langle r^{2k+1} \rangle. \quad (3.54)$$

It is possible to get an analytic result for these integrals. We obtain ($y \equiv \frac{m\pi}{\Lambda}$)

$$\begin{aligned}
 \langle r^{2k+1} \rangle_{(2)} & \simeq 2 \langle r^{2k+1} \rangle \simeq 2\Gamma(3/2+k) \frac{m_\pi^{1-2k}}{(4\pi F_0)^2} \left\{ \Gamma(3/2+k) \frac{2+4g_A^2(2+k)}{3+4(k^2-1)} \right. \\
 & + \frac{4}{9} g_{\pi N\Delta}^2 \frac{\pi(k+2)(-1)^{k+1}}{\Gamma[5/2-k]} y^2 {}_2F_1\left(\frac{3}{2}, 1; \frac{5}{2}-k; y^2\right) \\
 & \left. + \frac{32}{3} g_{\pi N\Delta}^2 y^{2k-1} \sum_{r=0}^{\infty} \frac{y^{2r}}{r!} \frac{(-1)^r}{\Gamma(-1/2-k-r)} \left[B_{2k+2r+4} - \frac{r+\frac{4}{3}k+\frac{2}{3}}{\frac{1}{2}+k+r} B_{2k+2r+2} \right] \right\}. \quad (3.55)
 \end{aligned}$$

²Note that comparison with Eq. (3.18) gives algebraic relations between the even charge, $\langle r^{2n} \rangle$, and Zemach, $\langle r^{2n} \rangle_{(2)}$, moments.

	$\langle r^3 \rangle$	$\langle r^4 \rangle$	$\langle r^5 \rangle$	$\langle r^6 \rangle$	$\langle r^7 \rangle$	$\langle r^3 \rangle_{(2)}$
π	0.4980	0.6877	1.619	5.203	20.92	0.9960
$\pi \& \Delta$	0.4071	0.6228	1.522	4.978	20.22	0.8142
Ref. [79]	0.7706	1.083	1.775	3.325	7.006	2.023
Ref. [80]	0.9838	1.621	3.209	7.440	19.69	2.526
Ref. [81]	1.16(4)	2.59(19)(04)	8.0(1.2)(1.0)	29.8(7.6)(12.6)	— — —	2.85(8)

Table 3.1: Values of $\langle r^n \rangle$ in fermi units. The first two rows give the prediction from the effective theory: the first row for the effective theory with only pions and the second for the theory with pions and Deltas. The third row corresponds to the standard dipole fit of Ref. [79] with $\langle r^2 \rangle = 0.6581 \text{ fm}^3$. The fourth and fifth rows correspond to different parameterizations of experimental data Ref. [80, 81], with the latest fit being the more recent analysis based on Mainz data. For completeness, we also quote $\langle r^3 \rangle_{(2)} = 2.71 \text{ fm}^3$ from Ref. [82].

In Table 3.1 we give our predictions for some selected charge and Zemach moments,³ both in the effective theory with only pions and in the effective theory with pions and Deltas. The even powers are obtained by direct Taylor expansion of Eq. (3.13), or using the analytic formulas in Eq. (3.19). The odd powers are obtained from Eq. (3.55). We have also numerically checked the values of $\langle r^{2k+1} \rangle$ directly using Eq. (3.20). In order to estimate the error of the charge/Zemach moments and the other quantities we compute in this work we proceed as follows. We count $m_\pi \sim \sqrt{\Lambda_{\text{QCD}} m_q}$ and $\Delta \sim \frac{\Lambda_{\text{QCD}}}{N_c}$. We then have the double expansion $\frac{m_\pi}{\Lambda_{\text{QCD}}} \sim \sqrt{\frac{m_q}{\Lambda_{\text{QCD}}}}$ and $\frac{\Delta}{\Lambda_{\text{QCD}}} \sim \frac{1}{N_c}$. We still have to determine the relative size between m_π and Δ . We observe that $m_\pi/\Delta \sim N_c \sqrt{\frac{m_q}{\Lambda_{\text{QCD}}}} \sim 1/2$. Therefore, we associate a 50% uncertainty to the pure chiral computation. For all Zemach moments we observe good convergence, with the contribution due to the Delta being much smaller than the pure chiral result, and well inside the 50% uncertainty. Leaving aside the Delta, the splitting with the next resonances suggest a mass gap of order $\Lambda_{\text{QCD}} \sim 500\text{-}770 \text{ MeV}$ depending on whether one considers the Roper resonance or the ρ . For practical purposes, we also count $m_K \sim \sqrt{\Lambda_{\text{QCD}} m_s} \sim 500 \text{ MeV}$ of order Λ_{QCD} . Therefore, we assign $\frac{m_\pi}{\Lambda_{\text{QCD}}} \sim 1/3$ and $\frac{\Delta}{\Lambda_{\text{QCD}}} \sim 1/2$, as the uncertainties of the pure chiral and the Delta-related contribution respectively. We add these errors linearly for the final error. This gives the expected size of the uncomputed corrections but numerical factors may change the real size of the correction.

The chiral prediction is expected to give the dominant contribution of $\langle r^n \rangle$ for $n \geq 3$. For $n = 2$ it could also give the leading chiral logarithm. For smaller n the chiral corrections are subleading. Note that for all $n \geq 3$, these expressions give the leading (non-analytic) dependence in the light quark mass as well as in $1/N_c$. This is a valuable information for eventual lattice simulations of these quantities where one can tune these parameters. In Table 3.1 we also compare with the standard dipole ansatz Ref. [79], and with different determinations using experimental data of the electric Sachs form factor fitted to more sophisticated functions Refs. [80, 81].⁴ The latest fit claims to be the more accurate. Nevertheless, we observe large differences, bigger than

³Note that $\langle r^{2k+1} \rangle_{(2)} \simeq 2\langle r^{2k+1} \rangle$ with the precision of our computation.

⁴The agreement with Ref. [80] for $n = 7$ is accidental. We have checked that the growth with n is different with respect the chiral prediction.

the errors. This is specially worrisome for large n , since the chiral prediction is expected to give the dominant contribution of $\langle r^n \rangle$ for $n \geq 3$. In this respect, we believe that the chiral result may help to shape the appropriated fit function and, thus, to discriminate between different options, as well as to assess uncertainties. The impact of choosing different fit functions can be fully appreciated, for instance, when dealing with renormalons such as in Ref. [83], where the lack of data points in the low $1/N_S$ region allows for very different behaviors of the fitted function unless extra theoretical constrains are introduced. Closer to our concerns, we can also see the effect of the chosen fitting function in the different values of the electromagnetic proton radius obtained in Ref. [84] vs. Refs. [50, 85] from direct fits to the ep scattering data. The first group found a satisfactory fit ($\chi^2 = 1.14$ for 1422 points) using flexible fitting functions (splines and polynomials). The second group found a fit with $\chi^2 = 1.4$ for the same set of points, fixing the normalization of the fitting function. The values of the proton radius which they yield differ by around three standard deviations. On the other hand, even if on general grounds one may expect the charge/Zemach moments will be more and more sensitive to the chiral region for $n \rightarrow \infty$, large fractions of the experimental numbers are determined by the subtraction terms included to render these objects finite (for odd powers of n). We stop the discussion here but the reason for such large discrepancies should be further understood.

Lastly, as we have already mentioned, $c_{3,\text{Born}}^{pl_i}$ can be related with (one of) the Zemach moments:

$$c_{3,\text{Born}} = \frac{\pi}{3} \alpha^2 m_p^2 \langle r^3 \rangle_{(2)}, \quad \langle r^3 \rangle_{(2)} = \frac{48}{\pi} \int_0^\infty \frac{dQ}{Q^4} \left(G_E^2(-Q^2) - 1 + \frac{Q^2}{3} \langle r^2 \rangle \right). \quad (3.56)$$

Note again that the terms proportional to "1" and r^2 vanish in dimensional regularization.

3.4.2 $c_{3,\text{pol}}$, the polarizability term

Finally, we consider the polarizability correction of c_3 . It is obtained from Eq. (3.46) but subtracting the Born term to the structure functions of the FVCT. The expressions to $\mathcal{O}(p^3)$ in HBChPT can be found in Sec. 3.3. The final expression reads

$$c_{3,\text{pol}} = -e^4 m_p^2 \frac{m_\mu}{m_\pi} \left(\frac{g_A}{F_\pi} \right)^2 \mathcal{I}_2^\pi - e^4 b_{1F}^2 \frac{m_\mu}{\Delta} \frac{4}{9} \mathcal{I}_2^\Delta - e^4 m_p^2 \frac{m_\mu}{\Delta} \frac{8}{3} \left(\frac{g_{\pi N \Delta}}{F_\pi} \right)^2 \mathcal{I}_2^{\Delta\pi}, \quad (3.57)$$

where

$$\begin{aligned} \mathcal{I}_2^i = & \int \frac{d^3k}{(2\pi)^3} \frac{1}{(1+\mathbf{k}^2)^4} \int_0^\infty \frac{d\omega}{\pi} \frac{1}{\omega} \frac{1}{\omega^2 + 4\hat{m}_i \frac{1}{(1+\mathbf{k}^2)^2}} \left\{ (2 + (1+\mathbf{k}^2)^2) A_E^i(\omega, \mathbf{k}^2) \right. \\ & \left. + (1+\mathbf{k}^2)^2 \mathbf{k}^2 \omega^2 B_E^i(\omega, \mathbf{k}^2) \right\}. \end{aligned} \quad (3.58)$$

For the case of only pions we have $\hat{m}_\pi = m_\mu/m_\pi$ and

$$A_E^\pi(\omega, \mathbf{k}^2) = -\frac{1}{4\pi} \left[-\frac{3}{2} + \sqrt{1+\omega^2} + \int_0^1 dx \frac{1-x}{\sqrt{1+x^2\omega^2+x(1-x)\omega^2\mathbf{k}^2}} \right], \quad (3.59)$$

$$B_E^\pi(\omega, \mathbf{k}^2) = \frac{1}{8\pi} \int_0^1 dx \left[\frac{1-2x}{\sqrt{1+x^2\omega^2+x(1-x)\omega^2\mathbf{k}^2}} - \frac{1}{2} \frac{(1-x)(1-2x)^2}{(1+x^2\omega^2+x(1-x)\omega^2\mathbf{k}^2)^{\frac{3}{2}}} \right]. \quad (3.60)$$

For the case of Delta at tree level we have $\hat{m}_\Delta = m_\mu/\Delta$ and

$$A_E^\Delta(\omega, \mathbf{k}^2) = \frac{1}{\pi^2} \frac{\omega^2 \mathbf{k}^2}{\omega^2 + 1}, \quad (3.61)$$

$$B_E^\Delta(\omega, \mathbf{k}^2) = -\frac{1}{\pi^2} \frac{1}{\omega^2 + 1}. \quad (3.62)$$

For the case of loops including the Delta we have $\hat{m}_{\Delta\pi} = m_\mu/\Delta$ and

$$\begin{aligned} A_E^{\Delta\pi}(\omega, \mathbf{k}^2) = & -\frac{1}{12\pi^2} \int_0^1 dx \left\{ 3\sqrt{1-t^2} \ln\left(\frac{1+\sqrt{1-t^2}}{t}\right) \right. \\ & + 2\sqrt{-t^2 - (i+\omega)^2} \left(\ln(t) - \ln\left(1 - i\omega + \sqrt{-t^2 - (i+\omega)^2}\right) \right) \\ & - (3-5x) \ln\left(1 + \frac{(1+\mathbf{k}^2)(1-x)x\omega^2}{t^2}\right) \\ & + 2 \frac{(t^2-1)(3-5x) + 2ix(3-5x)\omega + x(3-5x+3\mathbf{k}^2(1-x)(1-2x))\omega^2}{\sqrt{1-t^2+x\omega(-2i+(-1+\mathbf{k}^2(-1+x))\omega)}} \\ & \left. \ln\left(\frac{1-ix\omega + \sqrt{1-t^2+x\omega(-2i+(-1+\mathbf{k}^2(-1+x))\omega)}}{\sqrt{t^2-(1+\mathbf{k}^2)(-1+x)x\omega^2}}\right) \right\} + (\omega \rightarrow -\omega), \end{aligned} \quad (3.63)$$

$$\begin{aligned} B_E^{\Delta\pi}(\omega, \mathbf{k}^2) = & \frac{1}{24\pi^2} \int_0^1 dx (1-2x)^2 \\ & \left\{ \frac{\mathbf{k}^2(1-x)x^2\omega^2(1+i\omega x)}{(t^2-(1+\mathbf{k}^2)(-1+x)x\omega^2)(1-t^2+x\omega(2i+(-1+\mathbf{k}^2(-1+x))\omega))} \right. \\ & - \frac{-3+t^2(3-7x) + x(7+2i(-3+7x)\omega + (3-7x+3\mathbf{k}^2(1-x)(1-2x))\omega^2)}{(1-t^2+x\omega(2i+(-1+\mathbf{k}^2(-1+x))\omega))^{3/2}} \\ & \left. \ln\left(\frac{1+ix\omega + \sqrt{1-t^2+x\omega(2i+(-1+\mathbf{k}^2(-1+x))\omega)}}{\sqrt{t^2-(1+\mathbf{k}^2)(-1+x)x\omega^2}}\right) \right\} + (\omega \rightarrow -\omega), \end{aligned} \quad (3.64)$$

where $t = m_\pi/\Delta$. Note that the imaginary part of these expressions comes only from the Wick rotation of k_0 and will vanish upon integration.

It is also interesting to consider the limit $m_{l_i} \ll m_\pi$, which is relevant for the hydrogen atom. In this limit the general form of Eq. (3.57) approximates, with logarithmic accuracy, to

$$c_{3,\text{pol}}^{pl_i} = -\alpha m_p^2 m_{l_i} \left[5\alpha_E^{(p)} - \beta_M^{(p)} \right] \ln(m_{l_i}), \quad (3.65)$$

$$\begin{aligned} c_{3,\text{pol}}^{pl_i} = & -\frac{2}{9} \alpha^2 \frac{m_{l_i}}{\Delta} b_{1,F}^2 \ln \frac{\Delta}{m_{l_i}} + \frac{49}{12} \pi \alpha^2 g_A^2 \frac{m_{l_i}}{m_\pi} \frac{m_p^2}{(4\pi F_0)^2} \ln\left(\frac{m_\pi}{m_{l_i}}\right) \\ & + \frac{8}{27} \alpha^2 g_{\pi N\Delta}^2 \frac{m_{l_i}}{\sqrt{\Delta^2 - m_\pi^2}} \frac{m_p^2}{(4\pi F_0)^2} \left(\frac{45\Delta}{\sqrt{\Delta^2 - m_\pi^2}} + \frac{4\Delta^2 - 49m_\pi^2}{\Delta^2 - m_\pi^2} \ln[\mathcal{R}(m_\pi^2)] \right) \ln\left(\frac{m_\pi}{m_{l_i}}\right). \end{aligned} \quad (3.66)$$

These logarithms can be obtained by computing the ultraviolet behavior of the diagram in Fig. 3.5. This contribution is proportional to c_{A_1} and c_{A_2} or, in other words, the polarizabilities of the

proton (see Refs. [86,87]). For the pure pion cloud, the polarizabilities were computed in Ref. [8]. The contribution due to the Δ can be found in Ref. [88]. The scale in the logarithm is compensated by the next scale of the problem, which can be m_π or Δ . For contributions which are only due to the Δ or pions, the scale is unambiguous. In the case where pions and Δ are both present in the loop we will choose the pion mass (the difference being beyond the logarithmic accuracy). It is known that the pure chiral prediction of $\alpha_E^{(p)}$ and $\beta_M^{(p)}$ nicely agrees with the experimental values. This agreement deteriorates after the inclusion of the Delta effects, specially for $\beta_M^{(p)}$. Nevertheless, this object is comparatively small, and even more so for $5\alpha_E^{(p)} - \beta_M^{(p)}$, the combination that appears in the logarithmic approximation. Whereas the experimental number, Ref. [89], reads $5\alpha_E^{(p)} - \beta_M^{(p)} \simeq 54 \times 10^{-4} \text{ fm}^3$, the pure chiral result gives $(5\alpha_E^{(p)} - \beta_M^{(p)})(\pi) \simeq 60 \times 10^{-4} \text{ fm}^3$, and after the inclusion of the Delta we obtain $(5\alpha_E^{(p)} - \beta_M^{(p)})(\pi \& \Delta) \simeq 73 \times 10^{-4} \text{ fm}^3$. The inclusion of the Delta slightly deteriorates the agreement, the difference being of the order of one sigma according to our error analysis. We take this as an indication that EFT result will not be very far off from the real number for the case of muonic hydrogen.

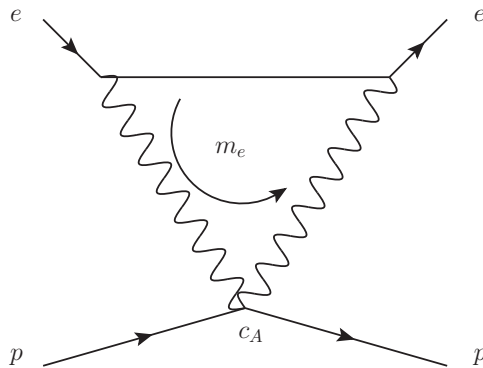


Figure 3.5: *Diagram contributing to the polarizability correction with $\ln m_e$ accuracy. The matching coefficients of the proton can be c_{A_1} or c_{A_2} , or, in other words, the proton polarizabilities.*

It is also customary to split the polarizability term (note that the Born term has already been subtracted from it) in what is called the inelastic and subtraction term:

$$\begin{aligned} c_{3,\text{sub}} &= -e^4 m_p m_\mu \int \frac{d^4 k_E}{(2\pi)^4} \frac{1}{k_E^4} \frac{1}{k_E^4 + 4m_\mu^2 k_{0,E}^2} (3k_{0,E}^2 + \mathbf{k}^2) S_1(0, -k_E^2) \\ &= -\frac{\alpha^2 m_p}{2m_\mu} \int_0^\infty \frac{dQ^2}{Q^2} \left\{ 1 + \left(1 - \frac{Q^2}{2m_\mu^2} \right) \left(\sqrt{\frac{4m_\mu^2}{Q^2} + 1} - 1 \right) \right\} S_1(0, -Q^2), \end{aligned} \quad (3.67)$$

$$\begin{aligned} c_{3,\text{inel}} &= -e^4 m_p m_\mu \int \frac{d^4 k_E}{(2\pi)^4} \frac{1}{k_E^4} \frac{1}{k_E^4 + 4m_\mu^2 k_{0,E}^2} \\ &\times \left\{ (3k_{0,E}^2 + \mathbf{k}^2) (S_1(ik_{0,E}, -k_E^2) - S_1(0, -k_E^2)) - \mathbf{k}^2 S_2(ik_{0,E}, -k_E^2) \right\}. \end{aligned} \quad (3.68)$$

It is argued that the inelastic term does not require further subtractions and can be obtained through dispersion relations. On the other hand, the subtraction term cannot be directly obtained from experiment. This fact has been used in Ref. [90] to emphasize that the polarizability term is affected by huge theoretical uncertainties. In this work, we can avoid making any assumption

about the dispersion relation properties of these quantities. This is possible within the framework of EFTs. In this setup the splitting between the inelastic and subtraction terms is unmotivated, and to some extent artificial (as it was the splitting between the Born and polarizability term). Let us elaborate on this point and see what EFTs have to say in this respect. The main problem comes, as it has already been pointed out in Ref. [72], from the diagram in Fig. 3.2. This diagram yields a finite (an small) contribution to $c_{3,\text{pol}}$ (and therefore to the energy shift, see Eq. (5.35)). Nevertheless, when split into $c_{3,\text{inel}}$ and $c_{3,\text{sub}}$, each term diverges in the following way

$$\delta c_{3,\text{sub}} \sim -\delta c_{3,\text{inel}} \simeq -\frac{4}{3}\alpha^2 \frac{m_\mu}{\Delta} b_{1,F}^2 \ln(\nu/m_\mu). \quad (3.69)$$

Obviously such contribution is fictitious but it may alter the value of the individual terms.

We relegate further discussion on the contribution of the coefficient c_3^{had} to Sec. 5.4, where we will discuss the Lamb energy shift.

3.5 Spin-dependent matching: c_4

In order to find the spin-dependent coefficient c_4 , we proceed in the same way as in the spin-independent case. We match HBET and NRQED order by order in a generic expansion in $1/m_p$, $1/m_{l_i}$ and α . We have two sorts of loops: chiral and electromagnetic. The former are always associated to $1/(4\pi F_0)^2$ factors, whereas the latter are always suppressed by α factors. Any scale left to get the dimensions right scales with m_π or Δ .

At $\mathcal{O}(\alpha^2)$, the contribution to $c_4^{pl_i}$ (see Fig. 2.1) from matching HBET to NRQED can be written in a compact way in terms of the structure functions of the FVCT. In Euclidean space it reads

$$c_4^{pl_i} = \frac{e^4}{3} \int \frac{d^D k}{(2\pi)^D} \frac{1}{k_E^2} \frac{1}{k_E^4 + 4m_{l_i}^2 k_{0,E}^2} \left\{ A_1(ik_{0,E}, -k_E^2)(k_{0,E}^2 + 2k_E^2) + i3k_E^2 \frac{k_{0,E}}{m_p} A_2(ik_{0,E}, -k_E^2) \right\} + \mathcal{O}(\alpha^3), \quad (3.70)$$

consistent with the expressions obtained long ago in Ref. [91]. This result keeps the complete dependence on m_{l_i} and is valid both for NRQED(μp) and NRQED(ep), i.e. for hydrogen and muonic hydrogen. From now on we will assume that we are doing the matching to NRQED(μp). Therefore, we keep the whole dependence on m_μ/m_π . Once again can recover the case for a general lepton just replacing $m_\mu \rightarrow m_{l_i}$. The NRQED(ep) case can then be derived by expanding m_e versus m_π .

Similarly to the spin-independent case, this contribution can be organized as in Eq. (2.27). From now on we focus on the matching of the hadronic part, which we again split in:

$$c_4^{\text{had}} = c_{4,\text{Born}}^{pl_i} + c_{4,\text{pol}}^{pl_i}. \quad (3.71)$$

These terms (associated to energies of $\mathcal{O}(m_\pi)$) were computed with $\mathcal{O}(\alpha^2 \times (\ln m_q, \ln \Delta, \ln m_{l_i}))$

accuracy in Ref. [59]. We quote them here for ease of reference⁵:

$$c_{4,\text{Born}} \simeq (4\pi\alpha)^2 m_p \frac{2}{3} \int \frac{d^{D-1}k}{(2\pi)^{D-1}} \frac{1}{\mathbf{k}^4} G_E^{(0)} G_M^{(1)} \quad (3.72)$$

$$\simeq \frac{m_p^2}{(4\pi F_0)^2} \alpha^2 \frac{2}{3} \pi^2 \left[g_A^2 \ln \frac{m_\pi^2}{\nu^2} + \frac{4}{9} g_{\pi N\Delta}^2 \ln \frac{\Delta^2}{\nu^2} \right], \quad (3.73)$$

$$c_{4,\text{pol}} = \frac{m_p^2}{(4\pi F_0)^2} \frac{\alpha^2}{\pi} \frac{8}{3} \left(\frac{7\pi}{8} - \frac{\pi^3}{12} \right) \left[g_A^2 \ln \frac{m_\pi^2}{\nu^2} - \frac{8}{9} g_{\pi N\Delta}^2 \ln \frac{\Delta^2}{\nu^2} \right] + \frac{b_{1,F}^2}{18} \alpha^2 \ln \frac{\Delta^2}{\nu^2}. \quad (3.74)$$

Note that Eq. (3.72) is independent of the lepton mass, while the last expression Eq. (3.74) does not include the whole dependence on the lepton mass anymore. Summing up the hadronic and point-like terms one has⁶

$$\begin{aligned} c_4 \simeq & \left(1 - \frac{\mu_p^2}{4} \right) \alpha^2 \ln \frac{m_\mu^2}{\nu^2} + \frac{b_{1,F}^2}{18} \alpha^2 \ln \frac{\Delta^2}{\nu^2} + \frac{m_p^2}{(4\pi F_0)^2} \alpha^2 \frac{2}{3} \left(\frac{2}{3} + \frac{7}{2\pi^2} \right) \pi^2 g_A^2 \ln \frac{m_\pi^2}{\nu^2} \\ & + \frac{m_p^2}{(4\pi F_0)^2} \alpha^2 \frac{8}{27} \left(\frac{5}{3} - \frac{7}{\pi^2} \right) \pi^2 g_{\pi N\Delta}^2 \ln \frac{\Delta^2}{\nu^2} \\ & \stackrel{(N_c \rightarrow \infty)}{\simeq} \alpha^2 \ln \frac{m_\mu^2}{\nu^2} + \frac{m_p^2}{(4\pi F_0)^2} \alpha^2 \pi^2 g_A^2 \ln \frac{m_\pi^2}{\nu^2}. \end{aligned} \quad (3.75)$$

Parametrically, the three contributions, Eqs. (2.31), (3.72) and (3.74), are of the same order. Nevertheless, the polarizability and the point-like term are much smaller. This is consistent with the fact that polarizability correction seems to be small (see Refs. [93–95]), if determined through dispersion relations. As already discussed in Ref. [59], the EFT computation gives a double explanation to this fact. On the one hand, this is due to the smallness of the numerical coefficient of the polarizability term, but there also seems to be some large N_c rationale behind. Since $g_{\pi N\Delta} = 3/(2\sqrt{2})g_A$ in the large N_c limit, the polarizability term vanishes (see Ref. [63]) except for the tree-level-like Delta contribution (the last term in Eq. (3.74)). Nevertheless, the latter also vanishes against the κ_p -dependent point-like contribution (which effectively becomes the result of a point-like particle) in the large N_c limit, since $b_1^F = 3/(2\sqrt{2})\kappa_V$ and $\kappa_p = \kappa_V/2$ Ref. [96]. Note also that the point-like term and the tree-level-like Delta contribution are suppressed by $1/\pi$ factors with respect the Born contribution.

This discussion also illustrates that splitting the total contribution into different terms may introduce spurious effects that vanish in the total sum. We have also seen a similar thing but in a different context for the case of the spin-independent computation.

Our computation allows us to relate $c_4^{pl\mu} \equiv c_4$ and $c_4^{pl_e}$ in a model independent way (now keeping the whole dependence on the lepton masses). Since $c_{4,R}^{pl_i} \simeq c_{4,R}^p$ up to terms of $\mathcal{O}(\alpha^2 m_i/\Lambda_{\text{QCD}})$, we can obtain the following relation

$$c_4 = c_4^{pl_e} + \left[c_{4,\text{point-like}} - c_{4,\text{point-like}}^{pl_e} \right] + \left[c_{4,\text{pol}} - c_{4,\text{pol}}^{pl_e} \right] + \mathcal{O}(\alpha^3, \alpha^2 m_\mu/\Lambda_{\text{QCD}}). \quad (3.76)$$

⁵In Ref. [59] $c_{4,\text{Born}}^{pl_i}$ was named $\delta c_{4,\text{Zemach}}^{pl_i}$, as Eq. (3.72) corresponds to the Zemach expression Ref. [92], the leading order in the NR expansion of the Born term. The point-like contribution diverges irrespectively of doing the computation in a relativistic or NR way (see the discussion in Ref. [59]). Here we only quote the NR expression, which is more natural from the EFT point of view, as it avoids any assumption about the behavior of the theory at the proton mass scale.

⁶Remember that, analogously to c_3 , within the EFT framework the contribution from energies of $\mathcal{O}(m_\rho)$ or higher in Eq. (2.27) are encoded in $c_{4,R}^{pl_i} \simeq c_{4,R}^p$.

Note that we have already used the fact that $c_{4,\text{Born}}^{pl_i}$ cancels in the difference, as it is independent of the lepton mass. The experimental and theoretical results discussed before suggest that $c_{4,\text{Born}}^{pl_i}$ is the leading contribution to the Wilson coefficient. Therefore, such contribution can be obtained from $c_4^{pl_e}$, which can be determined from the hyperfine splitting of Hydrogen. In Ref. [59] it was estimated to be $c_4^{pl_e} \simeq -48\alpha^2$. By considering differences in Eq. (3.76) the ultraviolet behavior gets regulated and the logarithmic divergences vanish. This renders these contributions very small and negligible in comparison with the uncertainties. For the point-like contribution we obtain

$$c_{4,\text{point-like}} - c_{4,\text{point-like}}^{pl_e} = \left(1 - \frac{\kappa_p^2}{4}\right) \alpha^2 \ln \frac{m_\mu^2}{m_e^2} \simeq 2.09\alpha^2, \quad (3.77)$$

and for the polarizability we obtain (note that this term vanishes in the large N_c limit, except for the tree-level-like contribution)

$$c_{4,\text{pol}} - c_{4,\text{pol}}^{pl_e} = 0.17\alpha^2(\pi) + 0.07\alpha^2(\Delta) + 0.008\alpha^2(\pi\&\Delta) = 0.24\alpha^2. \quad (3.78)$$

Overall we obtain $c_4 \simeq -46\alpha^2$. The bulk of this contribution is expected to come from the Born term, which in turn is related to the Zemach magnetic radius,

$$\langle r_Z \rangle = -\frac{4}{\pi} \int_0^\infty \frac{dQ}{Q^2} [G_E(Q^2)G_M(Q^2) - 1] \quad (3.79)$$

by the following relation

$$\langle r_Z \rangle = -\frac{3}{4\pi} \frac{1}{\alpha^2 m_p} c_{4,\text{Born}}^{pl_i} \simeq -\frac{\pi}{2} \frac{m_p}{(4\pi F_0)^2} \left[g_A^2 \ln \frac{m_\pi^2}{\nu^2} + \frac{4}{9} g_{\pi N \Delta}^2 \ln \frac{\Delta^2}{\nu^2} \right] \stackrel{(\nu=m_\rho)}{=} 1.35 \text{ fm}. \quad (3.80)$$

The chiral logarithm result compares well ($\sim 30\%$) with existing predictions ($\sim 1.04\text{-}1.08$ fm) from hydrogen hyperfine Refs. [97,98], from dispersion relations Refs. [81,82], or from the muonic hydrogen hyperfine Ref. [20]. Note that in the case of the determinations of $\langle r_Z \rangle$ from the hyperfine splitting (either from hydrogen or muonic hydrogen) one needs to control the relativistic hadronic effects associated to the Born term as well as the polarizability correction. On the other hand, if we are only interested in the hyperfine splitting it may make more sense to consider $c_4^{pl_i}$ as a whole. We relegate a more detailed discussion to future work.

Chapter 4

Matching NRQED to pNRQED

Now that we have fully set the NRQED Lagrangian and its Wilson coefficients, we move on to its matching to pNRQED. In this chapter we will give the form of the potentials that form the pNRQED Lagrangian in Sec. 2.4. We will organise them in terms of their power counting within the EFT framework. Once all the potentials that contribute to the spectrum at $\mathcal{O}(m_r\alpha^5)$ are collected we will be able to compute the Lamb shift in muonic hydrogen.

4.1 The static potential: $V^{(0)}$

The Fourier transform of $V^{(0)}$ reads

$$\tilde{V}^{(0)} \equiv -4\pi Z \frac{\alpha_{\tilde{V}}(k)}{\mathbf{k}^2} \equiv \sum_{n=1}^{\infty} \tilde{V}^{(0,n)}, \quad (4.1)$$

where $\tilde{V}^{(0,n)}$ have been defined in Eq. (2.38). The definition of $\alpha_{\tilde{V}}$, the coupling constant associated to the static potential is implicit in the previous equation. This coupling constant is gauge invariant and scheme/scale independent. The contribution to the static potential associated to the electron VP ($\Pi(0) = 0$)

$$\Pi(k^2) = \alpha\Pi_1(k^2) + \alpha^2\Pi_2(k^2) + \alpha^3\Pi_3(k^2) + \dots$$

provides with another very popular definition for the effective coupling that enjoys the nice properties of gauge invariance and scheme/scale independence:

$$\alpha_{\text{eff}}(k) = \alpha \frac{1}{1 + \Pi(-\mathbf{k}^2)} = \alpha - \frac{\alpha^2}{\pi}\Pi_1 + \frac{\alpha^3}{\pi^2}(\Pi_1^2 - \Pi_2) + \frac{\alpha^4}{\pi^3}(-\Pi_1^3 + 2\Pi_1\Pi_2 - \Pi_3) + \mathcal{O}(\alpha^5). \quad (4.2)$$

The coupling α_{eff} corresponds to Dyson summation. If we express $\alpha_{\tilde{V}}(k)$ in terms of $\alpha_{\text{eff}}(k)$, we have

$$\alpha_{\tilde{V}}(k) = \alpha_{\text{eff}}(k) + \sum_{\substack{n,m=0 \\ n+m=\text{even}>0}} Z_{\mu}^n Z_p^m \alpha_{\text{eff}}^{(n,m)}(k) \equiv \alpha_{\text{eff}}(k) + \delta\alpha(k), \quad \delta\alpha(k) = \mathcal{O}(\alpha^4). \quad (4.3)$$

The leading order contribution to the static potential is nothing but the Coulomb potential

$$\tilde{V}^{(0,1)} \equiv -4\pi Z \frac{\alpha}{\mathbf{k}^2}. \quad (4.4)$$

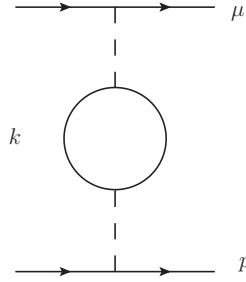


Figure 4.1: *One-loop electron VP contribution to the static potential. The dashed lines represent the A_0 fields, while the continuous lines represent the fermion and antifermion fields.*

In order to achieve $\mathcal{O}(m_r\alpha^5)$ accuracy we need to know $\Pi^{(1)}$, $\Pi^{(2)}$, $\Pi^{(3)}$ and the leading, non-vanishing, contributions to $\alpha_{\text{eff}}^{(2,0)}(k)$, $\alpha_{\text{eff}}^{(0,2)}(k)$ and $\alpha_{\text{eff}}^{(1,1)}(k)$.

The next-to-leading order (NLO) term of the static potential is displayed in Fig. 4.1 and reads

$$\tilde{V}_{\text{VP}}^{(0,2)}(k) = 4\pi Z \frac{\alpha^2}{\pi} \frac{\Pi_1(-\mathbf{k}^2)}{\mathbf{k}^2}, \quad (4.5)$$

where

$$\Pi_1(k^2) = k^2 \int_4^\infty dq^2 \frac{1}{q^2(m_e^2 q^2 - k^2)} u(q^2), \quad (4.6)$$

and

$$u(q^2) = \frac{1}{3} \sqrt{1 - \frac{4}{q^2}} \left(1 + \frac{2}{q^2}\right). \quad (4.7)$$

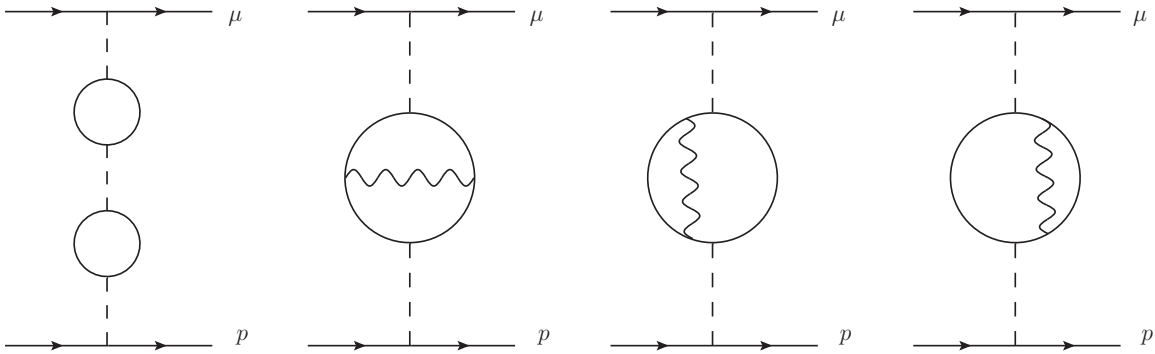


Figure 4.2: *Diagrams contributing to $V^{(0,3)}$. The dashed and wiggly lines represent the A_0 and A fields respectively, while the continuous lines represent the fermion and antifermion fields.*

The next-to-next-to-leading order (NNLO) term of the static potential is produced by the diagrams depicted in Fig. 4.2, which can be understood as a correction to the VP. It was computed

by Källen and Sabry Ref. [99] and reads

$$\tilde{V}_{\text{VP}}^{(0,3)}(k) = 4\pi Z \frac{\alpha^3}{\pi^2} \frac{\Pi_1^2(-\mathbf{k}^2) - \Pi_2(-\mathbf{k}^2)}{\mathbf{k}^2}, \quad (4.8)$$

$$\Pi_1^2(k^2) - \Pi_2(k^2) = k^2 \int_4^\infty dq^2 \frac{1}{q^2(m_e^2 q^2 - k^2)} u^{(2)}(q^2), \quad (4.9)$$

where

$$\begin{aligned} u^{(2)}(q^2) = & \frac{1}{3} \left[\tau \left(-\frac{19}{24} + \frac{55}{72}\tau^2 - \frac{1}{3}\tau^4 - \frac{3-\tau^2}{2} \ln \left(\frac{64\tau^4}{(1-\tau^2)^3} \right) \right) \right. \\ & + \ln \left(\frac{1+\tau}{1-\tau} \right) \left(\frac{33}{16} + \frac{23}{8}\tau^2 - \frac{23}{16}\tau^4 + \frac{1}{6}\tau^6 + \left(\frac{3}{2} + \tau^2 - \frac{\tau^4}{2} \right) \ln \left(\frac{(1+\tau)^3}{8\tau^2} \right) \right) \\ & \left. + (3 + 2\tau^2 - \tau^4) \left(2\text{Li}_2 \left(\frac{1-\tau}{1+\tau} \right) + \text{Li}_2 \left(\frac{-1+\tau}{1+\tau} \right) \right) \right], \end{aligned} \quad (4.10)$$

with

$$\tau = \sqrt{1 - \frac{4}{q^2}}, \quad (4.11)$$

and the polylogarithm function is defined as

$$\text{Li}_2(x) = - \int_0^z du \frac{\ln(1-u)}{u}, \quad z \in \mathbb{C} \setminus [1, \infty). \quad (4.12)$$

The N³LO term of the static potential coming from the VP reads

$$\tilde{V}_{\text{VP}}^{(0,4)}(k) = 4\pi Z \frac{\alpha^4}{\pi^3} \frac{-\Pi_1^3(-\mathbf{k}^2) + 2\Pi_1(-\mathbf{k}^2)\Pi_2(-\mathbf{k}^2) - \Pi_3(-\mathbf{k}^2)}{\mathbf{k}^2}. \quad (4.13)$$

This object (more specifically Π_3) has been computed in Ref. [100], see also Ref. [101] where the complete set of diagrams can be found.

The remaining N³LO contribution to the static potential is generated by diagrams that cannot be completely associated to the VP, and is encoded in $\delta\alpha(k)$. Its sum is constrained to fulfil $n+m = \text{even}$ because of the Furry theorem. Each $\alpha_{\text{eff}}^{(n,m)}(k)$ is also gauge invariant. The leading, non-vanishing, contributions are $\alpha_{\text{eff}}^{(2,0)}(k)$, $\alpha_{\text{eff}}^{(0,2)}(k)$ and $\alpha_{\text{eff}}^{(1,1)}(k)$. They have an expansion in α themselves. Since each of them is $\mathcal{O}(\alpha^4)$, we can approximate them by its leading order expression, which is produced by the light-by-light diagrams displayed in Fig. 4.3. This object could be deduced from the computation in Ref. [102] (we truncate the α_{eff} expressions to its leading order)

$$\tilde{V}_{\text{LbL}}^{(0,4)}(k) = -\frac{4\pi Z}{\mathbf{k}^2} \left((Z_\mu^2 + Z_p^2) \alpha_{\text{eff}}^{(2,0)}(k) + Z_\mu Z_p \alpha_{\text{eff}}^{(1,1)}(k) \right), \quad (4.14)$$

where we have already used that $\alpha_{\text{eff}}^{(2,0)}(k) = \alpha_{\text{eff}}^{(0,2)}(k)$.

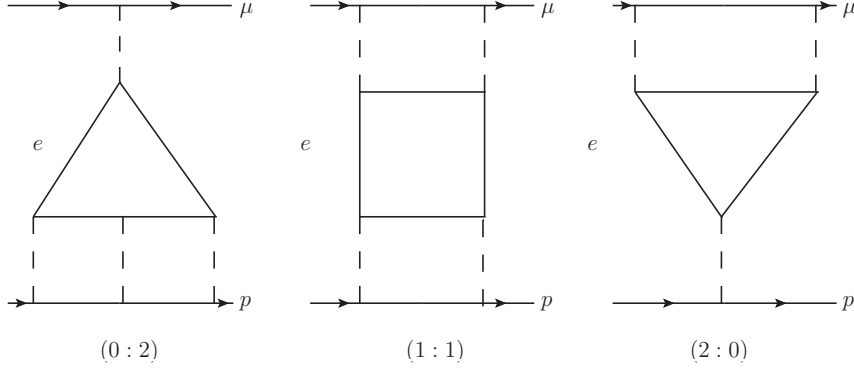


Figure 4.3: *Light-by-light contribution to the static potential. The first and third diagram are the contributions to $\alpha_{\text{eff}}^{(2,0)}(k)$ and $\alpha_{\text{eff}}^{(0,2)}(k)$ respectively. The second diagram contributes to $\alpha_{\text{eff}}^{(1,1)}(k)$.*

4.2 The potential beyond the static limit

We perform the matching computation through the off-shell matching scheme in the CG. In this scheme the $1/m$ potential is zero in QED as long as there are no light fermions (see Ref. [58]). However, in our computation we must include the electron as a massive light fermion. Yet, after inspection of the diagrams that may contribute, they would produce, at most, $\mathcal{O}(m_r\alpha^6)$ corrections to the energy, so they will be neglected in the following.

Up to order α^2/m^2 the expression of the potential in momentum space was obtained in Ref. [60]. We summarize its different contributions here.

$$\begin{aligned}
 \tilde{V}_{\text{tree+VP}}^{(2)} &= \frac{\pi\alpha_{\text{eff}}(k)}{2} \left(Z_p \frac{c_D^{(\mu)}}{m_\mu^2} + Z_\mu \frac{c_D^{(p)}}{m_p^2} \right) \\
 &\quad - i2\pi\alpha_{\text{eff}}(k) \frac{(\mathbf{p} \times \mathbf{k})}{\mathbf{k}^2} \cdot \left(Z_p \frac{c_S^{(\mu)} \mathbf{S}_\mu}{m_\mu^2} + Z_\mu \frac{c_S^{(p)} \mathbf{S}_p}{m_p^2} \right) \\
 &\quad - Z16\pi\alpha \left(\frac{d_2^{(\mu)}}{m_\mu^2} + \frac{d_2^{(\tau)}}{m_\tau^2} + \frac{d_2}{m_p^2} \right) \\
 &\quad - Z \frac{4\pi\alpha_{\text{eff}}(k)}{m_\mu m_p} \left(\frac{\mathbf{p}^2}{\mathbf{k}^2} - \frac{(\mathbf{p} \cdot \mathbf{k})^2}{\mathbf{k}^4} \right) \\
 &\quad - \frac{i4\pi\alpha_{\text{eff}}(k)}{m_\mu m_p} \frac{(\mathbf{p} \times \mathbf{k})}{\mathbf{k}^2} \cdot (Z_p c_F^{(\mu)} \mathbf{S}_\mu + Z_\mu c_F^{(p)} \mathbf{S}_p) \\
 &\quad + \frac{4\pi\alpha_{\text{eff}}(k) c_F^{(\mu)} c_F^{(p)}}{m_\mu m_p} \left(\mathbf{S}_\mu \cdot \mathbf{S}_p - \frac{\mathbf{S}_\mu \cdot \mathbf{k} \mathbf{S}_p \cdot \mathbf{k}}{\mathbf{k}^2} \right) \\
 &\quad - \frac{1}{m_p^2} (c_3 - 4c_4 \mathbf{S}_\mu \cdot \mathbf{S}_p), \tag{4.15}
 \end{aligned}$$

$$\tilde{V}_{1\text{-loop}}^{(2,2)} = \frac{Z^2 \alpha^2}{m_\mu m_p} \left(\frac{7}{3} \ln \frac{\mathbf{k}^2}{\nu^2} + \frac{1}{3} \right), \tag{4.16}$$

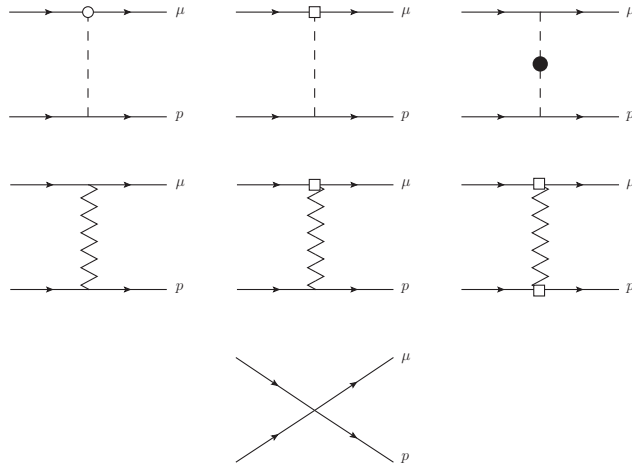


Figure 4.4: *The non-zero relevant diagrams for the matching at tree level in CG. For the A_0 (dashed line) the circle is the vertex proportional to c_D , the square to c_S (spin dependent) and the black dot to d_2 , while for \mathbf{A} (zigzag line) the square is the vertex proportional to c_F and the other vertex appears from the covariant derivative in the kinetic term. The last diagram is proportional to c_3 and c_4 . The symmetric diagrams are not displayed. Their sum corresponds to Eq. (4.15) (without VP).*

$$\tilde{V}_{\text{off-shell}}^{(2,2)} = -\frac{Ze^2}{4m_\mu m_p} \frac{(\mathbf{p}^2 - \mathbf{p}'^2)^2}{\mathbf{k}^2} \frac{\alpha}{\pi} m_e^2 \int_4^\infty d(q^2) \frac{1}{(m_e^2 q^2 + \mathbf{k}^2)^2} u(q^2), \quad (4.17)$$

where $\mathbf{S}_i = \boldsymbol{\sigma}_i/2$ is the spin of the particle i . We stress that Eq. (4.16) has been obtained in the $\overline{\text{MS}}$ scheme. If we switch off the electron VP effects, the computation would correspond to the muonium case (or positronium if we consider the equal masses). The relevant diagrams in such situation are presented in Figs. 4.4 and 4.5 (following the classification of Ref. [58] generalized to the non-equal mass case).

The tree-level diagrams of Fig. 4.4 produce the potential quoted in Eq. (4.15). Note that this equation depends on $\alpha_{\text{eff}} \simeq \alpha - \alpha^2 \Pi_1(-\mathbf{k}^2)$ (with the precision we are working). The effective coupling constant produces a leading order potential of $\mathcal{O}(\alpha)$. It also produces a NLO potential of $\mathcal{O}(\alpha^2)$, which corresponds to incorporating the electron VP effects. This means including the VP in the 1st, 2nd, 4th, 5th and 6th diagram in Fig. 4.4. On top of that one has to include the contribution coming from Fig. 4.6, which appears from the Taylor expansion in powers of the transfer energy of the VP when doing the matching computation off-shell (for further details see the discussion in Ref. [60]). It produces the potential quoted in Eq. (4.17). The one-loop diagrams in Fig. 4.5 produce the potential quoted in Eq. (4.16) (in the $\overline{\text{MS}}$ scheme).

The sum of these three potentials includes all terms of $\mathcal{O}(V^{(2,1)})$ and $\mathcal{O}(V^{(2,2)})$:

$$\tilde{V}^{(2)} = \tilde{V}_{\text{tree+VP}}^{(2)} + \tilde{V}_{1\text{-loop}}^{(2,2)} + \tilde{V}_{\text{off-shell}}^{(2,2)} + \mathcal{O}(\tilde{V}^{(2,3)}). \quad (4.18)$$

4.3 The potential in position space

The matrix elements of the potentials that appear in the energy shifts are more efficiently computed in position space. Therefore, we also write the potentials in position space.

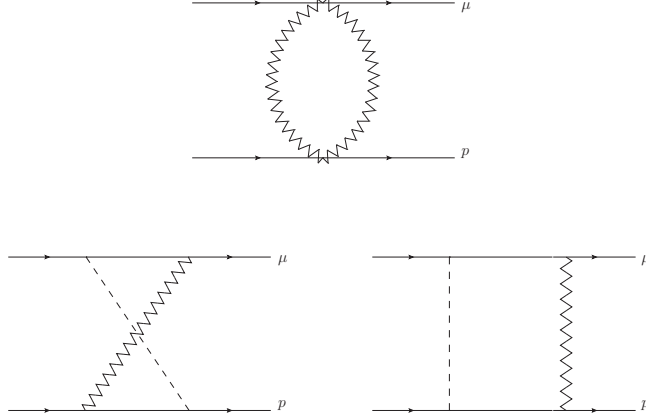


Figure 4.5: The non-zero relevant diagrams for the matching at one loop in CG. The interactions for \mathbf{A} (zigzag line) are the ones which appear from the covariant space derivatives in the kinetic term, while for A_0 (dashed line) comes from the covariant time derivative. The symmetric diagrams are not displayed. They correspond to Eq. (4.16).

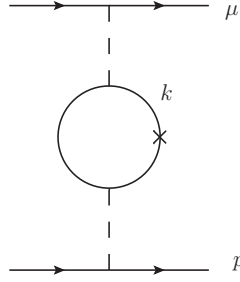


Figure 4.6: Symbolic representation of the leading correction to the static potential due to the Taylor expansion of the electron VP in CG in powers of $k^0 = E'_1 - E_1$. It corresponds to Eq. (4.17). The dashed lines represent the A_0 field, while the continuous lines represent the fermion and antifermion.

The static potential is trivially written in position space via Fourier transformation. It reads:

$$V^{(0,1)}(r) = -Z \frac{\alpha}{r}, \quad (4.19)$$

$$V_{\text{VP}}^{(0,2)}(r) = -\frac{Z\alpha}{r} \frac{\alpha}{\pi} \int_4^\infty \frac{dq^2}{q^2} u(q^2) e^{-2m_e r q}, \quad (4.20)$$

$$V_{\text{VP}}^{(0,3)}(r) = 4\pi Z \frac{\alpha^3}{\pi^2} \int_4^\infty \frac{dq^2}{q^2} u^{(2)}(q^2) e^{-2m_e r q}, \quad (4.21)$$

$$V_{\text{VP}}^{(0,4)}(r) = 4\pi Z \frac{\alpha^4}{\pi^3} \int \frac{d^3k}{(2\pi)^3} e^{-i\mathbf{k}\cdot\mathbf{r}} \frac{-\Pi_1^3(-\mathbf{k}^2) + 2\Pi_1(-\mathbf{k}^2)\Pi_2(-\mathbf{k}^2) - \Pi_3(-\mathbf{k}^2)}{\mathbf{k}^2}, \quad (4.22)$$

$$V_{\text{LbL}}^{(0,4)}(r) = -4\pi Z \int \frac{d^3k}{(2\pi)^3} e^{-i\mathbf{k}\cdot\mathbf{r}} \frac{1}{\mathbf{k}^2} \left((Z_\mu^2 + Z_p^2) \alpha_{\text{eff}}^{(2,0)}(k) + Z_\mu Z_p \alpha_{\text{eff}}^{(1,1)}(k) \right). \quad (4.23)$$

For the case of the $\frac{1}{m^2}$ potential it is convenient to split the potential in a slightly different

way than in momentum space. In particular, the VP contributions are dealt with in an isolated way. We follow the notation of Ref. [60]. The contributions coming from tree-level diagrams read

$$\begin{aligned}
 V_{\text{tree}}^{(2)} = & \frac{Z\alpha}{2m_\mu m_p} \left[-\left\{ \frac{1}{r}, \mathbf{p}^2 \right\} + \frac{1}{r^3} \mathbf{L}^2 + 4\pi \delta^{(3)}(\mathbf{r}) \right] - 16\pi Z\alpha \left(\frac{d_2^{(\mu)}}{m_\mu^2} + \frac{d_2^{(\tau)}}{m_\tau^2} + \frac{d_2}{m_p^2} \right) \delta^{(3)}(\mathbf{r}) \\
 & + \frac{\alpha}{2m_\mu m_p} \left[\left(\frac{Z_\mu c_D^{(p)} m_\mu^2 + Z_p c_D^{(\mu)} m_p^2}{m_\mu m_p} \right) \pi \delta^{(3)}(\mathbf{r}) \right. \\
 & + Z_p c_F^{(\mu)} \frac{2}{r^3} \mathbf{L} \cdot \mathbf{S}_\mu + Z_\mu c_F^{(p)} \frac{2}{r^3} \mathbf{L} \cdot \mathbf{S}_p + m_\mu m_p \left\{ \frac{Z_p c_S^{(\mu)}}{m_\mu^2} \frac{1}{r^3} \mathbf{L} \cdot \mathbf{S}_\mu + \frac{Z_\mu c_S^{(p)}}{m_p^2} \frac{1}{r^3} \mathbf{L} \cdot \mathbf{S}_p \right\} \left. \right] \\
 & + \frac{\alpha}{2m_\mu m_p} \left[\frac{16\pi}{3} c_F^{(\mu)} c_F^{(p)} \delta^{(3)}(\mathbf{r}) \mathbf{S}_\mu \mathbf{S}_p + \frac{c_F^{(\mu)} c_F^{(p)}}{2r^3} \hat{S}_{p\mu}(\hat{\mathbf{r}}) \right] + \frac{1}{m_p^2} (-c_3 + 4\mathbf{S}_\mu \mathbf{S}_p c_4) \delta^{(3)}(\mathbf{r}),
 \end{aligned} \tag{4.24}$$

where $\hat{S}_{ij}(\hat{\mathbf{r}}) = -4(\mathbf{S}_i \cdot \mathbf{S}_j) + 12(\mathbf{S}_i \cdot \hat{\mathbf{r}})(\mathbf{S}_j \cdot \hat{\mathbf{r}})$.

The Fourier transform of Eq. (4.16) reads

$$V_{1\text{-loop}}^{(2,2)} = \frac{Z^2 \alpha^2}{3m_p m_\mu} \left[\delta^{(3)}(\mathbf{r}) (1 - 7 \ln \nu^2) - \frac{7}{2\pi} \text{reg} \frac{1}{r^3} \right], \tag{4.25}$$

where

$$-\frac{1}{4\pi} \text{reg} \frac{1}{r^3} = \int \frac{d^3 k}{(2\pi)^3} e^{-i\mathbf{k} \cdot \mathbf{r}} \ln k. \tag{4.26}$$

Finally, the contributions associated to the one-loop VP read¹

$$\begin{aligned}
 V_{\text{VP},1\text{-loop}}^{(2)} + V_{\text{off-shell}}^{(2,2)} = & \frac{\alpha}{\pi} \int_4^\infty dq^2 \frac{u(q^2)}{q^2} \\
 & \times \left\{ \frac{\alpha}{8m_\mu^2 m_p^2} \left(Z_\mu c_D^{(p)} m_\mu^2 + Z_p c_D^{(\mu)} m_p^2 \right) \left(4\pi \delta^{(3)}(\mathbf{r}) - \frac{\lambda^2 e^{-\lambda r}}{r} \right) \right. \\
 & + \frac{\alpha}{2} \left(Z_\mu c_S^{(p)} \frac{\mathbf{L} \cdot \mathbf{S}_p}{m_p^2} + Z_p c_S^{(\mu)} \frac{\mathbf{L} \cdot \mathbf{S}_\mu}{m_\mu^2} \right) \left(\frac{e^{-\lambda r} (1 + \lambda r)}{r^3} \right) \\
 & - \frac{Z_p Z_\mu \alpha}{4m_\mu m_p} \left(\frac{\lambda^2 e^{-\lambda r}}{r} \left(1 - \frac{\lambda r}{2} \right) + 2p^i \frac{e^{-\lambda r}}{r} \left(\delta_{ij} + \frac{r_i r_j}{r^2} (1 + \lambda r) \right) p^j \right) \\
 & \left. + \frac{\alpha}{m_\mu m_p} \left(Z_p c_F^{(\mu)} \mathbf{L} \cdot \mathbf{S}_\mu + Z_\mu c_F^{(p)} \mathbf{L} \cdot \mathbf{S}_p \right) \left(\frac{e^{-\lambda r} (1 + \lambda r)}{r^3} \right) \right\}
 \end{aligned} \tag{4.28}$$

¹Note that the fourth line can be written in a way that makes the angular momentum structure more explicit:

$$\begin{aligned}
 & \int_4^\infty dq^2 \frac{u(q^2)}{q^2} \left(\frac{\lambda^2 e^{-\lambda r}}{r} \left(1 - \frac{\lambda r}{2} \right) + 2p^i \frac{e^{-\lambda r}}{r} \left(\delta_{ij} + \frac{r_i r_j}{r^2} (1 + \lambda r) \right) p^j \right) \\
 & = \int_4^\infty dq^2 \frac{u(q^2)}{q^2} \left(2 \left\{ \mathbf{p}^2, \frac{e^{-\lambda r}}{r} \left(1 + \frac{\lambda r}{2} \right) \right\} - 2 \frac{e^{-\lambda r}}{r^3} (1 + \lambda r) \mathbf{L}^2 + \frac{\lambda^2}{r} e^{-\lambda r} \left(1 + \frac{\lambda r}{2} \right) - 8\pi \delta^{(3)}(\mathbf{r}) \right).
 \end{aligned} \tag{4.27}$$

Nevertheless, one has to be careful when dealing with the right-hand-side of the equality, as the first and last term are separately divergent (but not their sum).

$$+ \frac{\alpha c_F^{(\mu)} c_F^{(p)}}{m_\mu m_p} \left(-\frac{2}{3} \frac{e^{-\lambda r} \lambda^2}{r} \mathbf{S}_\mu \cdot \mathbf{S}_p + \frac{8}{3} \pi \delta^{(3)}(\mathbf{r}) \mathbf{S}_\mu \cdot \mathbf{S}_p + \frac{e^{-\lambda r}}{4r^3} \left(1 + r\lambda + \frac{r^2 \lambda^2}{3} \right) \hat{S}_{p\mu}(\hat{\mathbf{r}}) \right) \Bigg\},$$

where $\lambda = m_e q$. Therefore, with the precision we aim at, we obtain

$$V^{(2)} = V_{\text{tree}}^{(2)} + V_{1\text{-loop}}^{(2,2)} + (V_{\text{VP},1\text{-loop}}^{(2)} + V_{\text{off-shell}}^{(2,2)}) + \mathcal{O}(V^{(2,3)}) = V^{(2,1)} + V^{(2,2)} + \mathcal{O}(V^{(2,3)}), \quad (4.29)$$

where in the second equality we organize the potential terms according to their powers in α . This requires expanding the NRQCD Wilson coefficients in powers of α . The leading non-vanishing contribution reads²

$$\begin{aligned} V^{(2,1)} &= \frac{Z\alpha}{2m_\mu m_p} \left[-\left\{ \frac{1}{r}, \mathbf{p}^2 \right\} + \frac{1}{r^3} \mathbf{L}^2 + 4\pi \left(1 + \frac{m_\mu^2 + m_p^2}{4m_\mu m_p} \right) \delta^{(3)}(\mathbf{r}) \right] \\ &+ \frac{\alpha}{2m_\mu m_p} \left[\frac{16}{3} \pi Z_\mu (Z_p + \kappa_p^{\text{had}}) \mathbf{S}_\mu \mathbf{S}_p \delta^{(3)}(\mathbf{r}) Z_\mu \frac{Z_p + \kappa_p^{\text{had}}}{2} \frac{1}{r^3} \hat{S}_{p\mu}(\hat{\mathbf{r}}) \right] \\ &+ \frac{\alpha}{2m_\mu m_p} \left[Z_\mu \left(2(Z_p + \kappa_p^{\text{had}}) + \frac{m_\mu}{m_p} (Z_p + 2\kappa_p^{\text{had}}) \right) \frac{1}{r^3} \mathbf{L} \cdot \mathbf{S}_p + Z \left(2 + \frac{m_p}{m_\mu} \right) \frac{1}{r^3} \mathbf{L} \cdot \mathbf{S}_\mu \right] \\ &+ \frac{\pi\alpha}{2m_p^2} Z_\mu \left[\frac{4}{3} r_p^2 m_p^2 \right] \delta^{(3)}(\mathbf{r}). \end{aligned} \quad (4.30)$$

For the organization of the computation it is also convenient to split $V^{(2,2)}$ in the following way:

$$V^{(2,2)} = V_{\text{no-VP}}^{(2,2)} + V_{\text{VP}}^{(2,2)}. \quad (4.31)$$

The first term is the potential if we switch off the interaction with the electrons. This is a well defined limit, as it corresponds to the case of muonium. The second term is the correction to the potential associated to the one-loop electron VP. They read:

$$\begin{aligned} V_{\text{no-VP}}^{(2,2)} &= -\frac{4Z\alpha^2}{15} \left(\frac{Z_p^2}{m_p^2} + \frac{Z_\mu^2}{m_\mu^2} + \frac{1}{m_\tau^2} \right) \delta^{(3)}(\mathbf{r}) + \frac{\alpha^2 Z Z_p^2}{2\pi m_p^2} \left(\frac{1}{r^3} \mathbf{L} \cdot \mathbf{S}_p + \frac{4}{3} \pi \ln \left(\frac{m_p^2}{\nu^2} \right) \delta^{(3)}(\mathbf{r}) \right) \\ &+ \frac{\alpha^2 Z Z_\mu^2}{2\pi m_\mu^2} \left(\frac{1}{r^3} \mathbf{L} \cdot \mathbf{S}_\mu + \frac{4}{3} \pi \ln \left(\frac{m_\mu^2}{\nu^2} \right) \delta^{(3)}(\mathbf{r}) \right) + \frac{\alpha^2 Z}{2\pi m_p m_\mu} \left(\frac{Z_p^2}{r^3} \mathbf{L} \cdot \mathbf{S}_p + \frac{Z_\mu^2}{r^3} \mathbf{L} \cdot \mathbf{S}_\mu \right. \\ &+ \left. (Z_p^2 + Z_\mu^2) \left(\frac{8\pi}{3} \mathbf{S}_\mu \mathbf{S}_p \delta^{(3)}(\mathbf{r}) + \frac{\hat{S}_{p\mu}(\hat{\mathbf{r}})}{4} \right) - \frac{14\pi Z}{3} \left(\ln(\nu^2) \delta^{(3)}(\mathbf{r}) + \frac{1}{2\pi} \text{reg} \frac{1}{r^3} \right) \right) \\ &+ \frac{\alpha^2 Z^2 \delta^{(3)}(\mathbf{r})}{m_p^2 - m_\mu^2} \left(4\mathbf{S}_\mu \mathbf{S}_p \ln \left(\frac{m_\mu^2}{m_p^2} \right) - \frac{m_p}{m_\mu} \ln \left(\frac{m_\mu^2}{\nu^2} \right) + \frac{m_\mu}{m_p} \ln \left(\frac{m_p^2}{\nu^2} \right) \right) \\ &- \frac{\delta^{(3)}(\mathbf{r})}{m_p^2} \left(c_3^{\text{had}} - 4c_4^{\text{had}} \mathbf{S}_\mu \mathbf{S}_p + 16Z\pi\alpha d_2^{\text{had}} \right) \\ &+ \frac{Z_\mu^3 \alpha^2 \kappa_p^{\text{had}}}{2\pi m_\mu m_p} \left(\frac{8\pi}{3} \mathbf{S}_\mu \mathbf{S}_p \delta^{(3)}(\mathbf{r}) + \frac{\hat{S}_{p\mu}(\hat{\mathbf{r}})}{4} \right), \end{aligned} \quad (4.32)$$

²Strictly speaking there could still be some $\mathcal{O}(\alpha)$ included in κ_p^{had} with the definition we are using, similarly as what happens with the proton radius.

$$\begin{aligned}
 V_{\text{VP}}^{(2,2)} = & \frac{\alpha^2}{\pi} \int_4^\infty dq^2 \frac{u(q^2)}{q^2} \left\{ \frac{Z_\mu m_\mu^2 + Z_p m_p^2}{8m_\mu^2 m_p^2} \left(4\pi \delta^{(3)}(\mathbf{r}) - \frac{\lambda^2 e^{-\lambda r}}{r} \right) \right. \\
 & + \left(Z_\mu \frac{\mathbf{L} \cdot \mathbf{S}_p}{m_p^2} + Z_p \frac{\mathbf{L} \cdot \mathbf{S}_\mu}{m_\mu^2} \right) \left(\frac{e^{-\lambda r} (1 + \lambda r)}{2r^3} \right) + \frac{Z_p \mathbf{L} \cdot \mathbf{S}_\mu + Z_\mu \mathbf{L} \cdot \mathbf{S}_p}{m_\mu m_p} \frac{e^{-\lambda r} (1 + \lambda r)}{r^3} \\
 & - \frac{Z_p Z_\mu}{4m_\mu m_p} \left(\frac{\lambda^2 e^{-\lambda r}}{r} \left(1 - \frac{\lambda r}{2} \right) + 2p^i \frac{e^{-\lambda r}}{r} \left(\delta_{ij} + \frac{r_i r_j}{r^2} (1 + \lambda r) \right) p^j \right) \\
 & \left. + \frac{1}{m_\mu m_p} \left(-\frac{2}{3} \frac{e^{-\lambda r} \lambda^2}{r} \mathbf{S}_\mu \cdot \mathbf{S}_p + \frac{8}{3} \pi \delta^{(3)}(\mathbf{r}) \mathbf{S}_\mu \cdot \mathbf{S}_p + \frac{e^{-\lambda r}}{4r^3} \left(1 + r\lambda + \frac{r^2 \lambda^2}{3} \right) \hat{S}_{p\mu}(\hat{\mathbf{r}}) \right) \right\}. \tag{4.34}
 \end{aligned}$$

Finally, the $1/m^3$ potential, which we directly consider in position space, just comes from the Taylor expansion of the relativistic expression of the dispersion relation:

$$V^{(3,0)} = -\frac{1}{8} \left(\frac{1}{m_\mu^3} + \frac{1}{m_p^3} \right) \mathbf{p}^4. \tag{4.35}$$

There are no $\mathcal{O}(\alpha/m^3)$ terms.

Chapter 5

The muonic hydrogen Lamb shift and the proton radius

In this chapter we review all the contributions to the energy shift $E(2P_{3/2}) - E(2S_{1/2})$ of $\mathcal{O}(m_r \alpha^5)$, as well as those that scale like $\alpha^6 \times \text{logarithms}$, in the context of pNRQED. Many of the computations were done before. We have checked most of them, and we provide some new analytical expressions.

In order to carry out the computations of this chapter we use the most updated PDG values (Ref. [70]) for the masses and fine structure constant.

$$\begin{aligned} m_e &= 0.510998928(11) \text{ MeV}, \\ m_\mu &= 105.6583715(35) \text{ MeV}, \\ \alpha &= 1/137.035999074(44) \text{ MeV}, \\ m_p &= 938.272046(21) \text{ MeV}, \\ m_\tau &= 1776.82(16) \text{ MeV}, \\ m_\pi &= 139.57018 \text{ MeV}, \\ \Delta &= 293.728 \text{ MeV}, \\ g_A &= 1.25, \\ g_{\pi N\Delta} &= 1.05, \\ F_\pi &= 92.5 \text{ MeV}, \\ b_{1F} &= 3.86. \end{aligned} \tag{5.1}$$

The values of the effective theory parameters $g_{\pi N\Delta}$ and b_{1F} correspond to the leading order expressions of the NR effective theory.

The muonic hydrogen Lamb shift is obtained by the combined use of NR quantum mechanics perturbation theory and perturbative quantum field theory computations (when ultrasoft photons show up). As we have definite counting rules to assess the relative importance of the different terms we know when we can stop computing. The application of this program to the muonic hydrogen produces the contributions we use in our analysis, listed in Table 5.5. Most of the results were already available in the literature, we have checked many. We now discuss them focusing on the novel aspects. Note that, even though most of the contributions can be associated to a pure QED calculation, the hadronic effects are also included in this computation. Their effects are

included in the NRQED Wilson coefficients discussed in Sec. 2.2, and are encoded in the different terms of the potential in the Lagrangian of pNRQED discussed in Sec. 4.

We define the following function which we will need for the $n = 2$ Lamb shift between the S - and P -wave bound states:

$$\rho(r) \equiv \rho_{2P}(r) - \rho_{2S}(r) = (m_r Z\alpha)^{3/2} e^{-m_r Z\alpha r} \left[\frac{1}{12} (m_r Z\alpha r)^2 - \left(1 - \frac{m_r Z\alpha r}{2} \right)^2 \right], \quad (5.2)$$

where ρ_{nl} is the NR charge density of the nl state.

We will use the following notation:

$$\delta E_{nlj}^V = \langle nlj | V | nlj \rangle \quad (5.3)$$

and

$$\delta E_L^V = \langle 2P_{1/2} | V | 2P_{1/2} \rangle - \langle 2S_{1/2} | V | 2S_{1/2} \rangle \quad (5.4)$$

for the correction to the Lamb shift of a generic potential V .

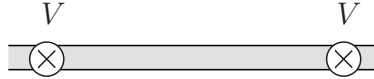


Figure 5.1: *2nd order perturbation theory of the bound-state Green function generated by a generic potential V .*

We will represent the second order perturbation theory correction to the bound-state Green function generated by a generic potential V by Fig. 5.1, where the double line represents the bound state and the vertices (local in time) the potentials. In case we want to obtain the associated energy shift we will compute objects like

$$\begin{aligned} \delta E_{nlj}^{V \times V} &= \langle \psi_{nlj} | V \frac{1}{(E_n - h)'} V | \psi_{nlj} \rangle \\ &= \int d\mathbf{r}_2 d\mathbf{r}_1 \psi_{nlj}^*(\mathbf{r}_2) V(\mathbf{r}_2) G'_{nl}(\mathbf{r}_1, \mathbf{r}_2) V(\mathbf{r}_1) \psi_{nlj}(\mathbf{r}_1), \end{aligned} \quad (5.5)$$

where

$$\frac{1}{(E_n - h)'} = \lim_{E \rightarrow E_n} \left(\frac{1}{E - h} - \frac{1}{E - E_n} \right), \quad h = \frac{\mathbf{p}^2}{2m_r} - \frac{\alpha}{r}, \quad (5.6)$$

$$G'_{nl}(\mathbf{r}_1, \mathbf{r}_2) \equiv \langle \mathbf{r}_1 | \frac{1}{(E_{nl} - h)'} | \mathbf{r}_2 \rangle \equiv \lim_{E \rightarrow E_n} \left(G(\mathbf{r}_1, \mathbf{r}_2; E) - \frac{|\psi_{nl}|^2}{E - E_n} \right), \quad (5.7)$$

$\psi_{nl}(\mathbf{r})$ is the bound state wave function of the (nl) -state and E_n is the energy of the state, h is the Hamiltonian in the Schrödinger equation and $G(\mathbf{r}_1, \mathbf{r}_2; E)$ is the Coulomb Green function. In the case of different potentials we use objects analogous to Eq. (5.5).

In order to perform the computation it is specially useful to use the following representation for a negative energy $E = -\frac{m_r Z^2 \alpha^2}{2\lambda^2}$ of the Coulomb Green function (see for instance, the appendix of Ref. [103]):

$$G(\mathbf{r}_1, \mathbf{r}_2; E) = \frac{-m_r^2 Z \alpha}{\lambda \pi} \sum_{l=0}^{\infty} (2l+1) P_l\left(\frac{\mathbf{r}_1 \cdot \mathbf{r}_2}{r_1 r_2}\right) \left(\frac{2m_r Z \alpha}{\lambda} r_1\right)^l \left(\frac{2m_r Z \alpha}{\lambda} r_2\right)^l e^{-\frac{m_r Z \alpha}{\lambda}(r_1+r_2)} \sum_{s=0}^{\infty} \frac{L_s^{2l+1}\left(\frac{2m_r Z \alpha}{\lambda} r_1\right) L_s^{2l+1}\left(\frac{2m_r Z \alpha}{\lambda} r_2\right) s!}{(s+l+1-\lambda)(s+2l+1)!}. \quad (5.8)$$

Then $G'_{nl}(\mathbf{r}_1, \mathbf{r}_2)$ is just the Coulomb Green function evaluated at $\lambda = n + \delta\lambda$, and subtracting the pole. In the case where the potentials that appear in Eq. (5.5) are only functions of the modulus of \mathbf{r} (i.e. they are invariant under rotations), the sum over l reduces to the single term that matches the angular momentum l of the bound state.

Obviously a similar discussion applies to higher order corrections from perturbation theory, and also similar expressions follow for the Lamb shift.

We will now study each relevant contributing term separately, both in the $1/m_\mu$ and in the α expansions. We will write explicitly the Z_μ, Z_p, Z dependence except for the dependence on Z that appears in the combination $m_r Z \alpha / m_e$ in the numerical integrals we perform. Therefore, such numerical values will change for different muonic atoms.

5.1 Corrections from the static potential: $V^{(0)}$

5.1.1 One-loop Vacuum Polarization: $\delta E_L^{V_{\text{VP}}^{(0,2)}} \sim \mathcal{O}(m_\mu \alpha^3)$

The Lamb shift in muonic hydrogen, unlike in hydrogen, receives its most important contribution from the electron VP. This is due to the fact that the typical atomic momentum of the muonic hydrogen is $m_\mu \alpha$, which is of the order of the electron mass: $m_\mu \alpha \sim 1.5 m_e$. This effect comes from the modification of the photon propagator, as we have already seen in the previous chapter (see Fig. 4.1). In order to compute it, we must take the first order in α of the expansion of $\Pi(-\mathbf{k}^2)$.

The integral in r and x can be done analytically. The result reads (see for instance Ref. [104])

$$\begin{aligned} \delta E_L^{V_{\text{VP}}^{(0,2)}} &= \int d^3 r V_{\text{VP}}^{(0,2)}(r) \rho(r) = \\ &= \frac{\alpha}{\pi} (Z\alpha)^2 m_r \left[\frac{8\pi\beta^3}{3} + \frac{1 - 26\beta^2 + 352\beta^4 - 768\beta^6}{18(1-4\beta^2)^2} \right. \\ &\quad \left. + \frac{4\beta^4(15 - 80\beta^2 + 128\beta^4)}{3(1-4\beta^2)^{5/2}} \ln\left(\frac{1 - \sqrt{1-4\beta^2}}{2\beta}\right) \right] = m_r \alpha^3 Z^2 0.005555 = 205.00737 \text{ meV}, \end{aligned} \quad (5.9)$$

where

$$\beta = \frac{m_e}{(Z\alpha m_r)} = 0.7373836. \quad (5.10)$$

Eq. (5.9) gives the first entry in Table 5.5.

For the case $m_e \ll Z\alpha m_r$ the computation can be checked with the result of heavy quarkonium. We have checked it. We also observe that $m_e \ll Z\alpha m_r$ is a bad approximation to this quantity, so we will not consider it further but only for checking. Actually, neither the $\beta \ll 1$ nor the $\beta \gg 1$ give a good approximation to Eq. (5.9).

5.1.2 Two-loop Vacuum Polarization: $\delta E_L^{V_{\text{VP}}^{(0,3)}} \sim \mathcal{O}(m_r \alpha^4)$

We now compute the $\mathcal{O}(m_r \alpha^4)$ contribution associated to the two-loop static potential. We obtain the second entry of Table 5.5:

$$\delta E_L^{V_{\text{VP}}^{(0,3)}} = m_r \alpha^4 Z^2 0.005599695 = 1.50795 \text{ meV}. \quad (5.11)$$

It agrees with the result of Pachucki's Ref. [105] with 5 significant digits.

We observe that this contribution is significantly bigger than the one coming from double insertions of the leading VP potential discussed in the next section. In a different context a similar situation has been found in heavy quarkonium physics, Ref. [106].

5.1.3 Double Vacuum Polarization: $\delta E_L^{V_{\text{VP}}^{(0,2)} \times V_{\text{VP}}^{(0,2)}} \sim \mathcal{O}(m_r \alpha^4)$

The second $\mathcal{O}(m_r \alpha^4)$ correction is generated by the second order perturbation theory of the $V_{\text{VP}}^{(0,2)}$ potential. Following Eq. (5.5) and the associated discussion we obtain

$$\begin{aligned} \delta E_L^{V_{\text{VP}}^{(0,2)} \times V_{\text{VP}}^{(0,2)}} &= \langle \psi_{2p} | V_{\text{VP}}^{(0,2)} \frac{1}{(E_{2p} - h)'} V_{\text{VP}}^{(0,2)} | \psi_{2p} \rangle - \langle \psi_{2s} | V_{\text{VP}}^{(0,2)} \frac{1}{(E_{2s} - h)'} V_{\text{VP}}^{(0,2)} | \psi_{2s} \rangle \\ &= (Z\alpha)^2 m_r \left(\frac{\alpha}{\pi} \right)^2 \int_4^\infty \int_4^\infty d\rho_1^2 d\rho_2^2 \frac{u(\rho_1^2)}{\rho_1^2} \frac{u(\rho_2^2)}{\rho_2^2} \\ &\times \left(\frac{[1 + \beta(\rho_1 + \rho_2)]^{-3} \beta^2 Q}{12(1 + \beta\rho_1)^5 (1 + \beta\rho_2)^5} + \frac{\beta^2 [\rho_1^2 + \rho_2^2 + 2(\beta\rho_1\rho_2)^2]}{(1 + \beta\rho_1)^4 (1 + \beta\rho_2)^4} \ln \left(\frac{(1 + \beta\rho_1)(1 + \beta\rho_2)}{1 + \beta(\rho_1 + \rho_2)} \right) \right), \end{aligned} \quad (5.12)$$

where

$$\begin{aligned} Q &= 12\beta^8 \rho_1^6 \rho_2^4 + 12\beta^8 \rho_1^5 \rho_2^5 + 36\beta^7 \rho_1^6 \rho_2^3 + 120\beta^7 \rho_1^5 \rho_2^4 + 12\beta^6 \rho_1^6 \rho_2^2 + 84\beta^6 \rho_1^5 \rho_2^3 + 74\beta^6 \rho_1^4 \rho_2^4 \\ &+ 33\beta^5 \rho_1^6 \rho_2 + 39\beta^5 \rho_1^5 \rho_2^2 - 62\beta^5 \rho_1^4 \rho_2^3 + 9\beta^4 \rho_1^6 + 111\beta^4 \rho_1^5 \rho_2 - 33\beta^4 \rho_1^4 \rho_2^2 - 142\beta^4 \rho_1^3 \rho_2^3 \\ &+ 24\beta^3 \rho_1^5 + 99\beta^3 \rho_1^4 \rho_2 - 189\beta^3 \rho_1^3 \rho_2^2 + 18\beta^2 \rho_1^4 - 3\beta^2 \rho_1^3 \rho_2 - 75\beta^2 \rho_1^2 \rho_2^2 - 24\beta \rho_1^2 \rho_2 - 3\rho_1^2 \\ &+ (\rho_1 \rightarrow \rho_2). \end{aligned} \quad (5.13)$$

This expression corrects several mistakes in Eq. (11) of Ref. [107] (which however gets the correct numerical result) and yields the 3rd entry of Table 5.5:

$$\delta E_L^{V_{\text{VP}}^{(0,3)} \times V_{\text{VP}}^{(0,3)}} = m_r \alpha^4 Z^2 \left(\frac{\alpha}{\pi} \right)^2 0.0055304 = 0.150897 \text{ meV}. \quad (5.14)$$

This numerical value agrees with Ref. [105] within the significant digits given in this reference.

5.1.4 Static potential (vacuum polarization): $\delta E_L \sim \mathcal{O}(m_r \alpha^5)$

The first four entries in Table 5.5 are the contributions to the Lamb shift associated to the electron VP corrections to the static potential $V^{(0)}$. Specially difficult is the 4th entry, as it corresponds to the three-loop static potential and to the third order iteration in perturbation theory. It was computed (numerically) in Ref. [101] (see also Ref. [108] for a small correction). It can be split into the following contributions:

$$\delta E_L^{V_{\text{VP}}^{(0,4)}} = m_r \alpha^5 Z^2 0.002694 = 5.295 \times 10^{-3} \text{ meV}. \quad (5.15)$$

5.2. Corrections from the $1/m_\mu$ potentials without vacuum polarization

The contribution from 2nd order perturbation theory yields Ref. [101] (this result includes all permutations):

$$\delta E_L^{V_{\text{VP}}^{(0,2)} \times V_{\text{VP}}^{(0,3)}} + \delta E_L^{V_{\text{VP}}^{(0,3)} \times V_{\text{VP}}^{(0,2)}} = m_r \alpha^5 Z^2 0.00109562 = 2.153 \times 10^{-3} \text{meV}. \quad (5.16)$$

And the contribution from 3rd order perturbation theory reads Refs. [101, 108]:

$$\delta E_L^{V_{\text{VP}}^{(0,2)} \times V_{\text{VP}}^{(0,2)} \times V_{\text{VP}}^{(0,2)}} = m_r \alpha^5 Z^2 0.0000377 = 0.0741 \times 10^{-3} \text{meV}. \quad (5.17)$$

The sum of the above three terms gives the final contribution:

$$\delta E_{L,\text{static}}^{\mathcal{O}(\alpha^5),\text{VP}} = 0.11868 m_r Z^2 \alpha^2 \left(\frac{\alpha}{\pi} \right)^3 = 0.00752 \text{meV}, \quad (5.18)$$

which is the 4th entry of Table 5.5. The computation has been done independently for a time-like ($q^2 > 0$) and a space-like ($q^2 < 0$) momentum of the photon. This last one involves the integration of the whole VP function $\Pi(q^2)$ to the desired order, and the other involves just its imaginary part evaluated at $q^2 = t m_e^2$.

5.1.5 Static potential (light-by-light): $\delta E_L^{V_{\text{LbL}}^{(0,4)}} \sim \mathcal{O}(m_r \alpha^5)$

The 5th entry of Table 5.5 corresponds to the contribution associated to the light-by-light corrections to the static potential $V^{(0)}$, i.e. to V_{LbL} (see Eq. (4.14)). It was obtained in Ref. [102], where a very long explanation was made to argue that the light-by-light contributions could be computed in the static approximation. This is evident in the EFT, as they correspond to a correction to the static potential, as already stated in Ref. [60].

The result for this contribution, given in Ref. [102], is

$$\begin{aligned} \delta E_L^{V_{\text{LbL}}^{(0,4)}} &= -m_r \alpha^5 Z^2 10^{-3} \left[(Z_p^2 + Z_\mu^2) 0.5185 - Z_p Z_\mu 0.5852 \right] \\ &= -m_r \alpha^5 0.000452 = -0.00089(2) \text{meV}. \end{aligned} \quad (5.19)$$

5.2 Corrections from the $1/m_\mu$ potentials without vacuum polarization

We jump directly into the $V^{(2)}$ potential, since we already discussed that the $V^{(1)}$ potential produces corrections of, utmost, $\mathcal{O}(m_r \alpha^6)$ and are then beyond the accuracy of our interest.

We now compute the corrections to the energy and Lamb shift associated to the potentials in Eqs. (4.24) and (4.25) to $\mathcal{O}(m_r \alpha^5)$. In other words, we compute the relativistic corrections that are not associated to the VP.

5.2.1 Relativistic corrections: $\delta E_L \sim \mathcal{O}(m_r \alpha^4)$

The potential in Eq. (4.24) is the EFT generalization of the Breit potential. Note that it is in this potential where the hadronic corrections arise at $\mathcal{O}(m_r \alpha^5 \frac{m_\mu^2}{m_p^2})$ (we will consider them in more detail later on). The energy associated to this potential for any given quantum numbers reads

$$\begin{aligned}
 \delta E_{nljj_\mu}^{V_{\text{tree}}^{(2)}} &= \frac{m_r^3 Z^3 \alpha^4}{2n^3 m_\mu^2} \left\{ Z_p c_D^{(\mu)} \delta_{l0} + Z_p c_S^{(\mu)} \frac{(1 - \delta_{l0})}{l(l+1)(2l+1)} d_{j_\mu, l} \right. \\
 &+ 2 \frac{m_\mu}{m_p} \left(Z \left(\frac{1}{n} + \frac{(1+4l)\delta_{l0} - 3}{2l+1} \right) + c_F^{(\mu)} c_F^{(p)} \left(\frac{(1 - \delta_{l0})\delta_{s1}}{2l(l+1)(2l+1)} c_{j,l} - 2\delta_{l0} + \frac{8}{3}\delta_{l0}\delta_{s1} \right) \right. \\
 &+ \frac{(1 - \delta_{l0})}{l(l+1)(2l+1)} \left(Z_p c_F^{(\mu)} d_{j_\mu, l} + Z_\mu c_F^{(p)} (2h_{j,l}\delta_{s1} - d_{j_\mu, l}) \right) \\
 &+ \left. \left. \frac{m_\mu^2}{m_p^2} \left(Z_\mu c_D^{(p)} \delta_{l0} + Z_\mu c_S^{(p)} \frac{(1 - \delta_{l0})}{l(l+1)(2l+1)} (2\delta_{s1} h_{j,l} - d_{j_\mu, l}) \right) \right\} \right. \\
 &- \left. \frac{m_r^3 Z^3 \alpha^3}{\pi n^3} \delta_{l0} \left\{ \frac{1}{m_p^2} (c_3 + (3 - 4\delta_{s1})c_4) + 16\pi Z \alpha \left(\frac{d_2}{m_p^2} + \frac{d_2^{(\mu)}}{m_\mu^2} + \frac{d_2^{(\tau)}}{m_\tau^2} \right) \right\}, \quad (5.20)
 \end{aligned}$$

where

$$c_{j,l} = 2 \begin{cases} -\frac{l+1}{2l-1} & j = l-1, \\ 1 & j = l, \\ -\frac{l}{2l+3} & j = l+1, \end{cases} \quad (5.21)$$

$$h_{j,l} = \begin{cases} -(l+1) & j = l-1, \\ -1 & j = l, \\ l & j = l+1, \end{cases} \quad (5.22)$$

$$d_{j_1, l} = \begin{cases} -(l+1) & j_1 = l - \frac{1}{2}, \\ l & j_1 = l + \frac{1}{2}. \end{cases} \quad (5.23)$$

The energy has been expressed in terms of the total angular momentum $\mathbf{J} = \mathbf{L} + \mathbf{S}$ (where $\mathbf{S} = \mathbf{S}_\mu + \mathbf{S}_p$) and in terms of the angular momentum of the muon $\mathbf{J}_\mu = \mathbf{L} + \mathbf{S}_\mu$. The basis is taken in terms of the lightest particle because it is the most convenient in which to express the energy shift. This is so since the lightest particle gives rise to larger effects in the terms which involve the ratio of the masses, and this comes out more clearly when using this basis. In our notation, the ill-defined quantity $(1 - \delta_{l0})/l \rightarrow 0$ when $l \rightarrow 0$.

In the last line of Eq. (5.20) we have still included the contribution associated to the tau VP. As its numerical effect is very small we will neglect it in the following.

$\delta E_{nljj_\mu}^{V_{\text{tree}}^{(2)}}$ encodes all the $\mathcal{O}(m_r \alpha^4)$ corrections to the spectrum due to the $1/m_\mu^2$. It also includes higher order effects through the $\mathcal{O}(\alpha)$ terms in the NRQCD Wilson coefficients. If we set them

to zero, we obtain the non-trivial leading-order contribution:

$$\begin{aligned}
 \delta E_{nlj\mu}^{V_{\text{tree}}(2)} &= \frac{m_r^3 Z^3 \alpha^4}{2n^3 m_\mu^2} \left\{ Z \delta_{l0} + Z \frac{(1 - \delta_{l0})}{l(l+1)(2l+1)} d_{j\mu,l} \right. \\
 &\quad + 2 \frac{m_\mu}{m_p} \left(Z \left(\frac{1}{n} + \frac{(1+4l)\delta_{l0} - 3}{2l+1} \right) \right. \\
 &\quad + Z_\mu (Z_p + \kappa_p^{\text{had}}) \left(\frac{(1 - \delta_{l0})\delta_{s1}}{2l(l+1)(2l+1)} c_{j,l} - 2\delta_{l0} + \frac{8}{3}\delta_{l0}\delta_{s1} \right) \\
 &\quad + \frac{(1 - \delta_{l0})}{l(l+1)(2l+1)} \left(Z d_{j\mu,l} + Z_\mu (Z_p + \kappa_p^{\text{had}}) (2h_{j,l}\delta_{s1} - d_{j\mu,l}) \right) \Big) \\
 &\quad + \frac{m_\mu^2}{m_p^2} \left(Z \delta_{l0} + Z_\mu (Z_p + 2\kappa_p^{\text{had}}) \frac{(1 - \delta_{l0})}{l(l+1)(2l+1)} (2\delta_{s1} h_{j,l} - d_{j\mu,l}) \right) \Big\} \\
 &\quad + \left[\frac{4}{3} r_p^2 m_p^2 \right] \frac{\pi \alpha}{2m_p^2} Z_\mu \delta_{l0} \frac{1}{\pi} \left(\frac{m_r Z \alpha}{n} \right)^3. \tag{5.24}
 \end{aligned}$$

We shall also take into account the correction to this order in α coming from the perturbative expansion of the relativistic kinetic term, i.e. from Eq. (4.35), which leads to the energy shift:

$$\delta E_{nl}^{V_{nl}^{(3,0)}} = \frac{m_r^3 Z^4 \alpha^4}{2m_\mu^2} \left[\left(1 - \frac{m_\mu}{m_p} + \left(\frac{m_\mu}{m_p} \right)^2 \right) \left(\frac{3}{4n^4} - \frac{2}{n^3(2l+1)} \right) \right]. \tag{5.25}$$

Summing up the contributions of Eqs. (5.24) and (5.25) we get for the transition of the $2S^{1/2} \rightarrow 2P^{1/2}$ states:

$$\delta E_L^{V_L^{(2,1)}} + \delta E_L^{V_L^{(3,0)}} = \frac{m_r^3 \alpha^4 Z^4}{48m_p^2} - \frac{m_r^3 \alpha^4 Z^3 Z_\mu}{16m_p^2} \left[\frac{4}{3} r_p^2 m_p^2 \right] = \left(0.05747 - 5.1975 \frac{r_p^2}{\text{fm}^2} \right) \text{meV}. \tag{5.26}$$

The first term agrees both analytically and numerically with the one obtained in Ref. [105]. We shall remark that it has an extra $\frac{m_\mu^2}{m_p^2}$ suppression factor, which was to be expected since this correction does not contribute for the case of the hydrogen (in the infinite proton mass limit). The 2nd term is the leading contribution associated to the proton radius. Both contributions appear as entries vi) and xi) in Table 5.5.

5.2.2 Relativistic corrections: $\delta E_L \sim \mathcal{O}(m_r \alpha^5)$

We now compute the $\mathcal{O}(m_r \alpha^5)$ contributions to the spectrum with no electron VP. As we have already mentioned, this is a well defined quantity, as it amounts to the corresponding evaluation of the muonium (μe) spectrum (if we turn off the hadronic effects). Taking the $\mathcal{O}(m_r \alpha^5)$ corrections generated from Eq. (5.20) (typically generated by the $\mathcal{O}(\alpha)$ corrections of the NRQCD Wilson coefficients) plus the energy shift produced by the expectation value of Eq. (4.25), we obtain

(note that this computation has been done in the $\overline{\text{MS}}$ scheme)

$$\begin{aligned}
 \delta E_{nljj_\mu}^{V_{\text{no-VF}}^{(2,2)}} &= \frac{m_r^3 Z^3 \alpha^5}{2\pi n^3} \left\{ \frac{ZZ_\mu^2}{m_\mu^2} \left(\frac{4}{3} \left(-\frac{2}{5} + \ln \left(\frac{m_\mu^2}{\nu^2} \right) \right) \delta_{l,0} + \frac{1 - \delta_{l,0}}{l(l+1)(2l+1)} d_{j_\mu, l} \right) \right. \\
 &+ \frac{Z_p^2 Z}{m_p^2} \left(\frac{4}{3} \left(-\frac{2}{5} + \ln \left(\frac{m_p^2}{\nu^2} \right) \right) \delta_{l,0} + \frac{1 - \delta_{l,0}}{l(l+1)(2l+1)} (2\delta_{s,1} h_{j,l} - d_{j_\mu, l}) \right) \\
 &+ \frac{1}{m_\mu m_p} \left(-2 \left(ZZ_\mu^2 + ZZ_p^2 - \frac{Z^2}{3} + Z_\mu^3 \kappa_p^{\text{had}} \right) \delta_{l,0} - \frac{14}{3} Z^2 \frac{1 - \delta_{l,0}}{l(l+1)(2l+1)} \right. \\
 &+ \frac{14}{3} Z^2 \delta_{l,0} \left(1 - \frac{1}{n} + 2S_1(n) + 2 \ln \left(\frac{2\alpha m_r}{n\nu} \right) \right) + \frac{8}{3} \left(ZZ_\mu^2 + ZZ_p^2 + Z_\mu^3 \kappa_p^{\text{had}} \right) \delta_{s,1} \delta_{l,0} \\
 &+ \frac{1 - \delta_{l,0}}{l(l+1)(2l+1)} \left(\frac{1}{2} \left(ZZ_\mu^2 + ZZ_p^2 + Z_\mu^3 \kappa_p^{\text{had}} \right) \delta_{s,1} c_{j,l} \right. \\
 &+ \left. \left. 2ZZ_p^2 \delta_{s,1} h_{j,l} + Z(Z_\mu^2 - Z_p^2) d_{j_\mu, l} \right) \right) + \frac{2Z^2 \delta_{l,0}}{m_\mu^2 - m_p^2} \left(\frac{m_p}{m_\mu} \left(\frac{1}{3} + \ln \left(\frac{m_\mu^2}{\nu^2} \right) \right) \right. \\
 &+ \left. \frac{m_\mu}{m_p} \left(\frac{1}{3} + \ln \left(\frac{m_p^2}{\nu^2} \right) \right) + \ln \left(\frac{m_\mu^2}{m_p^2} \right) (3 - 4\delta_{s,1}) - \frac{8Z_p Z_\mu}{15m_\tau^2} \delta_{l,0} \right\} \\
 &- \frac{m_r^3 Z^3 \alpha^3}{\pi n^3} \delta_{l,0} \left[\frac{1}{m_p^2} \left(c_3^{\text{had}} + (3 - 4\delta_{s,1}) c_4^{\text{had}} \right) + 16\pi\alpha \frac{d_2^{\text{had}}}{m_p^2} \right], \tag{5.27}
 \end{aligned}$$

where $S_1(n)$ is the n harmonic number defined in Appendix A. Note that in this expression the hadronic corrections that scale as α^2 : c_3^{had} , c_4^{had} and αd_2^{had} are also included, as they also produce an $m_r \alpha^5$ energy shift.

5.3 Ultrasoft effects: $\delta E_L \sim \mathcal{O}(m_r \alpha^5)$

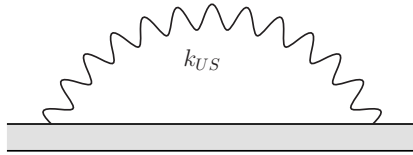


Figure 5.2: Correction due to ultrasoft photons.

The interaction of the bound state with ultrasoft photons (symbolically pictured in Fig. 5.2) produces an energy shift of $\mathcal{O}(m_r \alpha^5)$. It has been computed in the $\overline{\text{MS}}$ in Refs. [57, 58] for the case of hydrogen and positronium respectively. The application to muonic hydrogen is trivial, as we only have to rescale for the reduced mass. On top of that we introduce the changes for the case of particles with general charges Z_μ , Z_p . Finally, the energy shift reads (in the $\overline{\text{MS}}$ scheme)

$$\begin{aligned}
 \delta E_{nl}^{\text{US}} &= \frac{2}{3} \left(\frac{Z_\mu m_p + Z_p m_\mu}{m_p + m_\mu} \right)^2 \frac{\alpha}{\pi} \left(\left(\ln \frac{\nu}{m_r} + \frac{5}{6} - \ln 2 \right) \left(\frac{Ze^2}{2} \right) \frac{|\phi_n(0)|^2}{m_r^2} \right. \\
 &- \left. \sum_{n' \neq n} \left| \langle n | \frac{p}{m_r} | n' \rangle \right|^2 (E_n - E_{n'}) \ln \frac{m_r}{|E_n - E_{n'}|} \right)
 \end{aligned}$$

$$\begin{aligned} &\equiv \frac{m_r Z^4 \alpha^5}{n^3 \pi} \left(\frac{Z_\mu m_p + Z_p m_\mu}{m_p + m_\mu} \right)^2 \left(\delta_{l,0} \left(-\frac{4}{3} \left(\ln R(n, l) + \ln \frac{m_r Z^2 \alpha^2}{\nu} \right) + \frac{10}{9} \right) \right. \\ &\quad \left. - (1 - \delta_{l,0}) \frac{4}{3} \ln R(n, l) \right), \end{aligned} \quad (5.28)$$

where $|\phi_n(0)|^2 = \frac{1}{\pi} \left(\frac{m_r Z \alpha}{n} \right)^3$ and $\ln R(n, l)$ are the Bethe logarithms and are implicitly defined by the equality with Eq. (5.28). For their numerical values for the $2S$ and $2P$ states we have used the values quoted in Ref. [105].

We observe that $\delta E_{n,l}^{\text{US}}$ is factorization scale dependent. Such dependence cancels with the scale dependence of Eq. (5.27). The sum of both contributions gives all the $\mathcal{O}(m_r \alpha^5)$ corrections to the spectrum that are not associated to the electron VP:

$$\delta E_{nlj\mu}^{\mathcal{O}(\alpha^5), \text{no-VP}} = \delta E_{nlj\mu}^{V_{\text{no-VP}}(2,2)} + \delta E_{nl}^{\text{US}}, \quad (5.29)$$

and is independent of the factorization scale. It can also be split into the different hadronic contributions, associated to the fact that the proton is not point-like, and the $\mathcal{O}(\alpha^5)$ contribution to the spectrum of two point-like particles (relevant for muonium) in the following way:

$$\delta E_{nlj\mu}^{\mathcal{O}(\alpha^5), \text{no-VP}} = \delta E_{nlj\mu, \text{point-like}}^{\mathcal{O}(\alpha^5), \text{no-VP}} + \delta E_{nlj\mu, d_2^{\text{had}}}^{\mathcal{O}(\alpha^5), \text{no-VP}} + \delta E_{nlj\mu, c_3^{\text{had}}}^{\mathcal{O}(\alpha^5), \text{no-VP}} + \delta E_{nlj\mu, c_4^{\text{had}}}^{\mathcal{O}(\alpha^5), \text{no-VP}}. \quad (5.30)$$

Similar equations follow for the Lamb shift energy splitting: $\delta E_L^{\mathcal{O}(\alpha^5), \text{no-VP}}$, although in this last case the contribution proportional to c_4^{had} vanishes, since the spin-dependent term does not contribute to the average energy over polarizations.

The above computation keeps the complete proton and muon mass dependence. It is interesting to see the convergence of the m_μ/m_p expansion. We do so for $\delta E_{L, \text{point-like}}^{\mathcal{O}(\alpha^5), \text{no-VP}}$, which has a non-trivial dependence on this ratio. The first orders of the expansion in this ratio can be found in Table 5.1, where one can observe a clear convergence.

$\mathcal{O}(m_\mu \alpha^5) \frac{m_\mu^n}{m_p^n}$	$\delta E_{L, \text{point-like}}^{\mathcal{O}(\alpha^5), \text{no-VP}}$
$n = 0$	-0.900 meV
$n = 1$	0.226 meV
$n = 2$	-0.054 meV
$n = 3$	0.010 meV

Table 5.1: *Different orders of the expansion in $\frac{m_\mu^n}{m_p^n}$ for $\delta E_{L, \text{point-like}}^{\mathcal{O}(\alpha^5), \text{no-VP}}$.*

Summing up to all orders, leads to the following $\mathcal{O}(\alpha^5)$ energy contribution to the Lamb shift

$$\delta E_{L, \text{point-like}}^{\mathcal{O}(\alpha^5), \text{no-VP}} = -0.71896 \text{ meV}, \quad (5.31)$$

which corresponds to the 7th entry of Table 5.5. This result is very similar to the one computed by Pachucki's Ref. [105], where these effects sum up to $E(2P_{1/2} - 2S_{1/2}) = -0.663 - 0.045 - 0.010 = -0.718 \text{ meV}$ at $\mathcal{O}(m_\mu \alpha^5)$. The difference between both computations is the inclusion of the Tau VP plus a finite term proportional to $1/m_p^2$ in our computation. The latter is due to the fact that Eq.(51) in Ref. [105] is only computed with logarithmic accuracy, i.e. the finite terms are missing.

5.4 $1/m_\mu^2$ hadronic corrections: $\delta E_L \sim \mathcal{O}(m_r \alpha^5)$

We now consider the hadronic corrections. The energy shift associated to the hadronic VP can be fully obtained from dispersion relations (Ref. [66]) and reads

$$\delta E_{L,d_2^{\text{had}}}^{\mathcal{O}(\alpha^5),\text{no-VP}} = \frac{16\alpha Z d_2^{\text{had}}}{m_p^2} \left(\frac{m_r Z \alpha}{2} \right)^3 = 0.0111(2) \text{ meV}, \quad (5.32)$$

which corresponds to the 14th entry of Table 5.5.

Now we will focus on the energy shift associated to c_3^{had} , i.e. the hadronic contribution of TPE. Using the value found in Eq. (2.32) we obtain

$$\delta E_L^{\text{TPE}} \equiv \delta E_{L,c_3^{\text{had}}}^{\mathcal{O}(\alpha^5),\text{no-VP}} = \frac{c_3^{\text{had}}}{m_p^2} \frac{1}{\pi} \left(\frac{m_r Z \alpha}{2} \right)^3 = 0.0344(125) \text{ meV}, \quad (5.33)$$

which corresponds to the 15th entry of Table 5.5. The energy shift associated to the TPE is typically split into its Born and polarizability contributions. For ease of comparison with previous results we compute it in the same way (see discussion in Chapter 3). Now we present our results each contribution and compare them with other determinations.

First we obtain the Born contribution to δE_L^{TPE} , from the EFT.

$$\delta E_L^{\text{Born}} = \frac{c_{3,\text{Born}}}{m_p^2} \frac{1}{\pi} \left(\frac{m_r \alpha}{2} \right)^3, \quad (5.34)$$

We quote our results in Table 5.2. The pure chiral result was already obtained in Ref. [60]. The $\pi\&\Delta$ result corrects the evaluation made in that reference due to the error in its Eq. (61). Note that the new result is much more convergent, since the correction associated to the Delta is much smaller. On the other hand our result is now much more different with respect to standard values obtained from dispersion relations. We quote two of them in Table 5.2. One may wonder whether such difference is due to relativistic corrections. An estimate of the relativistic effects can be obtained from the analysis made in Ref. [105], which, however, is based on dipole form factors parameterizations. The difference between the relativistic and NR expression was found to be small ($\sim 3\mu\text{eV}$). It should be checked that this feature holds with different parameterizations. If so, the difference seems to be mainly due to the computation of the Zemach correction (see Table 3.1 and the discussion above).

μeV	DR	Ref. [109]	Ref. [110]	HBET	Ref. [60](π)	($\pi\&\Delta$)
δE_L^{Born}		23.2(1.0)	24.7(1.6)		10.1(5.1)	8.3(4.3)

Table 5.2: Predictions for the Born contribution to the $n = 2$ Lamb shift. The first two entries correspond to dispersion relations. The last two entries are the predictions of HBET: The 3rd entry is the prediction of HBET at leading order (only pions) and the last entry is the prediction of HBET at leading order and NLO (pions and Deltas).

We now look at the contribution from the polarizability term. The pure pion contribution was already found in Ref. [61], which we confirm. Our full prediction including the Delta effects

reads

$$\delta E_L^{\text{pol}} = \frac{c_{3,\text{pol}}}{m_p^2} \frac{1}{\pi} \left(\frac{m_r \alpha}{2} \right)^3 = 18.51(\pi\text{-loop}) - 1.58(\Delta\text{-tree}) + 9.25(\pi\Delta\text{-loop}) = 26.2(10.0)\mu\text{eV}. \quad (5.35)$$

In Table 5.3 we compare our determination with previous results. Most of them are obtained by a combination of dispersion relations plus some modelling of the subtraction term that we discuss below. The analysis of Ref. [72] has a different status. In this reference the polarizability correction was computed using $B\chi\text{PT}$ with only pions. Such computation treats the baryon relativistically. The result incorporates some subleading effects, which are sometimes used to give an estimate of higher order effects in HBChPT . Nevertheless, the computation also assumes that a theory with only baryons and pions is appropriate at the proton mass scale. This should be taken with due caution. Still, it would be desirable to have a deeper theoretical understanding of this difference, which may signal that relativistic corrections are important for the polarizability correction. In any case, the $B\chi\text{PT}$ computation differs of our chiral result by around 50% (this means around 1.5 times the error we use for the chiral contribution, once the Delta is incorporated in the calculation), which we consider reasonable.

We now combine the contribution from the Born and polarizability terms and summarize our final results for δE_L^{TPE} :

$$\delta E_L^{\text{TPE}} = \delta E_L^{\text{Born}} + \delta E_L^{\text{pol}} = 28.59(\pi) + 5.86(\pi\&\Delta) = 34.4(12.5)\mu\text{eV}. \quad (5.36)$$

We would like to emphasize that this result is a pure prediction of the EFT. It is also the most precise expression that can be obtained in a model independent way, since $\mathcal{O}(m_\mu \alpha^5 \frac{m_\mu^3}{\Lambda_{\text{QCD}}^3})$ effects are not controlled by the chiral theory and would require new counterterms. Our number is only marginally bigger than $\delta E_L^{\text{TPE}} = 33(2)\mu\text{eV}$ Ref. [73]. This number is the one used in Ref. [20] for its determination of the proton radius. It is obtained as the sum of the elastic and inelastic terms from Ref. [110] and the subtraction term from Ref. [73]. Note that this evaluation is model dependent. Even though the low energy behavior of the FVCT was computed to $\mathcal{O}(p^4)$, this does not reflect in an improved determination of the polarizability correction, since an effective dipole form factor is used, not only at the ρ mass scale, but also at the chiral scale. This problem also introduces a model dependence in its error estimate. Other existing determinations Refs. [109–111] yield quite similar numbers but suffer from the same systematic uncertainties. In this respect our calculation is model independent and have completely different systematics. The fact that we obtain similar numbers gives further significance for the reliability of the proton radius determinations obtained in Refs. [20, 44]. On the other hand, one should not forget that the individual contributions are quite different, and the reasons for that should be further investigated. Yet it is quite remarkable that the total sum gives such similar numbers. Therefore, as stated above, the reason for such large discrepancies should be investigated. In the mean time we will stick to our model independent prediction from the effective theory.

It is also worth discussing the LEX approximation used in Ref. [72]. This approximation consists in setting $q_0 = 0$ everywhere except in the denominator in Eq. (3.46). For the pure chiral result, this approximation works remarkably well (18.51(exact) vs 17.85 (LEX)). Nevertheless, such success does not survive the incorporation of the Δ particle. For the Delta tree-level contribution we find (-1.58(exact) vs 0 (LEX)). The real problem appears from the one-loop pion-Delta result. For such contribution there are $1/q_0$ singularities in the tensor that only cancel if the complete expression is used. Doing the LEX approximation leads to divergent expressions. Even

more worrisome is the fact that, at present, there is no theoretical justification for using the LEX approximation for the integral in Eq. (3.46). It is not correct to assume that the photon energy that appears in the integral, q_0 , corresponds to the energy in the atomic system. It rather reflects virtual fluctuations of order of the pion and muon mass (as well as of the Δ scale). Since those particles are relativistic at those scales it is theoretically incorrect, a priori, to neglect q_0 . In any case, on the light of the good agreement for the pure chiral case, it would be interesting to see whether one could find a theoretical justification for such behavior.

	DR + Model				B χ PT(π)	HBET(π)	(π & Δ)
	Ref. [109]	Ref. [111]	Ref. [110]	Ref. [112]	Ref. [72]	Ref. [61]	Ref. [44]
δE_L^{pol} (μeV)	12(2)	11.5	7.4(2.4)	15.3(5.6)	8.2($^{+1.2}_{-2.5}$)	18.5(9.3)	26.2(10.0)

Table 5.3: Predictions for the polarizability contribution to the $n = 2$ Lamb shift. The first four entries use dispersion relations for the inelastic term and different modeling functions for the subtraction term. The number of the fourth entry has been taken from [72]. The 5th entry is the prediction obtained using B χ PT. The last two entries are the predictions of HBET discussed in this paper. The 6th entry is the prediction at leading order (only pions) and the last entry is the prediction at leading and next-to-leading order (pions and Deltas).

The subtraction and inelastic terms in Eqs. (3.67) and (3.68) are individually divergent. If we set the ultraviolet cutoff in Eq. (3.69) to the ρ mass, $\nu = m_\rho$, the energy shift of each term is one order of magnitude bigger $\sim -11.37 \mu\text{eV}$ than the exact result for the sum. Obviously such contribution is fictitious and may alter the value of the individual terms. On the other hand it is possible to perform this splitting for the case of the pion and pion-Delta loop. We obtain the following:

$$\delta E_L^{\text{sub}}(\pi\text{-loop}) = -1.62 \mu\text{eV}; \quad \delta E_L^{\text{sub}}(\pi\Delta\text{-loop}) = -1.23 \mu\text{eV}. \quad (5.37)$$

They are of the same magnitude. Their size is barely one order of magnitude smaller than the total polarizability term. For the case of the pion loop it is possible to obtain analytic expressions in the limit $m_\mu = m_\pi$, which is a rather good approximation:

$$\delta E_L^{\text{sub}}(\pi\text{-loop}) \Big|_{m_\pi=m_\mu} = -\frac{g_A^2 \alpha^5 m_r^3}{64\pi^2 F_\pi^2} \frac{m_\mu}{m_\pi} (-1 + 3G - 2 \ln 2) = -1.40 \mu\text{eV}, \quad (5.38)$$

where $G \simeq 0.9160$ is the Catalan's constant. For these quantities the LEX approximation works quite well, both for the pion and the pion-Delta loop case. We find¹

$$\delta E_{L,\text{LEX}}^{\text{sub}}(\pi\text{-loop}) = -1.23 \mu\text{eV}; \quad \delta E_{L,\text{LEX}}^{\text{sub}}(\pi\Delta\text{-loop}) = -0.91 \mu\text{eV}, \quad (5.40)$$

which is again asking for a theoretical explanation of this relatively good agreement.

For comparison we show different values obtained for the subtraction and inelastic terms obtained in the literature in Table 5.4.

¹For $m_\mu = m_\pi$ an analytic expression can be found for the pion-loop case, Ref. [72]:

$$\delta E_{L,\text{LEX}}^{\text{sub}}(\pi\text{-loop}) \Big|_{m_\pi=m_\mu} = -\frac{g_A^2 \alpha^5 m_r^3}{64\pi^2 F_\pi^2} \frac{m_\pi}{m_\mu} \left(\frac{1}{2} - G + \ln 2 \right) = -1.08 \mu\text{eV}. \quad (5.39)$$

(μeV)	Ref. [109]	Ref. [111]	Ref. [110]	Ref. [73]	Ref. [112]	Ref. [72]
δE_L^{sub}	-1.8	-2.3	-5.3(1.9)	-4.2(1.0)	2.3(4.6) ⁽¹⁾	3.0
δE_L^{inel}	13.9	13.8	12.7(5)	---	13.0(6)	5.2

Table 5.4: Values for the subtraction and inelastic terms that one can find in the literature. ⁽¹⁾This number is the adjusted value of Ref. [112], given in Ref. [72].

5.5 $1/m_\mu^2$ electron VP corrections: $\delta E_L \sim \mathcal{O}(m_r \alpha^5)$

We now compute the $\mathcal{O}(m_r \alpha^5)$ energy shifts associated to the electron VP. They are produced by 2nd order NR quantum mechanics perturbation theory of $V_{\text{VP}}^{(0,2)} \sim \alpha^2/r$, together with the $V^{(2,1)} \sim \alpha/m^2$ and $V^{(3,0)} \sim 1/m^3$ potentials, as well as by the correction due to the $V_{\text{VP}}^{(2,2)} \sim \alpha^2/m^2$ potential. This sum constitutes a well defined set, as it can be parametrically distinguished from other contributions (formally through the number of light fermions). The energy shift then reads

$$\begin{aligned} & \delta E_{nl}^{V_{\text{VP}}^{(2,2)}} + \delta E_{nl}^{V^{(2,1)} \times V_{\text{VP}}^{(0,2)}} + \delta E_{nl}^{V^{(3,0)} \times V_{\text{VP}}^{(0,2)}} \\ &= \langle \psi_{nl} | V_{\text{VP}}^{(2,2)} | \psi_{nl} \rangle + 2 \langle \psi_{nl} | (V^{(2,1)} + V^{(3,0)}) \frac{1}{(E_{nl} - h')} V_{\text{VP}}^{(0,2)} | \psi_{nl} \rangle. \end{aligned} \quad (5.41)$$

For the Lamb shift corrections we obtain the explicit expressions

$$\begin{aligned} \delta E_L^{V_{\text{VP}}^{(2,2)}} &= (m_r Z \alpha)^3 \frac{\alpha}{8\pi} \int_4^\infty dq^2 \frac{u(q^2)}{q^2} \\ &\times \left\{ -\frac{1}{2} \left(\frac{Z_p c_D^{(\mu)}}{m_\mu^2} + \frac{Z_\mu c_D^{(p)}}{m_p^2} \right) \frac{(1+2\beta q)(1+2\beta q(1+\beta q))}{(1+\beta q)^4} + \frac{Z}{m_\mu m_p} \frac{1+2\beta q}{(1+\beta q)^2} \right. \\ &- \left. \frac{Z_p}{3} \left(\frac{c_S^{(\mu)}}{2m_\mu^2} + \frac{c_F^{(\mu)}}{m_\mu m_p} \right) \left(\frac{3\beta q + 1}{(\beta q + 1)^3} \right) \right\} = - \left(0.027714 + 0.0112 \frac{r_p^2}{\text{fm}^2} \right) \text{meV} \\ &+ \mathcal{O}(\alpha^6), \end{aligned} \quad (5.42)$$

$$\begin{aligned} \delta E_L^{V_{\text{VP}}^{(0,2)} \times V^{(2,1)}} + \delta E_L^{V_{\text{VP}}^{(0,2)} \times V^{(3,0)}} &= (m_r Z \alpha)^3 \frac{\alpha}{2\pi} \int_4^\infty dq^2 \frac{u(q^2)}{q^2} \\ &\times \left\{ \frac{m_r}{6} \left(\frac{Z}{m_\mu^3} + \frac{Z}{m_p^3} \right) \left(-\frac{4(1+3q^2\beta^2)}{(1+q\beta)^4} \ln \left(\frac{1}{1+q\beta} \right) \right. \right. \\ &+ \left. \frac{16+64q\beta+53q^2\beta^2+81q^3\beta^3+24q^4\beta^4}{4(1+q\beta)^5} \right) + \frac{Z}{m_\mu m_p} \left(-\frac{1+4q^2\beta^2}{(1+q\beta)^4} \ln \left(\frac{1}{1+q\beta} \right) \right. \\ &+ \left. \frac{(3+11q\beta)(1+q^2\beta^2)}{4(1+q\beta)^5} \right) + \frac{1}{2} \left(\frac{Z_p c_D^{(\mu)}}{m_\mu^2} + \frac{Z_\mu c_D^{(p)}}{m_p^2} \right) \left(-\frac{3+11q\beta+4q^2\beta^2+12q^3\beta^3+4q^4\beta^4}{4(1+q\beta)^5} \right. \\ &+ \left. \frac{1+2q^2\beta^2}{(1+q\beta)^4} \ln \left(\frac{1}{1+q\beta} \right) \right) + \left. \frac{Z_p}{3} \left(\frac{c_S^{(\mu)}}{2m_\mu^2} + \frac{c_F^{(\mu)}}{m_\mu m_p} \right) \left(-\frac{3+11q\beta+4q^2\beta^2}{4(1+q\beta)^5} + \frac{\ln \left(\frac{1}{1+q\beta} \right)}{(1+q\beta)^4} \right) \right\} \end{aligned}$$

$$= \left(0.046473 - 0.016953 \frac{r_p^2}{\text{fm}^2} \right) \text{meV} + \mathcal{O}(\alpha^6). \quad (5.43)$$

For this last result we have used Eq. (5.8). Summing up both contributions, Eqs. (5.42) and (5.43), we obtain

$$\begin{aligned} & \delta E_L^{V_{\text{VP}}^{(2,2)}} + \delta E_L^{V^{(2,1)} \times V_{\text{VP}}^{(0,2)}} + \delta E_L^{V^{(3,0)} \times V_{\text{VP}}^{(0,2)}} \\ &= m_r \alpha^5 0.0095460 - m_r \alpha^5 0.01433 \frac{r_p^2}{\text{fm}^2} = \left(0.018759 - 0.0282 \frac{r_p^2}{\text{fm}^2} \right) \text{meV}. \end{aligned} \quad (5.44)$$

As we have already stated, this sum constitutes a well defined set, as it can be parametrically distinguished from other contributions (formally through the number of light fermions). This is also so for each individual term in the last equality in Eq. (5.44). The first term corresponds to assuming the proton to be point-like (switching off the proton radius contribution) and gives the viii) entry in Table 5.5. This contribution was first computed in Ref. [105] and later corrected in Refs. [113, 114]. Nevertheless, a different number has been obtained in two recent analyses Refs. [104, 115]. We confirm this last number, which is the one we quote in Table 5.5.

The term proportional to the proton radius in Eq. (5.44) emanates from the coefficient $c_D^{(p)}$. It corresponds to the xi) entry of the table and it is in agreement with the result found in Ref. [105].

5.6 $\mathcal{O}(m_r \alpha^6 \times \ln)$ effects

The first eight entries in Table 5.5 give the complete $\mathcal{O}(m_r \alpha^5)$ result for a point-like proton. In this result we have kept the exact mass dependence. The $\mathcal{O}(m_r \alpha^6)$ contribution is dominated by the logarithmic enhanced terms. Here, we compute the leading ones. We assign a general counting of $m_r/m_p \lesssim \ln \alpha \sim \ln(m_e/m_\mu)$. Therefore, we only compute those contributions at leading order in the m_r/m_p expansion, i.e. those where the proton is infinitely massive. If we switch off electron VP effects (i.e. we switch off the interaction with the electron) the system corresponds to the standard hydrogen situation, which has no $\mathcal{O}(m_r \alpha^6 \ln \alpha)$ effects. Actually, this is also true if we consider the case of muonium (with finite recoil effects), which again has no $\mathcal{O}(m_r \alpha^6 \ln \alpha)$ effects. The reason is that the sum of all possible contributions vanishes for the case of the Lamb shift, since the effective energy shift, Ref. [116], is

$$\delta E_{nls} = \frac{1}{3} \frac{m_r^5}{m_p^2 m_\mu^2} \alpha^6 \ln \frac{1}{\alpha} \left(\delta_{s1} - \frac{3}{4} \right) \frac{\delta_{l0}}{n^3}, \quad (5.45)$$

which vanishes for the Lamb shift (for simplicity we set $Z_p = Z_\mu = 1$ in this section). Therefore, we can actually claim that all the $\mathcal{O}(m_r \alpha^6 \ln \alpha)$ logarithms are generated by the electron VP (for a point-like proton). Note that this would also be true if we consider proton-recoil corrections. In any case, as we have already mentioned, here we only consider the infinite proton mass limit. In this limit, for a point-like proton, only two contributions are produced (both of them generated by electron VP effects), listed in the the ix) and x) entries of Table 5.5, which we now discuss.

The 9th entry is due to the logarithmic-enhanced $\mathcal{O}(\alpha^2)$ corrections to the $c_D^{(\mu)}$ Wilson coefficient (see Eq. (2.19)) that appear in the tree-level potential (see the $c_D^{(p)}$ -dependent term of

Eq. (4.24)). It produces an $\alpha^3/m_\mu^2 \times$ logarithm-potential, the expectation value of which gives the following energy shift to the spectrum

$$\delta E_{nl} = \frac{m_r^3 \alpha^4}{2m_\mu^2} \frac{c_D^{(\mu)}}{n^3} \delta_{l0} \Big|_{\mathcal{O}(\alpha^6 \ln)}, \quad (5.46)$$

and to the Lamb shift

$$\delta E_L = -m_r \alpha^6 0.08885 = -0.0012741 \text{ meV}, \quad (5.47)$$

which is the number that we quote in the 9th entry of Table 5.5.

The 10th entry in Table 5.5 is generated in the same way as the 8th entry but multiplied by the (logarithmic enhanced) $\mathcal{O}(\alpha)$ term of $c_D^{(\mu)}(\nu)$ (see Eqs. (2.19) and (5.42)):

$$\begin{aligned} \delta E_L^{V_{\text{VP}}^{(2,2)}} \Big|_{\mathcal{O}(\alpha^6)} &= -(m_r \alpha)^3 \frac{\alpha}{16\pi} \int_4^\infty dq^2 \frac{u(q^2)}{q^2} \frac{c_D^{(\mu)}}{m_\mu^2} \left\{ \frac{(1+2\beta q)(1+2\beta q(1+\beta q))}{(1+\beta q)^4} \right. \\ &\quad \left. + \frac{4\beta^4 q^4 + 12\beta^3 q^3 + 4\beta^2 q^2 + 11\beta q + 3}{(\beta q + 1)^5} - \frac{4(2\beta^2 q^2 + 1) \ln\left(\frac{1}{\beta q + 1}\right)}{(\beta q + 1)^4} \right\} \Big|_{\mathcal{O}(\alpha^6 \ln)}. \end{aligned} \quad (5.48)$$

The ν dependence gets regulated by the ultrasoft scale, which we set to $\nu = m_\mu \alpha^2$, producing the number

$$\delta E_L^{V_{\text{VP}}^{(2,2)}} \Big|_{\mathcal{O}(\alpha^6 \ln)} = -m_r \alpha^6 0.31644 = -0.004538 \text{ meV}, \quad (5.49)$$

which we quote in the 10th entry in Table 5.5.

Both computations were considered before in Ref. [105]. We agree with them for the significant digits given in that reference. It is also interesting to see that both contributions can be understood from a renormalization group analysis in some appropriate limit Ref. [117]. This analysis also gives us information on the logarithmic structure of the recoil, m_r/m_p , corrections. At this order extra logarithmic terms appear. Nevertheless, they are at most linear: $\mathcal{O}(m_\mu \alpha^6 \frac{m_r}{m_p} \ln \alpha)$, i.e. there are no $\mathcal{O}(m_r \alpha^6 \frac{m_\mu}{m_p} \ln^2 \alpha)$ terms, contrary to the claim in Ref. [104].

For a point-like proton this computation would finish our analysis. The error would be due to uncomputed contributions of $\mathcal{O}(m_r \alpha^6)$ and $\mathcal{O}(m_r \alpha^6 \frac{m_\mu}{m_p} \ln \alpha)$. In Refs. [107, 118] several terms of this order were computed. We use these analyses to estimate the error. Specially useful to us are the (a) and (d) entries in Table IV of the last reference. They are related with the large logarithmic contributions discussed above but also include some finite pieces. We take the difference with the pure logarithmic terms for the generic $\mathcal{O}(m_r \alpha^6)$ error. Taking instead 1/2 of the sum of the 9th and 10th entries yields a similar error: $\sim 3 \mu\text{eV}$. This is the error we quote in the first term of Eq. (5.51), which encodes all the QED-like contributions assuming the proton to be point-like.

We now consider the $\mathcal{O}(m_r \alpha^6 \ln \alpha)$ correction associated to the proton radius. It scales like $\mathcal{O}(m_r \alpha^6 \ln \alpha \times m_r^2 r_p^2)$ and has been computed in Ref. [119]. Such effect would be generated by the 2nd order perturbation theory of the delta potential (note that a similar effect would also

exist in the analogous hydrogen computation). The infrared behaviour of this computation would be regulated by the inverse Bohr radius generated by the bound state dynamics, $\sim m_\mu\alpha$. The ultraviolet behaviour gets regulated by energy scales of order $m_\mu \sim m_\pi$. This produces the large logarithm: $\ln((m_\mu\alpha)/m_\mu) = \ln\alpha$. The explicit correction reads

$$\delta E_L = \frac{2\pi}{3} \left[\frac{m_r^3 \alpha^3}{2^3 \pi} \right] r_p^2 \alpha^3 \ln\alpha = -0.0014 \frac{r_p^2}{\text{fm}^2}, \quad (5.50)$$

and it is listed in the 13th entry of Table 5.5. We use 1/2 of this result for the error of the r_p^2 coefficient in Eq. (5.51).

i)	$\mathcal{O}(m_r\alpha^3)$	$V_{\text{VP}}^{(0)}$	Eq. (5.9)	205. 00737
ii)	$\mathcal{O}(m_r\alpha^4)$	$V_{\text{VP}}^{(0)}$	Eq. (5.11)	1. 50795
iii)	$\mathcal{O}(m_r\alpha^4)$	$V_{\text{VP}}^{(0)}$	Eq. (5.14)	0. 15090
iv)	$\mathcal{O}(m_r\alpha^5)$	$V_{\text{VP}}^{(0)}$	Eq. (5.18)	0. 00752
v)	$\mathcal{O}(m_r\alpha^5)$	$V_{\text{LbL}}^{(0)}$	Eq. (5.19)	-0. 00089(2)
vi)	$\mathcal{O}(m_r\alpha^4 \times \frac{m_\mu^2}{m_p^2})$	$V^{(2,1)} + V^{(3,0)}$	Eq. (5.26)	0. 05747
vii)	$\mathcal{O}(m_r\alpha^5)$	$V_{\text{no-VP}}^{(2,2)} + \text{ultrasoft}$	Eq. (5.31)	-0. 71896
viii)	$\mathcal{O}(m_r\alpha^5)$	$V_{\text{VP}}^{(2,2)} + V^{(2,1)} \times V_{\text{VP}}^{(0,2)}$	Eq. (5.44)	0. 01876
ix)	$\mathcal{O}(m_r\alpha^6 \times \ln(\frac{m_\mu}{m_e}))$	$V^{(2,3)}; c_D^{(\mu)}$	Eq. (5.47)	-0. 00127
x)	$\mathcal{O}(m_r\alpha^6 \times \ln\alpha)$	$V_{\text{VP}}^{(2,3)}; c_D^{(\mu)}$	Eq. (5.49)	-0. 00454
xi)	$\mathcal{O}(m_r\alpha^4 \times m_r^2 r_p^2)$	$V^{(2,1)}; c_D^{(p)}; r_p^2$	Eq. (5.26)	-5. 19745 $\frac{r_p^2}{\text{fm}^2}$
xii)	$\mathcal{O}(m_r\alpha^5 \times m_r^2 r_p^2)$	$V_{\text{VP}}^{(2,2)}; c_D^{(p)}; r_p^2$	Eq. (5.44)	-0. 02815 $\frac{r_p^2}{\text{fm}^2}$
xiii)	$\mathcal{O}(m_r\alpha^6 \ln\alpha \times m_r^2 r_p^2)$	$V^{(2,3)}; c_D^{(p)}; r_p^2$	Eq. (5.50)	-0. 00136 $\frac{r_p^2}{\text{fm}^2}$
xiv)	$\mathcal{O}(m_r\alpha^5 \times \frac{m_r^2}{m_p^2})$	$V_{\text{VP had}}^{(2)}; d_2^{\text{had}}$	Eq. (5.32)	0. 0111(2)
xv)	$\mathcal{O}(m_r\alpha^5 \times \frac{m_r^2 m_\mu}{m_p^2 m_\pi})$	$V^{(2)}; c_3^{\text{had}}$	Eq. (5.33)	0. 0344(125)

Table 5.5: *The different contributions to the Lamb shift in muonic hydrogen in meV units.*

5.7 The proton radius

Summarizing all contributions, our final prediction for the Lamb shift reads

$$\Delta E_L^{\text{this work}} = \left[206.070(13) - 5.2270(7) \frac{r_p^2}{\text{fm}^2} \right] \text{meV} \quad (5.51)$$

$$= \left[206.0243(30) - 5.2270(7) \frac{r_p^2}{\text{fm}^2} + 0.0455(125) \right] \text{meV}. \quad (5.52)$$

In the last equality the first term is the pure QED result, and its error is the estimate of the $\mathcal{O}(m_\mu\alpha^6)$ effects. The error of the coefficient of the term proportional to r_p^2 is the estimated

size of the $\mathcal{O}(m_\mu\alpha^6(m_\mu r_p)^2)$ terms. The last term encodes the r_p -independent hadronic effects. The error is the assigned uncertainty due to unknown terms of $\mathcal{O}(m_\mu\alpha^5\frac{m_\mu^3}{m_p^3})$. Using Eq. (1.1) we obtain

$$r_p = 0.8412(15) \text{ fm}, \tag{5.53}$$

where the theoretical and experimental errors have been combined in quadrature. Nevertheless, the latter is completely subdominant with respect to the total error, which is fully dominated by the hadronic effects.

Our central value is basically equal to the one quoted in [20] (even though some individual terms are quite different) but has significantly larger errors. The main reason is that the error associated to the two-photon exchange contribution is larger in our case, as it is the most one can do without model dependent assumptions. Nevertheless, we emphasize that with our model independent analysis, which yields a 6.8σ discrepancy with respect to the CODATA value, we give a model independent significance to the proton radius puzzle.

Chapter 6

Conclusions

In the first part of this dissertation we have established the necessary pNRQED terms that allow us to determine the Lamb shift in muonic hydrogen up to uncomputed terms of $\mathcal{O}(m_\mu\alpha^5\frac{m_\mu^3}{\Lambda_{\text{QCD}}^3}, m_\mu\alpha^6)$. Most importantly, for the relevant four-fermion Wilson coefficients, we have performed the matching of HBET to NRQED. The hadronic part of these coefficients arises from the TPE. In order to obtain it, we have computed the FVCT at leading order including the contributions of the pion and the Delta particle. This allows us to obtain a model independent prediction of the muonic hydrogen Lamb shift.

We have computed the spin-dependent and spin-independent structure functions of the FVCT of the proton at $\mathcal{O}(p^3)$ in HBChPT including the Delta particle. We include it not only because the Delta is the closest resonance to the proton (see [29]), but also because in the large N_c limit the Delta and the proton become degenerate in mass [32]. Moreover, we have given D -dimensional expressions for these functions. Those are relevant for future higher order loop computations. We have compared our results with previous computations. The $D = 4$ expressions for the spin-dependent structure functions were computed in Ref. [63]. We agree with their results. The $D = 4$ expressions for the pure chiral (without Delta contributions) spin-independent structure functions were computed in Ref. [61]. We agree with their results too. The Delta-associated contributions to the spin-independent structure functions are computed in this work for the first time. We also profit to present all these results obtained throughout the years in a unified form.

We have used these results to determine the leading chiral and large N_c structure of c_3^{pli} and c_4^{pli} , or, in other words, to determine their non-analytic dependence on m_q and N_c . The fact that we have full control over the quark mass dependence makes our result very useful for eventual lattice determinations of these quantities. In lattice simulations, by fine tuning the mass we can identify the results obtained in this work and up to which mass the chiral is a good approximation. One could also vary N_c to check how well the large- N_c approximation works.

These Wilson coefficients appear in the hyperfine splitting (spin-dependent) and the Lamb shift (spin-independent) in hydrogen and muonic hydrogen. The relevant Wilson coefficient for the Lamb shift, c_3^{pli} , is chiral enhanced. Therefore, the $\mathcal{O}(p^3)$ chiral result is a pure prediction of the effective theory, which we use to determine Eq. (5.36), the energy shift associated to the (hadronic) TPE of the Lamb shift.

We would like to emphasize that Eq. (5.36) is the most precise expression that can be obtained in a model independent way, since $\mathcal{O}(m_\mu\alpha^5\frac{m_\mu^3}{\Lambda_{\text{QCD}}^3})$ effects are not controlled by the chiral theory and would require new counterterms. Our final number is quite similar to previous estimates

existing in the literature. Nevertheless, those computations require the splitting of the TPE contribution into different terms. Such terms are then computed using different dispersion relations, except for a subtraction term which requires modelling of its Q^2 dependence. In contrast, we have used the same method for all computations contributing to our result, yielding a parameter-free prediction. On the other hand, one should not forget that the individual contributions we obtain are quite different to other determinations, and the reasons for that should be further investigated. In this respect we have discussed what the effective theory has to say about the separation into Born, polarizability, inelastic and subtraction term. The Born contribution is related with the Zemach moments. We profit of our computation to give the prediction of the effective theory for some charge, $\langle r^n \rangle$, and Zemach, $\langle r^n \rangle_{(2)}$ moments. To finalise the matching of HBET to NRQED, we have also discussed the chiral dependence of the spin-dependent four-fermion Wilson coefficient, $c_4^{pl_i}$, and obtained the relation between c_4^{pe} and $c_4^{p\mu}$ given by the effective theory.

All the contributions to the Lamb shift considered here are listed in Table 5.5. Their sum produces the theoretical prediction for the Lamb shift in Eqs. (5.51)-(5.52).

The first ten terms in Table 5.5 are those associated to a pure QED-like computation assuming the proton to be point-like. Their sum comprises the first term in Eq. (5.52), and its error is the estimate of the $\mathcal{O}(m_r\alpha^6)$ effects.

As a by-product of this computation, we give in Appendix E the exact $\mathcal{O}(m_r\alpha^5)$ expression for the muonium spectrum, keeping the complete mass dependence. It can be easily deduced from our muonic hydrogen computation by changing $m_p \rightarrow m_\mu$ and $m_\mu \rightarrow m_e$, and setting the hadronic coefficients, d_2^h , and the electron VP effects to zero.

The second line in Eq. (5.52) encodes all the corrections proportional to the proton radius, entries x)-xiii) in Table 5.5. The error of the coefficient of the term proportional to r_p^2 is the estimated size of the $\mathcal{O}(m_r\alpha^6(m_\mu^2 r_p^2))$ terms.

The last term encodes the r_p^2 -independent hadronic effects. The error is the assigned uncertainty due to unknown terms of $\mathcal{O}(m_r\alpha^5 \frac{m_\mu^3}{m_p^2})$.

We emphasize that a partial incorporation of subleading corrections in α to the above expression will not improve the precision of the result (unless arguments in favor that such contributions dominant are found), as the uncertainty is still dominated by unknown parametric terms of order $m_r\alpha^6$. For an account of some of such corrections see Ref. [120].

In order to obtain Eq. (5.51), the first and last term of Eq. (5.52) have been added and their error combined in quadrature. This, together with the experimental result in Eq. (1.1), yields the value for the proton radius quoted in Eq. (5.53), where the theoretical and experimental errors have been combined in quadrature. Nevertheless, the latter is completely subdominant with respect to the total error, which is fully dominated by the hadronic effects. In this respect it is also convenient to present our result in the following way

$$\begin{aligned}
\Delta E_L &= 206.0243 \text{ meV} \\
&- \left[\frac{1}{\pi} \frac{m_r^3 \alpha^3}{8} \right] \frac{\alpha}{m_p^2 \text{ fm}^2} \left[47.3525 + 35.1491\alpha + 47.3525\alpha^2 \ln(1/\alpha) \right] \\
&+ \left[\frac{1}{\pi} \frac{m_r^3 \alpha^3}{8} \right] \frac{1}{m_p^2} \left[c_3^{\text{had}} + 16\pi\alpha d_2^{\text{had}} \right] \\
&+ \mathcal{O}(m_r\alpha^6). \tag{6.1}
\end{aligned}$$

Note that since $c_3^{\text{had}} \sim \alpha^2$ and $\alpha d_2^{\text{had}} \sim \alpha^2$, the third line of the previous equation encodes all the hadronic effects unrelated to the proton radius of order $m_r\alpha^5$. This presentation of the result

where r_p and c_3^{had} are kept explicit could be important for the future. In the long term (once the origin of the proton radius puzzle is clarified) the natural place to provide the value of the proton radius is the hydrogen Lamb shift while, since c_3^{had} is suppressed by an extra factor of the lepton mass, it should be best determined in muonic hydrogen. In this scenario a complete evaluation of the $\mathcal{O}(m_r\alpha^6)$ term may improve the precision of an eventual experimental determination of c_3^{had} . Note that throughout this discussion we assume that we can determine d_2^{had} from alternative methods, like dispersion relations.

The value for the proton radius that we obtain is 6.8σ away from the CODATA value. This quantifies, in a model independent way, the significance to the proton radius puzzle. In the near future several experiments will take place in order to shed some light on this long-standing issue. On the one hand, looking for measurements at lower momentum and to clarify the aforementioned problems with the ep -scattering data, various scattering experiments will take place: MAMI [121], JLAB [122], MUSE [123]. On the other hand, the puzzle may be related to problems in previous measurements of the hydrogen spectrum. Experiments as MPQ [124], Garching [125], Toronto [126] or LKB [127] will get new measurements of different energy splittings. Finally, muonic experiments are much newer and rare, presenting the need to both confirm the PSI muonic hydrogen results and measure other muonic bound states. Theoretical understanding of nuclear effects will be of primary importance for the interpretation of the next muonic measurements which will deal with states such as muonic deuterium and muonic helium.

Part III

Heavy quarkonium: the B_c system

Chapter 7

Introduction

In Part II, we established the appropriate EFT for systems bounded by the electromagnetic interaction, and with it we computed the Lamb shift in muonic hydrogen and the proton radius. We now move on to a similar but more complicated system. We want to study systems bounded by the strong interaction, in particular, those formed by a heavy quark and heavy anti-quark (i.e. heavy quarkonium) with different masses. The contents of this part of the thesis are based on the work published in [128] by the author.

In analogy to the case of muonic hydrogen, the dynamical properties of quark-antiquark systems near threshold ($E \sim 2m$) and with large quark masses can be obtained by solving a properly generalized NR Schrödinger equation. The use of EFTs, in particular of pNRQCD (Refs. [15,129], for reviews see Refs. [103,130]), allows us to quantify this connection, and to derive the Schrödinger equation and its corrections from the underlying theory, in a model independent and efficient way (see the discussion in Part I). pNRQCD exploits both the NR nature of the problem and the wide hierarchy of the scales that govern the system:

$$m \gg mv \gg mv^2 \dots, \quad (7.1)$$

where $m \sim m_1 \sim m_2 \sim m_r \gg \Lambda_{\text{QCD}}$ and v is the heavy-quark velocity in the center of mass frame.

In this work we focus on the extreme weak-coupling limit $mv^2 \gg \Lambda_{\text{QCD}}$, where the EFT can be summarized schematically by

$$\left. \begin{aligned} & \left(i\partial_0 - \frac{\mathbf{p}^2}{2m_r} - V^{(0)}(r) \right) \phi(\mathbf{r}) = 0 \\ & + \text{corrections to the potential} \\ & + \text{interaction with other low-energy degrees of freedom} \end{aligned} \right\} \text{pNRQCD.} \quad (7.2)$$

Analogously to the QED case, a key ingredient in the EFT is the (heavy quarkonium) potential that appears in the Schrödinger equation. The potential is expanded in inverse powers of the heavy masses. At leading order in this expansion, i.e. $\mathcal{O}(m^0)$, it consists of the static potential $V^{(0)}$. Relativistic corrections are then further suppressed by inverse powers of the heavy quark masses. The potential is obtained by matching NRQCD Refs. [14, 131] to pNRQCD. As we discussed in Part I, there are several ways to carry out the matching in practice. The most common three are: on-shell matching, off-shell matching and Wilson-loop matching.

In the **on-shell** matching one equates S-matrix elements of NRQCD and pNRQCD order by order in an expansion in the QCD coupling constant α_s and the velocity v ($\sim \alpha_s$ in the

extreme weak-coupling regime). The S-matrix elements are defined for asymptotic external quark states satisfying the equations of motion (EOMs) of free quarks. This necessarily requires the incorporation of potential loops, i.e. loops with internal momenta $(k_0, \mathbf{k}) \sim (mv^2, mv)$, in both calculations, in order to carry out the matching. The reason is that the free-quark on-shell condition produces an imperfect cancellation between potential loops in NRQCD and pNRQCD, and mixes different orders in the $1/m$ expansion. This obscures the mass dependence of the potential, as it invalidates a strict $1/m$ expansion for the determination of the potentials. In other words, in the on-shell matching computation the potentials at a given order in $1/m$ also receive contributions from matrix elements involving operators of higher order. On the other hand, the on-shell matching result for the potential is gauge invariant (to a fixed order in v), as so are the S-matrix elements.

In the **off-shell** matching one equates off-shell Green functions computed in NRQCD with the corresponding off-shell Green functions in pNRQCD (still respecting global energy-momentum conservation). In other words, external quark fields need not fulfil the free equations of motion. This allows us to perform the matching within a strict $1/m$ expansion, since potential loops in NRQCD and pNRQCD exactly cancel each other. Hence we can keep exact track of the mass dependence of the resulting matching condition for the potentials. The drawback is that the expression we get from the off-shell matching for the individual potentials may depend on the gauge. The total expression for the potential, however, still yields of course gauge invariant results for observables, in particular for the bound state energies, within the accuracy of the computation. In addition, the potentials may acquire some energy dependence, of which one should get rid by using field redefinitions.¹

In the **Wilson-loop** matching one equates NRQCD and pNRQCD Green functions which are off-shell and gauge-invariant directly in position space. These Green functions are written in terms of Wilson loops with chromo-electric/magnetic insertions. Working in position space is obviously only a Fourier transformation and it is not the major difference with respect to the previous matching schemes. The key point is that the time of the quark and antiquark fields are set equal. This is not a restriction, and is in fact the natural thing to do for the heavy quark-antiquark system near threshold. We also incorporate gluon strings between the quark and the antiquark fields such that the whole system is gauge invariant. This description of the potential in terms of Wilson loops is also valid in the strong coupling regime. The details of how this matching is performed can be found in Refs. [42, 43]. In the static limit, it reduces to the original computation of the static potential by Wilson in Ref. [132]. The advantage of this procedure is twofold: the matching can be done in a strict $1/m$ expansion with no need of potential loops, and closed expressions in terms of the aforementioned rectangular Wilson loops can be obtained for each potential. They are therefore explicitly gauge invariant. This makes this procedure quite appealing. We will see that both the static potential and the relativistic corrections can be efficiently computed using this method.

The heavy quarkonium potential is known with N³LO precision for the equal mass case in the on-shell matching scheme since 2002 Ref. [133]. Nevertheless, there are several reasons why we would like to know the heavy quarkonium potential with N³LO precision for the unequal mass case, and also in other matching schemes. Let us highlight two of them:

- The B_c system: the LHC provides a unique opportunity to study the properties of the B_c bound states in great detail. In particular, the possibility to measure a good deal of the B_c

¹ Equivalently, at the order at which we are working, one can use the complete EOMs at the appropriate order.

spectrum and decays is now a reality, starting with the observation of the B_c ground state at LCHb [134] (which was first observed by CDF [135]), and of an excited B_c state consistent with $B_c(2S)$ at ATLAS, Ref. [136]. Obviously, a major ingredient in such analyses is a detailed knowledge of the heavy quarkonium potential and spectrum in the short distance limit. We will compute both in this work.

- The heavy quarkonium potential in terms of Wilson loops: It is possible to give closed expressions for the potentials in terms of Wilson loops that can be generalized beyond perturbation theory. They are therefore suitable objects for the study of the non-perturbative QCD dynamics by comparing different models with lattice simulations (the Wilson loop representation of the potentials indeed allows for exact results in the case of QED, e.g. that the $1/m$ potential is zero to all orders Ref. [42]). For such analyses it is also important to control the short distance behavior of the potentials.

Another important motivation for this work is to set the ground for higher order computations of the potentials, which we stress again are key ingredients in any observable related to heavy quarkonium we can think of (spectrum, decays, NR sum rules, and $t\bar{t}$ production near threshold, ...). We would like to systematize their computation as much as possible, since, as one goes to higher orders, and as soon as ultrasoft effects start to play a role, the understanding of the relation of the computed potential to the EFT framework becomes compulsory.

In this respect, we believe that it is important to clarify the relation between the different matching schemes and to explore their advantages and disadvantages. The three matching methods mentioned above have been employed more or less independently over the years. However, the results obtained with these methods often differ, which makes a comparison difficult. On top of that, there is the problem of how to renormalize the potentials in pNRQCD, i.e. how the ultrasoft divergences are subtracted from the bare potentials. There is much freedom here as well. One can perform the subtraction in momentum or position space. In the latter case, one can define the subtraction for the potentials in $D = 4 + 2\epsilon$ or in four dimensions. These different subtraction/renormalization prescriptions give rise to different expressions for the renormalized potentials (even if all of them only account for soft physics), but not for physical observables. We also note that, while computations using on-shell/off-shell Green functions are naturally done in momentum space, the Wilson loop calculations are naturally carried out in position space (as is the computation of the spectrum). We will discuss these issues in some detail, putting a special emphasis on matching schemes that admit a strict $1/m$ expansion of the potential.

In this work we will focus on the spin-independent potentials. The spin-dependent potentials are not affected by ultrasoft divergences, nor by field redefinitions, to the order required for the calculation of the heavy quarkonium mass with N³LO accuracy. Therefore, we will not consider them in detail in this work and only use known renormalized results for the final determination of the B_c spectrum. Nevertheless, we will present the spin-dependent results in a form compatible with our EFT computation.

Chapter 8

Effective field theories: Matching NRQCD to pNRQCD

8.1 NRQCD

The NRQCD Lagrangian is defined uniquely up to field redefinitions. In this work we use the following Lagrangian density for a quark ψ of mass m_1 , an antiquark χ_c of mass m_2 and n_f massless fermions q_i to $\mathcal{O}(1/m^2)$ [14, 67, 131, 137]:¹

$$\mathcal{L}_{\text{NRQCD}} = \mathcal{L}_g + \mathcal{L}_l + \mathcal{L}_\psi + \mathcal{L}_{\chi_c} + \mathcal{L}_{\psi\chi_c}, \quad (8.1)$$

$$\mathcal{L}_g = -\frac{1}{4}G^{\mu\nu a}G_{\mu\nu}^a + \frac{1}{4}\left(\frac{c_1^{g(1)}}{m_1^2} + \frac{c_1^{g(2)}}{m_2^2}\right)gf_{abc}G_{\mu\nu}^aG^{\mu b}{}_\lambda G^{\nu\lambda c}, \quad (8.2)$$

$$\mathcal{L}_l = \sum_{i=1}^{n_f} \bar{q}_i i\not{D} q_i + \frac{\delta\mathcal{L}_l^{(1)}}{m_1^2} + \frac{\delta\mathcal{L}_l^{(2)}}{m_2^2}, \quad (8.3)$$

$$\begin{aligned} \delta\mathcal{L}_l^{(1)} = & \frac{c_1^{ll(1)}}{8}g^2 \sum_{i,j=1}^{n_f} \bar{q}_i T^a \gamma^\mu q_i \bar{q}_j T^a \gamma_\mu q_j + \frac{c_2^{ll(1)}}{8}g^2 \sum_{i,j=1}^{n_f} \bar{q}_i T^a \gamma^\mu \gamma_5 q_i \bar{q}_j T^a \gamma_\mu \gamma_5 q_j \\ & + \frac{c_3^{ll(1)}}{8}g^2 \sum_{i,j=1}^{n_f} \bar{q}_i \gamma^\mu q_i \bar{q}_j \gamma_\mu q_j + \frac{c_4^{ll(1)}}{8}g^2 \sum_{i,j=1}^{n_f} \bar{q}_i \gamma^\mu \gamma_5 q_i \bar{q}_j \gamma_\mu \gamma_5 q_j, \end{aligned} \quad (8.4)$$

$$\delta\mathcal{L}_l^{(2)} = \delta\mathcal{L}_l^{(1)}((1) \rightarrow (2)), \quad (8.5)$$

$$\begin{aligned} \mathcal{L}_\psi = & \psi^\dagger \left\{ iD_0 + \frac{c_k^{(1)}}{2m_1} \mathbf{D}^2 + \frac{c_4^{(1)}}{8m_1^3} \mathbf{D}^4 + \frac{c_F^{(1)}}{2m_1} \boldsymbol{\sigma} \cdot g\mathbf{B} + \frac{c_D^{(1)}}{8m_1^2} (\mathbf{D} \cdot g\mathbf{E} - g\mathbf{E} \cdot \mathbf{D}) \right. \\ & \left. + i \frac{c_S^{(1)}}{8m_1^2} \boldsymbol{\sigma} \cdot (\mathbf{D} \times g\mathbf{E} - g\mathbf{E} \times \mathbf{D}) \right\} \psi + \frac{\delta\mathcal{L}_{\psi l}^{(1)}}{m_1^2}, \end{aligned} \quad (8.6)$$

$$\delta\mathcal{L}_{\psi l}^{(1)} = \frac{c_1^{hl(1)}}{8}g^2 \sum_{i=1}^{n_f} \psi^\dagger T^a \psi \bar{q}_i \gamma_0 T^a q_i + \frac{c_2^{hl(1)}}{8}g^2 \sum_{i=1}^{n_f} \psi^\dagger \gamma^\mu \gamma_5 T^a \psi \bar{q}_i \gamma_\mu \gamma_5 T^a q_i$$

¹We also include the $\mathbf{D}^4/(8m^3)$ terms since they will be necessary later on.

$$+ \frac{c_3^{hl(1)}}{8} g^2 \sum_{i=1}^{n_f} \psi^\dagger \psi \bar{q}_i \gamma_0 q_i + \frac{c_4^{hl(1)}}{8} g^2 \sum_{i=1}^{n_f} \psi^\dagger \gamma^\mu \gamma_5 \psi \bar{q}_i \gamma_\mu \gamma_5 q_i, \quad (8.7)$$

$$\mathcal{L}_{\chi_c} = \mathcal{L}_\psi(\psi \rightarrow \chi_c, g \rightarrow -g, T^a \rightarrow (T^a)^T, m_1 \rightarrow m_2, (1) \rightarrow (2)), \quad (8.8)$$

$$\begin{aligned} \mathcal{L}_{\psi\chi_c} = & -\frac{d_{ss}}{m_1 m_2} \psi^\dagger \psi \chi_c^\dagger \chi_c + \frac{d_{sv}}{m_1 m_2} \psi^\dagger \boldsymbol{\sigma} \psi \chi_c^\dagger \boldsymbol{\sigma} \chi_c \\ & - \frac{d_{vs}}{m_1 m_2} \psi^\dagger T^a \psi \chi_c^\dagger (T^a)^T \chi_c + \frac{d_{vv}}{m_1 m_2} \psi^\dagger T^a \boldsymbol{\sigma} \psi \chi_c^\dagger (T^a)^T \boldsymbol{\sigma} \chi_c. \end{aligned} \quad (8.9)$$

Here ψ is the NR fermion field represented by a Pauli spinor and $\chi_c \equiv -i\sigma_2 \chi^*$ is the respective antifermion field also represented by a Pauli spinor. The matrix $(T^a)^T$ is the transpose of the $SU(N_c)$ generator T^a in the fundamental representation, and $T^a \rightarrow (T^a)^T$ in Eq. (8.8) only applies to the matrices contracted with the heavy quark color indexes. The components of the vector $\boldsymbol{\sigma}$ are the Pauli matrices. We define $iD^0 = i\partial^0 - gA^0$, $i\mathbf{D} = i\nabla + g\mathbf{A}$, $\mathbf{E}^i = G^{i0}$ and $\mathbf{B}^i = -\epsilon_{ijk} G^{jk}/2$, where ϵ_{ijk} is the three-dimensional totally antisymmetric tensor with $\epsilon_{123} = 1$ and $(\mathbf{a} \times \mathbf{b})^i \equiv \epsilon_{ijk} \mathbf{a}^j \mathbf{b}^k$. For a list of the relevant Feynman rules derived from Eq. (8.1) we refer e.g. to Appendix B.2.

Due to reparametrization invariance, we know that $c_k^{(i)} = c_4^{(i)} = 1$ and $c_S^{(i)} = 2c_F^{(i)} - 1$, Ref. [67]. In Ref. [138], c_F was computed with NLO accuracy. The other NLO Wilson coefficients to $\mathcal{O}(1/m^2)$ were computed for the light and one heavy-quark sector in Ref. [67] and for the two heavy-quark sector in Ref. [71], both in Feynman gauge (FG). Here we only list the Wilson coefficients that are directly relevant for our analysis.² Their bare expressions read

$$c_F^{(i)} = c_F^{(i)\overline{\text{MS}}}(\nu) - c_F^{(i)} C_A \frac{g_B^2 \bar{\nu}^{2\epsilon}}{(4\pi)^2 \epsilon} + \mathcal{O}(\epsilon), \quad (8.11)$$

$$c_D^{(i)} = c_D^{(i)\overline{\text{MS}}}(\nu) - \left(\frac{2}{3} C_A c_D^{(i)} - \frac{16}{3} C_F - \frac{1}{3} C_A - \frac{5}{3} C_A c_F^{(i)2} + \frac{4}{3} T_F n_f c_1^{hl(i)} \right) \frac{g_B^2 \bar{\nu}^{2\epsilon}}{(4\pi)^2 \epsilon} + \mathcal{O}(\epsilon), \quad (8.12)$$

$$d_{ss} = d_{ss}^{\overline{\text{MS}}}(\nu) - C_F \left(\frac{C_A}{2} - C_F \right) \frac{g_B^4 \bar{\nu}^{2\epsilon}}{(4\pi)^2 \epsilon} + \mathcal{O}(\epsilon), \quad (8.13)$$

$$\begin{aligned} d_{vs} = & d_{vs}^{\overline{\text{MS}}}(\nu) - \left[2C_F - \frac{3C_A}{4} + \frac{3}{8} C_A \left(\frac{m_1}{m_2} c_D^{(2)} + \frac{m_2}{m_1} c_D^{(1)} \right) - \frac{5}{8} C_A \left(\frac{m_1}{m_2} + \frac{m_2}{m_1} \right) \right] \times \\ & \times \frac{g_B^4 \bar{\nu}^{2\epsilon}}{(4\pi)^2 \epsilon} + \mathcal{O}(\epsilon), \end{aligned} \quad (8.14)$$

$$d_{sv} = d_{sv}^{\overline{\text{MS}}}(\nu) + \mathcal{O}(\epsilon), \quad (8.15)$$

$$d_{vv} = d_{vv}^{\overline{\text{MS}}}(\nu) + \frac{C_A}{4} c_F^{(1)} c_F^{(2)} \frac{g_B^4 \bar{\nu}^{2\epsilon}}{(4\pi)^2 \epsilon} + \mathcal{O}(\epsilon), \quad (8.16)$$

where

$$\bar{\nu}^{2\epsilon} = \nu^{2\epsilon} \left(\frac{e^{\gamma_E}}{4\pi} \right)^\epsilon, \quad g_B^2 = g^2 \left[1 + \frac{g^2 \bar{\nu}^{2\epsilon}}{4\pi} \frac{\beta_0}{4\pi \epsilon} + \mathcal{O}(g^4) \right], \quad (8.17)$$

and $\alpha_s = g^2 \nu^{2\epsilon}/(4\pi)$. The color factors T_F , C_A , C_F as well as the QCD β -function coefficients (β_i) are given in Appendix A. In the following we will only distinguish between the bare coupling

²Except for

$$c_1^{g(1)} = \frac{\alpha_s(m)}{90\pi} T_F, \quad (8.10)$$

as this equation corrects Eq. (218) in Ref. [103].

g_B and the $\overline{\text{MS}}$ renormalized coupling g when necessary. The respective renormalized Wilson coefficients of the single quark sector in the $\overline{\text{MS}}$ scheme can be found in Appendix A.2.

At the order we are working, we can set $c_1^{(i)hl} = 0$. However, if we are interested in the resummation of large logarithms, we must keep $c_1^{(i)hl}$ due to its non-trivial RG evolution. For future purposes we will therefore retain the contribution proportional to $c_1^{(i)hl}$ in the potential and only set it to zero in the final determination of the heavy quarkonium mass with N³LO accuracy.

Since the basis of operators is not minimal, there are ambiguities in the values of some Wilson coefficients. In particular the expressions of d_{vs} and c_D depend on the gauge used to determine them (not only the finite pieces but also the logarithmic divergences, see the discussion in Ref. [139]). The expression we give here is the FG result. Note also that the coefficient d_{vv} is affected by the prescription used to deal with Pauli matrices in D -dimensions. In dimensional regularization several prescriptions are possible for the ϵ_{ijk} tensors and σ , and the same prescription as for the calculation of the Wilson coefficients must be used. Throughout this work we use the prescription $[\sigma_i, \sigma_j] = 2i\epsilon_{ijk}\sigma_k$ and $\epsilon_{ijk}\epsilon_{ijk'} = (D-2)\delta_{kk'}$.

8.2 pNRQCD: the potentials

Integrating out the soft modes in NRQCD we end up with the EFT pNRQCD. The most general pNRQCD Lagrangian compatible with the symmetries of QCD that can be constructed with a singlet and an octet (quarkonium) field, as well as an ultrasoft gluon field to NLO in the multipole expansion has the form (Refs. [15, 129])

$$\begin{aligned} \mathcal{L}_{\text{pNRQCD}} = & \int d^3\mathbf{r} \text{Tr} \left\{ S^\dagger (i\partial_0 - h_s(\mathbf{r}, \mathbf{p}, \mathbf{P}_\mathbf{R}, \mathbf{S}_1, \mathbf{S}_2)) S + O^\dagger (iD_0 - h_o(\mathbf{r}, \mathbf{p}, \mathbf{P}_\mathbf{R}, \mathbf{S}_1, \mathbf{S}_2)) O \right\} \\ & + V_A(r) \text{Tr} \left\{ O^\dagger \mathbf{r} \cdot g\mathbf{E} S + S^\dagger \mathbf{r} \cdot g\mathbf{E} O \right\} + \frac{V_B(r)}{2} \text{Tr} \left\{ O^\dagger \mathbf{r} \cdot g\mathbf{E} O + O^\dagger O \mathbf{r} \cdot g\mathbf{E} \right\} \\ & - \frac{1}{4} G_{\mu\nu}^a G^{\mu\nu a} + \sum_{i=1}^{n_f} \bar{q}_i i\not{D} q_i, \end{aligned} \quad (8.18)$$

$$h_s(\mathbf{r}, \mathbf{p}, \mathbf{P}_\mathbf{R}, \mathbf{S}_1, \mathbf{S}_2) = \frac{\mathbf{p}^2}{2m_r} + \frac{\mathbf{P}_\mathbf{R}^2}{2M} + V_s(\mathbf{r}, \mathbf{p}, \mathbf{P}_\mathbf{R}, \mathbf{S}_1, \mathbf{S}_2), \quad (8.19)$$

$$h_o(\mathbf{r}, \mathbf{p}, \mathbf{P}_\mathbf{R}, \mathbf{S}_1, \mathbf{S}_2) = \frac{\mathbf{p}^2}{2m_r} + \frac{\mathbf{P}_\mathbf{R}^2}{2M} + V_o(\mathbf{r}, \mathbf{p}, \mathbf{P}_\mathbf{R}, \mathbf{S}_1, \mathbf{S}_2), \quad (8.20)$$

$$V_s = V^{(0)} + \frac{V^{(1,0)}}{m_1} + \frac{V^{(0,1)}}{m_2} + \frac{V^{(2,0)}}{m_1^2} + \frac{V^{(0,2)}}{m_2^2} + \frac{V^{(1,1)}}{m_1 m_2} + \dots, \quad (8.21)$$

$$V_o = V_o^{(0)} + \frac{V_o^{(1,0)}}{m_1} + \frac{V_o^{(0,1)}}{m_2} + \frac{V_o^{(2,0)}}{m_1^2} + \frac{V_o^{(0,2)}}{m_2^2} + \frac{V_o^{(1,1)}}{m_1 m_2} + \dots, \quad (8.22)$$

where $iD_0 O \equiv i\partial_0 O - g[A_0(\mathbf{R}, t), O]$, $\mathbf{P}_\mathbf{R} = -i\nabla_\mathbf{R}$ for the singlet, $\mathbf{P}_\mathbf{R} = -i\mathbf{D}_\mathbf{R}$ for the octet (where the covariant derivative is in the adjoint representation), $\mathbf{p} = -i\nabla_\mathbf{r}$. The masses m_r and M have been defined in Eq. (2). We adopt the color normalization

$$S = S \mathbf{1}_c / \sqrt{N_c}, \quad O = O^a \mathbf{T}^a / \sqrt{T_F}, \quad (8.23)$$

for the singlet field $S = S(\mathbf{r}, \mathbf{R}, t)$ and the octet field $O = O^a(\mathbf{r}, \mathbf{R}, t)$.

Both, h_s and the potential V_s are operators acting on the Hilbert space of a heavy quark-antiquark system in the singlet configuration.³ In order to achieve the precision we are aiming for, we need to know the potentials up to terms of order $1/m^2$, since there is no $\mathcal{O}(\alpha_s/m^3)$ potential. For our calculation of the B_c spectrum we also have to include the leading correction to the NR dispersion relation:

$$\delta V_s = - \left(\frac{1}{8m_1^3} + \frac{1}{8m_2^3} \right) \mathbf{p}^4. \quad (8.24)$$

The static and the $1/m$ potentials are real-valued functions of r only. The $1/m^2$ potentials have an imaginary part proportional to $\delta^{(3)}(\mathbf{r})$ (which we will drop in this analysis) and a dependence on the momentum operator $\mathbf{p} = -i\partial/\partial\mathbf{r}$ of each particle. The real part may be decomposed as:

$$V^{(2,0)} = V_{SD}^{(2,0)} + V_{SI}^{(2,0)}, \quad V^{(0,2)} = V_{SD}^{(0,2)} + V_{SI}^{(0,2)}, \quad V^{(1,1)} = V_{SD}^{(1,1)} + V_{SI}^{(1,1)}, \quad (8.25)$$

$$V_{SI}^{(2,0)} = \frac{1}{2} \left\{ \mathbf{p}_1^2, V_{\mathbf{p}^2}^{(2,0)}(r) \right\} + V_{\mathbf{L}^2}^{(2,0)}(r) \frac{\mathbf{L}_1^2}{r^2} + V_r^{(2,0)}(r), \quad (8.26)$$

$$V_{SI}^{(0,2)} = \frac{1}{2} \left\{ \mathbf{p}_2^2, V_{\mathbf{p}^2}^{(0,2)}(r) \right\} + V_{\mathbf{L}^2}^{(0,2)}(r) \frac{\mathbf{L}_2^2}{r^2} + V_r^{(0,2)}(r), \quad (8.27)$$

$$V_{SI}^{(1,1)} = -\frac{1}{2} \left\{ \mathbf{p}_1 \cdot \mathbf{p}_2, V_{\mathbf{p}^2}^{(1,1)}(r) \right\} - V_{\mathbf{L}^2}^{(1,1)}(r) \frac{(\mathbf{L}_1 \cdot \mathbf{L}_2 + \mathbf{L}_2 \cdot \mathbf{L}_1)}{2r^2} + V_r^{(1,1)}(r), \quad (8.28)$$

$$V_{SD}^{(2,0)} = V_{LS}^{(2,0)}(r) \mathbf{L}_1 \cdot \mathbf{S}_1, \quad (8.29)$$

$$V_{SD}^{(0,2)} = -V_{LS}^{(0,2)}(r) \mathbf{L}_2 \cdot \mathbf{S}_2, \quad (8.30)$$

$$V_{SD}^{(1,1)} = V_{L_1 S_2}^{(1,1)}(r) \mathbf{L}_1 \cdot \mathbf{S}_2 - V_{L_2 S_1}^{(1,1)}(r) \mathbf{L}_2 \cdot \mathbf{S}_1 + V_{S_2^2}^{(1,1)}(r) \mathbf{S}_1 \cdot \mathbf{S}_2 + V_{\mathbf{S}_{12}}^{(1,1)}(r) \mathbf{S}_{12}(\mathbf{r}), \quad (8.31)$$

where the operators are the same as in those for pNRQED in Chapter 4: $\mathbf{S}_1 = \boldsymbol{\sigma}_1/2$, $\mathbf{S}_2 = \boldsymbol{\sigma}_2/2$, $\mathbf{L}_1 \equiv \mathbf{r} \times \mathbf{p}_1$, $\mathbf{L}_2 \equiv \mathbf{r} \times \mathbf{p}_2$ and $\mathbf{S}_{12}(\mathbf{r}) \equiv \frac{3\mathbf{r} \cdot \boldsymbol{\sigma}_1 \mathbf{r} \cdot \boldsymbol{\sigma}_2}{r^2} - \boldsymbol{\sigma}_1 \cdot \boldsymbol{\sigma}_2$.

By arguments of invariance under charge conjugation plus invariance under $m_1 \leftrightarrow m_2$ interchange we have that

$$V^{(1,0)}(r) = V^{(0,1)}(r), \quad \text{and so} \quad \frac{V^{(1,0)}}{m_1} + \frac{V^{(0,1)}}{m_2} = \frac{V^{(1,0)}}{m_r}. \quad (8.32)$$

The same arguments also imply:

$$\begin{aligned} V_{\mathbf{p}^2}^{(2,0)}(r) &= V_{\mathbf{p}^2}^{(0,2)}(r), & V_{\mathbf{L}^2}^{(2,0)}(r) &= V_{\mathbf{L}^2}^{(0,2)}(r), & V_r^{(2,0)}(r) &= V_r^{(0,2)}(r; m_2 \leftrightarrow m_1), \\ V_{LS}^{(2,0)}(r) &= V_{LS}^{(0,2)}(r; m_2 \leftrightarrow m_1), & V_{L_1 S_2}^{(1,1)}(r) &= V_{L_2 S_1}^{(1,1)}(r; m_1 \leftrightarrow m_2). \end{aligned} \quad (8.33)$$

Our aim is to calculate the potentials. In order to do so we can neglect the center-of-mass momentum, i.e. in the following we set $\mathbf{P}_{\mathbf{R}} = 0$ and thus $\mathbf{L}_1 \equiv \mathbf{r} \times \mathbf{p}_1 = \mathbf{r} \times \mathbf{p} \equiv \mathbf{L}$, $\mathbf{L}_2 \equiv \mathbf{r} \times \mathbf{p}_2 = -\mathbf{r} \times \mathbf{p} \equiv -\mathbf{L}$.

³Therefore, in a more mathematical notation: $h \rightarrow \hat{h}$, $V_s(\mathbf{r}, \mathbf{p}) \rightarrow \hat{V}_s(\hat{\mathbf{r}}, \hat{\mathbf{p}})$. We will however avoid this notation in order to facilitate the reading.

8.2.1 Potentials in momentum space

Unlike the position space potential V_s , the momentum space potential \tilde{V}_s is a c-number, not an operator. It is defined as the matrix element

$$\tilde{V}_s \equiv \langle \mathbf{p}' | V_s | \mathbf{p} \rangle. \quad (8.34)$$

For the static potential we have ($\mathbf{k} = \mathbf{p} - \mathbf{p}'$)

$$\tilde{V}^{(0)} = -\frac{1}{\mathbf{k}^2} \tilde{D}^{(0)}(k) = -\frac{1}{\mathbf{k}^2} C_F \sum_{n=0}^{\infty} \frac{g_B^{2n+2} \mathbf{k}^{2n\epsilon}}{(4\pi)^{2n}} \tilde{D}_{n+1}^{(0)}(\epsilon), \quad (8.35)$$

where the coefficients $\tilde{D}_i^{(0)}(\epsilon)$ can be found in Appendix G.2 up to $i = 3$. Throughout this work we will use the notation

$$D \equiv 4 + 2\epsilon, \quad d \equiv 3 + 2\epsilon. \quad (8.36)$$

For the $1/m$ potential we follow the standard practice of making the prefactor $1/k$ explicit:

$$\tilde{V}^{(1,0)} \equiv \frac{1}{k} \tilde{D}^{(1,0)}(k) = \frac{1}{k} C_F \frac{g_B^4 k^{2\epsilon}}{4\pi} \left(\tilde{D}_2^{(1,0)}(\epsilon) + \frac{g_B^2 k^{2\epsilon}}{(4\pi)^2} \tilde{D}_3^{(1,0)}(\epsilon) + \mathcal{O}(g_B^4) \right). \quad (8.37)$$

Implicit in the definitions above is the fact that the mass dependence of the potentials admits a Taylor expansion in powers of $1/m_1$ and $1/m_2$ (up to logarithms). This is so in the off-shell and Wilson-loop matching scheme but not in the on-shell scheme.

In momentum space we choose the following basis for the $1/m^2$ potentials:

$$\tilde{V}_{SI}^{(2,0)} = \frac{\mathbf{p}^2 + \mathbf{p}'^2}{2\mathbf{k}^2} \tilde{D}_{\mathbf{p}^2}^{(2,0)}(k) + \tilde{D}_r^{(2,0)}(k) + \frac{(\mathbf{p}'^2 - \mathbf{p}^2)^2}{\mathbf{k}^4} \tilde{D}_{\text{off}}^{(2,0)}(k), \quad (8.38)$$

$$\tilde{V}_{SI}^{(1,1)} = \frac{\mathbf{p}^2 + \mathbf{p}'^2}{2\mathbf{k}^2} \tilde{D}_{\mathbf{p}^2}^{(1,1)}(k) + \tilde{D}_r^{(1,1)}(k) + \frac{(\mathbf{p}'^2 - \mathbf{p}^2)^2}{\mathbf{k}^4} \tilde{D}_{\text{off}}^{(1,1)}(k). \quad (8.39)$$

The Wilson coefficients $\tilde{D}_{\mathbf{p}^2/r/\text{off}}^{(n)}$ are functions of d and $k = |\mathbf{p} - \mathbf{p}'|$. They have non-integer (mass) dimension $\sim M^{-2\epsilon}$, and the following expansion in powers of the bare parameter g_B^2 :

$$\tilde{D}_{\mathbf{p}^2}^{(2,0)} = C_F g_B^2 \left(\tilde{D}_{\mathbf{p}^2,1}^{(2,0)}(\epsilon) + \frac{g_B^2 k^{2\epsilon}}{(4\pi)^2} \tilde{D}_{\mathbf{p}^2,2}^{(2,0)}(\epsilon) + \mathcal{O}(g_B^4) \right), \quad (8.40)$$

$$\tilde{D}_{\text{off}}^{(2,0)} = C_F g_B^2 \left(\tilde{D}_{\text{off},1}^{(2,0)}(\epsilon) + \frac{g_B^2 k^{2\epsilon}}{(4\pi)^2} \tilde{D}_{\text{off},2}^{(2,0)}(\epsilon) + \mathcal{O}(g_B^4) \right), \quad (8.41)$$

$$\tilde{D}_r^{(2,0)} = C_F g_B^2 \left(\tilde{D}_{r,1}^{(2,0)}(\epsilon) + \frac{g_B^2 k^{2\epsilon}}{(4\pi)^2} \tilde{D}_{r,2}^{(2,0)}(\epsilon) + \mathcal{O}(g_B^4) \right), \quad (8.42)$$

$$\tilde{D}_{\mathbf{p}^2}^{(1,1)} = C_F g_B^2 \left(\tilde{D}_{\mathbf{p}^2,1}^{(1,1)}(\epsilon) + \frac{g_B^2 k^{2\epsilon}}{(4\pi)^2} \tilde{D}_{\mathbf{p}^2,2}^{(1,1)}(\epsilon) + \mathcal{O}(g_B^4) \right), \quad (8.43)$$

$$\tilde{D}_{\text{off}}^{(1,1)} = C_F g_B^2 \left(\tilde{D}_{\text{off},1}^{(1,1)}(\epsilon) + \frac{g_B^2 k^{2\epsilon}}{(4\pi)^2} \tilde{D}_{\text{off},2}^{(1,1)}(\epsilon) + \mathcal{O}(g_B^4) \right), \quad (8.44)$$

$$\tilde{D}_r^{(1,1)} = \tilde{D}_{r,0}^{(1,1)}(\epsilon) + C_F g_B^2 \left(\tilde{D}_{r,1}^{(1,1)}(\epsilon) + \frac{g_B^2 k^{2\epsilon}}{(4\pi)^2} \tilde{D}_{r,2}^{(1,1)}(\epsilon) + \mathcal{O}(g_B^4) \right). \quad (8.45)$$

In our convention the different coefficients of the Taylor expansion are dimensionless except for $\tilde{D}_{r,0}^{(1,1)}(\epsilon)$. Furthermore, this coefficient depends on the NRQCD four-fermion Wilson coefficients, which have a non-trivial mass dependence. This makes the assignment of (part of) the four-fermion NRQCD Wilson coefficient to $\tilde{D}_{r,0}^{(1,1)}$ or $\tilde{D}_{r,0}^{(2,0)}$ ambiguous. We choose to put these coefficients in $\tilde{D}_{r,0}^{(1,1)}$. We will discuss these issues further in the following sections.

8.2.2 The \mathbf{L}^2 operator and potentials in D dimensions

We work with dimensional regularization, hence we need to define the potentials in $D = 4 + 2\epsilon$ dimensions. In the previous section we have given D -dimensional expressions for the potentials in momentum space. In position space, for the spin-independent potentials, only the \mathbf{L}^2 operator differs from the four-dimensional case. The definition of the operator \mathbf{L}^2 in D dimensions is ambiguous. In this work we choose the definition

$$\frac{\mathbf{L}^2}{r^2} \equiv p^i \left(\delta^{ij} - \frac{r^i r^j}{r^2} \right) p^j. \quad (8.46)$$

The right-hand-side of the equation is equal to the usual $\frac{\mathbf{L}^2}{r^2}$ in four dimensions and it commutes with pure functions of r in D dimensions, i.e. $[f(r), \frac{\mathbf{L}^2}{r^2}] = 0$, as we would expect for an angular momentum operator.

8.2.3 Position versus momentum space

We now proceed to relate the potentials in position and momentum space. For the static and $1/m$ potentials the relation is straightforward. After Fourier transformation to position space Eq. (8.35) becomes

$$V^{(0)} = \int \frac{d^d q}{(2\pi)^d} e^{-i\mathbf{q}\cdot\mathbf{r}} \tilde{V}^{(0)}(\mathbf{q}) = -C_F \sum_{n=0}^{\infty} \frac{g_B^{2n+2}}{(4\pi)^{2n}} \mathcal{F}_{2-2n\epsilon}(r) \tilde{D}_{n+1}^{(0)}(\epsilon), \quad (8.47)$$

where

$$\mathcal{F}_n(r) = \int \frac{d^d k}{(2\pi)^d} \frac{e^{-i\mathbf{k}\cdot\mathbf{r}}}{|\mathbf{k}|^n} = \frac{2^{-n} \pi^{-d/2} \Gamma(d/2 - n/2)}{r^{d-n} \Gamma(n/2)} \quad (8.48)$$

is the d -dimensional Fourier transform of $|\mathbf{k}|^{-n}$.

For the $1/m$ potential we have

$$V^{(1,0)} = \int \frac{d^d q}{(2\pi)^d} e^{-i\mathbf{q}\cdot\mathbf{r}} \tilde{V}^{(1,0)}(\mathbf{q}) = C_F \sum_{n=1}^{\infty} \frac{g_B^{2n+2}}{(4\pi)^{2n-1}} \mathcal{F}_{1-2n\epsilon}(r) \tilde{D}_{n+1}^{(1,0)}(\epsilon). \quad (8.49)$$

In order to Fourier transform the $1/m^2$ potentials some preparation is required. Given two arbitrary functions of r , $f(r)$ and $g^{ij}(r) = A(r)\delta^{ij} + B(r)\frac{r^i r^j}{r^2}$, the following equalities hold:⁴

$$p^i f(r) p^i = [p^i, f(r)] p^i + f(r) \mathbf{p}^2 = \frac{1}{2} \left\{ f(r), \mathbf{p}^2 \right\} - \frac{1}{2} [p^i, [p^i, f(r)]], \quad (8.50)$$

$$p^i \left(A(r)\delta^{ij} + B(r)\frac{r^i r^j}{r^2} \right) p^j = -B(r) \frac{\mathbf{L}^2}{r^2} + \frac{1}{2} \left\{ A(r) + B(r), \mathbf{p}^2 \right\} - \frac{1}{2} [p^i, [p^i, A(r) + B(r)]]. \quad (8.51)$$

⁴Recall that in coordinate space $p^i = -i\partial/\partial r^i$ and $[p^i, [p^i, f(r)]] = -(\nabla^2 f(r))$ for an arbitrary function $f(r)$.

Furthermore, we can write

$$\frac{(\mathbf{p}'^2 - \mathbf{p}^2)^2}{\mathbf{k}^4} \tilde{D}_{\text{off}}^{(2,0)}(k) = p^i \left(4\tilde{D}_{\text{off}}^{(2,0)}(k) \frac{k^i k^j}{\mathbf{k}^4} \right) p^j + \tilde{D}_{\text{off}}^{(2,0)}(k), \quad (8.52)$$

and analogously for $\tilde{D}_{\text{off}}^{(1,1)}$. The last equality is especially useful, because the first term has the structure of the matrix element of the left-hand-side of Eq. (8.51). It allows us to relate

$$\tilde{V}_{\text{off}}^{(2,0)} \equiv \frac{(\mathbf{p}'^2 - \mathbf{p}^2)^2}{\mathbf{k}^4} \tilde{D}_{\text{off}}^{(2,0)}(k) \quad (8.53)$$

with the potentials in position space:

$$V_{\text{off}}^{(2,0)} = 4 \left(\frac{d^2 g_{\text{off}}^{(2,0)}}{dr^2} - \frac{1}{r} \frac{dg_{\text{off}}^{(2,0)}}{dr} \right) \frac{\mathbf{L}^2}{r^2} - 2 \left\{ \frac{d^2 g_{\text{off}}^{(2,0)}}{dr^2}, \mathbf{p}^2 \right\} + 2[p^i, [p^i, \frac{d^2 g_{\text{off}}^{(2,0)}}{dr^2}]] + h_{\text{off}}(r), \quad (8.54)$$

through

$$g_{\text{off}}^{(2,0)}(r) = \int \frac{d^d k}{(2\pi)^d} e^{-i\mathbf{k}\cdot\mathbf{r}} \frac{\tilde{D}_{\text{off}}^{(2,0)}(k)}{\mathbf{k}^4}, \quad h_{\text{off}}^{(2,0)}(r) = \int \frac{d^d k}{(2\pi)^d} e^{-i\mathbf{k}\cdot\mathbf{r}} \tilde{D}_{\text{off}}^{(2,0)}(k), \quad (8.55)$$

and similarly for $V_{\text{off}}^{(1,1)}$.⁵ Note that the three potentials $V_{\mathbf{L}^2}$, $V_{\mathbf{p}^2}$ and V_r receive contributions from the Fourier transform of \tilde{V}_{off} . On the other hand, $\tilde{V}_{\mathbf{p}^2}$ and \tilde{V}_r only directly contribute to $V_{\mathbf{p}^2}$ and V_r . We stress that $\tilde{V}_{\mathbf{p}^2/r}$ is not the Fourier transform of $V_{\mathbf{p}^2/r}$.

In summary, we have the following relations:

$$V_{\mathbf{L}^2}^{(2,0)} = 4 \left(\frac{d^2 g_{\text{off}}^{(2,0)}}{dr^2} - \frac{1}{r} \frac{dg_{\text{off}}^{(2,0)}}{dr} \right) \equiv C_F \sum_{n=0}^{\infty} \frac{g_B^{2n+2}}{(4\pi)^{2n+1}} \mathcal{F}_{2-2n\epsilon}(r) D_{\mathbf{L}^2, n+1}^{(2,0)}(\epsilon), \quad (8.59)$$

$$V_{\mathbf{p}^2}^{(2,0)} = \int \frac{d^d q}{(2\pi)^d} e^{-i\mathbf{q}\cdot\mathbf{r}} \tilde{V}_{\mathbf{p}^2}^{(2,0)}(\mathbf{q}) - 4 \frac{d^2 g_{\text{off}}^{(2,0)}}{dr^2} \equiv C_F \sum_{n=0}^{\infty} \frac{g_B^{2n+2}}{(4\pi)^{2n+1}} \mathcal{F}_{2-2n\epsilon}(r) D_{\mathbf{p}^2, n+1}^{(2,0)}(\epsilon), \quad (8.60)$$

$$V_r^{(2,0)} = \int \frac{d^d q}{(2\pi)^d} e^{-i\mathbf{q}\cdot\mathbf{r}} \tilde{V}_r^{(2,0)}(\mathbf{q}) + 2[p^i, [p^i, \frac{d^2 g_{\text{off}}^{(2,0)}}{dr^2}]] + h_{\text{off}}^{(2,0)}(r)$$

⁵For the inverse Fourier transform the following relation is useful:

$$\begin{aligned} \langle \mathbf{p}' | f(r) \mathbf{L}^2 | \mathbf{p} \rangle &= \frac{k^2}{4} \left(\tilde{f}''(k) - \frac{\tilde{f}'(k)}{k} \right) \left(\frac{(\mathbf{p}^2 - \mathbf{p}'^2)^2}{k^4} - 1 \right) - k^2 \left(\tilde{f}''(k) + (d-2) \frac{\tilde{f}'(k)}{k} \right) \frac{\mathbf{p}^2 + \mathbf{p}'^2}{2k^2} \\ &\quad + \frac{k^2}{2} \left(\tilde{f}''(k) + (d-2) \frac{\tilde{f}'(k)}{k} \right), \end{aligned} \quad (8.56)$$

where

$$f(r) = r^2 \int \frac{d^d k}{(2\pi)^d} e^{-i\mathbf{k}\cdot\mathbf{r}} \tilde{f}(k) \quad (8.57)$$

and $\tilde{f}'(k) = \frac{d}{dk} \tilde{f}(k)$. Finally, note that in four dimensions

$$\langle \mathbf{p}' | \frac{\mathbf{L}^2}{2\pi r^3} | \mathbf{p} \rangle = \left(\frac{\mathbf{p}^2 - \mathbf{p}'^2}{\mathbf{k}^2} \right)^2 - 1. \quad (8.58)$$

$$= C_F \left[\frac{g_B^2}{4\pi} \delta^{(d)}(\mathbf{r}) D_{r,1}^{(2,0)}(\epsilon) + \frac{g_B^4}{(4\pi)^3} \mathcal{F}_{-2\epsilon}(r) D_{r,2}^{(2,0)}(\epsilon) + \mathcal{O}(g_B^6) \right], \quad (8.61)$$

$$V_{\mathbf{L}^2}^{(1,1)} = 4 \left(\frac{d^2 g_{\text{off}}^{(1,1)}}{dr^2} - \frac{1}{r} \frac{dg_{\text{off}}^{(1,1)}}{dr} \right) \equiv C_F \sum_{n=0}^{\infty} \frac{g_B^{2n+2}}{(4\pi)^{2n+1}} \mathcal{F}_{2-2n\epsilon}(r) D_{\mathbf{L}^2, n+1}^{(1,1)}(\epsilon), \quad (8.62)$$

$$V_{\mathbf{p}^2}^{(1,1)} = \int \frac{d^d q}{(2\pi)^d} e^{-i\mathbf{q}\cdot\mathbf{r}} \tilde{V}_{\mathbf{p}^2}^{(1,1)}(\mathbf{q}) - 4 \frac{d^2 g_{\text{off}}^{(1,1)}}{dr^2} \equiv C_F \sum_{n=0}^{\infty} \frac{g_B^{2n+2}}{(4\pi)^{2n+1}} \mathcal{F}_{2-2n\epsilon}(r) D_{\mathbf{p}^2, n+1}^{(1,1)}(\epsilon), \quad (8.63)$$

$$V_r^{(1,1)} = \int \frac{d^d q}{(2\pi)^d} e^{-i\mathbf{q}\cdot\mathbf{r}} \tilde{V}_r^{(1,1)}(\mathbf{q}) + 2[p^i, [p^i, \frac{d^2 g_{\text{off}}^{(1,1)}}{dr^2}]] + h_{\text{off}}^{(1,1)}(r) \quad (8.64)$$

$$= \delta^{(d)}(\mathbf{r}) D_{r,0}^{(1,1)}(\epsilon) + C_F \left[\frac{g_B^2}{4\pi} \delta^{(d)}(\mathbf{r}) D_{r,1}^{(1,1)}(\epsilon) + \frac{g_B^4}{(4\pi)^3} \mathcal{F}_{-2\epsilon}(r) D_{r,2}^{(1,1)}(\epsilon) + \mathcal{O}(g_B^6) \right].$$

In the second equality of each expression we have explicitly expanded in powers of g_B^2 . Again, $\mathcal{F}_n(r)$ has been defined in Eq. (8.48) and expressions with $\mathcal{F}_{-2\epsilon}(r)$ should be treated with care, as such operators are singular.

In summary, at each order in g_B^2 it is possible to obtain closed expressions relating the $1/m^2$ coefficients in momentum and position space. The position space expressions are, however, more complicated than for the static and $1/m$ potentials. The off-shell potential \tilde{V}_{off} obscures the relation between the momentum and position space potentials. Note also that V_r can always be written as $[p^i, [p^i, \mathcal{V}_r(r)]]$, where $\mathcal{V}_r(r)$ has the same dimensions as $V_{\mathbf{p}^2}$ and $V_{\mathbf{L}^2}$.

8.3 Field redefinitions

The bases of potentials, Eqs. (8.49)-(8.59)-(8.64), in position space, and Eqs. (8.37)-(8.39) in momentum space, are ambiguous. There is a large freedom to reshuffle (parts of) some potentials into others using unitary transformations of the pNRQCD fields S and O , which leave the spectrum unchanged. In particular, this reshuffling takes place between the off-shell $1/m^2$ potential and the $1/m$ potential. It turns out that we can even eliminate the $1/m$ potential or, alternatively, the off-shell $1/m^2$ potential \tilde{V}_{off} , completely by such field redefinitions. In fact, the latter is achieved in the on-shell matching scheme, which provides us with a minimal basis of operators by construction. The drawback of this scheme is that, as it relies on the free EOMs, the determination of the potentials has to be corrected order by order in α_s , through potential loops. Still, once a minimal basis is fixed, there is no ambiguity left and each potential is well defined on its own. The fact that the potential is unambiguous also implies that unitary transformations that keep the Hamiltonian in a given minimal basis cannot move terms between the potentials.

In this work, however, we want to keep \tilde{V}_{off} , in order to enable a strict $1/m$ expansion and to maintain the Poincaré invariance relations, see Sec. 9.6. We are also not particularly interested in completely eliminating the $1/m$ potential, as it naturally appears in the Wilson loop matching, as well as in the off-shell/on-shell matching schemes.

Instead, the goal of this section is to determine the field redefinitions that translate the results of different matching schemes into each other. This will eventually allow us to combine our calculation of the $1/m^2$ potential with the result of the $1/m$ potential in the on-shell matching

scheme for the equal mass case computed in Ref. [140] to obtain the $1/m$ potential in the unequal mass case in Sec. 9.3. Following Ref. [42] we proceed as follows. The Hamiltonian has the form

$$h_s = \frac{\mathbf{p}^2}{2m_r} + V^{(0)}(r) + \frac{\delta V_1(r)}{m_r} + \dots, \quad (8.65)$$

where \dots stands for $\mathcal{O}(1/m)$ (or higher order) potentials that we are not interested in eliminating.

The unitary transformation

$$U = \exp\left(-\frac{i}{m_r}\{\mathbf{W}(r), \mathbf{p}\}\right) \quad (8.66)$$

transforms $h_s \rightarrow h'_s = U^\dagger h_s U$. Under the condition $\{\mathbf{W}, \mathbf{p}\} \ll m_r$ (which is necessary in order to maintain the standard form of the leading terms in the Hamiltonian, i.e. a kinetic term plus a potential) h'_s reads

$$\begin{aligned} h'_s &= \frac{\mathbf{p}^2}{2m_r} + V^{(0)} + \frac{\delta V_1}{m_r} + \frac{2}{m_r} \mathbf{W} \cdot (\nabla V^{(0)}) + \frac{2}{m_r^2} \mathbf{W} \cdot (\nabla \delta V_1) \\ &+ \frac{2}{m_r^2} W^i (\nabla^i W^j (\nabla^j V^{(0)})) - \frac{1}{2m_r^2} \{p^i, \{p^j, (\nabla^i W^j)\}\} + \mathcal{O}\left(\frac{1}{m_r^3}\right) + \dots \end{aligned} \quad (8.67)$$

By choosing

$$\mathbf{W} = -\frac{1}{2} \delta V_1 \frac{\nabla V^{(0)}}{(\nabla V^{(0)})^2} \quad (8.68)$$

we completely eliminate $\frac{\delta V_1}{m_r}$ from h'_s . Moreover, since $\delta V_1 \sim \alpha_s^2$ (there is no tree-level $1/m$ potential), for the precision of the calculations in this work, we can neglect some terms in Eq. (8.67) such that:

$$h'_s = \frac{\mathbf{p}^2}{2m_r} + V^{(0)} - \frac{1}{2m_r^2} \{p^i, \{p^j, (\nabla^i W^j)\}\} + \mathcal{O}\left(\frac{1}{m_r^3}, \frac{\alpha_s^3}{m_r^2}\right) + \dots \quad (8.69)$$

Therefore, eliminating $\delta V_1/m_r$ is equivalent to introducing an extra $1/m^2$ potential:

$$\delta V_{\text{FR}} = -\frac{1}{2m_r^2} \{p^i, \{p^j, (\nabla^i W^j)\}\}. \quad (8.70)$$

Using

$$\{p^i, \{p^j, (\nabla^i W^j)\}\} = 4p^i (\nabla^i W^j) p^j + [p^i, [p^j, (\nabla^i W^j)]] \quad (8.71)$$

and Eq. (8.51), we obtain

$$\begin{aligned} \{p^i, \{p^j, (\nabla^i \nabla^j g)\}\} &= -4 \left(g''(r) - \frac{g'(r)}{r} \right) \frac{\mathbf{L}^2}{r^2} + 2 \{ \mathbf{p}^2, g''(r) \} - 2 [p^i, [p^i, g''(r)]] \\ &+ \left[p^i, \left[p^j, \frac{g'(r)}{r} \delta_{ij} + \frac{r^i r^j}{r^2} \left(g''(r) - \frac{g'(r)}{r} \right) \right] \right], \end{aligned} \quad (8.72)$$

where, without loss of generality,

$$(\nabla^i W^j) = -\frac{1}{2} \nabla^i \left(\delta V_1 \frac{\nabla^j V_0}{(\nabla V_0)^2} \right) \equiv \nabla^i \nabla^j g(r) = \delta^{ij} \frac{g'(r)}{r} + \frac{r^i r^j}{r^2} \left(g''(r) - \frac{g'(r)}{r} \right). \quad (8.73)$$

Hence, we find in momentum space

$$\delta\tilde{V}_{\text{FR}} = \langle \mathbf{p}' | \delta V_{\text{FR}} | \mathbf{p} \rangle = \frac{1}{2m_r^2} \frac{(\mathbf{p}'^2 - \mathbf{p}^2)^2}{\mathbf{k}^4} \tilde{g}(k), \quad (8.74)$$

where we have defined

$$\nabla^i g(r) \equiv \nabla^i \int \frac{d^d k}{(2\pi)^d} e^{-i\mathbf{k}\cdot\mathbf{r}} \frac{\tilde{g}(k)}{\mathbf{k}^4} = -\frac{1}{2} \delta V_1 \frac{\nabla^i V_0}{(\nabla V_0)^2}. \quad (8.75)$$

This has the important consequence that through $\mathcal{O}(\alpha_s^2)$ the coefficients \tilde{D}_r and $\tilde{D}_{\mathbf{p}^2}$ remain invariant under the field redefinitions discussed above. One can also check that the $\mathcal{O}(\alpha_s/m^3)$ potential is invariant under the field redefinition Eq. (8.69). We will make use of these results in the following.

At higher orders in α_s the neglected terms in Eq. (8.67) and Eq. (8.69) may give an extra contribution to \tilde{D}_r . On the other hand, note that $\tilde{D}_{\mathbf{p}^2}$ is unaffected by the field redefinition, Eq. (8.66), at any order in the α_s expansion.

Finally, we stress that, since the unitary transformation used in this section can move us into a minimal basis, and, since the static and the α_s/m^3 potential remain invariant under such transformation, the result for these two potentials is independent of the specific matching scheme used to determine them.

Chapter 9

Determination of the potential for unequal masses

In this chapter we compute for the first time the spin-independent $\mathcal{O}(\alpha_s^2/m^2)$ potential for unequal masses. We do so explicitly in different matching schemes and with full ϵ dependence. Our results directly fix the bare coefficients \tilde{D} in each scheme. With little effort and using the equations in Sec. 8.2.3, one can then obtain the expressions for the bare coefficients D of the potential in position space. Note that all $1/m^2$ position space potentials depend on the matching procedure (albeit some of them weakly, in the sense that the matching scheme dependence vanishes when $\epsilon \rightarrow 0$), as do g_{off} and h_{off} in Eqs. (8.59)-(8.64). Therefore, instead of presenting explicit expressions, we give the position space results only in terms of the momentum space coefficients in Appendix G.1.

9.1 The $\mathcal{O}(\alpha_s^2/m^2)$ potential: matching with Green functions

In the off-shell matching we equate four-point off-shell Green functions computed in NRQCD with the analogous four-point off-shell Green functions in pNRQCD. The only restriction on the external momenta is total energy-momentum conservation. This allows us to perform the matching in a strict $1/m$ expansion, since NRQCD and pNRQCD potential loops cancel each other exactly. Hence, we can directly equate soft NRQCD diagrams (computed with static quarks) with the bare potentials in pNRQCD at a given order in $1/m$.

By contrast, in the on-shell matching S-matrix elements of NRQCD and pNRQCD are equated order by order in an expansion in v ($\sim \alpha_s$). These S-matrix elements are computed with asymptotic quarks satisfying the free EOM. The on-shell condition causes an imperfect cancellation between potential loops in NRQCD and pNRQCD, and so the matching requires the incorporation of potential loops in both calculations. Potential loops in pNRQCD mix different orders in the $1/m$ expansion, i.e. potential loops involving a potential at a given order can contribute to the matching of a potential at lower orders. See, for instance, Ref. [141] for an illustrative example.

Throughout Part II we have performed the matching between NRQED and pNRQED in CG and with the addition of a light massive fermion. Note that the CG expressions we will obtain here for the potential proportional to C_F^2 are the same as the ones in Chapter 4 taking the QED values $C_F = 1$, $C_A = 0$ and $T_f = 1$ (provided there are no hadronic contributions in the Wilson

coefficients). With some effort we can also derive the $C_F T_F n_f$ proportional terms of the potential from Chapter 4 for $n_f = 1$ taking the limit $m_e \rightarrow 0$.

9.1.1 Off-shell matching: Coulomb gauge

The off-shell matching between NRQED and pNRQED has been studied in detail with $\mathcal{O}(m\alpha_s^5)$ precision in CG in Refs. [57, 58]. The FG matching has also been discussed in Ref. [58] with $\mathcal{O}(m\alpha_s^4)$ precision.

We now perform the matching for the case of QCD. We focus on the relativistic $1/m^2$ corrections to the potential. The tree-level matching is analogous to the one in QED up to the straightforward incorporation of color factors:

$$\tilde{D}_{r,0}^{(1,1)}(\epsilon) = d_{ss} + C_F d_{vs}, \quad (9.1)$$

$$\tilde{D}_{\mathbf{p}^2,1}^{(2,0)}(\epsilon) = 0, \quad (9.2)$$

$$\tilde{D}_{\text{off},1,\text{CG}}^{(2,0)}(\epsilon) = 0, \quad (9.3)$$

$$\tilde{D}_{r,1}^{(2,0)}(\epsilon) = \frac{c_D^{(1)}}{8}, \quad (9.4)$$

$$\tilde{D}_{\mathbf{p}^2,1}^{(1,1)}(\epsilon) = -1, \quad (9.5)$$

$$\tilde{D}_{\text{off},1,\text{CG}}^{(1,1)}(\epsilon) = \frac{1}{4}, \quad (9.6)$$

$$\tilde{D}_{r,1}^{(1,1)}(\epsilon) = \frac{1}{4}. \quad (9.7)$$

The gauge-dependent off-shell coefficients \tilde{D} are given here in CG and labeled accordingly.

Now we consider the one-loop corrections. In Appendix F we present the result of the relevant diagrams in CG and give explicit expressions for the amplitudes diagram by diagram. It is usually assumed that the evaluation of Feynman diagrams in the CG can be quite cumbersome, especially for non-Abelian gauge theories. We find that this is not the case, at least for the computation we perform in this work.

The diagrams depend on the energies of the four external quarks E_i (see Appendix F). This dependence (at the order at which we are working) can be eliminated in the potentials using the complete EOMs at the appropriate order, which include the static potential.¹ Finally, we obtain the following (bare) CG results

$$\tilde{D}_{\mathbf{p}^2,2}^{(2,0)}(\epsilon) = \frac{2C_A}{3} \frac{\pi^{\frac{3}{2}-\epsilon}}{16^\epsilon} \frac{\csc(\pi\epsilon)}{\Gamma\left(\epsilon + \frac{1}{2}\right)} = \left(\frac{e^{\gamma_E}}{4\pi}\right)^\epsilon \frac{2}{3} C_A \frac{1}{\epsilon} + \mathcal{O}(\epsilon), \quad (9.8)$$

$$\begin{aligned} \tilde{D}_{r,2}^{(2,0)}(\epsilon) = & \frac{\pi^{\frac{3}{2}-\epsilon} \csc(\pi\epsilon)}{2^{4\epsilon+3} \Gamma\left(\epsilon + \frac{5}{2}\right)} \left\{ (c_D^{(1)} + c_1^{hl(1)}) T_F n_f (1 + \epsilon) \right. \\ & \left. - C_A \left[\frac{1}{4} (c_F^{(1)})^2 (1 + \epsilon)(5 + 4\epsilon) + \frac{1}{3} (2 + \epsilon)(3 + 2\epsilon)(3 + 4\epsilon) \right] \right\} \end{aligned}$$

¹Fortunately, for our purposes it is enough to use the free EOMs while still keeping $\mathbf{p}^2 \neq \mathbf{p}'^2$ (unlike in the on-shell matching), as we are not interested in performing the full computation of the $1/m$ potential. However, for completeness we give the contribution of the computed diagrams to the $1/m$ potential in Eq. (F.8).

$$\begin{aligned}
 &= \left(\frac{e^{\gamma_E}}{4\pi}\right)^\epsilon \left\{ \left[C_A \left(-1 + \frac{11}{24} c_D^{(1)} - \frac{5}{24} c_F^{(1)2} \right) + \frac{1}{6} c_1^{hl(1)} T_{Fn_f} - \frac{c_D^{(1)}}{8} \beta_0 \right] \frac{1}{\epsilon} \right. \\
 &\quad \left. + \left(\frac{1}{3} + \frac{13}{36} (c_F^{(1)})^2 \right) \frac{C_A}{2} - \frac{5}{18} (c_D^{(1)} + c_1^{hl(1)}) T_{Fn_f} \right\} + \mathcal{O}(\epsilon), \tag{9.9}
 \end{aligned}$$

$$\begin{aligned}
 \tilde{D}_{\mathbf{p}^2,2}^{(1,1)}(\epsilon) &= -\frac{1}{3} \frac{\pi^{\frac{3}{2}-\epsilon} \csc(\pi\epsilon)}{2^{4\epsilon+2} \Gamma\left(\epsilon + \frac{5}{2}\right)} \left\{ 12 T_{Fn_f}(\epsilon + 1) - C_A(40\epsilon^2 + 89\epsilon + 45) \right\} \\
 &= \left(\frac{e^{\gamma_E}}{4\pi}\right)^\epsilon \left\{ -a_1 + \left(\frac{4}{3} C_A + \beta_0\right) \frac{1}{\epsilon} \right\} + \mathcal{O}(\epsilon), \tag{9.10}
 \end{aligned}$$

$$\begin{aligned}
 \tilde{D}_{r,2}^{(1,1)}(\epsilon) &= \frac{1}{3} \frac{\pi^{\frac{3}{2}-\epsilon} \csc(\pi\epsilon)}{2^{4\epsilon+3} \Gamma\left(\epsilon + \frac{5}{2}\right)} \left\{ 2 C_F(1 + \epsilon)(3 + 2\epsilon)(7 + 8\epsilon) + 6 T_{Fn_f}(1 + \epsilon) \right. \\
 &\quad \left. - C_A(8\epsilon^3 + 47\epsilon^2 + 74\epsilon + 33) \right\} \\
 &= \left(\frac{e^{\gamma_E}}{4\pi}\right)^\epsilon \left\{ \frac{a_1}{4} - \frac{1}{12} C_A + \frac{1}{3} C_F - \left(\frac{11}{12} C_A - \frac{7}{3} C_F + \frac{\beta_0}{4} \right) \frac{1}{\epsilon} \right\} + \mathcal{O}(\epsilon), \tag{9.11}
 \end{aligned}$$

$$\begin{aligned}
 \tilde{D}_{\text{off},2,\text{CG}}^{(2,0)}(\epsilon) &= C_A \frac{(3 + 2\epsilon)}{3} \frac{\pi^{\frac{3}{2}-\epsilon} \csc(\pi\epsilon)}{2^{4\epsilon+3} \Gamma\left(\epsilon + \frac{5}{2}\right)} \left\{ 4 + \epsilon(7 + 4\epsilon) - \frac{2^{3+2\epsilon}(1 + \epsilon)\Gamma^2\left(\epsilon + \frac{3}{2}\right)}{\sqrt{\pi}\Gamma\left(2\epsilon + \frac{3}{2}\right)} \right\} \\
 &= \left(\frac{e^{\gamma_E}}{4\pi}\right)^\epsilon C_A \left(\frac{1}{2} - \frac{4}{3} \ln 2 \right) + \mathcal{O}(\epsilon), \tag{9.12}
 \end{aligned}$$

$$\begin{aligned}
 \tilde{D}_{\text{off},2,\text{CG}}^{(1,1)}(\epsilon) &= \frac{\pi^{\frac{3}{2}-\epsilon} \csc(\pi\epsilon)}{2^{4\epsilon+3} \Gamma\left(\epsilon + \frac{5}{2}\right)} \left\{ 2 T_{Fn_f}(1 - \epsilon^2) + \frac{C_A}{6} \left(- \frac{2^{5+2\epsilon}(3 + 2\epsilon)(1 + \epsilon)\Gamma^2\left(\epsilon + \frac{3}{2}\right)}{\sqrt{\pi}\Gamma\left(2\epsilon + \frac{3}{2}\right)} \right. \right. \\
 &\quad \left. \left. + 56\epsilon^3 + 137\epsilon^2 + 92\epsilon + 15 \right) \right\} \\
 &= \left(\frac{e^{\gamma_E}}{4\pi}\right)^\epsilon \left\{ \frac{a_1}{4} + C_A + \frac{\beta_0}{4} - \frac{8}{3} C_A \ln 2 - \frac{\beta_0}{4} \frac{1}{\epsilon} \right\} + \mathcal{O}(\epsilon), \tag{9.13}
 \end{aligned}$$

where a_1 and β_0 are defined in Appendix A. Note that, strictly speaking, there are subleading contributions in powers of α_s encoded in the NRQCD Wilson coefficients.

9.1.2 Off-shell matching: Feynman gauge

The matching in FG involves considerably more (soft) NRQCD diagrams. In particular, diagrams with only A^0 gluon exchanges now give a non-zero contribution. As a consequence, the dependence on the (off-shell) external quark energies is more complicated. The complete expression for the sum of all one-loop diagrams can be found in Appendix F. Yet, after using the complete EOMs we find that the coefficients \tilde{D}_r and $\tilde{D}_{\mathbf{p}^2}$ agree with the CG results. This is indeed what we expected, as these potentials remain the same in the on-shell limit, and are therefore separately matching scheme and gauge invariant. The differences to CG therefore manifest themselves only in the \tilde{D}_{off} coefficients.

At tree level in FG (and at one loop in the CG) an energy-dependent term $\propto k_0^2 = (E'_1 - E_1)^2$ occurs. In principle, the redefinition of the quark energies in terms of three-momenta is ambiguous. In this special case, however, there is a preferred prescription (see Ref. [58]) to

transform away the energy dependence, namely Eq. (F.7). It is the only way to preserve the $1/(m_1 m_2)$ structure and at the same time leave the $1/m$ potential unchanged, see Appendix F for details. Adopting this prescription we arrive at the same result as in CG:

$$\tilde{D}_{\text{off},1,\text{FG}}^{(1,1)} = \tilde{D}_{\text{off},1,\text{CG}}^{(1,1)}, \quad \tilde{D}_{\text{off},1,\text{FG}}^{(2,0)} = \tilde{D}_{\text{off},1,\text{CG}}^{(2,0)}. \quad (9.14)$$

Replacing the energy dependence as detailed in Appendix F we obtain at one loop

$$\begin{aligned} \tilde{D}_{\text{off},2,\text{FG}}^{(2,0)}(\epsilon) &= \tilde{D}_{\text{off},2,\text{CG}}^{(2,0)}(\epsilon) + \frac{C_A}{3} \frac{\pi^{\frac{3}{2}-\epsilon} \csc(\pi\epsilon)}{2^{4\epsilon+3} \Gamma(\epsilon + \frac{5}{2})} \left(\frac{2^{2\epsilon+3} (\epsilon+1)(2\epsilon+3) \Gamma^2(\epsilon + \frac{3}{2})}{\sqrt{\pi} \Gamma(2\epsilon + \frac{3}{2})} \right. \\ &\quad \left. + 20\epsilon^3 + 39\epsilon^2 + \frac{25\epsilon}{4} - 12 \right) \\ &= \tilde{D}_{\text{off},2,\text{CG}}^{(2,0)}(\epsilon) + C_A \left(\frac{35}{24} + \frac{4 \ln 2}{3} \right) + \mathcal{O}(\epsilon), \end{aligned} \quad (9.15)$$

$$\begin{aligned} \tilde{D}_{\text{off},2,\text{FG}}^{(1,1)}(\epsilon) &= \tilde{D}_{\text{off},2,\text{CG}}^{(1,1)}(\epsilon) + \frac{C_A}{3} \frac{\pi^{\frac{3}{2}-\epsilon} \csc(\pi\epsilon)}{2^{4\epsilon+2} \Gamma(\epsilon + \frac{5}{2})} \left(\frac{2^{2\epsilon+3} (\epsilon+1)(2\epsilon+3) \Gamma^2(\epsilon + \frac{3}{2})}{\sqrt{\pi} \Gamma(2\epsilon + \frac{3}{2})} \right. \\ &\quad \left. + 20\epsilon^3 + 39\epsilon^2 + \frac{25\epsilon}{4} - 12 \right) \\ &= \tilde{D}_{\text{off},2,\text{CG}}^{(1,1)}(\epsilon) + C_A \left(\frac{35}{12} + \frac{8 \ln 2}{3} \right) + \mathcal{O}(\epsilon). \end{aligned} \quad (9.16)$$

9.1.3 On-shell matching

Finally, we determine the potential in the on-shell matching scheme. In this scheme we have $\tilde{D}_{\text{off,on-shell}} = 0$ by construction. At the order we are working at, this means

$$\tilde{D}_{\text{off},1,\text{on-shell}}^{(2,0)}(\epsilon) = \tilde{D}_{\text{off},1,\text{on-shell}}^{(1,1)}(\epsilon) = \tilde{D}_{\text{off},2,\text{on-shell}}^{(2,0)}(\epsilon) = \tilde{D}_{\text{off},2,\text{on-shell}}^{(1,1)}(\epsilon) = 0. \quad (9.17)$$

It turns out that for the other potentials a dedicated on-shell matching computation is not necessary. A priori, we must take into account potential loops, which are not needed in the off-shell computation, in addition to the soft NRQCD loops. The discussion on field redefinitions in Sec. 8.3 however shows that the transformation from an off-shell to the on-shell scheme leaves the coefficients $\tilde{D}_{\mathbf{p}^2}$ and \tilde{D}_r , as well as the $\mathcal{O}(\alpha_s/m^3)$ potential, unchanged at the order we are working at. Hence, potential loops can neither contribute to $\tilde{D}_{\mathbf{p}^2,2}$ and $\tilde{D}_{r,2}$,² nor to the $\mathcal{O}(\alpha_s/m^3)$ potential. Therefore, these coefficients are equal irrespectively of computing them on- or off-shell, and in the latter case they are independent of the gauge, as we have seen.

For equal masses and in the on-shell matching scheme the potential has been computed in Refs. [133,141–145]. The complete ϵ dependence for the equal mass case can be found in Ref. [142]. We agree with their results. The novel results of the present section are the potentials for unequal masses (keeping track of the NRQCD Wilson coefficients).

As another cross check we have calculated the $\mathcal{O}(\alpha_s^2/m^2)$ potential for unequal masses from soft on-shell scattering amplitudes in vNRQCD, Ref. [146], using the Feynman rules given in Ref. [145]. We found complete agreement with our momentum space results in the on-shell matching scheme.

²At higher orders in α_s potential loop contributions to V_r are possible.

9.2 The $\mathcal{O}(\alpha_s^2/m^2)$ potential: matching with Wilson loops

9.2.1 The quasi-static energy and general formulas

An alternative determination of the potentials is the direct matching of NRQCD and pNRQCD gauge-invariant Green functions in position space. One key point is that the time of the quark and antiquark are now set equal. This is not a restriction. Instead, it is rather natural to describe quark-antiquark bound states by fields that depend on a single time coordinate. Another difference to the off-shell matching scheme is the insertion of gluon strings (Wilson lines) between the static quark and antiquark in order to form a Wilson loop, so that the whole system is gauge invariant.

The details of the Wilson-loop matching procedure are given in Refs. [42, 43]. In these references the emphasis was put on the matching in the non-perturbative scenario without ultrasoft degrees of freedom. Two alternative methods were worked out in detail. One is the direct matching between NRQCD and pNRQCD Wilson loops, and the other one is a generalized “quantum-mechanical” matching, which gives the spectral decomposition of the potentials, allowing them to be rewritten in terms of Wilson loops. Either way, the matching can be done in a strict $1/m$ expansion (potential loops do not have to be considered at all) and closed expressions in terms of Wilson loops can be obtained for each potential, which are then manifestly gauge invariant. This allows for a non-perturbative definition of the potential E_s , to which we will refer to as the “quasi-static” energy in the following. Formally it would be

$$\begin{aligned}
 E_s(\mathbf{r}, \mathbf{p}, \mathbf{P}_R, \mathbf{S}_1, \mathbf{S}_2) = & \frac{\mathbf{p}^2}{2m_r} + \frac{\mathbf{P}_R^2}{2M} + E^{(0)} + \frac{E^{(1,0)}}{m_1} + \frac{E^{(0,1)}}{m_2} \\
 & + \frac{E^{(2,0)}}{m_1^2} + \frac{E^{(0,2)}}{m_2^2} + \frac{E^{(1,1)}}{m_1 m_2} + \dots .
 \end{aligned} \tag{9.18}$$

We use “ E ” to make the distinction to the potentials “ V ” explicit. In the strong-coupling regime (and provided there are no ultrasoft degrees of freedom), the quasi-static energy replaces the potential in the Schrödinger equation describing the non-perturbative heavy quarkonium bound state. Once ultrasoft effects are included (as e.g. in our calculation of the B_c spectrum) this is not true anymore. The potential “ V ” is the particularization of the quasi-static energy once the ultrasoft effects have been subtracted in the weak coupling regime. That is why we explicitly distinguish between E and V . We will elaborate on this in Sec. 9.2.2 and in a forthcoming paper.

We shall use the following definitions for the Wilson-loop operators (see Ref. [43] for extra details). The angular brackets $\langle \dots \rangle$ denote the average value over the Yang–Mills action, W_\square is the rectangular static Wilson loop of dimensions $r \times T_W$:

$$W_\square \equiv \text{P exp} \left\{ -ig \oint_{r \times T_W} dz^\mu A_\mu(z) \right\}, \tag{9.19}$$

and $\langle \langle \dots \rangle \rangle \equiv \langle \dots W_\square \rangle / \langle W_\square \rangle$; P is the path-ordering operator. Moreover, we define the *connected* Wilson loop with $O_1(t_1), O_2(t_2), \dots, O_n(t_n)$ operator insertions for $T_W/2 \geq t_1 \geq t_2 \geq \dots \geq t_n \geq$

$-T_W/2$ by

$$\langle\langle O_1(t_1)O_2(t_2) \rangle\rangle_c = \langle\langle O_1(t_1)O_2(t_2) \rangle\rangle - \langle\langle O_1(t_1) \rangle\rangle \langle\langle O_2(t_2) \rangle\rangle, \quad (9.20)$$

$$\langle\langle O_1(t_1)O_2(t_2)O_3(t_3) \rangle\rangle_c = \langle\langle O_1(t_1)O_2(t_2)O_3(t_3) \rangle\rangle \quad (9.21)$$

$$\begin{aligned} & - \langle\langle O_1(t_1) \rangle\rangle \langle\langle O_2(t_2)O_3(t_3) \rangle\rangle_c - \langle\langle O_1(t_1)O_2(t_2) \rangle\rangle_c \langle\langle O_3(t_3) \rangle\rangle - \langle\langle O_1(t_1) \rangle\rangle \langle\langle O_2(t_2) \rangle\rangle \langle\langle O_3(t_3) \rangle\rangle, \\ \langle\langle O_1(t_1)O_2(t_2)O_3(t_3)O_4(t_4) \rangle\rangle_c & = \langle\langle O_1(t_1)O_2(t_2)O_3(t_3)O_4(t_4) \rangle\rangle \\ & - \langle\langle O_1(t_1) \rangle\rangle \langle\langle O_2(t_2)O_3(t_3)O_4(t_4) \rangle\rangle_c - \langle\langle O_1(t_1)O_2(t_2) \rangle\rangle_c \langle\langle O_3(t_3)O_4(t_4) \rangle\rangle_c \\ & - \langle\langle O_1(t_1)O_2(t_2)O_3(t_3) \rangle\rangle_c \langle\langle O_4(t_4) \rangle\rangle - \langle\langle O_1(t_1) \rangle\rangle \langle\langle O_2(t_2) \rangle\rangle \langle\langle O_3(t_3)O_4(t_4) \rangle\rangle_c \\ & - \langle\langle O_1(t_1) \rangle\rangle \langle\langle O_2(t_2)O_3(t_3) \rangle\rangle_c \langle\langle O_4(t_4) \rangle\rangle - \langle\langle O_1(t_1)O_2(t_2) \rangle\rangle_c \langle\langle O_3(t_3) \rangle\rangle \langle\langle O_4(t_4) \rangle\rangle \\ & - \langle\langle O_1(t_1) \rangle\rangle \langle\langle O_2(t_2) \rangle\rangle \langle\langle O_3(t_3) \rangle\rangle \langle\langle O_4(t_4) \rangle\rangle, \end{aligned} \quad (9.22)$$

...

At leading order in the $1/m$ expansion, we get nothing but the static energy already found by Wilson many years ago Ref. [132]

$$E^{(0)}(r) = \lim_{T \rightarrow \infty} \frac{i}{T} \ln \langle W_{\square} \rangle. \quad (9.23)$$

The complete expression of the $1/m$ and $1/m^2$ potentials in the quenched approximation (no light quarks) in terms of Wilson loops has been determined in Refs. [42, 43] (partial results for the $1/m^2$ potential can be found in Refs. [147–150]). For these we define the shorthand notation

$$\lim_{T \rightarrow \infty} \equiv \lim_{T \rightarrow \infty} \lim_{T_W \rightarrow \infty}, \quad (9.24)$$

where T_W is the time length of the Wilson loop and T is the time length appearing in the time integrals shown below. By performing the limit $T_W \rightarrow \infty$ first, the averages $\langle\langle \dots \rangle\rangle$ become independent of T_W and thus are invariant under global time translations.

The incorporation of light quarks introduces extra terms in $E_r^{(2,0)}$, which we include here. The other Wilson loop expressions for the quasi-static energies equal the ones in Refs. [42, 43], with the exception that we rewrite some of them so that they remain valid in D dimensions. For the spin-independent quasi-static energies we have

$$E^{(1,0)}(r) = -\frac{1}{2} \lim_{T \rightarrow \infty} \int_0^T dt t \langle\langle g\mathbf{E}_1(t) \cdot g\mathbf{E}_1(0) \rangle\rangle_c, \quad (9.25)$$

$$E_{\mathbf{p}^2}^{(2,0)}(r) = \frac{i}{2} \frac{r^i r^j}{r^2} \lim_{T \rightarrow \infty} \int_0^T dt t^2 \langle\langle g\mathbf{E}_1^i(t) g\mathbf{E}_1^j(0) \rangle\rangle_c, \quad (9.26)$$

$$E_{\mathbf{L}^2}^{(2,0)}(r) = \frac{i}{2(d-1)} \left(\delta^{ij} - d \frac{r^i r^j}{r^2} \right) \lim_{T \rightarrow \infty} \int_0^T dt t^2 \langle\langle g\mathbf{E}_1^i(t) g\mathbf{E}_1^j(0) \rangle\rangle_c, \quad (9.27)$$

$$E_{\mathbf{p}^2}^{(1,1)}(r) = i \frac{r^i r^j}{r^2} \lim_{T \rightarrow \infty} \int_0^T dt t^2 \langle\langle g\mathbf{E}_1^i(t) g\mathbf{E}_2^j(0) \rangle\rangle_c, \quad (9.28)$$

$$E_{\mathbf{L}^2}^{(1,1)}(r) = \frac{i}{d-1} \left(\delta^{ij} - d \frac{r^i r^j}{r^2} \right) \lim_{T \rightarrow \infty} \int_0^T dt t^2 \langle\langle g\mathbf{E}_1^i(t) g\mathbf{E}_2^j(0) \rangle\rangle_c, \quad (9.29)$$

$$E_r^{(2,0)}(r) = -\frac{c_D^{(1)}}{8} \lim_{T_W \rightarrow \infty} \langle\langle [\mathbf{D}_1 \cdot, g\mathbf{E}_1](t) \rangle\rangle_c \quad (9.30)$$

$$- \frac{ic_F^{(1)2}}{4} \lim_{T \rightarrow \infty} \int_0^T dt \langle\langle g\mathbf{B}_1(t) \cdot g\mathbf{B}_1(0) \rangle\rangle_c + \frac{1}{2} (\nabla_r^2 E_{\mathbf{p}^2}^{(2,0)})$$

$$\begin{aligned}
 & - \frac{i}{2} \lim_{T \rightarrow \infty} \int_0^T dt_1 \int_0^{t_1} dt_2 \int_0^{t_2} dt_3 (t_2 - t_3)^2 \langle\langle g_{\mathbf{E}_1}(t_1) \cdot g_{\mathbf{E}_1}(t_2) g_{\mathbf{E}_1}(t_3) \cdot g_{\mathbf{E}_1}(0) \rangle\rangle_c \\
 & + \frac{1}{2} \left(\nabla_r^i \lim_{T \rightarrow \infty} \int_0^T dt_1 \int_0^{t_1} dt_2 (t_1 - t_2)^2 \langle\langle g_{\mathbf{E}_1}^i(t_1) g_{\mathbf{E}_1}(t_2) \cdot g_{\mathbf{E}_1}(0) \rangle\rangle_c \right) \\
 & - \frac{i}{2} \left(\nabla_r^i E^{(0)} \right) \lim_{T \rightarrow \infty} \int_0^T dt_1 \int_0^{t_1} dt_2 (t_1 - t_2)^3 \langle\langle g_{\mathbf{E}_1}^i(t_1) g_{\mathbf{E}_1}(t_2) \cdot g_{\mathbf{E}_1}(0) \rangle\rangle_c \\
 & + \frac{1}{4} \left(\nabla_r^i \lim_{T \rightarrow \infty} \int_0^T dt t^3 \langle\langle g_{\mathbf{E}_1}^i(t) g_{\mathbf{E}_1}^j(0) \rangle\rangle_c (\nabla_r^j E^{(0)}) \right) \\
 & - \frac{i}{12} \lim_{T \rightarrow \infty} \int_0^T dt t^4 \langle\langle g_{\mathbf{E}_1}^i(t) g_{\mathbf{E}_1}^j(0) \rangle\rangle_c (\nabla_r^i E^{(0)}) (\nabla_r^j E^{(0)}) \\
 & - \frac{c_1^{g(1)}}{4} f_{abc} \int d^3 \mathbf{x} \lim_{T_W \rightarrow \infty} g \langle\langle G_{\mu\nu}^a(x) G_{\mu\lambda}^b(x) G_{\nu\lambda}^c(x) \rangle\rangle \\
 & - \frac{1}{2} \lim_{T \rightarrow \infty} \int_0^T dt_1 \int_0^{t_1} dt_2 (t_1 - t_2)^2 \langle\langle [\mathbf{D}_{1\cdot}, g_{\mathbf{E}_1}](t_1) g_{\mathbf{E}_1}(t_2) \cdot g_{\mathbf{E}_1}(0) \rangle\rangle_c \\
 & + \frac{i}{8} \lim_{T \rightarrow \infty} \int_0^T dt t^2 \langle\langle [\mathbf{D}_{1\cdot}, g_{\mathbf{E}_1}](t) [\mathbf{D}_{1\cdot}, g_{\mathbf{E}_1}](0) \rangle\rangle_c \\
 & - \frac{i}{4} \left(\nabla_r^i \lim_{T \rightarrow \infty} \int_0^T dt t^2 \langle\langle g_{\mathbf{E}_1}^i(t) [\mathbf{D}_{1\cdot}, g_{\mathbf{E}_1}](0) \rangle\rangle_c \right) \\
 & - \frac{1}{4} \lim_{T \rightarrow \infty} \int_0^T dt t^3 \langle\langle [\mathbf{D}_{1\cdot}, g_{\mathbf{E}_1}](t) g_{\mathbf{E}_1}^j(0) \rangle\rangle_c (\nabla_r^j E^{(0)}) \\
 & - \frac{c_1^{hl(1)}}{8} g^2 \sum_{i=1}^{n_f} \lim_{T_W \rightarrow \infty} \langle\langle T_1^a \bar{q}_i \gamma_0 T_1^a q_i(t) \rangle\rangle_c - \frac{c_2^{hl(1)}}{8} g^2 \sum_{i=1}^{n_f} \lim_{T_W \rightarrow \infty} \langle\langle \bar{q}_i \gamma_0 q_i(t) \rangle\rangle_c \\
 & - \int d^3 \mathbf{x} \lim_{T_W \rightarrow \infty} \langle\langle \delta \mathcal{L}_l^{(1)} \rangle\rangle,
 \end{aligned}$$

where in the second-to-last line the light-quark operators are located in the heavy-quark Wilson line (i.e. at the position \mathbf{x}_1). The last term contains the $1/m^2$ operators in the NRQCD Lagrangian that only involve light degrees of freedom. Irrespectively of this, all the Wilson-loop expectation values should be computed with dynamical light quarks. The quasi static energy in Eq. (9.30) generalizes the result of Ref. [43] to the case with light fermions (as usual neglecting ultrasoft effects). Note that, although, formally, the first, the second-to-last, and the last lines of Eq. (9.30) depend on the time where the operators are inserted on the heavy-quark lines. Due to time translation invariance, this is not so after performing the $T_W \rightarrow \infty$ limit.

Finally, the last term we need in Eq. (9.18) is³

$$\begin{aligned}
 E_r^{(1,1)}(r) &= \frac{1}{2} (\nabla_r^2 E_{\mathbf{p}^2}^{(1,1)}) \tag{9.31} \\
 & - i \lim_{T \rightarrow \infty} \int_0^T dt_1 \int_0^{t_1} dt_2 \int_0^{t_2} dt_3 (t_2 - t_3)^2 \langle\langle g_{\mathbf{E}_1}(t_1) \cdot g_{\mathbf{E}_1}(t_2) g_{\mathbf{E}_2}(t_3) \cdot g_{\mathbf{E}_2}(0) \rangle\rangle_c \\
 & + \frac{1}{2} \left(\nabla_r^i \lim_{T \rightarrow \infty} \int_0^T dt_1 \int_0^{t_1} dt_2 (t_1 - t_2)^2 \langle\langle g_{\mathbf{E}_1}^i(t_1) g_{\mathbf{E}_2}(t_2) \cdot g_{\mathbf{E}_2}(0) \rangle\rangle_c \right) \\
 & + \frac{1}{2} \left(\nabla_r^i \lim_{T \rightarrow \infty} \int_0^T dt_1 \int_0^{t_1} dt_2 (t_1 - t_2)^2 \langle\langle g_{\mathbf{E}_2}^i(t_1) g_{\mathbf{E}_1}(t_2) \cdot g_{\mathbf{E}_1}(0) \rangle\rangle_c \right)
 \end{aligned}$$

³The first term of this equation corrects a sign error in the first term of Eqs. (48) and (54) in Ref. [43]. Note that its spectral decomposition in Eq. (23) of that reference is nevertheless correct.

$$\begin{aligned}
 & -\frac{i}{2} \left(\nabla_r^i E^{(0)} \right) \lim_{T \rightarrow \infty} \int_0^T dt_1 \int_0^{t_1} dt_2 (t_1 - t_2)^3 \langle\langle g\mathbf{E}_1^i(t_1) g\mathbf{E}_2(t_2) \cdot g\mathbf{E}_2(0) \rangle\rangle_c \\
 & -\frac{i}{2} \left(\nabla_r^i E^{(0)} \right) \lim_{T \rightarrow \infty} \int_0^T dt_1 \int_0^{t_1} dt_2 (t_1 - t_2)^3 \langle\langle g\mathbf{E}_2^i(t_1) g\mathbf{E}_1(t_2) \cdot g\mathbf{E}_1(0) \rangle\rangle_c \\
 & + \frac{1}{4} \left(\nabla_r^i \lim_{T \rightarrow \infty} \int_0^T dt t^3 \left\{ \langle\langle g\mathbf{E}_1^i(t) g\mathbf{E}_2^j(0) \rangle\rangle_c + \langle\langle g\mathbf{E}_2^i(t) g\mathbf{E}_1^j(0) \rangle\rangle_c \right\} (\nabla_r^j E^{(0)}) \right) \\
 & - \frac{i}{6} \lim_{T \rightarrow \infty} \int_0^T dt t^4 \langle\langle g\mathbf{E}_1^i(t) g\mathbf{E}_2^j(0) \rangle\rangle_c (\nabla_r^i E^{(0)}) (\nabla_r^j E^{(0)}) \\
 & + (d_{ss} + d_{vs} C_F) \delta^{(3)}(\mathbf{x}_1 - \mathbf{x}_2) \\
 & - \frac{1}{2} \lim_{T \rightarrow \infty} \int_0^T dt_1 \int_0^{t_1} dt_2 (t_1 - t_2)^2 \langle\langle [\mathbf{D}_{1\cdot}, g\mathbf{E}_1](t_1) g\mathbf{E}_2(t_2) \cdot g\mathbf{E}_2(0) \rangle\rangle_c \\
 & + \frac{1}{2} \lim_{T \rightarrow \infty} \int_0^T dt_1 \int_0^{t_1} dt_2 (t_1 - t_2)^2 \langle\langle [\mathbf{D}_{2\cdot}, g\mathbf{E}_2](t_1) g\mathbf{E}_1(t_2) \cdot g\mathbf{E}_1(0) \rangle\rangle_c \\
 & - \frac{i}{4} \lim_{T \rightarrow \infty} \int_0^T dt t^2 \langle\langle [\mathbf{D}_{1\cdot}, g\mathbf{E}_1](t) [\mathbf{D}_{2\cdot}, g\mathbf{E}_2](0) \rangle\rangle_c \\
 & + \frac{i}{4} \left(\nabla_r^i \lim_{T \rightarrow \infty} \int_0^T dt t^2 \left\{ \langle\langle g\mathbf{E}_1^i(t) [\mathbf{D}_{2\cdot}, g\mathbf{E}_2](0) \rangle\rangle_c - \langle\langle g\mathbf{E}_2^i(t) [\mathbf{D}_{1\cdot}, g\mathbf{E}_1](0) \rangle\rangle_c \right\} \right) \\
 & - \frac{1}{4} \lim_{T \rightarrow \infty} \int_0^T dt t^3 \left\{ \langle\langle [\mathbf{D}_{1\cdot}, g\mathbf{E}_1](t) g\mathbf{E}_2^j(0) \rangle\rangle_c - \langle\langle [\mathbf{D}_{2\cdot}, g\mathbf{E}_2](t) g\mathbf{E}_1^j(0) \rangle\rangle_c \right\} (\nabla_r^j E^{(0)}).
 \end{aligned}$$

Let us further elaborate on the expressions for $E_r^{(2,0)}$ and $E_r^{(1,1)}$. The first term of $E_r^{(2,0)}$ admits the alternative representation

$$\lim_{T_W \rightarrow \infty} \langle\langle [\mathbf{D}_{1\cdot}, g\mathbf{E}_1](t) \rangle\rangle_c = - \left(\nabla_r^2 E^{(0)} + 2i \lim_{T \rightarrow \infty} \int_0^T dt \langle\langle g\mathbf{E}_1(t) \cdot g\mathbf{E}_1(0) \rangle\rangle_c \right). \quad (9.32)$$

It is also possible to use the Gauss law

$$(\mathbf{D} \cdot \mathbf{E})^a | \text{phys} \rangle = g(\bar{\psi}^\dagger T^a \psi - \chi_c (T^a)^T \chi_c) | \text{phys} \rangle + \sum_{i=1}^{n_f} \bar{q}_i \gamma_0 T^a q_i | \text{phys} \rangle \quad (9.33)$$

to simplify Eq. (9.32). This was done in Ref. [43] for the case without light fermions. Including them we find

$$\lim_{T_W \rightarrow \infty} \langle\langle [\mathbf{D}_{1\cdot}, g\mathbf{E}_1](t) \rangle\rangle_c = -g^2 \delta^{(d)}(\mathbf{x}_1 - \mathbf{x}_2) + g^2 \sum_{i=1}^{n_f} \lim_{T_W \rightarrow \infty} \langle\langle T_1^a \bar{q}_i \gamma_0 T_1^a q_i(t) \rangle\rangle_c. \quad (9.34)$$

It is quite remarkable that Eqs. (9.32) and (9.34) are equal, because, unlike in the former, it is obvious in the latter that only the delta-function term survives for $n_f = 0$.

For the other terms of $E_r^{(2,0)}$ and $E_r^{(1,1)}$ that involve the commutator $[\mathbf{D}\cdot, g\mathbf{E}]$ we can make the replacement $[\mathbf{D}\cdot, g\mathbf{E}] \rightarrow g^2 T^a \bar{q}_i \gamma_0 T^a q_i$ everywhere, as the first term in the right-hand-side of Eq. (9.33) only contributes in the term proportional to c_D . This makes their dependence on the

light fermions more explicit. We obtain

$$\begin{aligned}
 E_r^{(2,0)}(r) = & -\frac{c_D^{(1)}}{8} \left[-g^2 \delta^d(\mathbf{x}_1 - \mathbf{x}_2) + g^2 \sum_{i=1}^{n_f} \lim_{T_W \rightarrow \infty} \langle\langle T_1^a \bar{q}_i \gamma_0 T_1^a q_i(t) \rangle\rangle_c \right] \quad (9.35) \\
 & - \frac{i c_F^{(1)2}}{4} \lim_{T \rightarrow \infty} \int_0^T dt \langle\langle g \mathbf{B}_1(t) \cdot g \mathbf{B}_1(0) \rangle\rangle_c + \frac{1}{2} (\nabla_r^2 E_{\mathbf{p}^2}^{(2,0)}) - \frac{c_1^{hl(1)}}{8} g^2 \sum_{i=1}^{n_f} \lim_{T_W \rightarrow \infty} \langle\langle T_1^a \bar{q}_i \gamma_0 T_1^a q_i(t) \rangle\rangle_c \\
 & - \frac{i}{2} \lim_{T \rightarrow \infty} \int_0^T dt_1 \int_0^{t_1} dt_2 \int_0^{t_2} dt_3 (t_2 - t_3)^2 \langle\langle g \mathbf{E}_1(t_1) \cdot g \mathbf{E}_1(t_2) g \mathbf{E}_1(t_3) \cdot g \mathbf{E}_1(0) \rangle\rangle_c \\
 & + \frac{1}{2} \left(\nabla_r^i \lim_{T \rightarrow \infty} \int_0^T dt_1 \int_0^{t_1} dt_2 (t_1 - t_2)^2 \langle\langle g \mathbf{E}_1^i(t_1) g \mathbf{E}_1(t_2) \cdot g \mathbf{E}_1(0) \rangle\rangle_c \right) \\
 & - \frac{i}{2} \left(\nabla_r^i E^{(0)} \right) \lim_{T \rightarrow \infty} \int_0^T dt_1 \int_0^{t_1} dt_2 (t_1 - t_2)^3 \langle\langle g \mathbf{E}_1^i(t_1) g \mathbf{E}_1(t_2) \cdot g \mathbf{E}_1(0) \rangle\rangle_c \\
 & + \frac{1}{4} \left(\nabla_r^i \lim_{T \rightarrow \infty} \int_0^T dt t^3 \langle\langle g \mathbf{E}_1^i(t) g \mathbf{E}_1^j(0) \rangle\rangle_c (\nabla_r^j E^{(0)}) \right) \\
 & - \frac{i}{12} \lim_{T \rightarrow \infty} \int_0^T dt t^4 \langle\langle g \mathbf{E}_1^i(t) g \mathbf{E}_1^j(0) \rangle\rangle_c (\nabla_r^i E^{(0)}) (\nabla_r^j E^{(0)}) \\
 & - \frac{c_1^{g(1)}}{4} f_{abc} \int d^3 \mathbf{x} \lim_{T_W \rightarrow \infty} g \langle\langle G_{\mu\nu}^a(x) G_{\mu\lambda}^b(x) G_{\nu\lambda}^c(x) \rangle\rangle \\
 & - \frac{1}{2} g^2 \sum_{j=1}^{n_f} \lim_{T \rightarrow \infty} \int_0^T dt_1 \int_0^{t_1} dt_2 (t_1 - t_2)^2 \langle\langle T_1^a \bar{q}_j \gamma_0 T_1^a q_j(t_1) g \mathbf{E}_1(t_2) \cdot g \mathbf{E}_1(0) \rangle\rangle_c \\
 & + \frac{i}{8} g^4 \sum_{j,s=1}^{n_f} \lim_{T \rightarrow \infty} \int_0^T dt t^2 \langle\langle T_1^a \bar{q}_s \gamma_0 T_1^a q_s(t) T_1^a \bar{q}_j \gamma_0 T_1^a q_j(0) \rangle\rangle_c \\
 & - \frac{i}{4} g^2 \sum_{j=1}^{n_f} \left(\nabla_r^i \lim_{T \rightarrow \infty} \int_0^T dt t^2 \langle\langle g \mathbf{E}_1^i(t) T_1^a \bar{q}_j \gamma_0 T_1^a q_j(0) \rangle\rangle_c \right) \\
 & - \frac{1}{4} g^2 \sum_{j=1}^{n_f} \lim_{T \rightarrow \infty} \int_0^T dt t^3 \langle\langle [T_1^a \bar{q}_j \gamma_0 T_1^a q_j(t) g \mathbf{E}_1^j(0)] \rangle\rangle_c (\nabla_r^j E^{(0)}) \\
 & - \frac{c_2^{hl(1)}}{8} g^2 \sum_{i=1}^{n_f} \lim_{T_W \rightarrow \infty} \langle\langle \bar{q}_i \gamma_0 q_i(t) \rangle\rangle_c - \int d^3 \mathbf{x} \lim_{T_W \rightarrow \infty} \langle\langle \delta \mathcal{L}_i^{(1)} \rangle\rangle,
 \end{aligned}$$

where the last six lines are due to light fermions, and the light quark operators are located on the heavy quark Wilson line (i.e. at the position \mathbf{x}_1) except for the last operator, and

$$\begin{aligned}
 E_r^{(1,1)}(r) = & \frac{1}{2} (\nabla_r^2 E_{\mathbf{p}^2}^{(1,1)}) \quad (9.36) \\
 & - i \lim_{T \rightarrow \infty} \int_0^T dt_1 \int_0^{t_1} dt_2 \int_0^{t_2} dt_3 (t_2 - t_3)^2 \langle\langle g \mathbf{E}_1(t_1) \cdot g \mathbf{E}_1(t_2) g \mathbf{E}_2(t_3) \cdot g \mathbf{E}_2(0) \rangle\rangle_c \\
 & + \frac{1}{2} \left(\nabla_r^i \lim_{T \rightarrow \infty} \int_0^T dt_1 \int_0^{t_1} dt_2 (t_1 - t_2)^2 \langle\langle g \mathbf{E}_1^i(t_1) g \mathbf{E}_2(t_2) \cdot g \mathbf{E}_2(0) \rangle\rangle_c \right) \\
 & + \frac{1}{2} \left(\nabla_r^i \lim_{T \rightarrow \infty} \int_0^T dt_1 \int_0^{t_1} dt_2 (t_1 - t_2)^2 \langle\langle g \mathbf{E}_2^i(t_1) g \mathbf{E}_1(t_2) \cdot g \mathbf{E}_1(0) \rangle\rangle_c \right) \\
 & - \frac{i}{2} \left(\nabla_r^i E^{(0)} \right) \lim_{T \rightarrow \infty} \int_0^T dt_1 \int_0^{t_1} dt_2 (t_1 - t_2)^3 \langle\langle g \mathbf{E}_1^i(t_1) g \mathbf{E}_2(t_2) \cdot g \mathbf{E}_2(0) \rangle\rangle_c
 \end{aligned}$$

$$\begin{aligned}
 & -\frac{i}{2} \left(\nabla_r^i E^{(0)} \right) \lim_{T \rightarrow \infty} \int_0^T dt_1 \int_0^{t_1} dt_2 (t_1 - t_2)^3 \langle \langle g \mathbf{E}_2^i(t_1) g \mathbf{E}_1(t_2) \cdot g \mathbf{E}_1(0) \rangle \rangle_c \\
 & + \frac{1}{4} \left(\nabla_r^i \lim_{T \rightarrow \infty} \int_0^T dt t^3 \left\{ \langle \langle g \mathbf{E}_1^i(t) g \mathbf{E}_2^j(0) \rangle \rangle_c + \langle \langle g \mathbf{E}_2^i(t) g \mathbf{E}_1^j(0) \rangle \rangle_c \right\} (\nabla_r^j E^{(0)}) \right) \\
 & - \frac{i}{6} \lim_{T \rightarrow \infty} \int_0^T dt t^4 \langle \langle g \mathbf{E}_1^i(t) g \mathbf{E}_2^j(0) \rangle \rangle_c (\nabla_r^i E^{(0)}) (\nabla_r^j E^{(0)}) \\
 & + (d_{ss} + d_{vs} C_F) \delta^{(3)}(\mathbf{x}_1 - \mathbf{x}_2) \\
 & - \frac{1}{2} g^2 \sum_{j=1}^{n_f} \lim_{T \rightarrow \infty} \int_0^T dt_1 \int_0^{t_1} dt_2 (t_1 - t_2)^2 \langle \langle T_1^a \bar{q}_j \gamma_0 T_1^a q_j(t_1) g \mathbf{E}_2(t_2) \cdot g \mathbf{E}_2(0) \rangle \rangle_c \\
 & + \frac{1}{2} g^2 \sum_{j=1}^{n_f} \lim_{T \rightarrow \infty} \int_0^T dt_1 \int_0^{t_1} dt_2 (t_1 - t_2)^2 \langle \langle T_2^a \bar{q}_j \gamma_0 T_2^a q_j(t_1) g \mathbf{E}_1(t_2) \cdot g \mathbf{E}_1(0) \rangle \rangle_c \\
 & - \frac{i}{4} g^4 \sum_{j,s=1}^{n_f} \lim_{T \rightarrow \infty} \int_0^T dt t^2 \langle \langle T_1^a \bar{q}_j \gamma_0 T_1^a q_j(t) T_2^a \bar{q}_s \gamma_0 T_2^a q_s(0) \rangle \rangle_c \\
 & + \frac{i}{4} g^2 \sum_{j=1}^{n_f} \left(\nabla_r^i \lim_{T \rightarrow \infty} \int_0^T dt t^2 \left\{ \langle \langle g \mathbf{E}_1^i(t) T_2^a \bar{q}_j \gamma_0 T_2^a q_j(0) \rangle \rangle_c - \langle \langle g \mathbf{E}_2^i(t) T_1^a \bar{q}_j \gamma_0 T_1^a q_j(0) \rangle \rangle_c \right\} \right) \\
 & - \frac{1}{4} g^2 \sum_{j=1}^{n_f} \lim_{T \rightarrow \infty} \int_0^T dt t^3 \left\{ \langle \langle T_1^a \bar{q}_j \gamma_0 T_1^a q_j(t) g \mathbf{E}_2^j(0) \rangle \rangle_c - \langle \langle T_2^a \bar{q}_j \gamma_0 T_2^a q_j(t) g \mathbf{E}_1^j(0) \rangle \rangle_c \right\} (\nabla_r^j E^{(0)}).
 \end{aligned}$$

In summary, the results of this subsection are the generalization of the results of Ref. [43] for the strong-coupling version of the $1/m^2$ pNRQCD potential after the inclusion of light fermions (and neglecting ultrasoft degrees of freedom). The expressions of the potentials in terms of Wilson loops are equal to the quenched ($n_f=0$) case except for $E_r^{(2,0)}$ and $E_r^{(1,1)}$ (and one should keep in mind that dynamical light quarks should be included in the computation at loop level). We have presented expressions valid in D dimensions.

9.2.2 Results in perturbation theory: the $\mathcal{O}(\alpha_s^2/m^2)$ potential

Once we focus on the weak-coupling regime, ultrasoft degrees of freedom certainly contribute to the quasi-static energies. They do so with energies/momenta of order $\Delta V \equiv V_o^{(0)} - V^{(0)} \sim C_A \alpha_s / r \sim m v^2$. Nevertheless, for a consistent description of the weakly-coupled quark-antiquark system, the potentials in the Schrödinger equation (i.e. in the pNRQCD Lagrangian) should only include contributions associated with the soft modes. Taylor expanding in powers of $1/m$ before integrating over the gauge or light-quark dynamical variables effectively sets the potential loops to zero. However, this does not eliminate the ultrasoft contributions from the potential expressed in terms of Wilson loops. Actually, as far as the ultrasoft modes are concerned, the $1/m$ expansion can be formally understood as exploiting the hierarchy $\Delta V \gg \mathbf{p}^2/m$, which is the limit implicit in the discussion of Sec. 9.2.1.⁴

In order to obtain the potentials in perturbation theory, the ultrasoft contribution has to be subtracted. This can be easily achieved by expanding in the ultrasoft scale *before* performing the loop integration. Thus, only the soft scale appears in the integrals, which become homogeneous

⁴Obviously, this is not the kinematic situation we face in the bound state, where $\Delta V \sim \mathbf{p}^2/m$.

in that scale. The potentials then take the form of a power series in g^2 (and, eventually, in ΔV , when working beyond the order we are interested in). In summary we have,

$$V_{s,W}(r) = E_s(r)|_{\text{soft}}, \quad (9.37)$$

where we have put the subscript W to indicate the Wilson-loop matching scheme.

For the static potential $V^{(0)}$, the Wilson loop definition is given in Eq. (9.23). Its perturbative evaluation in powers of α_s can be transformed into a calculation in momentum space, where the energies of the external quark and antiquark are set to zero for $T_W \rightarrow \infty$, since the time-dependent part of the external quark propagator, $\theta(T_W - t)$, can be approximated by 1. See also Ref. [151] for a detailed discussion. In addition, for a certain class of gauges (including FG and CG), one can neglect the exchange of asymptotic gluons from the boundaries of the Wilson loop at $\pm T_W/2$ for $T_W \rightarrow \infty$, see the discussion in Refs. [36, 151]. In this setup, the Wilson-loop matching for the static potential is equivalent to a standard diagrammatic S-matrix calculation with off-shell static quarks, i.e. with zero (kinetic) quark energies, but non-zero external three-momenta. This is indeed equivalent to the off-shell matching computation at leading order in the $1/m$, E_1 and E_2 expansion.

In fact, it is also equivalent to the on-shell matching computation. This is so because at $\mathcal{O}(m^0)$ no kinetic propagator insertions are involved in a soft NRQCD S-matrix calculation, as they would inevitably come with factors of $1/m$. It therefore does actually not matter for the latter calculation, whether the external quarks are on- or off-shell. Furthermore, potential loop contributions to the static potential in the on-shell matching scheme must vanish, because there are no field redefinitions (compatible with the symmetries of QCD) that could possibly remove them by modifying a higher order potential. Hence, we conclude, that the static potential is the same in any of the matching schemes discussed in this work.

The Wilson-loop calculation for the higher-order potentials cannot be related to a purely momentum space S-matrix calculation due to the insertions of gluonic/light-quark operators that are integrated over time. Nevertheless, we will see that we can also compute the higher-order potentials in the Wilson-loop matching scheme efficiently based on Feynman diagrams. It is worth emphasizing that the expressions for the potentials in terms of Wilson loops encapsulate all effects at the soft scale in a compact way, and they are correct to any finite order in perturbation theory. In particular, compared to the standard calculation of the static potential, only a few extra Feynman rules for the operator insertions have to be introduced (see Appendix B.3) once the exchange of asymptotic gluons from the boundaries of the Wilson loop at $\pm T_W/2$ for $T_W \rightarrow \infty$ is neglected. This is to be contrasted with the matching of Green functions, where higher-order kinetic insertions on the propagators must be taken into account, both for on-shell and off-shell matching, which can be quite tedious at higher orders. When matching on-shell, in addition, potential loops must be considered.

Let us now compute $V_{\mathbf{L}^2,W}^{(2,0)} = E_{\mathbf{L}^2}^{(2,0)}|_{\text{soft}}$ and $V_{\mathbf{L}^2,W}^{(1,1)} = E_{\mathbf{L}^2}^{(1,1)}|_{\text{soft}}$. We use this case in order to illustrate how we perform the Wilson loop calculations.

At $\mathcal{O}(\alpha_s)$ we only have contributions to $V_{\mathbf{L}^2,W}^{(1,1)}$. The diagrams contributing are drawn in Fig. 9.1. In CG only the second diagram contributes and using the Feynman rules derived in

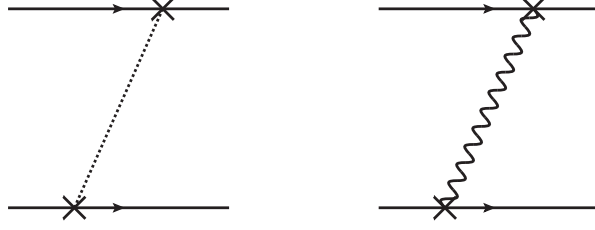


Figure 9.1: Tree-level Wilson-loop diagrams contributing to $V_{\mathbf{L}^2, W}^{(1,1)}(r)$. Dotted and wavy lines represent A_0 and \mathbf{A} gluons, respectively. The crossed vertices denote insertions of the chromoelectric field operator \mathbf{E}^i according to Eq. (9.29). Their horizontal displacement indicates that they are located at different times (0 and t).

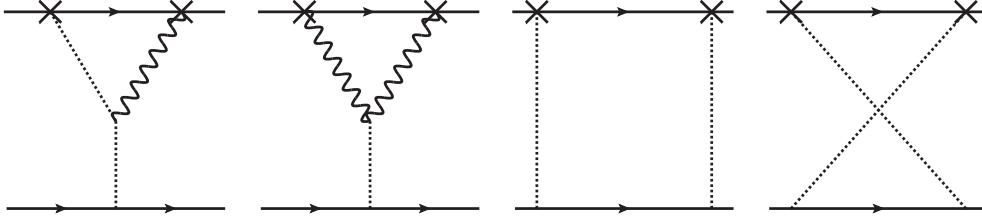


Figure 9.2: One-loop diagrams contributing to $V_{\mathbf{L}^2, W}^{(2,0)}(r)$. Left-right mirror graphs are understood.

Appendix B.3, the detailed calculation reads

$$\begin{aligned}
 V_{\mathbf{L}^2, W}^{(1,1)}(r) &= \frac{i}{(d-1)} \left(\delta^{ij} - d \frac{r^i r^j}{r^2} \right) g_B^2 C_F \lim_{T \rightarrow \infty} \int_0^T dt t^2 \int \frac{d^D k}{(2\pi)^D} e^{ikr} \frac{ik_0^2}{k^2 + i0} P_{ij}(\mathbf{k}) \\
 &= \frac{i}{(d-1)} \left(\delta^{ij} - d \frac{r^i r^j}{r^2} \right) g_B^2 C_F \int \frac{d^d k}{(2\pi)^d} e^{-i\mathbf{k}\mathbf{r}} P_{ij}(\mathbf{k}) \int \frac{dk_0}{(2\pi)} \frac{ik_0^2}{k^2 + i0} \left(-\frac{\partial^2}{\partial k_0^2} \right) \int_0^\infty dt e^{ik_0 t} \\
 &= \frac{1}{(d-1)} \left(\delta^{ij} - d \frac{r^i r^j}{r^2} \right) g_B^2 C_F \int \frac{d^d k}{(2\pi)^d} e^{-i\mathbf{k}\mathbf{r}} P_{ij}(\mathbf{k}) \int \frac{dk_0}{(2\pi)} \frac{k_0^2}{k_0^2 - \mathbf{k}^2 + i0} \frac{\partial^2}{\partial k_0^2} \frac{i}{k_0 + i0} \\
 &= \frac{C_F g_B^2}{8\pi} \frac{(1 + 2\epsilon)\Gamma(\frac{1}{2} + \epsilon)}{\pi^{\frac{1}{2} + \epsilon} r^{1+2\epsilon}} = \frac{C_F \alpha_s}{2r} + \mathcal{O}(\epsilon), \tag{9.38}
 \end{aligned}$$

where the projector $P_{ij}(\mathbf{k}) = \delta_{ij} - \frac{k^i k^j}{k^2}$.

In FG both diagrams in Fig. 9.1 contribute, but we still obtain the same result, as expected due to gauge invariance of the Wilson loop. At this order the result coincides with the result obtained using off-shell matching.⁵ Therefore

$$\tilde{D}_{\text{off}, 1, W}^{(2,0)}(\epsilon) = \tilde{D}_{\text{off}, 1, \text{CG}}^{(2,0)}(\epsilon), \quad \tilde{D}_{\text{off}, 1, W}^{(1,1)}(\epsilon) = \tilde{D}_{\text{off}, 1, \text{CG}}^{(1,1)}(\epsilon). \tag{9.39}$$

⁵In CG it coincides exactly, in FG only after using the EOMs as discussed before.

At $\mathcal{O}(\alpha_s^2)$ the diagrams needed for $V_{\mathbf{L}^2, W}^{(2,0)}$ are drawn in Fig. 9.2 and the calculation reads

$$\begin{aligned}
 V_{\mathbf{L}^2, W}^{(2,0)}(r) &= \\
 &= \frac{g_B^2}{2(d-1)} \left(\delta^{ij} - d \frac{r^i r^j}{r^2} \right) \int \frac{d^d k}{(2\pi)^d} e^{-i\mathbf{k}\mathbf{r}} \int \frac{d^D q}{(2\pi)^D} \int_0^\infty dt t^2 e^{-iq_0 t} \int \frac{dl_0}{2\pi} e^{-il_0 t} \frac{i\mathcal{M}_{ij}(q)}{l_0 + i0} \\
 &= \frac{g_B^2}{2(d-1)} \left(\delta^{ij} - d \frac{r^i r^j}{r^2} \right) \int \frac{d^d k}{(2\pi)^d} e^{-i\mathbf{k}\mathbf{r}} \int \frac{d^D q}{(2\pi)^D} \mathcal{M}_{ij}(q) \int_0^\infty dt t^2 e^{-iq_0 t} \theta(t) \\
 &= \frac{ig_B^2}{2(d-1)} \left(\delta^{ij} - d \frac{r^i r^j}{r^2} \right) \int \frac{d^d k}{(2\pi)^d} e^{-i\mathbf{k}\mathbf{r}} \int \frac{d^D q}{(2\pi)^D} \mathcal{M}_{ij}(q) \left(\frac{\partial^2}{\partial q_0^2} \frac{1}{q_0 - i0} \right). \tag{9.40}
 \end{aligned}$$

Here we chose the energy l_0 to flow along the arrow between the crossed vertices in Fig. 9.2 and the momentum q to flow counter-clockwise in the loop. The (integrand of) the one-loop amplitude \mathcal{M}_{ij} can be obtained by applying standard static Wilson-loop Feynman rules together with the additional rules for the \mathbf{E}^i operator insertions as given in Appendix B.3. Note that we have pulled out a factor $1/(l_0 + i0)$, corresponding to the upper static quark propagator from the amplitude's integrand, in order to render \mathcal{M}_{ij} l_0 -independent.

We emphasize that the pinch singular terms are explicitly removed in the definition of connected Wilson loops according to Eq. (9.20). A similar thing happens in the calculation of soft on/off-shell Green functions, where these pinch singularities are cancelled with the potential loops, see the discussion in Ref. [103].

In CG only the first two diagrams of Fig. 9.2 contribute (the first gives a divergent contribution). Using our Wilson-loop Feynman rules in Appendix B.3 we find the (unintegrated) amplitude

$$\mathcal{M}_{ij}^{\text{CG}}(q) = \frac{C_F C_A g_B^2}{\mathbf{k}^2} \left(\frac{P_{il}(\mathbf{q}) P_{jl}(\mathbf{q} - \mathbf{k}) q_0^3}{((q - k)^2 + i0)(q^2 + i0)} - 2 \frac{k^l (q^j - k^j) P_{il}(\mathbf{q}) q_0}{(\mathbf{q} - \mathbf{k})^2 (q^2 + i0)} \right). \tag{9.41}$$

Plugging this in Eq. (9.40) gives

$$\begin{aligned}
 V_{\mathbf{L}^2, W}^{(2,0)}(r) &= - \left(\frac{g_B^2}{4\pi} \right)^2 \frac{C_F C_A}{6} \mathcal{F}_{2-2\epsilon}(r) \frac{(4\epsilon + 1)(\epsilon(4\epsilon + 7) + 4) \csc(\pi\epsilon)}{2^{4\epsilon} \pi^{\epsilon - \frac{3}{2}} (\epsilon - 1) \Gamma\left(\epsilon + \frac{3}{2}\right)} \\
 &= \frac{4\pi C_F C_A}{3} \mathcal{F}_2(r) \frac{g_B^4}{16\pi^3} \bar{\nu}^{2\epsilon} \left(\frac{1}{\epsilon} + \frac{19}{4} - 2 \ln(r\nu e^{\gamma_E}) + \mathcal{O}(\epsilon) \right). \tag{9.42}
 \end{aligned}$$

We have also checked that we get the same result performing the calculation in FG, where all four diagrams in Fig. 9.2 contribute. Note that $V_{\mathbf{L}^2, W}^{(2,0)}$ differs from $V_{\mathbf{L}^2, \text{CG/FG}}^{(2,0)}$ obtained by off-shell matching, not only in the finite but also in the divergent part.

The calculation of $V_{\mathbf{L}^2, W}^{(1,1)}$ is carried out along the same lines. The diagrams contributing at $\mathcal{O}(\alpha_s^2)$ are displayed in Fig. 9.3. In order to have a cross check we compute again in both, CG

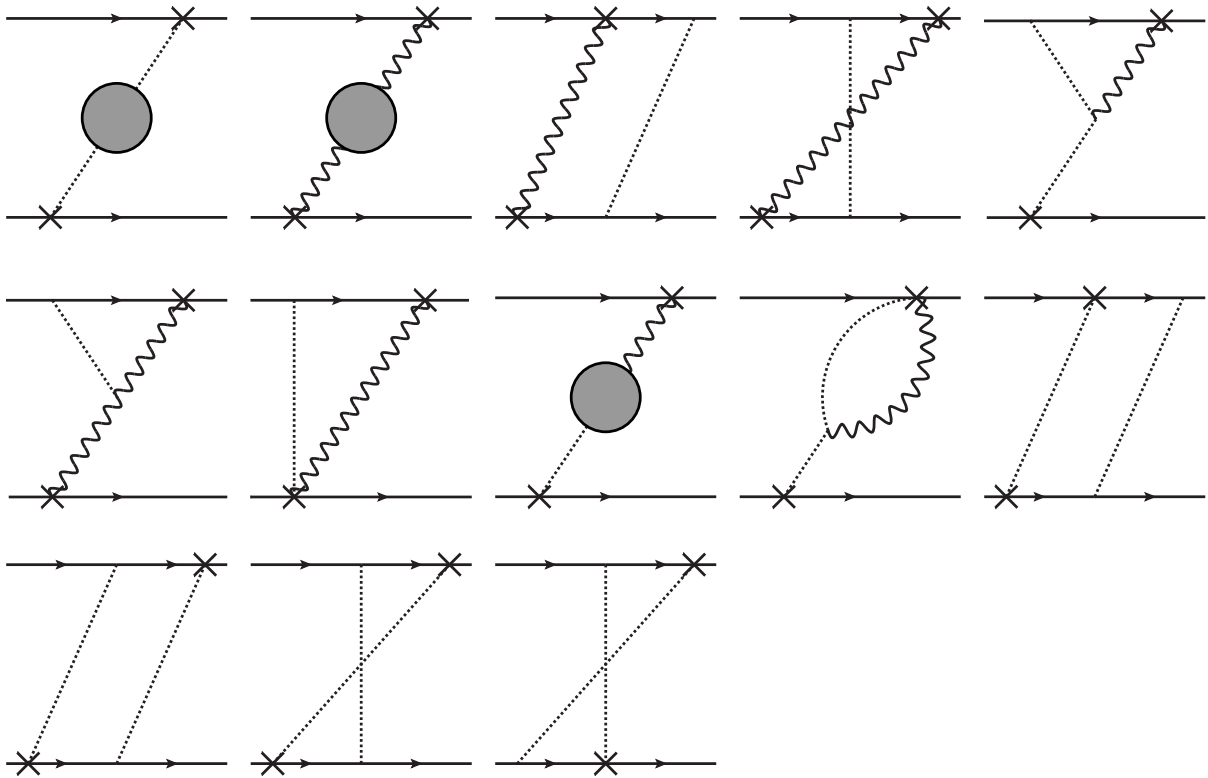


Figure 9.3: One-loop diagrams contributing to $V_{\mathbf{L}^2, W}^{(1,1)}(r)$. Left-right and up-down mirror graphs give the same result as the original diagram and are understood. In all diagrams (including the mirrored ones) the upper and lower crossed vertices are located at times t and 0 , respectively. In CG only the first seven diagrams contribute. In FG also the other six diagrams have to be evaluated.

and FG, and indeed obtain the same result:

$$\begin{aligned}
 V_{\mathbf{L}^2, W}^{(1,1)}(r) &= \frac{g_B^2 C_F}{4\pi} \frac{1}{2} \left\{ 4\pi(1+2\epsilon)\mathcal{F}_2(r) + \frac{g_B^2}{(4\pi)^2} \mathcal{F}_{2-2\epsilon}(r) \frac{\pi^{\frac{5}{2}-\epsilon}(4\epsilon+1) \csc(\pi\epsilon)}{4^{2\epsilon}(1-\epsilon)\Gamma(\epsilon+\frac{5}{2})} \left[4T_F n_f(1-\epsilon^2) \right. \right. \\
 &\quad \left. \left. + \frac{C_A}{3}(15+92\epsilon+137\epsilon^2+56\epsilon^3) \right] \right\} \\
 &= C_F \frac{g_B^2}{2} \mathcal{F}_2(r) \left\{ 1 + \frac{g_B^2 \bar{\nu}^{2\epsilon}}{4\pi^2} \left[\left(\frac{4}{3} C_A - \frac{\beta_0}{4} \right) \left(\frac{1}{\epsilon} - 2 \ln(r\nu e^{\gamma_E}) \right) \right. \right. \\
 &\quad \left. \left. + \frac{127}{36} C_A + \frac{7}{9} T_F n_f \right] + \mathcal{O}(\epsilon) \right\}. \tag{9.43}
 \end{aligned}$$

The above calculations of the $V_{\mathbf{L}^2, W}$ potentials to $\mathcal{O}(\alpha_s^2)$ are actually all we need to fix also the other spin-independent position space potentials $V_{\mathbf{p}^2, W}$ and $V_{r, W}$ with $\mathcal{O}(\alpha_s^2)$ precision. The reason is that we can use Eqs. (8.59) and (8.62) to determine $g_{\text{off}, W}$ and then (by inverse Fourier transformation) $\tilde{D}_{\text{off}, W}(k)$ in momentum space. We find

$$\tilde{D}_{\text{off}, 1, W}^{(1,1)}(\epsilon) = \frac{1}{4}, \tag{9.44}$$

$$\tilde{D}_{\text{off}, 2, W}^{(2,0)}(\epsilon) = \frac{C_A \pi^{\frac{3}{2}-\epsilon} (\epsilon(4\epsilon+7)+4) \csc(\pi\epsilon)}{12 \cdot 4^{2\epsilon} \Gamma(\epsilon+\frac{3}{2})} = \frac{C_A}{6} \left(\frac{e^{\gamma_E}}{4\pi} \right)^\epsilon \left(\frac{4}{\epsilon} - 1 + \mathcal{O}(\epsilon) \right), \tag{9.45}$$

$$\begin{aligned}
 \tilde{D}_{\text{off}, 2, W}^{(1,1)}(\epsilon) &= \frac{\pi^{\frac{3}{2}-\epsilon} \csc(\pi\epsilon)}{16^{\epsilon+1} \Gamma(\epsilon+\frac{5}{2})} \left(\frac{1}{3} C_A (56\epsilon^3 + 137\epsilon^2 + 92\epsilon + 15) + 4T_F n_f (1-\epsilon^2) \right) \\
 &= \left(\frac{e^{\gamma_E}}{4\pi} \right)^\epsilon \left[\frac{1}{\epsilon} \left(\frac{4}{3} C_A - \frac{\beta_0}{4} \right) + \frac{13}{9} C_A - \frac{8}{9} T_F n_f + \mathcal{O}(\epsilon) \right]. \tag{9.46}
 \end{aligned}$$

These are the only $1/m^2$ Wilson coefficients that are affected by the field redefinition in Eq. (8.69) at $\mathcal{O}(\alpha_s^2)$. Therefore, by the same argument as in Sec. 9.1.3, $\tilde{D}_{\mathbf{p}^2, W}(k) = \tilde{D}_{\mathbf{p}^2}(k)$ and $\tilde{D}_{r, W}(k) = \tilde{D}_r(k)$ with the precision of our computation. Then, using Eqs. (8.60), (8.61), (8.63) and (8.64), we obtain

$$\begin{aligned}
 V_{\mathbf{p}^2, W}^{(2,0)}(r) &= \left(\frac{g_B^2}{4\pi} \right)^2 \frac{C_F C_A}{3} \mathcal{F}_{2-2\epsilon}(r) \frac{(\epsilon+1)(8\epsilon^2+8\epsilon-1) \csc(\pi\epsilon)}{4^{2\epsilon} \pi^{\epsilon-\frac{3}{2}} (\epsilon-1) \Gamma(\epsilon+\frac{3}{2})} \\
 &= \frac{C_F C_A}{6} \mathcal{F}_2(r) \frac{g_B^4 \bar{\nu}^{2\epsilon}}{4\pi^2} \left(\frac{1}{\epsilon} - 8 - 2 \ln(r\nu e^{\gamma_E}) + \mathcal{O}(\epsilon) \right), \tag{9.47}
 \end{aligned}$$

$$\begin{aligned}
 V_{r, W}^{(2,0)}(r) &= \frac{C_F g_B^2}{8} \left\{ c_D^{(1)} \delta^{(d)}(\mathbf{r}) - \frac{g_B^2}{4\pi^2} \frac{(\epsilon+1) \csc(\pi\epsilon)}{3(\epsilon-1) 2^{4\epsilon+4} \pi^{\epsilon-\frac{3}{2}} \Gamma(\epsilon+\frac{5}{2})} \right. \\
 &\quad \left. \times \left[3(c_F^{(1)})^2 C_A (4\epsilon^2 + \epsilon - 5) - 12T_F n_f (\epsilon-1) (c_D^{(1)} + c_1^{hl(1)}) \right] \mathcal{F}_{-2\epsilon}(r) \right\} \\
 &\quad + \frac{1}{2} \nabla^2 V_{\mathbf{p}^2, B}^{(2,0), W}, \tag{9.48}
 \end{aligned}$$

where

$$\nabla^2 V_{\mathbf{p}^2, B}^{(2,0), W} = -g_B^4 C_F C_A \frac{16^{-\epsilon-1} \pi^{-\epsilon-\frac{1}{2}} (\epsilon+1) (8\epsilon^2 + 8\epsilon - 1) \csc(\pi\epsilon)}{3(\epsilon-1)\Gamma\left(\epsilon + \frac{3}{2}\right)} \mathcal{F}_{-2\epsilon}(r), \quad (9.49)$$

$$\begin{aligned} V_{\mathbf{p}^2, W}^{(1,1)}(r) &= -\frac{g_B^2}{4\pi} C_F \left\{ 4\pi(1+\epsilon) \mathcal{F}_2(r) + \frac{g_B^2}{(4\pi)^2} \mathcal{F}_{2-2\epsilon}(r) \frac{4^{-2\epsilon} \pi^{\frac{5}{2}-\epsilon} (\epsilon+1) \csc(\pi\epsilon)}{(\epsilon-1)\Gamma\left(\epsilon + \frac{5}{2}\right)} \right. \\ &\quad \left. \times \left[-4(1+\epsilon-2\epsilon^2) T_F n_f + \frac{C_A}{3} (45 - 31\epsilon - 202\epsilon^2 - 112\epsilon^3) \right] \right\} \\ &= -C_F g_B^2 \mathcal{F}_2(r) \left\{ 1 - \frac{g_B^2 \bar{\nu}^{2\epsilon}}{4\pi^2} \left(\frac{C_A}{3} + \frac{\beta_0}{4} \right) \left(\frac{1}{\epsilon} - 2 \ln(r\nu e^{\gamma_E}) \right) \right. \\ &\quad \left. + \frac{61}{36} C_A + \frac{1}{9} T_F n_f \right\} + \mathcal{O}(\epsilon), \end{aligned} \quad (9.50)$$

$$\begin{aligned} V_{r, W}^{(1,1)}(r) &= (d_{ss} + C_F d_{vs}) \delta^{(d)}(\mathbf{r}) + \frac{1}{2} \nabla^2 V_{\mathbf{p}^2, B}^{(1,1), W} + \left(\frac{g_B^2}{4\pi} \right)^2 \frac{C_F \pi^{\frac{3}{2}-\epsilon} (\epsilon+1) \csc(\pi\epsilon)}{3 \cdot 16^{\epsilon+1} \Gamma\left(\epsilon + \frac{5}{2}\right)} \\ &\quad \times \left[C_A (40\epsilon^2 + 83\epsilon + 39) + 4C_F (2\epsilon + 3) (8\epsilon + 7) - 12T_F n_f \epsilon \right] \mathcal{F}_{-2\epsilon}(r), \end{aligned} \quad (9.51)$$

and

$$\begin{aligned} \nabla^2 V_{\mathbf{p}^2, W}^{(1,1)}(r) &= g_B^2 C_F \left\{ (\epsilon+1) \delta^{(d)}(r) + \frac{g_B^2}{(4\pi)^3} \frac{4^{-2\epsilon} \pi^{\frac{5}{2}-\epsilon} (\epsilon+1) \csc(\pi\epsilon)}{(\epsilon-1)\Gamma\left(\epsilon + \frac{5}{2}\right)} \right. \\ &\quad \left. \times \left[\frac{1}{3} C_A (-112\epsilon^3 - 202\epsilon^2 - 31\epsilon + 45) - 4T_F n_f (1-\epsilon)(2\epsilon+1) \right] \mathcal{F}_{-2\epsilon}(r) \right\}. \end{aligned} \quad (9.52)$$

As a check, we have also directly computed $V_{\mathbf{p}^2, W}^{(2,0)}(r)$ in the same way as $V_{\mathbf{L}^2}^{(2,0)}(r)$. Note that the diagrams are the same (Fig. 9.2) and only the prefactor changes, cf. Eqs. (9.26) and (9.27). Using Eq. (9.41), we obtain

$$V_{\mathbf{p}^2, W}^{(2,0)}(r) = \frac{ig_B^2}{2} \frac{r^i r^j}{r^2} \int \frac{d^d k}{(2\pi)^d} e^{-i\mathbf{k}\mathbf{r}} \int \frac{d^D q}{(2\pi)^D} \mathcal{M}_{ij}^{\text{CG}}(q) \left(\frac{\partial^2}{\partial q_0^2} \frac{1}{q_0 - i0} \right), \quad (9.53)$$

which yields the same result as Eq. (9.47). On top of that, we have also checked that we obtain the same result in FG.

We have also computed $V_{\mathbf{p}^2}^{(1,1)}(r)$ directly in CG and FG finding agreement with Eq. (9.50). This is an even stronger check, because the calculation is more difficult, as it involves more diagrams.

From the above analysis we can also determine (the soft part of) some Wilson loops that contribute to $V_{r, W}$ and can be treated separately, because they are multiplied by different NRQCD Wilson coefficients. Let us first focus on $V_{r, W}^{(2,0)}$. Comparing all terms proportional to c_D in Eq. (9.48), with the c_D -dependent terms of the Wilson loop expression in (the first line of) Eq. (9.30), we find

$$\begin{aligned} \lim_{T \rightarrow \infty} \int_0^T dt \langle \langle g \mathbf{E}_1^i(t) g \mathbf{E}_1^i(0) \rangle \rangle_c \Big|_{\text{soft}} \\ = -i \left(\frac{g_B^2}{4\pi} \right)^2 C_F C_A \frac{2^{-3-4\epsilon} \pi^{\frac{3}{2}-\epsilon} (1+\epsilon) (11+8\epsilon) \csc(\pi\epsilon)}{\Gamma\left(\frac{5}{2} + \epsilon\right)} \mathcal{F}_{-2\epsilon}(r), \end{aligned} \quad (9.54)$$

where we have used the relation in Eq. (9.32). We can also directly compute the Wilson loop and check this result. The relevant diagrams are the same as in Fig. 9.2. A calculation analogous to the one for the $V_{\mathbf{L}^2, W}$ potentials yields

$$\lim_{T \rightarrow \infty} \int_0^T dt \left\langle \langle g \mathbf{E}_1^i(t) g \mathbf{E}_1^i(0) \rangle \right\rangle_c \Big|_{\text{soft}} = -g_B^2 \int \frac{d^d k}{(2\pi)^d} e^{-i\mathbf{k}\mathbf{r}} \int \frac{d^D q}{(2\pi)^D} \mathcal{M}_{ii}^{\text{CG}}(q) \frac{1}{q_0 - i0}, \quad (9.55)$$

which is equal to Eq. (9.54).

Using this result and Eq. (9.32) we obtain

$$g^2 \sum_{i=1}^{n_f} \lim_{T_W \rightarrow \infty} \left\langle \langle T_1^a \bar{q}_i \gamma_0 T_1^a q_i(t) \rangle \right\rangle_c \Big|_{\text{soft}} = -C_F \frac{g_B^4}{4\pi^2} \frac{(\epsilon + 1) \csc(\pi\epsilon)}{2^{4\epsilon+2} \pi^{\epsilon-\frac{3}{2}} \Gamma\left(\epsilon + \frac{5}{2}\right)} T_F n_f \mathcal{F}_{-2\epsilon}(r) \quad (9.56)$$

from the comparison to Eq. (9.34). Note that this results from a non-trivial cancellation of non-Abelian contributions so that only light-quark effects survive. This is precisely what should happen according to Eq. (9.34). We can also confirm Eq. (9.56) by direct inspection of the $c_D + c_1^{hl}$ term of $V_{r,W}^{(2,0)}$ (but now written in terms of light-quark operators), which, thus, provides us with an independent check.

Finally, by comparing the terms proportional to c_F^2 we find

$$i \lim_{T \rightarrow \infty} \int_0^T dt \left\langle \langle g \mathbf{B}_1(t) \cdot g \mathbf{B}_1(0) \rangle \right\rangle_c \Big|_{\text{soft}} = \frac{C_F C_A}{2} \frac{g_B^4}{4\pi^2} \frac{(\epsilon + 1) \csc(\pi\epsilon)}{(\epsilon - 1) 2^{4\epsilon+4} \pi^{\epsilon-\frac{3}{2}} \Gamma\left(\epsilon + \frac{5}{2}\right)} \times \left(4\epsilon^2 + \epsilon - 5\right) \mathcal{F}_{-2\epsilon}(r). \quad (9.57)$$

With this we have already exhausted all contributions to $V_{r,W}^{(2,0)}$. Therefore, we conclude that all the remaining terms contribute only at higher orders in α_s , i.e., the last eleven lines in Eq. (9.35) are $\mathcal{O}(\alpha_s^3)$.

Unfortunately a similar analysis for $V_{r,W}^{(1,1)}$ gives much less information on the values of the different contributing Wilson loops.

9.3 Determination of the $\mathcal{O}(\alpha_s^3/m)$ potential for unequal masses

The $\mathcal{O}(\alpha_s^2/m)$ potential for the unequal mass scheme was computed first in the on-shell matching in Ref. [141]. The D -dimensional expression in the same matching scheme, but for the equal mass case, can be found in Ref. [152]. The $\mathcal{O}(\alpha_s^3/m)$ potential for equal masses was obtained in Ref. [140] using on-shell matching and the $\mathcal{O}(\epsilon)$ piece can be found in Ref. [153]. Overall, the equal mass result (to the highest order in ϵ presently known) reads

$$\left[\tilde{V}_{\text{on-shell}}^{(1,0)} + \tilde{V}_{\text{on-shell}}^{(0,1)} \right]_{m=m_1=m_2} = \frac{g^2 \pi C_F}{4\mathbf{k}} \left\{ \frac{g^2}{4\pi} \mathbf{k}^{2\epsilon} b_1 \left(1 + \left(\frac{g^2 \bar{\nu}^{2\epsilon}}{4\pi} \right) \frac{\beta_0}{2\pi} \frac{1}{\epsilon} \left(1 - \frac{\mathbf{k}^{2\epsilon}}{\nu^{2\epsilon}} \right) \right) + \frac{1}{\pi} \left(\frac{g^2 \bar{\nu}^{2\epsilon}}{4\pi} \right)^2 \left(\frac{\mathbf{k}^{2\epsilon}}{\nu^{2\epsilon}} \right)^2 \left(\frac{b_{2L}}{2} \frac{1}{\epsilon} + b_2 + \epsilon b_{2\epsilon} + \mathcal{O}(\epsilon^2) \right) \right\}, \quad (9.58)$$

where

$$\begin{aligned}
 b_1 &= (4\pi)^{-\epsilon} \frac{\Gamma^2\left(\frac{1}{2} + \epsilon\right) \Gamma\left(\frac{1}{2} - \epsilon\right)}{\pi^{3/2} \Gamma(1 + 2\epsilon)} \left(\frac{C_F}{2} (1 + 2\epsilon) - C_A (1 + \epsilon) \right), \\
 b_{2L} &= \frac{4}{3} (C_A^2 + 2C_A C_F), \\
 b_2 &= -C_A^2 \left(\frac{101}{36} + \frac{4}{3} \ln 2 \right) + C_A C_F \left(\frac{65}{18} - \frac{8}{3} \ln 2 \right) + \frac{49}{36} C_A T_F n_f - \frac{2}{9} C_F T_F n_f, \\
 b_{2\epsilon} &= -C_F C_A \left(\frac{-631}{108} - \frac{15}{16} \pi^2 + \frac{65}{9} \ln 2 - \frac{8}{3} \ln^2 2 \right) - C_F T_F n_f \left(\frac{17}{27} - \frac{11}{36} \pi^2 - \frac{4}{9} \ln 2 \right) \\
 &\quad + C_A^2 \left(\frac{1451}{216} + \frac{161}{72} \pi^2 + \frac{101}{18} \ln 2 + \frac{4}{3} \ln^2 2 \right) - C_A T_F n_f \left(\frac{115}{54} + \frac{5}{18} \pi^2 + \frac{49}{18} \ln 2 \right).
 \end{aligned} \tag{9.59}$$

Note that, unlike the expressions for the potentials in the previous sections, we have written the potential in Eq. (9.58) in terms of the $\overline{\text{MS}}$ renormalized coupling g^2 evaluated at the scale ν ,⁶ because this allows for an easier comparison with the results of Refs. [140, 153]. It is however straightforward to change this back to g_B through Eq. (8.17).

It is the aim of this section to obtain the expression for the $1/m$ potential in the unequal mass case for the on-shell, off-shell (CG and FG) and the Wilson-loop matching schemes described in Secs. 9.2 and 9.1. We will rely on the $1/m^2$ results obtained in Secs. 9.1 and 9.2, as well as on the results of Ref. [140]. A key point in our derivation will be the use of the field redefinitions discussed in Sec. 8.3.

In Secs. 9.1 and 9.2 we have argued that through $\mathcal{O}(\alpha_s^2)$ the potential coefficients $\tilde{D}_{\mathbf{p}^2}$ and \tilde{D}_r are the same in all three matching schemes, based on field redefinitions. We have checked this prediction explicitly for the on-shell and off-shell matching. We have also determined all other $1/m^2$ potentials at $\mathcal{O}(\alpha_s^2)$.

The scheme differences can be compactly expressed in momentum space:

$$\tilde{V}_{s,X} \Big|_{\mathcal{O}(1/m^2)} = \tilde{V}_{s,\text{on-shell}} \Big|_{\mathcal{O}(1/m^2)} + \delta\tilde{V}_X^{(2)}, \tag{9.60}$$

where

$$\delta\tilde{V}_X^{(2)} = \frac{(\mathbf{p}'^2 - \mathbf{p}^2)^2}{\mathbf{k}^4} \left(\tilde{D}_{\text{off},X}^{(2,0)}(k) \left(\frac{1}{m_1^2} + \frac{1}{m_2^2} \right) + \tilde{D}_{\text{off},X}^{(1,1)}(k) \frac{1}{m_1 m_2} \right), \tag{9.61}$$

and the subscript X stands for the matching scheme: Wilson-loop (W), CG or FG. The term $\delta\tilde{V}_X^{(2)}$ has the same structure as Eq. (8.74), and can therefore be completely eliminated through the field redefinition in Eqs. (8.66), (8.68), generating a new $1/m$ potential: $\delta\tilde{V}_X^{(1)}$. Note that this potential can have a non-trivial dependence on the masses.

This $\delta\tilde{V}_X^{(1)}$, plus the on-shell scheme expression of the $1/m$ potential in the equal-mass case, is all we need to derive the $\mathcal{O}(\alpha_s^3/m)$ potential for unequal masses in the X or on-shell schemes. To achieve this one just needs to realize that

$$\frac{\tilde{V}_X^{(1,0)}}{m} + \frac{\tilde{V}_X^{(0,1)}}{m} + \delta\tilde{V}_X^{(1)} \Big|_{m=m_1=m_2} = \left[\frac{\tilde{V}_{\text{on-shell}}^{(1,0)}}{m} + \frac{\tilde{V}_{\text{on-shell}}^{(0,1)}}{m} \right]_{m=m_1=m_2}. \tag{9.62}$$

⁶For brevity, we avoid writing out the argument, i.e. $g \equiv g(\nu)$ is understood in the following.

9.3. Determination of the $\mathcal{O}(\alpha_s^3/m)$ potential for unequal masses

The potentials $\tilde{V}_X^{(1,0)}$ and $\tilde{V}_X^{(0,1)}$ are the unknown quantities in this equation. Since all schemes X admit a strict $1/m_i$ expansion, they do not depend on the mass. Hence Eq. (9.62) allows us to completely fix the (original) $1/m$ potential $\tilde{V}_X^{(1,0)} = \tilde{V}_X^{(0,1)}$. We emphasize that this is possible because we know the complete off-shell $1/m^2$ potential. In addition, our $1/m^2$ results contain the full information on the m_i dependence of the potentials. Therefore, we are also able to determine the $\mathcal{O}(\alpha_s^3/m)$ potential for unequal masses in the on-shell matching scheme, as we will see below.

We start with the results in the Wilson-loop scheme, where the appropriate field redefinition gives

$$\begin{aligned}
m \delta \tilde{V}_W^{(1)} \Big|_{m=m_1=m_2} &= \left(\frac{g_B^2}{4\pi} \right)^2 \frac{\mathbf{k}^{2\epsilon}}{\mathbf{k}} \pi^2 C_F^2 d_1 + \left(\frac{g_B^2}{4\pi} \right)^3 \frac{\mathbf{k}^{4\epsilon}}{\mathbf{k}} C_F^2 \frac{4^{-3\epsilon-1} \pi^{2-2\epsilon} \csc(\pi\epsilon) \sec(2\pi\epsilon)}{3(2\epsilon+1)(2\epsilon+3)\Gamma(2-\epsilon)\Gamma(3\epsilon+1)} \\
&\times \left\{ C_A \left(136\epsilon^4 + 363\epsilon^3 + 297\epsilon^2 + 89\epsilon + 15 \right) - 12T_F n_f (\epsilon-1)(\epsilon+1)(3\epsilon+1) \right\} \\
&= \frac{\pi C_F^2 g^2}{4\mathbf{k}} \left\{ \frac{g^2}{4\pi} \mathbf{k}^{2\epsilon} d_1 \left(1 + \left(\frac{g^2 \bar{\nu}^{2\epsilon}}{4\pi} \right) \frac{\beta_0}{2\pi} \frac{1}{\epsilon} \left(1 - \frac{\mathbf{k}^{2\epsilon}}{\nu^{2\epsilon}} \right) \right) \right. \\
&+ \frac{1}{\pi} \left(\frac{g^2 \bar{\nu}^{2\epsilon}}{4\pi} \right)^2 \left(\frac{\mathbf{k}^{2\epsilon}}{\nu^{2\epsilon}} \right)^2 \left(\frac{4}{3} C_A \frac{1}{\epsilon} + \left(\frac{65}{18} - \frac{8}{3} \ln 2 \right) C_A - \frac{2}{9} T_F n_f \right. \\
&+ \left. \left. \epsilon \left[C_A \left(\frac{631}{108} + \frac{15\pi^2}{16} - \frac{65 \ln 2}{9} + \frac{8 \ln^2 2}{3} \right) + T_F n_f \left(-\frac{17}{27} + \frac{11\pi^2}{36} + \frac{4 \ln 2}{9} \right) \right] \right. \right. \\
&\left. \left. + \mathcal{O}(\epsilon^2) \right\}, \tag{9.63}
\end{aligned}$$

with

$$d_1 = \frac{2^{-2\epsilon} \pi^{\frac{1}{2}-\epsilon} \Gamma\left(\frac{3}{2} + \epsilon\right) \sec(\pi\epsilon)}{\Gamma(1+2\epsilon)}. \tag{9.64}$$

We can now use Eq. (9.62) to determine $\tilde{V}_W^{(1,0)}$. We find the following momentum space coefficients according to Eq. (8.37):

$$\tilde{D}_{2,W}^{(1,0)} = -C_A \frac{\pi(1+\epsilon)}{4(1+2\epsilon)} d_1 = -\frac{C_A \pi}{8} + \mathcal{O}(\epsilon), \tag{9.65}$$

$$\begin{aligned}
\tilde{D}_{3,W}^{(1,0)} &= \frac{C_A \pi}{4} \left(\frac{e^{\gamma_E}}{4\pi} \right)^\epsilon \frac{2(1+\epsilon)}{1+2\epsilon} d_1 \beta_0 \frac{1}{\epsilon} \\
&+ \frac{C_A \pi}{2} \left(\frac{e^{\gamma_E}}{4\pi} \right)^{2\epsilon} \left(\frac{2}{3} C_A \frac{1}{\epsilon} + \frac{49}{36} T_F n_f - C_A \left(\frac{101}{36} + \frac{4}{3} \ln 2 \right) \right) \\
&+ \left. \left. \epsilon \left[C_A \left(\frac{1451}{216} + \frac{161\pi^2}{72} + \frac{101}{18} \ln 2 + \frac{4}{3} \ln^2 2 \right) - T_F n_f \left(\frac{115}{54} + \frac{5\pi^2}{18} + \frac{49}{18} \ln 2 \right) \right] \right. \right. \\
&\left. \left. + \mathcal{O}(\epsilon^2) \right. \right. \tag{9.66}
\end{aligned}$$

Note that these coefficients refer to the expansion of the $1/m$ potential in powers of g_B^2 . After

Fourier transformation to position space we obtain

$$\begin{aligned}
 V_W^{(1,0)}(r) &= -\frac{1}{2} \lim_{T \rightarrow \infty} \int_0^T dt t \left\langle \langle g \mathbf{E}_1(t) \cdot g \mathbf{E}_1(0) \rangle \right\rangle_c \Big|_{\text{soft}} \\
 &= \frac{\pi C_A C_F g^2}{8} \left\{ -\frac{g^2}{4\pi} \frac{2(1+\epsilon)}{1+2\epsilon} d_1 \mathcal{F}_{1-2\epsilon}(r) \left(1 + \left(\frac{g^2 \bar{\nu}^{2\epsilon}}{4\pi} \right) \frac{\beta_0}{2\pi} \frac{1}{\epsilon} \left(1 - \frac{\mathcal{F}_{1-4\epsilon}(r)}{\nu^{2\epsilon} \mathcal{F}_{1-2\epsilon}(r)} \right) \right) \right. \\
 &\quad + \left(\frac{g^2 \bar{\nu}^{2\epsilon}}{4\pi} \right)^2 \frac{1}{\pi} \frac{\mathcal{F}_{1-4\epsilon}(r)}{\nu^{4\epsilon}} \left(\frac{2}{3} C_A \frac{1}{\epsilon} + \frac{49}{36} T_F n_f - C_A \left(\frac{101}{36} + \frac{4}{3} \ln 2 \right) \right) \\
 &\quad + \epsilon \left[C_A \left(\frac{1451}{216} + \frac{161\pi^2}{72} + \frac{101}{18} \ln 2 + \frac{4}{3} \ln^2 2 \right) - T_F n_f \left(\frac{115}{54} + \frac{5\pi^2}{18} + \frac{49}{18} \ln 2 \right) \right] \\
 &\quad \left. + \mathcal{O}(\epsilon^2) \right\}. \tag{9.67}
 \end{aligned}$$

Note that this expression does not have terms proportional to the color factors $C_F^2 C_A$ and $C_F^2 T_F n_f$. A similar situation takes place in the static potential, where there are no C_F^2 terms at $\mathcal{O}(\alpha_s^2)$ due to the exponentiation of diagrams. Here, it is the fact that we consider connected Wilson loops, which seems to eliminate such contributions, see Eq. (9.20).

It is straightforward to identify the field redefinitions that relate the potentials obtained in the Wilson-loop and the CG/FG off-shell matching schemes, developing equations similar to Eq. (9.63). We emphasize that the differences $\delta \tilde{V}_W^{(2)} - \delta \tilde{V}_{\text{CG}}^{(2)}$ and $\delta \tilde{V}_W^{(2)} - \delta \tilde{V}_{\text{FG}}^{(2)}$ are precisely of the form of Eq. (8.74) with a mass-independent $\tilde{g}(k)$. Hence, according to the field redefinition in Eq. (8.69), the corresponding differences in the $1/m$ potential are proportional to $1/m_r = 1/m_1 + 1/m_2$. This explicitly verifies that the strict $1/m$ expansion also holds for the CG and FG off-shell schemes.

We now give expressions for the $1/m$ potentials in the CG and FG schemes. The coefficients in Eq. (8.37) read

$$\tilde{D}_{2,W}^{(1,0)} = \tilde{D}_{2,\text{CG}}^{(1,0)} = \tilde{D}_{2,\text{FG}}^{(1,0)}, \tag{9.68}$$

$$\tilde{D}_{3,\text{CG}}^{(1,0)} = \tilde{D}_{3,W}^{(1,0)} + \frac{\pi C_F C_A}{3} \frac{\sec(2\pi\epsilon) \Gamma\left(\epsilon + \frac{3}{2}\right) \Gamma(2\epsilon + 3)}{(8\pi)^{2\epsilon} (1-\epsilon) \epsilon \Gamma\left(2\epsilon + \frac{3}{2}\right) \Gamma(3\epsilon + 1)}, \tag{9.69}$$

$$\begin{aligned}
 \tilde{D}_{3,\text{FG}}^{(1,0)} &= \tilde{D}_{3,\text{CG}}^{(1,0)} - \frac{\pi C_A C_F}{6} \frac{\sec(2\pi\epsilon) \Gamma(\epsilon - 1)}{(8\pi)^{2\epsilon} \Gamma(3\epsilon + 1) (3 + 2\epsilon)} \left(12 - 20\epsilon^3 - 39\epsilon^2 - \frac{25\epsilon}{4} \right. \\
 &\quad \left. - \frac{4\Gamma\left(\epsilon + \frac{5}{2}\right) \Gamma(2\epsilon + 3)}{\Gamma(\epsilon + 1) \Gamma\left(2\epsilon + \frac{3}{2}\right)} \right). \tag{9.70}
 \end{aligned}$$

In the CG computation it is easy to see that there are no $C_F^2 T_F n_f$ contributions to the $1/m$ potential by inspection of the possible diagrams at $\mathcal{O}(\alpha_s^3)$.

Furthermore, as stated above, we can determine the NLO $1/m$ potential in the on-shell scheme for unequal masses. Now, however, the field redefinition relating it to the off-shell potentials induces a non-trivial dependence on the masses, because $2D_{\text{off},X}^{(2,0)} \neq D_{\text{off},X}^{(1,1)}$ in Eq. (9.61). We

obtain⁷

$$\frac{V_{\text{on-shell}}^{(1,0)}}{m_1} + \frac{V_{\text{on-shell}}^{(0,1)}}{m_2} = \frac{m_r}{m_1 m_2} 2\pi^2 C_F^2 \left(\frac{g_B^2}{4\pi}\right)^2 \left\{ d_1 \mathcal{F}_{1-2\epsilon}(r) \right. \quad (9.71)$$

$$\begin{aligned} & + \frac{g_B^2}{4\pi} \mathcal{F}_{1-4\epsilon}(r) \frac{(\epsilon+1)(3\epsilon+1) \csc(\pi\epsilon) \sec(2\pi\epsilon)}{(8\pi)^{2\epsilon} (2\epsilon+1)(2\epsilon+3) \Gamma(1-\epsilon) \Gamma(3\epsilon+1)} \left(T_F n_f - \frac{C_A}{4} (11+8\epsilon) \right) \Big\} \\ & - \frac{C_F C_A \pi^2}{m_r} \left(\frac{g_B^2}{4\pi}\right)^2 \left\{ \frac{1+\epsilon}{1+2\epsilon} d_1 \mathcal{F}_{1-2\epsilon}(r) \right. \\ & - \frac{g_B^2}{4\pi} \mathcal{F}_{1-4\epsilon}(r) \left(\frac{1+\epsilon}{1+2\epsilon} d_1 \frac{\beta_0 \bar{\nu}^{2\epsilon}}{2\pi \nu^{2\epsilon}} \frac{1}{\epsilon} + \frac{C_F}{3} \frac{(\epsilon(4\epsilon+7)+4) \csc(\pi\epsilon) \sec(2\pi\epsilon)}{2(8\pi)^{2\epsilon} \Gamma(2-\epsilon) \Gamma(3\epsilon+1)} \right. \\ & + \frac{\bar{\nu}^{4\epsilon}}{\nu^{4\epsilon}} \frac{1}{2\pi} \left\{ \frac{2}{3} C_A \frac{1}{\epsilon} - \left(\frac{101}{36} + \frac{4 \ln 2}{3} \right) C_A + \frac{49}{36} T_F n_f \right. \\ & \left. \left. + \epsilon \left[C_A \left(\frac{161\pi^2}{72} + \frac{1451}{216} + \frac{4 \ln^2 2}{3} + \frac{101 \ln 2}{18} \right) - T_F n_f \left(\frac{5\pi^2}{18} + \frac{115}{54} + \frac{49 \ln 2}{18} \right) \right] \right\} \right. \\ & \left. \left. + \mathcal{O}(\epsilon^2) \right\} \right\} \\ & = \frac{\pi C_F^2 g^2}{2(m_1+m_2)} \left\{ \frac{g^2}{4\pi} d_1 \mathcal{F}_{1-2\epsilon}(r) \left(1 + \left(\frac{g^2 \bar{\nu}^{2\epsilon}}{4\pi} \right) \frac{\beta_0}{2\pi \epsilon} \left(1 - \frac{\mathcal{F}_{1-4\epsilon}(r)}{\nu^{2\epsilon} \mathcal{F}_{1-2\epsilon}(r)} \right) \right) \right. \quad (9.72) \\ & + \left(\frac{g^2 \bar{\nu}^{2\epsilon}}{4\pi} \right)^2 \frac{1}{\pi} \frac{\mathcal{F}_{1-4\epsilon}(r)}{\nu^{4\epsilon}} \left(\frac{1}{4} (a_1 - \beta_0) + \frac{\epsilon}{2} \left[C_A \left(\frac{91}{54} - \frac{121\pi^2}{72} + \frac{2 \ln 2}{9} \right) \right. \right. \\ & \left. \left. + T_F n_f \left(-\frac{34}{27} + \frac{11\pi^2}{18} + \frac{8 \ln 2}{9} \right) \right] + \mathcal{O}(\epsilon^2) \right) \Big\} \\ & + \frac{\pi C_A C_F g^2}{8m_r} \left\{ -\frac{g^2}{4\pi} \frac{2(1+\epsilon)}{1+2\epsilon} d_1 \mathcal{F}_{1-2\epsilon}(r) \left(1 + \left(\frac{g^2 \bar{\nu}^{2\epsilon}}{4\pi} \right) \frac{\beta_0}{2\pi \epsilon} \left(1 - \frac{\mathcal{F}_{1-4\epsilon}(r)}{\nu^{2\epsilon} \mathcal{F}_{1-2\epsilon}(r)} \right) \right) \right. \\ & + \left(\frac{g^2 \bar{\nu}^{2\epsilon}}{4\pi} \right)^2 \frac{1}{\pi} \frac{\mathcal{F}_{1-4\epsilon}(r)}{\nu^{4\epsilon}} \left(\frac{2}{3} (C_A + 2C_F) \frac{1}{\epsilon} - C_A \left(\frac{101}{36} + \frac{4}{3} \ln 2 \right) + C_F \left(\frac{11}{3} - \frac{8}{3} \ln 2 \right) \right. \\ & + \frac{49}{36} T_F n_f + \epsilon \left[C_F \left(5 + \frac{16\pi^2}{9} - \frac{22}{3} \ln 2 + \frac{8}{3} \ln^2 2 \right) - T_F n_f \left(\frac{115}{54} + \frac{5\pi^2}{18} + \frac{49}{18} \ln 2 \right) \right. \\ & \left. \left. + C_A \left(\frac{1451}{216} + \frac{161\pi^2}{72} + \frac{101 \ln 2}{18} + \frac{4 \ln^2 2}{3} \right) \right] + \mathcal{O}(\epsilon^2) \right\}. \end{aligned}$$

We remark that in the first equality we keep the complete ϵ dependence of the terms proportional to the color factors $C_F^2 C_A$ and $C_F^2 T_F n_f$. This is an outcome of our calculation. In the second equality we expand to $\mathcal{O}(\epsilon)$.

Finally, note that, unlike for the off-shell and Wilson-loop potentials, it does not make sense to define the $1/m$ potential $V_{\text{on-shell}}^{(1,0)}$ alone. Only the combination $\frac{V_{\text{on-shell}}^{(1,0)}}{m_1} + \frac{V_{\text{on-shell}}^{(0,1)}}{m_2}$ is meaningful. A similar argument applies to $1/m$ potential in momentum space.

⁷We give here the result in position space. Note however that through the relations in Sec. A.4 it is straightforward to translate this into momentum space.

9.4 Renormalized potentials

So far we have obtained the bare potentials for different matching procedures. The different results can be related by unitary field redefinitions. Therefore, the physical spectrum of the quark-antiquark system will be the same irrespectively of the matching scheme used to determine the potentials.⁸ In order to produce physical results one always has to add the ultrasoft contribution to the respective observable. The ultrasoft calculation relevant for the determination of the B_c spectrum yields the following contribution to the (singlet) heavy quarkonium self-energy (in the quasi-static limit), Refs. [38, 39, 57]:

$$\Sigma_B(1\text{-loop}) = -g_B^2 C_F V_A^2 (1 + \epsilon) \frac{\Gamma(2 + \epsilon)\Gamma(-3 - 2\epsilon)}{\pi^{2+\epsilon}} \mathbf{r} (h_s - E + \Delta V)^{3+2\epsilon} \mathbf{r}, \quad (9.73)$$

where $\Delta V \equiv V_o^{(0)} - V^{(0)}$.

In general, ultrasoft contributions will depend on the basis of potentials used, but, up to the order we work at here, it only depends on the static octet potential, which is not affected by the field redefinition in Eq. (8.68).

The (ultraviolet) divergences of Eq. (9.73) that are associated with the pole of the heavy quarkonium propagator (i.e. those independent of $h_s - E$) should cancel the divergences of the bare potential V_s . We collect them in δV_s :

$$V_s^{\overline{\text{MS}}} + \delta V_s = V_s, \quad (9.74)$$

so that $V_s^{\overline{\text{MS}}}$ produces finite physical results. This does not necessarily mean that $V_s^{\overline{\text{MS}}}$ is finite in the four-dimensional limit, as the cancellation of divergences should only occur in physical quantities and not necessarily for each individual potential separately.

Let us elaborate on this point. In order to transform Eq. (9.73) into Eq. (9.74) we need to get rid of the factors $h_s - E$. The way to do this is not unique. In fact, we do it in two different ways. In the first one we take Eq. (9.73) and move one factor of $(h_s - E)$ to the left, one to the right, and the remaining one in is moved such that one obtains a $(h_s - E)$ -free divergence that is cancelled by the counterterm (note that $V_{\mathbf{L}^2}$ does not appear in this expression):

$$\begin{aligned} \delta V_s^{(\text{GF})} = & \left(\mathbf{r}^2 (\Delta V)^3 - \frac{1}{2m_r^2} \left[\mathbf{p}, \left[\mathbf{p}, V_o^{(0)} \right] \right] + \frac{1}{2m_r^2} \left\{ \mathbf{p}^2, \Delta V \right\} + \frac{2}{m_r} \Delta V \left(r \frac{d}{dr} V^{(0)} \right) \right. \\ & \left. + \frac{1}{2m_r} \left[(\Delta V)^2 (3d - 5) + 4\Delta V \left(\left(r \frac{d}{dr} \Delta V \right) + \Delta V \right) + \left(\left(r \frac{d}{dr} \Delta V \right) + \Delta V \right)^2 \right] \right) \\ & \times \frac{1}{\epsilon} C_F V_A^2 \frac{1}{3\pi} \frac{g_B^2 \bar{V}^{2\epsilon}}{4\pi}. \end{aligned} \quad (9.75)$$

This expression was used in Ref. [103]. In a second way, we take $(h_s - E)^3$ and move one factor of $(h_s - E)$ to the left, one to the right, and the remaining one is split in half and symmetrically

⁸Nevertheless, one should be careful with other observables such as decays. The Wilson coefficients of the corresponding operators will potentially depend on the basis of potentials used.

moved to the left and right in Eq. (9.73). We obtain

$$\begin{aligned}
 \delta V_s^{(W)} = & \left(\mathbf{r}^2 (\Delta V)^3 - \frac{1}{2m_r^2} \left[\mathbf{p}, \left[\mathbf{p}, V_o^{(0)} \right] \right] + \frac{1}{2m_r^2} \left\{ \mathbf{p}^2, \Delta V \right\} + \frac{i}{2m_r^2} \left\{ \mathbf{p}^i, \left\{ \mathbf{p}^j, \left[\mathbf{p}^j, \Delta V r^i \right] \right\} \right\} \right) \\
 & + \frac{1}{2m_r} \left[(\Delta V)^2 (3d - 5) + 4\Delta V \left(\left(r \frac{d}{dr} \Delta V \right) + \Delta V \right) + \left(\left(r \frac{d}{dr} \Delta V \right) + \Delta V \right)^2 \right] \\
 & \times \frac{1}{\epsilon} C_F V_A^2 \frac{1}{3\pi} \frac{g_B^2 \bar{\nu}^{2\epsilon}}{4\pi}. \tag{9.76}
 \end{aligned}$$

Therefore, even if Eq. (9.73) is not ambiguous, Eqs. (9.75) and (9.76) are. Still, they are related by field redefinitions, or in other words, they differ by terms of $\mathcal{O}(h_s - E)$.⁹ Hence, combining Eq. (9.75) or Eq. (9.76) with our expressions for the potential yields the same physical result for the spectrum. Yet, note that, e.g. in $V_{s,\text{CG}} - \delta V_s^{(W)}$ there is no cancellation of the divergences and therefore it does not yield finite four-dimensional expressions for the potentials. Formally this is not a problem, because the uncanceled divergences vanish in the calculation of the spectrum, but we are then forced to compute intermediate results in D dimensions. In practice, it is therefore convenient to find finite renormalized expressions that allow us to work in four dimensions. This is achieved by subtracting $\delta V_s^{(W)}$ from $V_{s,W}$ and $\delta V_s^{(\text{GF})}$ from the bare potentials in the CG/FG off-shell and on-shell schemes. Finally, Eq. (8.17) plus the fact that $V_A = 1$ with leading logarithmic accuracy (Ref. [155]), and the relation between the bare and renormalized expressions of the NRQCD Wilson coefficients presented in Sec. 8.1, we obtain the renormalized potentials for the different matching prescriptions.

In order to simplify the notation we drop the index $\overline{\text{MS}}$ of the NRQCD Wilson coefficients in the expressions of the renormalized potentials we give below. Note also that the divergences of the bare NRQCD Wilson coefficient d_{sv} we use in this work (computed in FG), do not cancel the divergences of $V_r^{(1,1)}$, they rather compensate the divergences of $V_r^{(2,0)}$ and $V_r^{(0,2)}$. One should bare in mind that, had we computed the NRQCD Wilson coefficients in CG, we would find no mixing between these potentials for the cancellation of divergences. See the renormalization group equations in Ref. [139] for the latter case.

We now list the final expressions for the renormalized potentials obtained in the different matching schemes in position space. In the off-shell CG scheme they read

$$\begin{aligned}
 V_{r,\text{CG}}^{(2,0),\overline{\text{MS}}}(r) = & \frac{C_F \alpha_s}{8} \left(c_D^{(1)} + \frac{\alpha_s}{\pi} \left\{ -\frac{5}{9} \left(c_D^{(1)} + c_1^{hl(1)} \right) T_F n_f + \left(\frac{13}{36} c_F^{(1)2} + \frac{4}{3} - \frac{8}{3} \ln 2 \right) C_A \right. \right. \\
 & \left. \left. + \left(\left(4 + \frac{5}{6} c_F^{(1)2} \right) C_A - \frac{2}{3} \left(c_D^{(1)} + c_1^{hl(1)} \right) T_F n_f \right) \ln(\nu) \right\} \right) 4\pi \delta^{(3)}(\mathbf{r}) \\
 & + \frac{C_F \alpha_s^2}{8\pi} \left\{ \left(4 + \frac{5}{6} c_F^{(1)2} \right) C_A - \frac{2}{3} \left(c_D^{(1)} + c_1^{hl(1)} \right) T_F n_f \right\} \text{reg} \frac{1}{r^3}, \tag{9.77}
 \end{aligned}$$

$$V_{\mathbf{L}^2,\text{CG}}^{(2,0),\overline{\text{MS}}}(r) = \frac{C_F \alpha_s^2}{4\pi} \frac{1}{r} C_A \left(1 - \frac{8}{3} \ln 2 \right), \tag{9.78}$$

$$V_{\mathbf{p}^2,\text{CG}}^{(2,0),\overline{\text{MS}}}(r) = -\frac{C_F \alpha_s^2}{3\pi} \frac{1}{r} C_A \ln(\nu r e^{\gamma_E}), \tag{9.79}$$

$$V_{r,\text{CG}}^{(1,1),\overline{\text{MS}}}(r) = \left[\frac{1}{4\pi} (d_{ss} + C_F d_{vs}) + \frac{C_F \alpha_s}{2} \left(1 + \frac{\alpha_s}{\pi} \left\{ \frac{31}{36} C_A + \frac{C_F}{6} - \frac{4}{3} C_A \ln 2 \right. \right. \right.$$

⁹See also the discussion in Ref. [154].

$$\begin{aligned}
 & - \frac{7}{18} T_F n_f + \left(\frac{11}{12} C_A - \frac{7}{3} C_F + \frac{\beta_0}{2} \right) \ln(\nu) \Big\} \Big] 4\pi \delta^{(3)}(\mathbf{r}) \\
 & + \frac{C_F \alpha_s^2}{2 \pi} \left(\frac{11}{12} C_A - \frac{7}{3} C_F + \frac{\beta_0}{2} \right) \text{reg} \frac{1}{r^3}, \tag{9.80}
 \end{aligned}$$

$$V_{\mathbf{L}^2, \text{CG}}^{(1,1), \overline{\text{MS}}}(r) = \frac{C_F \alpha_s (e^{-\gamma_E}/r)}{2r} \left\{ 1 + \frac{\alpha_s}{\pi} \left(\frac{C_A}{36} - \frac{8}{3} C_A \ln 2 + \frac{1}{9} T_F n_f \right) \right\}, \tag{9.81}$$

$$V_{\mathbf{p}^2, \text{CG}}^{(1,1), \overline{\text{MS}}}(r) = - \frac{C_F \alpha_s (e^{-\gamma_E}/r)}{r} \left\{ 1 + \frac{\alpha_s}{\pi} \left(-\frac{C_A}{18} - \frac{2}{9} n_f T_F + \frac{2}{3} C_A \ln(\nu r e^{\gamma_E}) \right) \right\}, \tag{9.82}$$

$$\begin{aligned}
 V_{\text{CG}}^{(1,0), \overline{\text{MS}}}(r) = & - \frac{C_F C_A \alpha_s^2 (e^{-\gamma_E}/r)}{4r^2} \left\{ 1 + \frac{\alpha_s}{\pi} \left(\frac{89}{36} C_A - \frac{49}{36} T_F n_f - \frac{8}{3} C_F \ln 2 \right. \right. \\
 & \left. \left. + \frac{4}{3} (C_A + 2C_F) \ln(\nu r e^{\gamma_E}) \right) \right\}. \tag{9.83}
 \end{aligned}$$

In the off-shell FG scheme, we have

$$V_{SI, \text{FG}}^{(2,0), \overline{\text{MS}}}(r) = V_{SI, \text{Coulomb}}^{(2,0), \overline{\text{MS}}}(r) + \frac{C_F C_A \alpha_s^2}{3\pi} \left(2 \ln 2 + \frac{35}{16} \right) \left[2\pi \delta^3(\mathbf{r}) + \frac{1}{r^3} \mathbf{L}^2 \right], \tag{9.84}$$

$$V_{SI, \text{FG}}^{(1,1), \overline{\text{MS}}}(r) = V_{SI, \text{Coulomb}}^{(1,1), \overline{\text{MS}}}(r) + \frac{2C_F C_A \alpha_s^2}{3\pi} \left(2 \ln 2 + \frac{35}{16} \right) \left[2\pi \delta^3(\mathbf{r}) + \frac{1}{r^3} \mathbf{L}^2 \right], \tag{9.85}$$

$$V_{\text{FG}}^{(1,0), \overline{\text{MS}}}(r) = V_{\text{Coulomb}}^{(1,0), \overline{\text{MS}}}(r) - \frac{C_F^2 \alpha_s^3}{3\pi r^2} C_A \left(2 \ln 2 + \frac{35}{16} \right). \tag{9.86}$$

The renormalized potentials obtained from the Wilson-loop prescription are

$$\begin{aligned}
 V_{r, W}^{(2,0), \overline{\text{MS}}}(r) = & \frac{C_F \alpha_s}{8} \left(c_D^{(1)} + \frac{\alpha_s}{\pi} \left\{ -\frac{5}{9} (c_D^{(1)} + c_1^{hl(1)}) T_F n_f + \left(\frac{13}{36} c_F^{(1)2} + \frac{8}{3} \right) C_A \right. \right. \\
 & \left. \left. + \left(\left(\frac{4}{3} + \frac{5}{6} c_F^{(1)2} \right) C_A - \frac{2}{3} (c_D^{(1)} + c_1^{hl(1)}) T_F n_f \right) \ln(\nu) \right\} \right) 4\pi \delta^{(3)}(\mathbf{r}) \\
 & + \frac{C_F \alpha_s^2}{8\pi} \left\{ \left(\frac{4}{3} + \frac{5}{6} c_F^{(1)2} \right) C_A - \frac{2}{3} (c_D^{(1)} + c_1^{hl(1)}) T_F n_f \right\} \text{reg} \frac{1}{r^3}, \tag{9.87}
 \end{aligned}$$

$$V_{\mathbf{L}^2, W}^{(2,0), \overline{\text{MS}}}(r) = \frac{C_A C_F \alpha_s^2}{4\pi r} \left(\frac{11}{3} - \frac{8}{3} \ln(\nu r e^{\gamma_E}) \right), \tag{9.88}$$

$$V_{\mathbf{p}^2, W}^{(2,0), \overline{\text{MS}}}(r) = - \frac{C_A C_F \alpha_s^2}{\pi r} \left(\frac{2}{3} + \frac{1}{3} \ln(\nu r e^{\gamma_E}) \right), \tag{9.89}$$

$$\begin{aligned}
 V_{r, W}^{(1,1), \overline{\text{MS}}}(r) = & \left[\frac{1}{4\pi} (d_{ss} + C_F d_{vs}) + \frac{C_F \alpha_s}{2} \left(1 + \frac{\alpha_s}{\pi} \left\{ \frac{55}{36} C_A + \frac{C_F}{6} - \frac{7}{18} T_F n_f \right. \right. \right. \\
 & \left. \left. + \left(-\frac{5}{12} C_A - \frac{7}{3} C_F + \frac{\beta_0}{2} \right) \ln(\nu) \right\} \right] 4\pi \delta^{(3)}(\mathbf{r}) \\
 & + \frac{C_F \alpha_s^2}{2 \pi} \left(-\frac{5}{12} C_A - \frac{7}{3} C_F + \frac{\beta_0}{2} \right) \text{reg} \frac{1}{r^3}, \tag{9.90}
 \end{aligned}$$

$$V_{\mathbf{L}^2, W}^{(1,1), \overline{\text{MS}}}(r) = \frac{C_F \alpha_s (e^{-\gamma_E}/r)}{2r} \left\{ 1 + \frac{\alpha_s}{\pi} \left(\frac{97 C_A}{36} + \frac{1}{9} T_F n_f - \frac{8}{3} C_A \ln(\nu r e^{\gamma_E}) \right) \right\}, \tag{9.91}$$

$$V_{\mathbf{p}^2, W}^{(1,1), \overline{\text{MS}}}(r) = -C_F \frac{\alpha_s (e^{-\gamma_E}/r)}{r} \left\{ 1 + \frac{\alpha_s}{\pi} \left(\frac{23}{18} C_A - \frac{2}{9} T_F n_f + \frac{2}{3} C_A \ln(\nu r e^{\gamma_E}) \right) \right\}, \tag{9.92}$$

$$V_W^{(1,0), \overline{\text{MS}}}(r) = - \frac{C_F C_A \alpha_s^2 (e^{-\gamma_E}/r)}{4r^2} \left\{ 1 + \frac{\alpha_s}{\pi} \left(\frac{89}{36} C_A - \frac{49}{36} T_F n_f + \frac{4}{3} C_A \ln(\nu r e^{\gamma_E}) \right) \right\}. \tag{9.93}$$

Finally, we present the renormalized potentials in the on-shell scheme:

$$\begin{aligned}
 V_{r,\text{on-shell}}^{(2,0),\overline{\text{MS}}}(r) &= \frac{C_F\alpha_s}{8} \left(c_D^{(1)} + \frac{\alpha_s}{\pi} \left\{ -\frac{5}{9} (c_D^{(1)} + c_1^{hl(1)}) T_{Fn_f} + \left(\frac{13}{36} c_F^{(1)2} + \frac{1}{3} \right) C_A \right. \right. \\
 &\quad \left. \left. + \left(\left(\frac{5}{6} c_F^{(1)2} + 4 \right) C_A - \frac{2}{3} (c_D^{(1)} + c_1^{hl(1)}) T_{Fn_f} \right) \ln(\nu) \right\} \right) 4\pi\delta^{(3)}(\mathbf{r}) \\
 &\quad + \frac{C_F\alpha_s^2}{8\pi} \left\{ \left(\frac{5}{6} c_F^{(1)2} + 4 \right) C_A - \frac{2}{3} (c_D^{(1)} + c_1^{hl(1)}) T_{Fn_f} \right\} \text{reg} \frac{1}{r^3}, \quad (9.94)
 \end{aligned}$$

$$V_{\mathbf{p}^2,\text{on-shell}}^{(2,0),\overline{\text{MS}}}(r) = -\frac{C_F\alpha_s^2}{3\pi} \frac{1}{r} C_A \ln(\nu r e^{\gamma_E}), \quad (9.95)$$

$$\begin{aligned}
 V_{r,\text{on-shell}}^{(1,1),\overline{\text{MS}}}(r) &= \left[\frac{1}{4\pi} (d_{ss} + C_F d_{vs}) + \frac{C_F\alpha_s}{2} \left(1 + \frac{\alpha_s}{\pi} \left\{ \frac{a_1}{4} - \frac{1}{12} C_A + \frac{C_F}{3} \right. \right. \right. \\
 &\quad \left. \left. + \left(\frac{11}{6} C_A - \frac{14}{3} C_F + \frac{\beta_0}{2} \right) \ln(\nu) \right\} \right) \right] 4\pi\delta^{(3)}(\mathbf{r}) \\
 &\quad + \frac{C_F\alpha_s^2}{4\pi} \left(\frac{11}{6} C_A - \frac{14}{3} C_F + \frac{\beta_0}{2} \right) \text{reg} \frac{1}{r^3}, \quad (9.96)
 \end{aligned}$$

$$V_{\mathbf{p}^2,\text{on-shell}}^{(1,1),\overline{\text{MS}}}(r) = -\frac{C_F\alpha_s(e^{-\gamma_E}/r)}{r} \left\{ 1 + \frac{\alpha_s}{4\pi} \left(a_1 + \frac{8}{3} C_A \ln(\nu r e^{\gamma_E}) \right) \right\}, \quad (9.97)$$

$$\begin{aligned}
 \frac{V_{\text{on-shell}}^{(1,0),\overline{\text{MS}}}(r)}{m_1} + \frac{V_{\text{on-shell}}^{(0,1),\overline{\text{MS}}}(r)}{m_2} &= \frac{C_F^2\alpha_s^2(e^{-\gamma_E}/r)}{2r^2} \frac{m_r}{m_1 m_2} \left(1 + \frac{\alpha_s}{2\pi} (a_1 - \beta_0) \right) \\
 &\quad - \frac{C_F C_A \alpha_s^2(e^{-\gamma_E}/r)}{4m_r r^2} \left\{ 1 + \frac{\alpha_s}{\pi} \left(\frac{89}{36} C_A - \frac{49}{36} T_{Fn_f} - C_F + \frac{4}{3} (C_A + 2C_F) \ln(\nu r e^{\gamma_E}) \right) \right\}. \quad (9.98)
 \end{aligned}$$

We remark again that in Eqs. (9.87)-(9.93), the renormalized expressions of the Wilson loop potentials have been obtained by subtracting Eq. (9.76) from the soft Wilson loop result, whereas the rest of renormalized potentials have been obtained by subtracting Eq. (9.75) from the respective soft results. Any of the above sets of potentials produces the same spectrum. We also stress that our renormalization procedure does not just subtract the $1/\epsilon$ poles, but also adds some finite pieces and an ϵ dependence to the renormalized potentials. We do this in such a way that the ultrasoft bound state calculation is simplified, as we will see in Sec. 10.1.

We quote the corresponding expressions for the renormalized potentials in the different matching schemes in momentum space in Appendix G.3. Note that what we get is not the result one obtains by just subtracting the $1/\epsilon$ poles in momentum space (which is what it is usually named $\overline{\text{MS}}$ scheme). This renormalization scheme would complicate the (ultrasoft part of the) bound state calculation for the spectrum. For our purposes, it is more convenient to do the subtraction in position space, and the prescription we have proposed here is particularly useful, because it avoids spurious logarithms of \mathbf{k}^2 . We will refer to it as $\overline{\text{MS}}$ scheme here. In this way we can efficiently carry out the bound state computations in four dimensions.

9.5 Static and spin-dependent potentials

The static and spin-dependent potentials are needed in order to achieve the precision we are aiming for in the computation of the spectrum. Their expressions in momentum space can be found in Appendix G.3.

The static potential, as we have already mentioned, is gauge invariant by itself, and therefore, the previous discussion on matching schemes and field redefinitions does not apply. Note that the static potential is affected by ultrasoft divergences, which we renormalize following the discussion of Sec. 9.4. The $\overline{\text{MS}}$ renormalized static potential reads

$$V_{s,\overline{\text{MS}}}^{(0)}(r) = -\frac{C_F \alpha_s(\nu)}{r} \left\{ 1 + \sum_{n=1}^3 \left(\frac{\alpha_s(\nu)}{4\pi} \right)^n a_n(r) \right\}, \quad (9.99)$$

with the coefficients

$$\begin{aligned} a_1(r) &= a_1 + 2\beta_0 \ln(\nu e^{\gamma_E} r), \\ a_2(r) &= a_2 + \frac{\pi^2}{3} \beta_0^2 + (4a_1\beta_0 + 2\beta_1) \ln(\nu e^{\gamma_E} r) + 4\beta_0^2 \ln^2(\nu e^{\gamma_E} r), \\ a_3(r) &= a_3 + a_1\beta_0^2\pi^2 + \frac{5\pi^2}{6} \beta_0\beta_1 + 16\zeta_3\beta_0^3 \\ &\quad + \left(2\pi^2\beta_0^3 + 6a_2\beta_0 + 4a_1\beta_1 + 2\beta_2 + \frac{16}{3}C_A^3\pi^2 \right) \ln(\nu e^{\gamma_E} r) \\ &\quad + \left(12a_1\beta_0^2 + 10\beta_0\beta_1 \right) \ln^2(\nu e^{\gamma_E} r) + 8\beta_0^3 \ln^3(\nu e^{\gamma_E} r). \end{aligned} \quad (9.100)$$

Explicit expressions for the coefficients a_i can be found in the literature Refs. [36–41]. For ease of reference we list them in Appendix A.

The spin-dependent potentials have been defined in Eqs. (8.29)-(8.31). Their D -dimensional structure requires a further study and examination, since objects such as the Pauli matrices and the Levi-Civita symbol are only well-defined in integer dimensions. This study is beyond the scope of this thesis, and so we relegate it for a future work. However, one should bare in mind that this potential is not affected by field redefinitions, and it is therefore gauge invariant. For completeness we quote here their renormalized expressions that read (renormalized NRQCD Wilson coefficients are understood)

$$V_{LS}^{(2,0)}(r) = \frac{C_F \alpha_s(e^{1-\gamma_E}/r)}{2 r^3} \left\{ c_S^{(1)} - \frac{\alpha_s}{\pi} \left[\left(\frac{5}{36} + \ln \left(\frac{r\nu}{e^{1-\gamma_E}} \right) \right) C_A + \frac{5}{9} T_F n_f \right] \right\}, \quad (9.101)$$

$$V_{LS}^{(0,2)}(r) = V_{LS}^{(2,0)}(r; c_S^{(1)} \rightarrow c_S^{(2)}), \quad (9.102)$$

$$\begin{aligned} V_{S^2}^{(1,1)}(r) &= \frac{2C_F}{3} \left\{ c_F^{(1)} c_F^{(2)} \alpha_s - \frac{3}{2\pi C_F} (d_{sv} + C_F d_{vv}) \right. \\ &\quad \left. + \frac{\alpha_s^2}{\pi} \left(\frac{-1}{72} C_A - \frac{5}{9} n_f T_F + \left(\frac{\beta_0}{2} - \frac{7}{4} C_A \right) \ln(\nu) \right) \right\} 4\pi \delta^3(\mathbf{r}) \\ &\quad + \frac{C_F \alpha_s^2}{6 \pi} \left(\frac{\beta_0}{2} - \frac{7}{4} C_A \right) \text{reg} \frac{1}{r^3}, \end{aligned} \quad (9.103)$$

$$V_{S_{12}}^{(1,1)}(r) = \frac{C_F \alpha_s(e^{4/3-\gamma_E}/r)}{4 r^3} \left\{ c_F^{(1)} c_F^{(2)} + \frac{\alpha_s}{\pi} \left[\left(\frac{13}{36} - \ln \left(\frac{\nu r}{e^{4/3-\gamma_E}} \right) \right) C_A - \frac{5}{9} n_f T_F \right] \right\}, \quad (9.104)$$

$$V_{L_2 S_1}^{(1,1)}(r) = C_F \frac{\alpha_s(e^{1-\gamma_E}/r)}{r^3} \left\{ c_F^{(1)} + \frac{\alpha_s}{\pi} \left[\left(\frac{13}{36} - \frac{1}{2} \ln \left(\frac{\nu r}{e^{1-\gamma_E}} \right) \right) C_A - \frac{5}{9} n_f T_F \right] \right\}, \quad (9.105)$$

$$V_{L_1 S_2}^{(1,1)}(r) = V_{L_2 S_1}^{(1,1)}(r; c_F^{(1)} \rightarrow c_F^{(2)}), \quad (9.106)$$

where the reg function has been defined in Eq. (4.26).

Eqs. (9.101) and (9.104)-(9.106) correct misprints in Eqs. (70) and (71) of Ref. [103] (when setting the masses equal). For the spin-dependent potentials, and for our purposes, we can work with the four dimensional expressions for $\mathbf{L} \cdot \mathbf{S}_i$, \mathbf{S}_{12} and \mathbf{S}^2 . Even though the (soft) matching calculation for these spin-dependent potentials exhibits ultraviolet divergences, they do not require renormalization in pNRQCD. The divergences exactly cancel the ones of the NRQCD Wilson coefficients, so that the overall spin-dependent potential in pNRQCD is finite (to the order of interest), cf. Eqs. (9.101)-(9.106).

The spin-dependent potentials are unambiguous (at least to the order we are working at). They were originally computed in Ref. [141] at NNLO, in Ref. [156] for the N³LO hyperfine splitting, and in Ref. [143] the complete expression for unequal masses was obtained.

9.6 Poincaré invariance constraints

The Poincaré algebra induces non trivial constraints on the form of the Hamiltonian of NR systems where Poincaré invariance is no longer explicit. In the context of our computation the following two relations for the heavy quark potential can be derived

$$2V_{\mathbf{L}^2}^{(2,0)} - V_{\mathbf{L}^2}^{(1,1)} + \frac{r}{2} \frac{dV^{(0)}(r)}{dr} = 0, \quad (9.107)$$

$$-4V_{\mathbf{p}^2}^{(2,0)} + 2V_{\mathbf{p}^2}^{(1,1)} - V^{(0)}(r) + r \frac{dV^{(0)}(r)}{dr} = 0. \quad (9.108)$$

Note that they do not involve the NRQCD Wilson coefficients.

These relations were originally found in Ref. [149] by explicit calculation of the potentials in terms of Wilson loops. In the context of pNRQCD, and explicitly using the Poincaré algebra, they were deduced in Refs. [157, 158]. We have checked that our results fulfill these equalities: we have explicitly verified that Eqs. (9.107) and (9.108) are fulfilled by the bare and renormalized potentials obtained from off-shell matching in CG and FG and from Wilson-loop matching.

On the other hand, we stress that the Poincaré invariance constraints cannot be applied to the results in the on-shell matching scheme. The reason is that Eqs. (9.107) and (9.108) are derived assuming a certain mass scaling of the potentials. This assumption does not hold for the potentials obtained by on-shell matching, as the latter mixes different orders in the $1/m$ expansion.

Finally, it is easy to see that the above Poincaré invariance relations are not affected by our field redefinition in Eq. (8.69), as the latter produces shifts of the form $\delta V_{\mathbf{L}^2}^{(1,1)} = 2\delta V_{\mathbf{L}^2}^{(2,0)}$, $\delta V_{\mathbf{p}^2}^{(1,1)} = 2\delta V_{\mathbf{p}^2}^{(2,0)}$, and leaves the static potential $V^{(0)}$ invariant.

Chapter 10

The B_c mass to N³LO

We are now in the position to compute the spectrum of a heavy quarkonium bound state made of two heavy quarks with different masses with N³LO accuracy in the weak coupling limit. We have obtained explicit expressions both for the static potential and its relativistic corrections in Chapter 9. In Sec. 10.1 we quote the energy shift produced by the ultrasoft contribution. In Sec. 10.2 we quote the energy shifts associated with the static potential. In Sec. 10.3 we compute the energy shifts associated with the relativistic corrections to the potential, and in Sec. 10.4 we present our final expression for the heavy quarkonium mass.

10.1 The ultrasoft energy correction

Combining the results given in Refs. [39, 58, 159] we find for the ultrasoft contribution to the energy:

$$\begin{aligned} \delta E_{nl}^{US} = & -E_n^C \frac{\alpha_s^3}{\pi} \left[\frac{2}{3} C_F^3 L_{nl}^E + \frac{1}{3} C_A \left(L_\nu - L_{US} + \frac{5}{6} \right) \left(\frac{C_A^2}{2} + \frac{4C_A C_F}{(2l+1)n} \right. \right. \\ & \left. \left. + 2C_F^2 \left(\frac{8}{(2l+1)n} - \frac{1}{n^2} \right) \right) + \frac{8\delta_{l0}}{3n} C_F^2 \left(C_F - \frac{C_A}{2} \right) \left(L_\nu - L_{US} + \frac{5}{6} \right) \right], \end{aligned} \quad (10.1)$$

where $E_n^C = -\frac{C_F^2 \alpha_s^2 m_r}{2n^2}$, $L_\nu = \ln\left(\frac{n\nu}{2m_r C_F \alpha_s}\right) + S_1(n+l)$, $L_{US} = \ln\left(\frac{C_F \alpha_s n}{2}\right) + S_1(n+l)$, and the Bethe logarithm is defined as

$$L_n^E = \frac{1}{(C_F \alpha_s)^2 E_n^C} \int_0^\infty \frac{d^3 k}{(2\pi)^3} |\langle \mathbf{r} | \mathbf{k} n | \rangle|^2 \left(E_n^C - \frac{k^2}{2m_r} \right)^3 \ln \frac{E_1^C}{E_n^C - \frac{k^2}{2m_r}}. \quad (10.2)$$

Numerical determinations of these non-Abelian Bethe logarithms were obtained for low values of n in Ref. [39] for $l=0$ and in Ref. [160] also for $l \neq 0$.

10.2 Energy correction associated with the static potential

We extract this contribution from the results of Ref. [160] for equal masses, as it has a trivial dependence on the mass. We (partially) adopt their notation in the following. For the ground state and first excitations the contribution was computed in Refs. [161–163]. It follows from

standard (time-independent) quantum mechanical perturbation theory up to third order and reads

$$\delta E(n, l, s, j) \Big|_{V^{(0)}} = E_n^C \left(1 + \frac{\alpha_s}{\pi} P_1(L_\nu) + \left(\frac{\alpha_s}{\pi} \right)^2 P_2^c(L_\nu) + \left(\frac{\alpha_s}{\pi} \right)^3 P_3^c(L_\nu) \right), \quad (10.3)$$

where

$$P_1(L_\nu) = \beta_0 L_\nu + \frac{a_1}{2}, \quad (10.4)$$

$$P_2^c(L_\nu) = \frac{3}{4} \beta_0^2 L_\nu^2 + \left(-\frac{\beta_0^2}{2} + \frac{\beta_1}{4} + \frac{3\beta_0 a_1}{4} \right) L_\nu + c_2^c, \quad (10.5)$$

$$\begin{aligned} P_3^c(L_\nu) = & \frac{1}{2} \beta_0^3 L_\nu^3 + \left(-\frac{7\beta_0^3}{8} + \frac{7\beta_0 \beta_1}{16} + \frac{3}{4} \beta_0^2 a_1 \right) L_\nu^2 \\ & + \left(\frac{\beta_0^3}{4} - \frac{\beta_0 \beta_1}{4} + \frac{\beta_2}{16} - \frac{3}{8} \beta_0^2 a_1 + 2\beta_0 c_2^c + \frac{3\beta_1 a_1}{16} \right) L_\nu + c_3^c + \pi^2 \frac{C_A^3}{6} L_\nu, \end{aligned} \quad (10.6)$$

and

$$c_2^c = \frac{a_1^2}{16} + \frac{a_2}{8} - \frac{\beta_0 a_1}{4} + \beta_0^2 \left(\frac{n}{2} \zeta(3) + \frac{\pi^2}{8} \left(1 - \frac{2n}{3} \Delta S_{1a} \right) - \frac{1}{2} S_2(n+l) + \frac{n}{2} \Sigma_a(n, l) \right), \quad (10.7)$$

$$c_3^c = \frac{\beta_0^2 a_1}{8} + \frac{3\beta_0 a_1^2}{32} - \frac{\beta_0 a_2}{16} - \frac{\beta_1 a_1}{16} - \frac{a_1^3}{16} - \frac{3a_1 a_2}{32} + \frac{a_3}{32} + a_1 c_2^c + \beta_0 \beta_1 \sigma(n, l) + \beta_0^3 \tau(n, l). \quad (10.8)$$

Expressions for the different parameters and functions involved in these formulae are quoted in Appendix A.

10.3 Energy correction associated with the relativistic potentials

Here we explicitly compute the energy correction up to N³LO associated with our results for the relativistic $1/m$ and $1/m^2$ potentials. Recall that there is no $\mathcal{O}(\alpha_s/m^3)$ potential.

The non-static (i.e. relativistic) NNLO correction to the bound state energy reads

$$\delta E(n, l, s, j) = E_n^C \left(\frac{\alpha_s}{\pi} \right)^2 c_2^{\text{nc}}, \quad (10.9)$$

where

$$\begin{aligned} c_2^{\text{nc}} = & -\frac{2m_r^2 \pi^2 C_F^2}{nm_1 m_2} \left\{ \frac{1 - \delta_{l0}}{l(l+1)(2l+1)} \left(\frac{m_2}{m_1} X_{LS_1} + (D_S + 2X_{LS}) + \frac{m_1}{m_2} X_{LS_2} \right) + \frac{8\delta_{l0}}{3} \mathcal{S}_{12} \right\} \\ & + \frac{m_r^2 \pi^2 C_F}{4n^2} \left\{ \frac{1}{m_1 m_2} C_F + \frac{1}{m_r^2} \left[-3C_F + \frac{8n}{2l+1} \left(C_F + \frac{C_A}{2} \right) - 4nC_F \delta_{l0} \right] \right\} \\ \equiv & c_2^{\text{nc,SD}} + c_2^{\text{nc,SI}}, \end{aligned} \quad (10.10)$$

and X_{LS} , X_{LS_i} , D_S and \mathcal{S}_{12} have been defined in Appendix H.1.

By default we will use the on-shell potential for the computation, as it will ease the comparison with other results, in particular those of Ref. [160]. However, we emphasize that using any other scheme will not change this results. We split the computation of the N³LO correction to the

bound state energy into a spin-dependent and a spin-independent part. The spin-dependent contribution can be organized as follows:

$$\begin{aligned}
 \delta E_{jj_1 n l s}^{SD} &= \langle nl | \left(\frac{V_{SD}^{(2,0)}}{m_1^2} + \frac{V_{SD}^{(0,2)}}{m_2^2} + \frac{V_{SD}^{(1,1)}}{m_1 m_2} \right) \Big|_{\mathcal{O}(\alpha_s^2)} |nl\rangle + \frac{16 C_F \pi \alpha_s}{3 m_1 m_2} \mathcal{S}_{12} \langle nl | V_1 \frac{1}{(E_n^C - h)'} \delta^3(\mathbf{r}) |nl\rangle \\
 &+ \frac{\alpha_s C_F}{m_1 m_2} \left(D_S + 2X_{LS} + \frac{m_1}{m_2} X_{LS_2} + \frac{m_2}{m_1} X_{LS_1} \right) \langle nl | V_1 \frac{1}{(E_n^C - h)'} \frac{1}{r^3} |nl\rangle \\
 &= E_n^C \left(\frac{\alpha_s}{\pi} \right)^3 \left(c_3^{\text{nc,SD}} - 2\beta_0 L_\nu c_2^{\text{nc,SD}} \right), \tag{10.11}
 \end{aligned}$$

where

$$V_C \equiv -\frac{C_F \alpha_s}{r}, \quad V_1 \equiv V_C \frac{\alpha_s}{4\pi} (2\beta_0 \ln(\nu r e^{\gamma_E}) + a_1), \tag{10.12}$$

and

$$\frac{1}{(E_n^C - h)'} = \lim_{E \rightarrow E_n^C} \left(\frac{1}{E - h} - \frac{1}{E - E_n^C} \right), \quad h = \frac{\mathbf{p}^2}{2m_r} + V_C. \tag{10.13}$$

Note that this procedure is exactly the same as the analogous one in Chapter 5. In fact, the way to compute it is through Eq. (5.5) (generalised for two different potentials), where the Coulomb Green function is the one in Eq. (5.8) for $Z = 1$ and making the change $\alpha \rightarrow C_F \alpha_s$.

Using the expectation values given in Appendix H.1 for single and Appendix H.2 for double potential operator insertions we find

$$c_3^{\text{nc,SD}} = \pi^2 \left(C_F^3 \xi_{\text{FFF}}^{\text{SD}} + C_F^2 C_A \xi_{\text{FFA}}^{\text{SD}} + C_F^2 T_F n_f \xi_{\text{FFnf}}^{\text{SD}} - \frac{n}{6} \beta_0 c_2^{\text{nc,SD}} \right), \tag{10.14}$$

where,

$$\begin{aligned}
 \xi_{\text{FFF}}^{\text{SD}} &= \frac{2}{3n} \frac{m_r^2}{m_1 m_2} \left\{ \frac{-3(1 - \delta_{l0})}{l(l+1)(2l+1)} \left(D_S + X_{LS} + \frac{m_1}{m_2} X_{LS_2} + \frac{m_2}{m_1} X_{LS_1} \right) \right. \\
 &\quad \left. - 4\mathcal{S}_{12} \delta_{l0} \left[2 + 3 \frac{m_1 m_2}{m_2^2 - m_1^2} \ln \left(\frac{m_1^2}{m_2^2} \right) \right] \right\}, \tag{10.15}
 \end{aligned}$$

$$\begin{aligned}
 \xi_{\text{FFnf}}^{\text{SD}} &= \frac{2m_r^2}{9n^2 m_1 m_2} \left\{ \frac{1 - \delta_{l0}}{l(l+1)(2l+1)} \left[2n(4\mathcal{S}_{12} - D_S) \right. \right. \\
 &\quad \left. \left. + 6 \left(D_S + \frac{m_2}{m_1} X_{LS_1} + \frac{m_1}{m_2} X_{LS_2} + 2X_{LS} \right) \left(\frac{3n}{2l+1} + \frac{n}{2l(l+1)(2l+1)} + l + \frac{1}{2} \right) \right. \right. \\
 &\quad \left. \left. + 2n \left\{ S_1(l+n) + S_1(2l-1) - 2S_1(2l+1) - l(\Sigma_1^{(k)} + \Sigma_1^{(m)}) + n\Sigma_b - \Sigma_1^{(m)} + \frac{1}{6} \right\} \right] \right. \\
 &\quad \left. + 8\delta_{l0} \mathcal{S}_{12} \left[1 + 4n \left(\frac{11}{12} - \frac{1}{n} - S_1(n-1) - S_1(n) + nS_2(n) \right) \right] \right\}, \tag{10.16}
 \end{aligned}$$

$$\begin{aligned}
 \xi_{\text{FFA}}^{\text{SD}} &= \frac{m_r^2}{m_1 m_2} \left\{ \frac{1 - \delta_{l0}}{l(l+1)(2l+1)n} \left[\frac{2}{3} \left(D_S + \frac{m_2}{m_1} X_{LS_1} + \frac{m_1}{m_2} X_{LS_2} + 2X_{LS} \right) \right. \right. \\
 &\quad \left. \left. \times \left\{ 22S_1(2l+1) - 17S_1(l+n) - 5S_1(2l-1) + 11 \left[l(\Sigma_1^{(k)} + \Sigma_1^{(m)}) - n\Sigma_b + \Sigma_1^{(m)} \right] \right\} \right] \right\}
 \end{aligned}$$

$$\begin{aligned}
 & \left. - \frac{5(2l+1)}{4n} - \frac{15}{2(2l+1)} - \frac{5}{4(l(l+1)(2l+1))} + \frac{1}{6} + \frac{3}{2} \ln \left(\frac{m_1 m_2}{4m_r^2} \right) + 3L_H \right\} \\
 & - \frac{2}{9} (2D_S + \mathcal{S}_{12}) + \ln \left(\frac{m_1}{m_2} \right) \left(\frac{m_1 m_2 X_{LS_1}}{m_r^2} - \frac{m_1 X_{LS}}{m_2} \right) \\
 & - 2X_{LS} \left(2(\mathcal{S}_1(2l-1) - \mathcal{S}_1(l+n)) + \frac{2l+1}{2n} + \frac{1}{2(l(l+1)(2l+1))} + \frac{3}{2l+1} \right. \\
 & \quad \left. - 2 + \frac{1}{2} \ln \left(\frac{m_1^2}{4m_r^2} \right) + L_H \right) \Bigg] \\
 & - \frac{4\delta_{l0}\mathcal{S}_2}{3n} \left[-\frac{67}{3}\mathcal{S}_1(l+n) - 7L_H + \frac{65\mathcal{S}_1(n)}{3} + \frac{44n\Sigma_2^{(k)}}{3} + \frac{1}{6n} + \frac{41}{18} \right. \\
 & \quad \left. + \frac{1}{m_1 - m_2} \left((5m_2 - 2m_1) \ln \left(\frac{m_1}{2m_r} \right) - (5m_1 - 2m_2) \ln \left(\frac{m_2}{2m_r} \right) \right) \right] \Bigg\}, \quad (10.17)
 \end{aligned}$$

and $L_H = \ln \left(\frac{n}{C_{F\alpha_s}} \right) + \mathcal{S}_1(n+l)$.

For the spin-independent part of the energy we proceed in the same way. In this case the energy shift can be written as

$$\begin{aligned}
 \delta E_{nl}^{SI} &= \langle nl | \left(\frac{V^{(1,0)}}{m_1} + \frac{V^{(0,1)}}{m_2} \right) \Big|_{\mathcal{O}(\alpha_s^3)} |nl\rangle + \langle nl | \left(\frac{V_{SI}^{(2,0)}}{m_1^2} + \frac{V_{SI}^{(0,2)}}{m_2^2} + \frac{V_{SI}^{(1,1)}}{m_1 m_2} \right) \Big|_{\mathcal{O}(\alpha_s^2)} |nl\rangle \\
 &+ \delta E_{US} - \frac{1}{4} \left(\frac{1}{m_1^3} + \frac{1}{m_2^3} \right) \langle nl | V_1 \frac{1}{(E_n^C - h)'} p^4 |nl\rangle - \frac{C_F \alpha_s}{m_1 m_2} \langle nl | V_1 \frac{1}{(E_n^C - h)'} \left\{ \frac{1}{r}, p^2 \right\} |nl\rangle \\
 &+ C_F \alpha_s^2 \left(C_F \frac{m_r}{m_1 m_2} - \frac{C_A}{2m_r} \right) \langle nl | V_1 \frac{1}{(E_n^C - h)'} \frac{1}{r^2} |nl\rangle + \frac{C_F \pi \alpha_s}{m_r^2} \langle nl | V_1 \frac{1}{(E_n^C - h)'} \delta^3(\mathbf{r}) |nl\rangle \\
 &= \langle nl | \left(\frac{V^{(1,0)}}{m_1} + \frac{V^{(0,1)}}{m_2} \right) \Big|_{\mathcal{O}(\alpha_s^3)} |nl\rangle + \langle nl | \left(\frac{V_{SI}^{(2,0)}}{m_1^2} + \frac{V_{SI}^{(0,2)}}{m_2^2} + \frac{V_{SI}^{(1,1)}}{m_1 m_2} \right) \Big|_{\mathcal{O}(\alpha_s^2)} |nl\rangle \\
 &+ \delta E_{US} + \frac{1}{2m_r} \left(1 - \frac{m_r^2}{m_1 m_2} \right) \left(\langle nl | V_1 |nl\rangle \langle nl | V_C |nl\rangle - \langle nl | V_1 V_C |nl\rangle \right) \\
 &+ \frac{C_F^3 \alpha_s^3 m_r}{n^2} \langle nl | V_1 \frac{1}{(E_n^C - h)'} \frac{1}{r} |nl\rangle - \frac{\alpha_s^2}{2m_r} C_F \left(C_F + \frac{C_A}{2} \right) \langle nl | V_1 \frac{1}{(E_n^C - h)'} \frac{1}{r^2} |nl\rangle \\
 &+ \frac{C_F \pi \alpha_s}{2m_r^2} \langle nl | V_1 \frac{1}{(E_n^C - h)'} \delta^3(\mathbf{r}) |nl\rangle = E_n^C \left(\frac{\alpha_s}{\pi} \right)^3 \left(c_3^{\text{nc,SI}} - 2\beta_0 L_\nu c_2^{\text{nc,SI}} - \frac{\pi^2}{6} C_A^3 L_\nu \right). \quad (10.18)
 \end{aligned}$$

Using again the expectation values in Appendix H.1 for single and Appendix H.2 for double potential insertions we obtain

$$\begin{aligned}
 c_3^{\text{nc,SI}} &= \pi^2 \left(C_A^3 \xi_{AAA} + C_A^2 C_F \xi_{AAF} + C_A C_F T_F n_f \xi_{AFn_f} + C_F^2 T_F \xi_{FF} + C_F^3 \xi_{FFF}^{\text{SI}} \right. \\
 & \quad \left. + C_F^2 C_A \xi_{FFA}^{\text{SI}} + C_F T_F n_f \xi_{FFn_f}^{\text{SI}} - \frac{n}{6} \beta_0 c_2^{\text{nc,SI}} \right), \quad (10.19)
 \end{aligned}$$

where,

$$\xi_{AAA} = \frac{1}{6} L_{US} - \frac{5}{36}, \quad (10.20)$$

$$\xi_{AAF} = \frac{1}{(2l+1)n} \left(\frac{5}{4} - \frac{7}{3(2l+1)} + \frac{8}{3}[S_1(2l) - S_1(l+n)] + \frac{11n}{3}\Sigma_b + \frac{4}{3}L_{US} \right), \quad (10.21)$$

$$\xi_{AFn_f} = -\frac{4}{3n(2l+1)} \left(\frac{65}{48} - \frac{1}{2l+1} + n\Sigma_b \right), \quad (10.22)$$

$$\xi_{FF} = \frac{8}{15n} \delta_{l0} \left(1 - 2\frac{m_r^2}{m_1 m_2} \right), \quad (10.23)$$

$$\xi_{FFF}^{SI} = \frac{2}{3n} \left\{ \frac{7m_r^2}{m_1 m_2} \left[\frac{1 - \delta_{l0}}{l(l+1)(2l+1)} + \delta_{l0} \left(\frac{1}{n} - 1 - 2(S_1(l+n) + S_1(n)) \right) \right] \right. \quad (10.24)$$

$$\left. - nL_{nl}^E + 2\delta_{l0}L_H \left(7\frac{m_r^2}{m_1 m_2} - 2 \right) - \frac{2m_r^2 \delta_{l0}}{m_1 m_2} \left[\frac{m_2}{m_1} \ln \left(\frac{m_1^2}{4m_r^2} \right) + \frac{m_1}{m_2} \ln \left(\frac{m_2^2}{4m_r^2} \right) \right. \right. \\ \left. \left. + \frac{3m_1 m_2}{2(m_1^2 - m_2^2)} \left(\frac{m_2}{m_1} \ln \left(\frac{m_1^2}{4m_r^2} \right) - \frac{m_1}{m_2} \ln \left(\frac{m_2^2}{4m_r^2} \right) \right) \right] - 2\delta_{l0} \left(\frac{5}{3} - 2L_{US} \right) \right\},$$

$$\xi_{FFA}^{SI} = \frac{1}{3n} \left\{ -\frac{\delta_{l0}}{4} \left(1 + \frac{29}{n} + 20L_H + 16L_{US} + 8S_1(n) - 124S_1(l+n) + 44n\Sigma_2^{(k)} \right) \right. \\ \left. - \frac{29(1 - \delta_{l0})}{4l(l+1)(2l+1)} - \frac{32}{2l+1} \left(\frac{5}{24} - \frac{1}{2}L_{US} + S_1(l+n) - S_1(2l+1) - \frac{11n\Sigma_b}{16} \right) \right. \\ \left. - \frac{38}{(2l+1)^2} - \frac{2}{n}L_{US} - \frac{7}{12n} - \frac{11\pi^2}{8} \right\} + \frac{m_r^2}{m_1 m_2 n} \left\{ \frac{7(1 - \delta_{l0})}{6l(l+1)(2l+1)} \right. \\ \left. + \frac{\delta_{l0}}{6} \left(\frac{7}{n} + 17 - 14(S_1(l+n) + S_1(n) - L_H) \right) + \frac{11}{3(2l+1)} - \frac{35}{36n} + \frac{11\pi^2}{72} \right\} \\ \left. + \frac{\delta_{l0} m_r^2}{6n(m_1 - m_2)} \left\{ \frac{1}{m_2^2} (2m_2 - 5m_1) \ln \left(\frac{m_2^2}{4m_r^2} \right) - \frac{1}{m_1^2} (2m_1 - 5m_2) \ln \left(\frac{m_1^2}{4m_r^2} \right) \right\}, \quad (10.25)$$

$$\xi_{FFn_f}^{SI} = \frac{2}{3n} \left\{ \frac{1 - \delta_{l0}}{2l(l+1)(2l+1)} + \frac{m_r^2}{m_1 m_2} \left(\frac{1}{6n} - \frac{\pi^2}{12} - \frac{2}{2l+1} \right) + \frac{3}{2n} - \frac{4n}{2l+1} \Sigma_b \right. \\ \left. - \frac{14}{3(2l+1)} + \frac{4}{(2l+1)^2} + \frac{1}{2} \delta_{l0} \left(4(n\Sigma_2^{(k)} - S_1(n)) + \frac{1}{n} + \frac{11}{3} \right) + \frac{\pi^2}{4} \right\}. \quad (10.26)$$

10.4 The $\mathcal{O}(m\alpha_s^5)$ spectrum for unequal masses

Summarizing the previous results, we can present the complete expression for the energy levels of a heavy quark-antiquark bound state with unequal quark masses and N³LO accuracy:

$$E(n, l, s, j) = E_n^C \left(1 + \frac{\alpha_s}{\pi} P_1(L_\nu) + \left(\frac{\alpha_s}{\pi} \right)^2 P_2(L_\nu) + \left(\frac{\alpha_s}{\pi} \right)^3 P_3(L_\nu) \right), \quad (10.27)$$

$$P_1(L_\nu) = \beta_0 L_\nu + \frac{a_1}{2}, \quad (10.28)$$

$$P_2(L_\nu) = \frac{3}{4} \beta_0^2 L_\nu^2 + \left(-\frac{\beta_0^2}{2} + \frac{\beta_1}{4} + \frac{3\beta_0 a_1}{4} \right) L_\nu + c_2, \quad (10.29)$$

$$P_3(L_\nu) = \frac{1}{2} \beta_0^3 L_\nu^3 + \left(-\frac{7\beta_0^3}{8} + \frac{7\beta_0 \beta_1}{16} + \frac{3}{4} \beta_0^2 a_1 \right) L_\nu^2 \\ + \left(\frac{\beta_0^3}{4} - \frac{\beta_0 \beta_1}{4} + \frac{\beta_2}{16} - \frac{3}{8} \beta_0^2 a_1 + 2\beta_0 c_2 + \frac{3\beta_1 a_1}{16} \right) L_\nu + c_3, \quad (10.30)$$

where $c_i = c_i^c + c_i^{\text{nc}}$.

We have checked that for the ground state the result agrees with the NNLO B_c energy given in Ref. [164]. For arbitrary quantum numbers the NNLO result can be found in Ref. [165] (though in a basis different from ours), and in Ref. [166] for the equal mass case. We have also checked that our results agree with the N³LO energy in the equal mass case, which was obtained in Ref. [161] for the ground state, in Refs. [162, 163] for S -wave states, and in Ref. [160] for general quantum numbers. We also agree with the numerical results given in Ref. [167].

All relevant definitions for the functions and parameters in the previous formulae can be found in Appendix A.

Chapter 11

Conclusions

In the second part of this thesis we have studied heavy quarkonium systems with different quark masses in the extreme weak-coupling limit. These systems are very similar to the ones studied in the first part of the thesis, with two main differences: their gauge group is different (U(1) vs. SU(3)) and so is the theory of their hard dynamics (HBET vs. QCD). The product of the latter is encoded in the Wilson coefficients of the effective theory NRQED/QCD. Once in this theory, the only difference is related to the gauge groups. We performed the matching computation of NRQCD and weakly-coupled pNRQCD for heavy quarkonium with different masses that allows us to obtain the spectrum to N³LO.

We have computed the $\mathcal{O}(\alpha_s^2/m^2)$ contribution to the heavy quarkonium spin-independent potential in the unequal mass case. We have obtained the bare D -dimensional expressions for different matching schemes in momentum and position space. We have performed all our calculations in CG and CF. Perturbative evaluations of loop diagrams in CG have always been thought of to be complicated and difficult to handle, especially for non-abelian theories. On the other hand one typically has to compute less diagrams in that gauge. For the one-loop calculations (using dimensional regularization) carried out in this work, CG has proven to be a competitive method.

In momentum space, the results are encoded in the coefficients \tilde{D}_2 . The coefficients $\tilde{D}_{\mathbf{p}^2,2}^{(2,0)}$, $\tilde{D}_{r,2}^{(2,0)}$, $\tilde{D}_{\mathbf{p}^2,2}^{(1,1)}$ and $\tilde{D}_{r,2}^{(1,1)}$ are independent of the matching procedure. Their expressions can be found in Eqs. (9.8)-(9.11). The expressions for $\tilde{D}_{\text{off},2}^{(2,0)}$, $\tilde{D}_{\text{off},2}^{(1,1)}$ are matching-scheme dependent. They vanish in the on-shell matching scheme. For off-shell matching in CG and FG we give their results in Eqs. (9.12), (9.13), and in Eqs. (9.15), (9.16), respectively. Wilson-loop matching yields the corresponding expressions in Eqs. (9.45), (9.46). The results for the individual potentials in terms of Wilson loops are manifestly gauge invariant.

These results, obtained from different matching procedures, can be related by field redefinitions. We have identified the field redefinitions that relate the $\mathcal{O}(\alpha_s^2/m^2)$ heavy quarkonium potentials in the different matching schemes. These field redefinitions are valid in D dimensions and can be applied to the bare potentials.

Our calculation yields an independent determination of the bare $\mathcal{O}(\alpha_s^3/m)$ potential piece proportional to the color factors $C_F^2 C_A$ and $C_F^2 T_F n_f$ for unequal masses and for the different matching schemes considered in this work. For the equal-mass on-shell case it agrees with the results of Refs. [140,153] up to $\mathcal{O}(\epsilon)$, but we remark that we also predict the complete ϵ dependence of these terms of the potential. Using the equal-mass on-shell result of Refs. [140,153] together

with our new $\mathcal{O}(\alpha_s^2/m^2)$ potentials we have determined the other terms of the $\mathcal{O}(\alpha_s^3/m)$ potential (proportional to $C_F C_A^2$ and $C_F C_A T_F n_f$) for unequal masses and the three different matching schemes to $\mathcal{O}(\epsilon)$.

For the $1/m$ potential in terms of Wilson loops we summarize our results in Eq. (9.67), and the corresponding momentum space coefficients $\tilde{D}_{2,W}^{(1,0)}$ and $\tilde{D}_{3,W}^{(1,0)}$ can be found in Eqs. (9.65) and (9.66). In the off-shell CG and FG matching schemes, the coefficients $\tilde{D}_2^{(1,0)}$ and $\tilde{D}_3^{(1,0)}$ can be found in Eqs. (9.68)-(9.70). In Eq. (9.71) we present the position-space expression for the unequal-mass $1/m$ potential in the on-shell scheme (note the non-trivial mass dependence). In the latter case it is actually meaningless to define the coefficients $\tilde{D}^{(1,0)}$, as they would depend on the heavy quark masses.

We remark that, in the Wilson-loop scheme, the terms of the $\mathcal{O}(\alpha_s^3/m)$ potential proportional to the color factors $C_F^2 C_A$ and $C_F^2 T_F n_f$ vanish. For the CG/FG off-shell matching the $C_F^2 T_F n_f$ term is zero, whereas in the on-shell scheme all possible color structures contribute. This suggests that using Wilson loops might be the optimal setup to determine the $1/m$ potential.

In summary, we have obtained the bare heavy quarkonium potential for unequal masses with the required precision to compute the B_c mass with N³LO accuracy. We have determined the renormalized potentials in the different matching schemes in Sec. 9.4 and discussed their dependence on the specific ultrasoft subtraction scheme. We have seen that the relativistic potentials obtained in the Wilson-loop and off-shell matching schemes (both the renormalized and bare expressions) satisfy certain constraints due to Poincaré invariance, unlike those obtained in the on-shell matching scheme.

We have performed the computation of the B_c mass with N³LO accuracy for arbitrary quantum numbers in Sec. 10. The final theoretical expression is given in Eq. (10.27). Note that, even though the expressions have been obtained in the weak-coupling limit, one can easily obtain expressions valid for $m_r \alpha_s^2 \sim \Lambda_{\text{QCD}}$ by subtracting the perturbative expression of the ultrasoft contribution, Eq. (10.1), and adding the corresponding expression in that regime (which then includes non-perturbative effects). A phenomenological analysis will be carried out elsewhere.

Other important results of our computation are the NLO expressions for the soft contribution of the $1/m$ and spin-independent (and velocity-dependent) $1/m^2$ quasi-static energies in the short-distance limit. These quasi-static energies represent non-perturbative definitions of the heavy quarkonium potentials. At this order, the quasi-static energies start to be sensitive to ultrasoft effects. Therefore, our results are, in fact, factorization scale dependent. To obtain “physical” results that can be compared with Monte Carlo lattice simulations, like those obtained in Refs. [168–170], the ultrasoft contributions to the relevant Wilson loops must be computed and added to the results of this work. This calculation will be carried out in a forthcoming publication.

The analysis of this work allows us to grasp the advantages and inconveniences of each matching scheme for perturbative evaluations of the potential. As a matter of fact, we find that all methods appear to be feasible in practice. In particular we found that perturbative computations using Wilson loops are not only feasible but may even have some advantages: The potentials in terms of Wilson loops encapsulate in a compact way all the information related to the soft scale, they are correct to any finite order in perturbation theory, and neither kinetic operator insertions nor potential loops have to be considered in the computation (which otherwise can be quite cumbersome at higher orders). We emphasize that, in the case of pure QED, it is possible to obtain closed expressions for some potentials, so that only a few orders in perturbation theory contribute. This implies some all-orders non-renormalization theorems (for the QED part) and, thus, also constrains the ultrasoft contributions.

Part IV

Final Remarks

In this thesis we have studied the physics of weakly bound states made of two heavy fermions with different masses. Their description is performed in the framework of EFTs, more specifically pNRQED and pNRQCD. We have computed the potentials up to N³LO and, as an application, we have used them to determine some energy levels.

We have established that the right theory in which to perform computations for these bound states is a theory at the ultrasoft scale. In the case of states bounded by QED it is clearly perturbative, since at low energies the coupling constant is a small parameter comparable to the relative velocity between the constituents, $\alpha \sim v$. However, in the case of systems bounded by QCD we also need to take into account the relation of the scales of the bound state with the energy scale that characterises the strong interaction, Λ_{QCD} . We work with bound states that, in the potential energy regime, fulfil $mv \gg \Lambda_{\text{QCD}}$. These systems can be described perturbatively, which allows us to compute a model independent potential for them, independently of the size of mv^2 . However, in order to obtain the spectrum we need to take into account the ultrasoft corrections to the energy. These corrections can be computed perturbatively in the limit $mv^2 \gg \Lambda_{\text{QCD}}$.

The first part of the dissertation is devoted to pNRQED, with special dedication to the Lamb shift in muonic hydrogen. We have obtained the potential terms that allows us to compute the Lamb shift up to $\mathcal{O}(\alpha^6 \ln \alpha)$. Within this computation the hadronic part of the NRQED Wilson coefficients is of utmost importance, as it is the main source of the theoretical uncertainty. Conducive to computing such Wilson coefficients in a model independent way, we perform the matching of the hadronic TPE from HBET to NRQED.

In order to describe such matching, we need to compute the effects of the hadronic structure of the proton on the Lamb shift in muonic hydrogen in terms of the interaction with photons and pions. We have computed and studied the spin-dependent and spin-independent structure functions of the FVCT of the proton to $\mathcal{O}(p^3)$ in HBChPT. These functions come out of the exchange of two photons between the proton and the muon. We have included the contribution of the Delta particle, not only because it is the closest resonance to the proton (and not so far away in terms of mass), but also because in the large- N_c limit proton and Delta become degenerate in mass. We have provided the computation of the FVCT structure functions associated to the m_π and Δ scales in D -dimensions. This completes previous partial results.

By incorporating these results to the NRQED coefficients $c_3^{pl_i}$ and $c_4^{pl_i}$, which appear in the $1/m^2$ delta-like potential in pNRQED, we obtain the hadronic TPE corrections to the muonic hydrogen Lamb shift. Moreover, with this computation, we obtain the leading chiral and large N_c structure of both coefficients, i.e. we determine their non-analytic dependence on m_q and N_c . This makes our result useful for eventual comparison to the lattice.

The contribution of this potential to the Lamb shift is therefore a pure prediction of the chiral theory, and hence it is model independent. We would like to emphasize that the energy shift associated to the TPE which we obtain is the most precise expression that can be obtained in a model independent way, since $\mathcal{O}(m_\mu \alpha^5 \frac{m_\mu^3}{\Lambda_{\text{QCD}}^3})$ effects are not controlled by the chiral theory and would require new counterterms.

The remaining of the first part of the thesis is devoted to reviewing the QED-like contributions to the Lamb shift in muonic hydrogen, and organising them within an EFT language. We have checked most of the results, and corrected some of the analytical formulae obtained previously in the literature. We have used the well-defined power counting of the EFT to estimate the size of the uncomputed terms and therefore the uncertainty of our result. We have reorganised the potentials making their dependence on the Wilson coefficients explicit, which is suitable to obtain

information of higher order contributions. As a by-product of these study we have obtained the full N³LO spectrum for muonium.

We have used the computation of the Lamb shift to determine the size of the electric proton radius. We do so via the comparison with the experimental measurement of the Lamb shift in muonic hydrogen first carried out at PSI in 2010. Our expression for the Lamb shift has a **pure QED-like term**, encoding all the contributions that consider the interaction of point-like fermions, a **hadronic term**, which takes into account the radius-independent effects of the hadronic structure of the proton, and a **term proportional to the proton radius**, which arises from the finite-size effects of the proton and allows us to obtain its value. In fact, in the EFT language, the latter is encoded in a Wilson coefficient, hence it is a well-defined quantity. The value for the proton radius that we obtain here is still 6.8σ away from the CODATA value. Therefore, we give model-independent significance to the proton radius puzzle. In this respect, we hope that all the new experiments related to this puzzle that are taking (or will take) place, will shed some light on the origin of this discrepancy.

On the second part of this work, we have studied heavy quarkonium with different masses at weak coupling. In particular, we have computed the relativistic corrections to the heavy quarkonium spin-independent potential at N³LO.

For the $\mathcal{O}(\alpha_s^2/m^2)$ potential we have obtained the bare expressions (in D -dimensions) for different matching schemes in momentum and position space. We have performed all our calculations in CG and FG. It is usually assumed that perturbative computations in the CG (specially for non-Abelian theories) are complicated and cumbersome, due mainly to the structure of the propagators. However, the number of Feynman diagrams contributing to a given process is usually smaller than in FG. We concluded that the Coulomb gauge is in fact a competitive framework in which to carry out these computations.

In momentum space we have split the potential into three different structures. Two of them only contain on-shell information, and thus are independent of the matching procedure: in position space one is related to the momentum operator and the other only depends on the position operator. The third structure is what we define as off-shell potential. It is related to the fact that we are not working in a minimal basis of potential structures, and therefore there is some mixing between this structure and the $1/m$ potential. Therefore, the off-shell potential is matching-scheme dependent. We have compared the main different matching schemes: on-shell, off-shell (in CG and FG) and performing the matching with Wilson loops. The first two matching schemes come out of equating the truncated on-/off-shell Green functions in NRQCD and pNRQCD, while the last one is given by the formulae that come out of equating the gauge invariant off-shell Green functions in both theories. The results for the individual potentials in terms of Wilson loops are manifestly gauge invariant. Moreover, the results obtained from different matching procedures, can be related by field redefinitions. We have identified the D -dimensional field redefinitions that relate the $\mathcal{O}(\alpha_s^2/m^2)$ heavy quarkonium potentials in the different matching schemes.

Our bare calculation yields an independent determination of the bare $\mathcal{O}(\alpha_s^3/m)$ potential proportional to the color factors $C_F^2 C_A$ and $C_F^2 T_F n_f$ for unequal masses and for the different matching schemes considered. Using the equal-mass on-shell result in the literature, together with our new $\mathcal{O}(\alpha_s^2/m^2)$ potentials, we have determined, through field redefinitions, the other terms of the $\mathcal{O}(\alpha_s^3/m)$ potential (proportional to $C_F C_A^2$ and $C_F C_A T_F n_f$) in the three different matching schemes to $\mathcal{O}(D-4)$. It is worth noting that in the Wilson-loops scheme, the terms of the $\mathcal{O}(\alpha_s^3/m)$ potential proportional to the color factors $C_F^2 C_A$ and $C_F^2 T_F n_f$ vanish. This only

happens for the $C_F^2 T_F n_f$ term in the off-shell matching schemes we have studied. This suggests that using Wilson loops might be the optimal setup to determine the $1/m$ potential.

From our computations it is straightforward to obtain the bare and renormalized potentials both in momentum and position space. We use a renormalization scheme similar to the usual $\overline{\text{MS}}$ but making the subtraction in position space. This subtraction is optimal to then perform the ultrasoft computation of the energy in the most natural way.

Altogether, we have obtained the bare heavy quarkonium potential for unequal masses with the required precision to compute the B_c mass with N³LO accuracy. We have also checked that the potentials, bare and renormalized, satisfy certain constraints due to Poincaré invariance. This does not apply to the on-shell scheme.

As an application of these results we have computed the B_c mass for arbitrary quantum numbers. This calculation is analogous to the muonic hydrogen we performed in the previous part and it also involves the contribution of lower order potentials through perturbation theory, which has been carried out using Voloshin's Green function formula.

Note that, even though the expressions have been obtained in the weak-coupling limit, one can easily obtain expressions valid for $m_r \alpha_s^2 \sim \Lambda_{\text{QCD}}$. To do so one should subtract the perturbative expression of the ultrasoft contribution from our final result, and add in its place the corresponding expression appropriate for that energy regime, which would include non-perturbative effects.

Through our analysis we wanted to grasp the advantages and inconveniences of each matching scheme for perturbative evaluations of the potential. As expected, all the schemes we have studied are indeed feasible. However, we find the matching through Wilson loops more advantageous: they encapsulate in a compact way all the information related to the soft scale, they are correct to any finite order in perturbation theory, and neither kinetic operator insertions nor potential loops have to be considered in the computation.

There are many possibilities for further work along the lines of the one presented here. In relation to the pNRQED section, it would be extremely interesting to obtain the contribution of the TPE to the Lamb shift from muonic hydrogen experiments. This could be achieved if the proton radius puzzle was clarified, and the value of the proton radius was then obtained from $e-p$ experiments. In this scenario, muonic hydrogen data would provide a better value of the hadronic TPE, as this quantity is suppressed by a power of the lepton mass. Moreover, we could work to obtain the spectrum at higher orders, which would then improve the determination of the TPE upon comparison to the experiment. On a different footing, the work carried out here could be of use to describe other light muonic atoms. One could also use the EFT tools to describe nucleon-nucleon interactions, e.g. for He atoms. Finally, it would be of great interest to analyse in depth the EFT determination of the fine and the hyperfine splittings in muonic hydrogen.

On the side of pNRQCD the possibilities are vast. On the one hand, a phenomenological analysis of the results obtained here is being carried out, which will allow for eventual comparison with experimental data. As a part of this analysis we will determine the ground state mass of the B_c from which we could obtain a new measure of the charm mass, provided the bottom mass has been obtained from another source. With this determination we could also study how important the US effects are, and hence how good our perturbative approximation is. The B_c ground state and its $2S$ excitation have already been measured experimentally, but we are hoping that many other related measurements will come out of the LHC experiment.

On top of that, some important results of our computation are the NLO expressions for the soft contribution of the $1/m$ and spin-independent $1/m^2$ quasi-static energies in the short-distance

limit. These quasi-static energies represent non-perturbative definitions of the heavy quarkonium potentials. At this order, the quasi-static energies start to be sensitive to ultrasoft effects, which makes our results factorization scale dependent. To obtain results that can be compared with Monte Carlo lattice simulations, the ultrasoft contributions to the relevant Wilson loops must be computed and added to the results of this work. We are actually performing this calculation.

On a broader scenario, the application of EFTs to somewhat different areas of research has proven very useful (for example in condensed matter). A specially relevant case in which NREFTs seem to be of relevance is in the direct detection of a possible heavy dark matter candidate. Some work has been carried out in this direction, although there is still much to be done. We plan to further extend this work.

Appendix A

Parameters and functions

A.1 QCD-related parameters

$$T_F = \frac{1}{2}; \quad C_A = N_c; \quad C_F = \frac{N_c^2 - 1}{2N_c}. \quad (\text{A.1})$$

$$\beta_0 = \frac{11}{3}C_A - \frac{4}{3}n_f T_F; \quad \beta_1 = \frac{34}{3}C_A^2 - \frac{20}{3}C_A T_F n_f - 4C_F T_F n_f; \quad (\text{A.2})$$

$$\beta_2 = \frac{2857}{54}C_A^3 - \frac{1415}{27}C_A^2 T_F n_f + \frac{158}{27}C_A T_F^2 n_f^2 - \frac{205}{9}C_A C_F T_F n_f + \frac{44}{9}C_F T_F^2 n_f^2 + 2C_F^2 T_F n_f. \quad (\text{A.3})$$

$$a_1 = \frac{31C_A - 20T_F n_f}{9}; \quad (\text{A.4})$$

$$a_2 = \frac{400 T_F^2 n_f^2}{81} - C_F T_F n_f \left(\frac{55}{3} - 16 \zeta(3) \right) + C_A^2 \left(\frac{4343}{162} + \frac{16 \pi^2 - \pi^4}{4} + \frac{22 \zeta(3)}{3} \right) - C_A T_F n_f \left(\frac{1798}{81} + \frac{56 \zeta(3)}{3} \right);$$

$$a_3 = a_3^{(3)} n_f^3 + a_3^{(2)} n_f^2 + a_3^{(1)} n_f + a_3^{(0)}, \quad (\text{A.5})$$

where

$$\begin{aligned} a_3^{(3)} &= - \left(\frac{20}{9} \right)^3 T_F^3, \\ a_3^{(2)} &= \left(\frac{12541}{243} + \frac{368 \zeta(3)}{3} + \frac{64 \pi^4}{135} \right) C_A T_F^2 + \left(\frac{14002}{81} - \frac{416 \zeta(3)}{3} \right) C_F T_F^2, \\ a_3^{(1)} &= (-709.717) C_A^2 T_F + \left(-\frac{71281}{162} + 264 \zeta(3) + 80 \zeta(5) \right) C_A C_F T_F \\ &\quad + \left(\frac{286}{9} + \frac{296 \zeta(3)}{3} - 160 \zeta(5) \right) C_F^2 T_F + (-56.83(1)) \frac{d_F^{abcd} d_A^{abcd}}{N_A}, \\ a_3^{(0)} &= 502.24(1) C_A^3 - 136.39(12) \frac{d_F^{abcd} d_A^{abcd}}{N_A} \end{aligned} \quad (\text{A.6})$$

and

$$\frac{d_F^{abcd} d_A^{abcd}}{N_A} = \frac{N_c(N_c^2 + 6)}{48}, \quad \frac{d_F^{abcd} d_F^{abcd}}{N_A} = \frac{N_c^4 - 6N_c^2 + 18}{96N_c^2}. \quad (\text{A.7})$$

A.2 $\overline{\text{MS}}$ renormalized NRQCD Wilson coefficients

In the $\overline{\text{MS}}$ scheme the respective renormalized Wilson coefficients of the single quark sector are (for $m_j \neq m_i$)¹

$$\begin{aligned} c_F^{(i)\overline{\text{MS}}}(\nu) &= 1 + \frac{\alpha_s(\nu)}{2\pi}(C_F + C_A) - \frac{\alpha_s(\nu)}{2\pi}C_A \ln \frac{m_i}{\nu}, \\ c_D^{(i)\overline{\text{MS}}}(\nu) &= 1 + \frac{\alpha_s(\nu)}{2\pi}C_A - \frac{4\alpha_s(\nu)}{15\pi} \left(1 + \frac{m_i^2}{m_j^2}\right) T_F + \frac{\alpha_s(\nu)}{\pi} \left(\frac{8}{3}C_F + \frac{2}{3}C_A\right) \ln \frac{m_i}{\nu}. \end{aligned} \quad (\text{A.8})$$

The four-quark Wilson coefficients for unequal masses are given by (note that for the equal mass case the annihilation contribution should be included, see Ref. [71] for the specific expressions):

$$d_{sv}^{\overline{\text{MS}}}(\nu) = \alpha_s^2 C_F \left(\frac{C_A}{2} - C_F\right) \frac{m_1 m_2}{m_1^2 - m_2^2} \ln \left(\frac{m_1^2}{m_2^2}\right), \quad (\text{A.9})$$

$$\begin{aligned} d_{vv}^{\overline{\text{MS}}}(\nu) &= 2\alpha_s^2 C_F \frac{m_1 m_2}{m_1^2 - m_2^2} \ln \left(\frac{m_1^2}{m_2^2}\right) + \frac{\alpha_s^2 C_A}{4(m_1^2 - m_2^2)} \left\{ m_1^2 \left(\ln \left(\frac{m_2^2}{\nu^2}\right) + 3\right) \right. \\ &\quad \left. - m_2^2 \left(\ln \left(\frac{m_1^2}{\nu^2}\right) + 3\right) - 3m_1 m_2 \ln \left(\frac{m_1^2}{m_2^2}\right) \right\}, \end{aligned} \quad (\text{A.10})$$

$$d_{ss}^{\overline{\text{MS}}}(\nu) = -C_F \left(\frac{C_A}{2} - C_F\right) \frac{\alpha_s^2}{m_1^2 - m_2^2} \left(m_1^2 \left(\ln \left(\frac{m_2^2}{\nu^2}\right) + \frac{1}{3}\right) - m_2^2 \left(\ln \left(\frac{m_1^2}{\nu^2}\right) + \frac{1}{3}\right) \right), \quad (\text{A.11})$$

$$\begin{aligned} d_{vs}^{\overline{\text{MS}}}(\nu) &= -2C_F \frac{\alpha_s^2}{m_1^2 - m_2^2} \left(m_1^2 \left(\ln \left(\frac{m_2^2}{\nu^2}\right) + \frac{1}{3}\right) - m_2^2 \left(\ln \left(\frac{m_1^2}{\nu^2}\right) + \frac{1}{3}\right) \right) \\ &\quad + \frac{C_A}{4} \frac{\alpha_s^2}{m_1^2 - m_2^2} \left[3 \left(m_1^2 \left(\ln \left(\frac{m_2^2}{\nu^2}\right) + \frac{1}{3}\right) - m_2^2 \left(\ln \left(\frac{m_1^2}{\nu^2}\right) + \frac{1}{3}\right) \right) \right. \\ &\quad \left. + \frac{1}{m_1 m_2} \left(m_1^4 \left(\ln \left(\frac{m_2^2}{\nu^2}\right) + \frac{10}{3}\right) - m_2^4 \left(\ln \left(\frac{m_1^2}{\nu^2}\right) + \frac{10}{3}\right) \right) \right]. \end{aligned} \quad (\text{A.12})$$

A.3 Finite Sums for the spectrum computation

The following functions are defined here in order to lighten the notation of the spectrum. We follow the notation of [160] for ease of comparison, and quote the functions here for completeness.

These functions are associated with finite sums that we have used throughout the computation of the spectrum:

¹The term in c_D proportional to T_F does not appear in the result quoted in Ref. [67]. It is generated by the field redefinition that eliminates the operator GD^2G from the NRQCD Lagrangian, see the discussion in Ref. [43].

$$S_p(N) = \sum_{i=1}^N \frac{1}{i^p}, \quad S_{p,q}(N) = \sum_{i=1}^N \sum_{j=1}^i \frac{1}{i^p j^q}, \quad (\text{A.13})$$

$$\Delta S_{1a} = S_1(n+l) - S_1(n-l-1), \quad \Delta S_{1b} = S_1(n+l) - S_1(2l+1), \quad (\text{A.14})$$

$$\Sigma_a(n, l) = \Sigma_3^{(m)} + \Sigma_3^{(k)} + \frac{2}{n} \Sigma_2^{(k)}, \quad \Sigma_b(n, l) = \Sigma_2^{(m)} + \Sigma_2^{(k)} - \frac{2}{n} \Delta S_{1b}, \quad (\text{A.15})$$

$$\Sigma_p^{(m)}(n, l) = \frac{(n+l)!}{(n-l-1)!} \sum_{m=-l}^l \frac{R(l, m)}{(n+m)^p} S_1(n+m), \quad (\text{A.16})$$

$$\Sigma_p^{(k)}(n, l) = \frac{(n-l-1)!}{(n+l)!} \sum_{k=1}^{n-l-1} \frac{(k+2l)!}{(k-1)!(k+l-n)^p}, \quad (\text{A.17})$$

where

$$R(l, m) = \frac{(-1)^{l-m}}{(l+m)!(l-m)!}. \quad (\text{A.18})$$

These functions are present in the energy correction associated to the static potential:

$$\begin{aligned} \sigma(n, l) &= \frac{\pi^2}{64} - \frac{1}{16} S_2(n+l) + \frac{1}{8} \Sigma_2^{(k)} \\ &+ \frac{1}{2} \left(\frac{n}{2} \zeta(3) + \frac{\pi^2}{8} \left(1 - \frac{2n}{3} \Delta S_{1a} \right) - \frac{1}{2} S_2(n+l) + \frac{n}{2} \Sigma_a(n, l) \right), \end{aligned} \quad (\text{A.19})$$

$$\begin{aligned} \tau(n, l) &= \frac{3}{2} \zeta(5) n^2 - \frac{\pi^2}{8} \zeta(3) n^2 + \frac{\pi^4}{1440} n (5n \Delta S_{1a} - 4) \\ &- \frac{1}{4} \zeta(3) \left[(n \Delta S_{1a} - 2)^2 + n^2 \{ 2S_2(n+l) - S_2(n-l-1) \} + n - 4 \right] \\ &+ \frac{\pi^2}{12} \left[\frac{n}{2} \Delta S_{1a} \{ n S_2(n+l) + 1 \} + \frac{n^2}{2} S_3(n+l) - \frac{3}{4} - n^2 \Sigma_a(n, l) \right] \\ &- \frac{n^2}{2} S_{4,1}(n-l-1) + n S_{3,1}(n-l-1) + \frac{1}{4} S_2(n+l) + \frac{1}{2} S_3(n+l) \\ &+ \Sigma_{\tau,1}(n, l) + \Sigma_{\tau,2}(n, l) + \Sigma_{\tau,3}(n, l). \end{aligned} \quad (\text{A.20})$$

$$\begin{aligned} \Sigma_{\tau,1} &= -\frac{n^2(n+l)!}{4(n-l-1)!} \sum_{k=1}^{n-l-1} \frac{(k-1)! S_1(n-l-k)}{(k+2l)!(k+l-n)^4} + \frac{(n-l-1)!}{4(n+l)!} \sum_{k=1}^{n-l-1} \frac{(k+2l)!}{(k-1)!(k+l-n)^4} \\ &\times \left[(k+l-n)(2k+2l-n) \{ 2n S_2(n-l-k-1) - 1 \} \right. \\ &- 6 \left\{ (k+l-n)(2k+2l-n) + n \left(k+l - \frac{n}{3} \right) \right\} S_1(n-l-k-1) \\ &\left. + \{ 3(k+l-n)(2k+2l-n) + n(k+l) \} \{ S_1(k+2l) - S_1(n+l) \} \right], \end{aligned} \quad (\text{A.21})$$

$$\Sigma_{\tau,2} = \frac{n(n+l)!}{8(n-l-1)!} \sum_{m=-l}^l \frac{R(l, m)}{(n+m)^5}$$

$$\begin{aligned}
 & \times \left[4n(n+m)^2 S_{2,1}(n+m) - (4m+3n)(n+m)S_2(n+m) \right. \\
 & + S_1(n+m) \{ -2(n+m)^2 - 8n + 8(n+m)^2 S_1(2l+1) - 2n(n+m)S_1(l+m) \\
 & \left. - 2(4m+3n)(n+m)S_1(l+n) - (4m-n)(n+m)S_1(n+m) \} \right], \tag{A.22}
 \end{aligned}$$

$$\Sigma_{\tau,3} = n^2 \sum_{m=-l}^l \sum_{k=1}^{n-l-1} \frac{(k+2l)! S_1(n+m) R(l,m)}{(k-1)!(n+m)^2(k+l+m)} \left\{ \frac{1}{2(k+l-n)^2} - \frac{1}{n(n+m)} \right\}. \tag{A.23}$$

A.4 List of transformations from momentum to position space

Unlike the position space potential V_s , the momentum space potential \tilde{V}_s is a c-number, not an operator. It is defined as the matrix element

$$\tilde{V}_s \equiv \langle \mathbf{p}' | V_s | \mathbf{p} \rangle. \tag{A.24}$$

In this section we give a list of the different related spin-independent potential structures in d -dimensions.

\tilde{V}_s	V_s
$\frac{1}{k^n}$	$\mathcal{F}_n(r)$
1	$\delta^{(d)}(\mathbf{r}) = [p^i, [p^i, \mathcal{F}_2(r)]]$
$k^{2\epsilon}$	$[p^i, [p^i, \mathcal{F}_{2-2\epsilon}(r)]]$
$\frac{\mathbf{p}^2 + \mathbf{p}'^2}{k^2}$	$\{\mathcal{F}_2(r), \mathbf{p}^2\}$
$\frac{\mathbf{p}^2 + \mathbf{p}'^2}{k^2} k^{2\epsilon}$	$\{\mathcal{F}_{2-2\epsilon}(r), \mathbf{p}^2\}$
$\frac{(\mathbf{p}^2 - \mathbf{p}'^2)^2}{k^4} - 1$	$2\mathcal{F}_2(r)(1+2\epsilon)\frac{\mathbf{L}^2}{r^2} - 2\epsilon\{\mathcal{F}_2(r), \mathbf{p}^2\} + 2\epsilon[p^i, [p^i, \mathcal{F}_2(r)]]$
$\left(\frac{(\mathbf{p}^2 - \mathbf{p}'^2)^2}{k^4} - 1 \right) k^{2\epsilon}$	$2\mathcal{F}_{2-2\epsilon}(r)\frac{4\epsilon+1}{1-\epsilon}\frac{\mathbf{L}^2}{r^2} - 4\frac{\epsilon}{1-\epsilon}\{\mathcal{F}_{2-2\epsilon}(r), \mathbf{p}^2\} + 4\frac{\epsilon}{1-\epsilon}[p^i, [p^i, \mathcal{F}_{2-2\epsilon}(r)]]$
$\frac{(\mathbf{p}^2 - \mathbf{p}'^2)^2}{k^4}$	$2\mathcal{F}_2(r)(1+2\epsilon)\frac{\mathbf{L}^2}{r^2} - 2\epsilon\{\mathcal{F}_2(r), \mathbf{p}^2\} + (1+2\epsilon)[p^i, [p^i, \mathcal{F}_2(r)]]$
$\frac{(\mathbf{p}^2 - \mathbf{p}'^2)^2}{k^4} k^{2\epsilon}$	$2\mathcal{F}_{2-2\epsilon}(r)\frac{1+4\epsilon}{1-\epsilon}\frac{\mathbf{L}^2}{r^2} - 4\frac{\epsilon}{1-\epsilon}\{\mathcal{F}_{2-2\epsilon}(r), \mathbf{p}^2\} + \frac{1+3\epsilon}{1-\epsilon}[p^i, [p^i, \mathcal{F}_{2-2\epsilon}(r)]]$

We make use of the following definition:

$$\mathcal{F}_n(r) = \int \frac{d^d k}{(2\pi)^d} \frac{e^{-i\mathbf{k}\cdot\mathbf{r}}}{|\mathbf{k}|^n} = \frac{2^{-n}\pi^{-d/2}\Gamma(d/2 - n/2)}{r^{d-n}\Gamma(n/2)} \tag{A.25}$$

Appendix B

Feynman rules

B.1 Feynman rules for HBET

In this appendix we present the set of Feynman rules from the HBET Lagrangian that we have used in order to compute the FVCT, $T^{\mu\nu}$, including the Delta particle. First we quote the different vertices that play a role in our computation (Ref. [64]¹):

	$2ie g^{\mu\nu} (\delta^{ab} - \delta^{a3} \delta^{b3})$		$e\epsilon^{a3b} (q_1^\mu + q_2^\mu)$
	$\frac{ie}{2} (1 + \tau^3) v^\mu$		$\frac{g_A}{F_\pi} S \cdot q \tau^a$
	$ie \frac{g_A}{F_\pi} S^\mu \epsilon^{a3b} \tau^b$		$ie\eta^{ab} g^{\alpha\beta} v^\mu$

¹Note that, in contrast to the notation of the coupling b_1 in Ref. [64], we use the notation $b_{1F} = 2b_1$.

$$\begin{aligned}
 & i e \frac{b_{1F}}{m_p} \delta^{a3} \left(S \cdot k g^{\mu\beta} - S^\beta k^\mu \right) & \frac{g_{\pi N \Delta}}{F_\pi} \delta^{ab} q^\mu \\
 & -i e \frac{g_{\pi N \Delta}}{F_\pi} \epsilon^{a3b} \epsilon^\mu(k)
 \end{aligned}$$

where $\eta^{ab} = \frac{1}{2} (1 + \tau^3) \delta^{ab} - i \epsilon^{ab3}$. The values of the Wilson coefficients can be found in Eq. (3). Vertices and propagators in the muon line are the usual QED vertices, since the muon is still relativistic.

The propagators read (Refs. [64, 65]):

$$\begin{aligned}
 & -i \frac{g^{\mu\nu}}{q^2 + i\eta} & \frac{i}{v \cdot q + i\eta} \\
 & i \frac{\delta^{ab}}{q^2 - m^2 + i\eta} & -i \frac{P_{\alpha\beta}^{3/2} \xi_{3/2}^{ab}}{v \cdot p - \Delta + i\eta}
 \end{aligned}$$

where we define the spin operator $S_\mu = \frac{i}{2} \gamma_5 \sigma_{\mu\nu} v^\nu$ and the following functions,

$$\xi_{3/2}^{ab} = \delta^{ab} - \frac{1}{3} \tau^a \tau^b, \quad (\text{B.1})$$

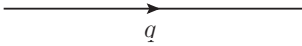
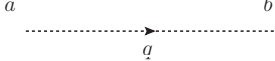
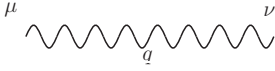
$$P_{\alpha\beta}^{3/2} = \frac{D-2}{D-1} (g_{\alpha\beta} - v_\alpha v_\beta) - \frac{2}{D-1} [S_\alpha, S_\beta]. \quad (\text{B.2})$$

These completes the set of HBET Feynman rules needed for our computation.

B.2 Feynman rules for NRQCD

In this appendix we present the set of NRQCD Feynman rules needed in order to compute the potential at N³leading order.

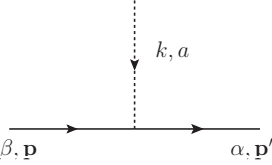
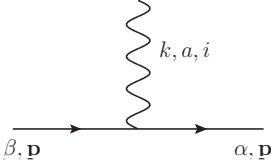
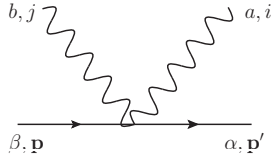
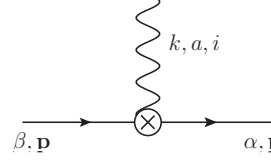
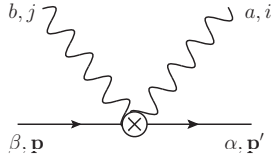
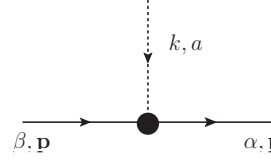
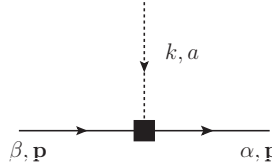
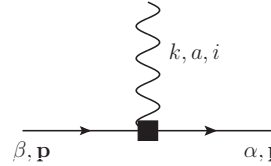
We start with the propagators. The propagator for particles ψ and antiparticles χ_c is the same.

	$\frac{i}{q_0 - \frac{\mathbf{q}^2}{2m} + i\eta} = \frac{i}{q_0 + i\eta} + \mathcal{O}\left(\frac{1}{m}\right)$
	$\frac{-i\delta^{ab}}{q^2 + i\eta}$ in FG, $\frac{i}{\mathbf{q}^2}\delta^{ab}$ in CG
	$\frac{i\delta^{ab}\delta^{ij}}{q^2 + i\eta}$ in FG, $\frac{i\delta^{ab}}{q^2 + i\eta}P^{ij}(\mathbf{q})$ in CG

where

$$P^{ij}(\mathbf{q}) = \delta^{ij} - \frac{q^i q^j}{\mathbf{q}^2}. \quad (\text{B.3})$$

We have used the following Feynman rules for the vertices:

	$-igT_{\alpha\beta}^a$		$\frac{ig}{2m}(p^i + p'^i)T_{\alpha\beta}^a$
	$-\frac{ig^2}{2m}\{T^a, T^b\}_{\alpha\beta}\delta^{ij}$		$\frac{c_F^{(x)}g}{2m_x}(\boldsymbol{\sigma} \times \mathbf{k})^i T_{\alpha\beta}^a$
	$\frac{c_F^{(x)}g^2}{2m_x}\epsilon^{ijk}\boldsymbol{\sigma}^k [T^a, T^b]_{\alpha\beta}$		$\frac{c_S^{(x)}g}{4m_x^2}\boldsymbol{\sigma} \cdot (\mathbf{p}' \times \mathbf{p}) T_{\alpha\beta}^a$
	$i\frac{c_D^{(x)}g}{8m_x^2}\mathbf{k}^2 T_{\alpha\beta}^a$		$-i\frac{c_D^{(x)}g}{8m_x^2}k_0 k^i T_{\alpha\beta}^a$

Appendix B. Feynman rules

All the momenta are taken to be incoming to the vertex. In CG the last vertex can be reduced to $-i \frac{c_D^{(x)} g^2}{4m_x^2} (p'^i - p^i) [T^a, T^b]_{\alpha\beta}$.

We use the NRQCD/NRQED convention for NR scattering amplitudes, where the antiquarks are treated as particles living in the anti-representation of $SU(3)$, i.e. the fermion flow (little arrows) of the antifermion is the same as for the fermion. The corresponding Feynman rules for the antifermion are then obtained by replacing $g \rightarrow -g$ and $T^a \rightarrow (T^a)^T$.

Finally, for the four-quark operators we get:

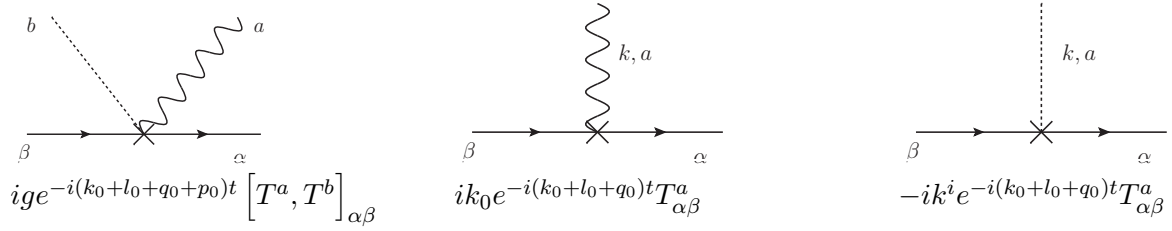
Throughout this work we project the states onto the singlet sector, i.e. $|s\rangle = \frac{1}{\sqrt{N_c}} \delta_{\alpha\alpha'}$, where α and α' are the indexes for the ingoing quarks. For the octet sector we would project onto $|o\rangle = \frac{1}{\sqrt{T_F}} \delta_{\alpha\alpha'}$.

B.3 Feynman rules for the matching with Wilson loops

In this appendix, we present a set of Feynman rules that can be used to calculate the soft contribution to Wilson-loop expectation values that contain insertions of the chromoelectric field $\mathbf{E}(t)$, diagrammatically. In our computation we use them regarding Eqs. (9.27) and (9.29).

Besides the standard set of (static) Feynman rules of NRQCD at leading order in $1/m$, the only additional Feynman rules needed for our computation are the following three vertices with an insertion of the chromo-electric field operator $\mathbf{E}^i(t)$.

B.3. Feynman rules for the matching with Wilson loops



The $\mathbf{E}^i(t)$ operator insertion is denoted by a cross in the diagram on a static quark line. Dotted and wavy lines represent A_0 and \mathbf{A} gluons, respectively. All momenta (k, l, q, p) are incoming. We again use the "NRQCD" convention for NR scattering amplitudes and so the corresponding Feynman rules for the antiquark are then obtained by replacing $g \rightarrow -g$ and $T^a \rightarrow (T^a)^T$.

Because of the explicit factors of t in the Wilson-loop expectation values (see e.g. Eqs. (9.27) and Eq. (9.29)) we are forced to retain the t dependence in the Feynman rules for $\mathbf{E}^i(t)$. As a consequence there is no energy conservation at these vertices, however three-momentum conservation is understood as usual.

Appendix C

Master integrals

C.1 Master integrals in HBET

The integrals presented in this Appendix are related to those presented in Refs. [64,65]. Here we give the full D -dependence of the functions in terms of which the integrals are decomposed.

$$\int \frac{d^D l}{(2\pi)^D} \frac{\{1, l_\mu, l_\mu l_\nu, l_\mu l_\nu l_\alpha, l_\mu l_\nu l_\alpha l_\beta\}}{(v \cdot l - q_0 - i\eta)(l^2 - m^2 + i\eta)} =$$

$$-i\{J_0(q_0, m), v_\mu J_1(q_0, m), g_{\mu\nu} J_2(q_0, m) + v_\mu v_\nu J_3(q_0, m),$$

$$(g_{\mu\nu} v_\alpha + g_{\mu\alpha} v_\nu + g_{\nu\alpha}) v_\mu J_4(q_0, m) + v_\mu v_\nu v_\alpha J_5(q_0, m),$$

$$(g_{\mu\nu} g_{\alpha\beta} + g_{\mu\alpha} g_{\nu\beta} + g_{\nu\alpha} g_{\mu\beta}) J_6(q_0, m) + (g_{\mu\nu} v_\alpha v_\beta$$

$$+ g_{\mu\alpha} v_\nu v_\beta + g_{\mu\beta} v_\nu v_\alpha + g_{\nu\alpha} v_\mu v_\beta) + g_{\alpha\beta} v_\mu v_\nu\} J_7(q_0, m) + \dots\}, \quad (\text{C.1})$$

where we can express all the J -functions in terms of the D -dimensional integrations:

$$\mathcal{D}_\pi(m) = m^{D-2} (4\pi)^{-D/2} \Gamma\left(1 - \frac{D}{2}\right), \quad (\text{C.2})$$

$$J_0(q_0, m) = \frac{2}{(4\pi)^{D/2}} \Gamma\left(2 - \frac{D}{2}\right) \int_{-q_0}^{\infty} dy \frac{1}{(m^2 - q_0^2 + y^2)^{2-D/2}}$$

$$= \begin{cases} \frac{2(-q_0)^{D-3} \Gamma\left(2 - \frac{D}{2}\right) {}_2F_1\left(\frac{3-D}{2}, 2 - \frac{D}{2}; \frac{5-D}{2}; 1 - \frac{m^2}{q_0^2}\right)}{(4\pi)^{D/2} (D-3)} & |q_0| < m, \\ i^{-D} q_0 (q_0^2 - m^2)^{\frac{D}{2}-2} {}_2F_1\left(\frac{1}{2}, 2 - \frac{D}{2}; \frac{3}{2}; \frac{q_0^2}{q_0^2 - m^2}\right) & \\ \frac{i^{1-D} \left(\sqrt{\pi} \Gamma\left(\frac{3}{2} - \frac{D}{2}\right)\right) (q_0^2 - m^2)^{\frac{D-3}{2}}}{2\Gamma\left(2 - \frac{D}{2}\right)} & q_0 < -m, \end{cases} \quad (\text{C.3})$$

$$\quad (\text{C.4})$$

since we will also want the renormalized result we give the results also expanded in $D = 4 + 2\epsilon$:

$$\mathcal{D}_\pi(m) = \frac{m^2}{16\pi^2} \tilde{L} + \mathcal{O}(\epsilon), \quad (\text{C.5})$$

$$J_0(q_0, m) = \begin{cases} \frac{q_0}{8\pi^2}(1 - \tilde{L}) - \frac{1}{4\pi^2} \sqrt{m^2 - q_0^2} \cos^{-1} \frac{-q_0}{m} + \mathcal{O}(\epsilon) & |q_0| < m, \quad (\text{C.6}) \\ \frac{q_0}{8\pi^2}(1 - \tilde{L}) + \frac{\sqrt{q_0^2 - m^2}}{4\pi^2} \ln \left(\frac{\sqrt{q_0^2 - m^2} - q_0}{m} \right) + \mathcal{O}(\epsilon) & q_0 < -m, \quad (\text{C.7}) \end{cases}$$

where

$$\tilde{L} = \mu^{2\epsilon} \left(\frac{1}{\epsilon} + (\gamma_E - 1 - \ln 4\pi) \right) + \ln \left(\frac{m^2}{\mu^2} \right). \quad (\text{C.8})$$

All the other functions are related to Eqs. (C.7)/(C.6) and (C.5) by:

$$J_1(q_0, m) = q_0 J_0(q_0, m) + \mathcal{D}_\pi(m), \quad (\text{C.9})$$

$$J_2(q_0, m) = \frac{1}{D-1} ((m^2 - q_0^2) J_0(q_0, m) - q_0 \mathcal{D}_\pi(m)), \quad (\text{C.10})$$

$$J_3(q_0, m) = q_0 J_1(q_0, m) - J_2(q_0, m), \quad (\text{C.11})$$

$$J_4(q_0, m) = q_0 J_2(q_0, m) + \frac{m^2}{D} \mathcal{D}_\pi(m), \quad (\text{C.12})$$

$$J_5(q_0, m) = q_0 J_3(q_0, m) - 2J_4(q_0, m), \quad (\text{C.13})$$

$$J_6(q_0, m) = \frac{1}{D+1} \left((m^2 - q_0^2) J_2(q_0, m) - \frac{m^2 q_0}{d} \mathcal{D}_\pi(m) \right), \quad (\text{C.14})$$

$$J_7(q_0, m) = m^2 J_2(q_0, m) + (D+2) J_6(q_0, m). \quad (\text{C.15})$$

We also define the derivative function which we use in our computation

$$J_i^{(n)}(q_0, m) = \frac{\partial^n}{\partial (m^2)^n} J_i(q_0, m). \quad (\text{C.16})$$

C.2 Master integrals for NRQCD in the Coulomb gauge

First we have computed the following master integrals in $d = D - 1$ dimensions in Euclidean space:

$$\int \frac{d^d q}{(2\pi)^d} \frac{\{1, q^i, q^i q^j, q^i, q^j, q^l\}}{(\mathbf{q}^2)^r ((\mathbf{q} - \mathbf{k})^2)^s} = \{I_1(r, s, \mathbf{k}), I_2^i(r, s, \mathbf{k}), I_3^{ij}(r, s, \mathbf{k}), I_4^{ijl}(r, s, \mathbf{k})\}, \quad (\text{C.17})$$

where we find:

$$I_1(r, s, \mathbf{k}) = \left(\frac{\mathbf{k}^2}{4\pi}\right)^{\frac{d}{2}} \left(\frac{1}{\mathbf{k}^2}\right)^{r+s} \frac{\Gamma\left(\frac{d}{2}-r\right)\Gamma\left(\frac{d}{2}-s\right)\Gamma\left(r+s-\frac{d}{2}\right)}{\Gamma(r)\Gamma(s)\Gamma(d-r-s)}, \quad (\text{C.18})$$

$$I_2^i(r, s, \mathbf{k}) = k^i \left(\frac{\mathbf{k}^2}{4\pi}\right)^{\frac{d}{2}} \left(\frac{1}{\mathbf{k}^2}\right)^{r+s} \frac{\Gamma\left(\frac{d}{2}-r+1\right)\Gamma\left(\frac{d}{2}-s\right)\Gamma\left(r+s-\frac{d}{2}\right)}{\Gamma(r)\Gamma(s)\Gamma(d-r-s+1)}, \quad (\text{C.19})$$

$$I_3^{ij}(r, s, \mathbf{k}) = \left(\frac{\mathbf{k}^2}{4\pi}\right)^{\frac{d}{2}} \left(\frac{1}{\mathbf{k}^2}\right)^{r+s} \left\{ k^i k^j \frac{\Gamma\left(\frac{d}{2}-r+2\right)\Gamma\left(\frac{d}{2}-s\right)\Gamma\left(r+s-\frac{d}{2}\right)}{\Gamma(r)\Gamma(s)\Gamma(d-r-s+2)} \right. \\ \left. + \delta^{ij} \frac{\mathbf{k}^2}{2} \frac{\Gamma\left(\frac{d}{2}-r+1\right)\Gamma\left(\frac{d}{2}-s+1\right)\Gamma\left(r+s-\frac{d}{2}-1\right)}{\Gamma(r)\Gamma(s)\Gamma(d-r-s+2)} \right\}, \quad (\text{C.20})$$

$$I_4^{ijkl}(r, s, \mathbf{k}) = \left(\frac{\mathbf{k}^2}{4\pi}\right)^{d/2} \left(\frac{1}{\mathbf{k}^2}\right)^{r+s} \left\{ k^i k^j k^l \frac{\Gamma\left(\frac{d}{2}-r+3\right)\Gamma\left(\frac{d}{2}-s\right)\Gamma\left(-\frac{d}{2}+r+s\right)}{\Gamma(r)\Gamma(s)\Gamma(d-r-s+3)} \right. \\ \left. + \mathbf{k}^2 (k^l \delta^{ij} + k^j \delta^{il} + k^i \delta^{jl}) \frac{\Gamma\left(\frac{d}{2}-r+2\right)\Gamma\left(\frac{d}{2}-s+1\right)\Gamma\left(-\frac{d}{2}+r+s-1\right)}{2\Gamma(r)\Gamma(s)\Gamma(d-r-s+3)} \right\}, \quad (\text{C.21})$$

and

$$\int \frac{dq^d}{(2\pi)^d} \frac{(\mathbf{q}^2)^s}{(\mathbf{q}^2 + m^2)^r} = I_5(r, s, \mathbf{k}, m^2) = \left(\frac{m^2}{4\pi}\right)^{\frac{d}{2}} (m^2)^{s-r} \frac{\Gamma\left(\frac{d}{2}+s\right)\Gamma\left(r-s-\frac{d}{2}\right)}{\Gamma(r)\Gamma\left(\frac{d}{2}\right)}. \quad (\text{C.22})$$

Now we can compute the following integrals in D -dimensions in terms of the previous master integrals (to the order of our interest in the loop integrals $k_0 \sim 0$). To do so we first perform the integration in the 0-component of the loop momentum:

$$\int \frac{dq^D}{(2\pi)^D} \frac{\{1, q^i, q^i q^j, q^i q^j q^l\}}{(q_0^2 - \mathbf{q}^2 + i\eta)(\mathbf{q} - \mathbf{k})^2 \mathbf{q}^{2n}} = \quad (\text{C.23}) \\ - \frac{i}{2} \{I_1(1/2+n, 1, \mathbf{k}), I_2^i(1/2+n, 1, \mathbf{k}), I_3^{ij}(1/2+n, 1, \mathbf{k}), I_4^{ijkl}(1/2+n, 1, \mathbf{k})\}.$$

Note that the following relation holds $\delta^{ij} I_3^{ij}(n, 1, \mathbf{k}) = I_1(n-1, 1, \mathbf{k})$.

$$\int \frac{dq^D}{(2\pi)^D} \frac{\{1, q^i, q^i q^j, q^i q^j q^l\}}{(\mathbf{q} - \mathbf{k})^2 \mathbf{q}^2 (q_0^2 - (\mathbf{q} - \mathbf{k})^2 + i\eta) q_0^2} = \quad (\text{C.24}) \\ - \frac{i}{2} \{I_1(1, 5/2, \mathbf{k}), I_2^i(1, 5/2, \mathbf{k}), I_3^{ij}(1, 5/2, \mathbf{k}), I_4^{ijkl}(1, 5/2, \mathbf{k})\}.$$

Some other useful integrals in terms of Feynman parameters are:

$$\int \frac{dq^D}{(2\pi)^D} \frac{\{1, q^i, q^i q^j\}}{(q_0^2 - \mathbf{q}^2 + i\eta)(q_0^2 - (\mathbf{q} - \mathbf{k})^2 + i\eta)} = \quad (\text{C.25}) \\ \frac{i}{4} \int_0^1 dz \left\{ I_5(3/2, 0, \mathbf{k}, \Delta_1^2), k^i z I_5(3/2, 0, \mathbf{k}, \Delta_1^2), \frac{\delta^{ij}}{d} I_5(3/2, 1, \mathbf{k}, \Delta_1^2) + k^i k^j z^2 I_5(3/2, 0, \mathbf{k}, \tilde{m}^2) \right\},$$

where $\Delta_1^2 = \mathbf{k}^2 z(1-z)$.

$$\begin{aligned}
 \int \frac{dq^D}{(2\pi)^D} \frac{\{1, q^i, q^i q^j, q^i q^j q^n\}}{(q_0^2 - \mathbf{q}^2 + i\eta)(q_0^2 - (\mathbf{q} - \mathbf{k})^2 + i\eta)\mathbf{q}^2} = & \quad (C.26) \\
 i \frac{3}{8} \int_0^1 dz \int_0^1 ds \sqrt{s} \left\{ I_5(5/2, 0, \mathbf{k}, \Delta_2^2), k^i z s I_5(5/2, 0, \mathbf{k}, \Delta_2^2), \right. \\
 \frac{\delta^{ij}}{d} I_5(5/2, 1, \mathbf{k}, \Delta_2^2) + s^2 z^2 k^i k^j I_5(5/2, 0, \mathbf{k}, \Delta_2^2), \\
 \left. s^3 z^3 k^i k^j k^n I_5(5/2, 0, \mathbf{k}, \Delta_2^2) + \frac{s z}{d} (k^i \delta^{jn} + k^j \delta^{in} + k^n \delta^{ij}) I_5(5/2, 1, \mathbf{k}, \Delta_2^2) \right\},
 \end{aligned}$$

where $\Delta_2^2 = \mathbf{k}^2 s z (1 - s z)$.

$$\begin{aligned}
 \int \frac{dq^D}{(2\pi)^D} \frac{\{1, q^i, q^i q^j\}}{(q_0^2 - \mathbf{q}^2 + i\eta)(q_0^2 - (\mathbf{q} - \mathbf{k})^2 + i\eta)\mathbf{q}^2(\mathbf{q} - \mathbf{k})^2} = & \quad (C.27) \\
 \frac{15}{16} \int_0^1 dz \int_0^1 dt \int_0^1 ds s \sqrt{1-s} \left\{ I_5(7/2, 0, \mathbf{k}, \Delta_3^2), k^i (z - s(t + z - 1)) I_5(7/2, 0, \mathbf{k}, \Delta_3^2), \right. \\
 \left. \frac{\delta^{ij}}{d} I_5(7/2, 1, \mathbf{k}, \Delta_3^2) + (z - s(t + z - 1))^2 k^i k^j I_5(7/2, 0, \mathbf{k}, \Delta_3^2) \right\},
 \end{aligned}$$

where $\Delta_3^2 = \mathbf{k}^2 (z - s(t + z - 1))(s(t + z - 1) - z + 1)$.

Appendix D

HBET amplitudes

Throughout our HBET computations we use the normalization $\bar{u}(p)u(p) = 2m_p$ and we define $\Delta = m_\Delta - m_p$. In what follows $\tilde{m}^2 = m_\pi^2 - q^2x(1-x)$ and the function Z has been defined in Eq. (3.45). We work in the rest frame where $v = (1, \mathbf{0})$.

D.1 Pion loops

Here we collect the amplitudes of all the diagrams contributing to the proton polarizability through a loop of pions, represented in Fig. 3.1, plus the ones with a crossed photon lines or permutations, which are assumed to be implicit in the representation. For all the diagrams here we consider the overall factor $\mathcal{A} = 2m_p \frac{g_A^2}{F_\pi^2}$. The J -functions are defined in Appendix C.1, and in this case the computation for J_0 in Eq. (C.3) applies. Diagrams with only one pion are zero due to the fact that we are working in the static limit.

$$\mathcal{M}_1^{\mu\nu} = \mathcal{A} g^{\mu\nu} h_0(q^2, q_0), \quad (\text{D.1})$$

$$\mathcal{M}_2^{\mu\nu} = \mathcal{A} \left\{ h_1(q^2, q_0)(g^{\mu\nu} - v^\mu v^\nu) + h_2(q^2, q_0) i \epsilon^{\mu\nu\alpha\beta} v_\alpha S_\beta \right\}, \quad (\text{D.2})$$

$$\mathcal{M}_3^{\mu\nu} = \mathcal{A} \left\{ h_3(q^2, q_0) g^{\mu\nu} + h_4(q^2, q_0) q^\mu q^\nu + h_5(q^2, q_0)(q^\mu v^\nu + v^\mu q^\nu) + h_6(q^2, q_0) v^\mu v^\nu \right\}, \quad (\text{D.3})$$

$$\begin{aligned} \mathcal{M}_4^{\mu\nu} = \mathcal{A} \left\{ h_7(q^2, q_0) g^{\mu\nu} + h_8(q^2, q_0) q^\mu q^\nu + h_9(q^2, q_0) v^\nu v^\mu + h_{10}(q^2, q_0)(q^\mu v^\nu + q^\nu v^\mu) \right. \\ \left. + h_{13}(q^2, q_0) i(\epsilon^{\mu\lambda\alpha\beta} v^\nu - \epsilon^{\nu\lambda\alpha\beta} v^\mu) q_\lambda S_\beta v_\alpha + h_{11}(q^2, q_0) i \epsilon^{\mu\nu\alpha\beta} S_\beta v_\alpha \right. \\ \left. + h_{12}(q^2, q_0) i(\epsilon^{\mu\lambda\alpha\beta} q^\nu - \epsilon^{\nu\lambda\alpha\beta} q^\mu) q_\lambda S_\beta v_\alpha \right\}, \end{aligned} \quad (\text{D.4})$$

$$\begin{aligned} \mathcal{M}_5^{\mu\nu} = \mathcal{A} \left\{ h_{14}(q^2, q_0) v^\mu v^\nu + h_{15}(q^2, q_0)(q^\mu v^\nu + q^\nu v^\mu) \right. \\ \left. + h_{16}(q^2, q_0) i(\epsilon^{\mu\lambda\alpha\beta} v^\nu - \epsilon^{\nu\lambda\alpha\beta} v^\mu) q_\lambda S_\beta v_\alpha \right\}, \end{aligned} \quad (\text{D.5})$$

$$\mathcal{M}_6^{\mu\nu} = \mathcal{A} h_{17}(q^2, q_0) v^\mu v^\nu, \quad (\text{D.6})$$

$$\mathcal{M}_7^{\mu\nu} = \mathcal{A} h_{18}(q^2, q_0) v^\mu v^\nu, \quad (\text{D.7})$$

$$\mathcal{M}_8^{\mu\nu} = \mathcal{A} h_{19}(q^2, q_0) v^\mu v^\nu, \quad (\text{D.8})$$

where the h functions read:

$$h_0(q^2, q_0) = -J_0(0, m_\pi) - m_\pi^2 J'_0(0, m_\pi), \quad (\text{D.9})$$

$$h_1(q^2, q_0) = \frac{1}{2} \left(J_0(q_0, m_\pi^2) + J_0(-q_0, m_\pi^2) \right), \quad (\text{D.10})$$

$$h_2(q^2, q_0) = -J_0(q_0, m_\pi^2) + J_0(-q_0, m_\pi^2), \quad (\text{D.11})$$

$$h_3(q^2, q_0) = 2 \int_0^1 dx (1-x) \left\{ (D+1) \left(J_6''(q_0x, \tilde{m}^2) + J_6''(-q_0x, \tilde{m}^2) \right) - x^2 \mathbf{q}^2 \left(J_2''(q_0x, \tilde{m}^2) + J_2''(-q_0x, \tilde{m}^2) \right) \right\}, \quad (\text{D.12})$$

$$h_4(q^2, q_0) = \frac{1}{2} \int_0^1 dx (1-x)(2x-1) \left\{ (D(2x-1) + 6x+1) \left(J_2''(q_0x, \tilde{m}^2) + J_2''(-q_0x, \tilde{m}^2) \right) - (2x-1)x^2 \mathbf{q}^2 \left(J_0''(q_0x, \tilde{m}^2) + J_0''(-q_0x, \tilde{m}^2) \right) \right\}, \quad (\text{D.13})$$

$$h_5(q^2, q_0) = \int_0^1 dx (1-x) \left\{ (-2Dx + D - 2x - 1) \left(J_4''(q_0x, \tilde{m}^2) - J_4''(-q_0x, \tilde{m}^2) \right) + x(2x-1) \left(x \mathbf{q}^2 \left(J_1''(q_0x, \tilde{m}^2) - J_1''(-q_0x, \tilde{m}^2) \right) - 2q_0 \left(J_2''(q_0x, \tilde{m}^2) + J_2''(-q_0x, \tilde{m}^2) \right) \right) \right\}, \quad (\text{D.14})$$

$$h_6(q^2, q_0) = 2 \int_0^1 dx (1-x) \left\{ (D-1) \left(J_7''(q_0x, \tilde{m}^2) + J_7''(-q_0x, \tilde{m}^2) \right) + x \left(-x \mathbf{q}^2 \left(J_3''(q_0x, \tilde{m}^2) + J_3''(-q_0x, \tilde{m}^2) \right) + 4q_0 \left(J_4''(q_0x, \tilde{m}^2) - J_4''(-q_0x, \tilde{m}^2) \right) - 2 \left(J_6''(q_0x, \tilde{m}^2) + J_6''(-q_0x, \tilde{m}^2) \right) \right) \right\}, \quad (\text{D.15})$$

$$h_7(q^2, q_0) = -2 \int_0^1 dx \left\{ J_2'(q_0x, \tilde{m}^2) + J_2'(-q_0x, \tilde{m}^2) \right\}, \quad (\text{D.16})$$

$$h_8(q^2, q_0) = \int_0^1 dx x(1-2x) \left\{ J_0'(q_0x, \tilde{m}^2) + J_0'(-q_0x, \tilde{m}^2) \right\}, \quad (\text{D.17})$$

$$h_9(q^2, q_0) = 2 \int_0^1 dx \left\{ -q_0x \left(J_1'(q_0x, \tilde{m}^2) - J_1'(-q_0x, \tilde{m}^2) \right) + J_2'(q_0x, \tilde{m}^2) + J_2'(-q_0x, \tilde{m}^2) \right\}, \quad (\text{D.18})$$

$$h_{10}(q^2, q_0) = \int_0^1 dx x \left\{ \frac{q_0}{2} (2x-1) \left(J_0'(q_0x, \tilde{m}^2) + J_0'(-q_0x, \tilde{m}^2) \right) + J_1'(q_0x, \tilde{m}^2) - J_1'(-q_0x, \tilde{m}^2) \right\}, \quad (\text{D.19})$$

$$h_{11}(q^2, q_0) = 4 \int_0^1 dx \left\{ J_2'(q_0x, \tilde{m}^2) - J_2'(-q_0x, \tilde{m}^2) \right\}, \quad (\text{D.20})$$

$$h_{12}(q^2, q_0) = - \int_0^1 dx x(1-2x) \left\{ J_0'(q_0x, \tilde{m}^2) - J_0'(-q_0x, \tilde{m}^2) \right\}, \quad (\text{D.21})$$

$$h_{13}(q^2, q_0) = -2 \int_0^1 dx x \left\{ J_1'(q_0x, \tilde{m}^2) + J_1'(-q_0x, \tilde{m}^2) \right\}, \quad (\text{D.22})$$

$$h_{14}(q^2, q_0) = \frac{2}{q_0} \int_0^1 dx \left\{ (D-1) \left(J_4'(q_0x, \tilde{m}^2) - J_4'(-q_0x, \tilde{m}^2) \right) + \mathbf{q}^2 (1-x)x \left(J_1'(q_0x, \tilde{m}^2) - J_1'(-q_0x, \tilde{m}^2) \right) - q_0(1-2x) \left(J_2'(q_0x, \tilde{m}^2) + J_2'(-q_0x, \tilde{m}^2) \right) \right\}, \quad (\text{D.23})$$

$$h_{15}(q^2, q_0) = \frac{1}{2q_0} \int_0^1 dx (1-2x) \left\{ (D+1) \left(J_2'(q_0x, \tilde{m}^2) + J_2'(-q_0x, \tilde{m}^2) \right) \right\}$$

$$+ \mathbf{q}^2 x(1-x) \left(J'_0(q_0 x, \tilde{m}^2) + J'_0(-q_0 x, \tilde{m}^2) \right) \}, \quad (\text{D.24})$$

$$h_{16}(q^2, q_0) = -\frac{2}{q_0} \int_0^1 dx \left\{ J'_2(q_0 x, \tilde{m}^2) - J'_2(-q_0 x, \tilde{m}^2) \right\}, \quad (\text{D.25})$$

$$h_{17}(q^2, q_0) = -2 \frac{D-1}{4} \frac{1}{q_0^2} \left(-2J_2(0, m_\pi^2) + J_2(-q_0, m_\pi^2) + J_2(q_0, m_\pi^2) \right), \quad (\text{D.26})$$

$$h_{18}(q^2, q_0) = 3 \frac{D-1}{4} \frac{1}{q_0^2} \left(J_2(q_0, m_\pi^2) + J_2(-q_0, m_\pi^2) - \left(J_2(0, m^2) + J_2(0, m_\pi^2) \right) \right), \quad (\text{D.27})$$

$$h_{19}(q^2, q_0) = \frac{D-1}{4} \frac{1}{q_0} \left(\frac{1}{q_0} \left(J_2(q_0, m_\pi^2) + J_2(-q_0, m_\pi^2) - 2J_2(0, m_\pi^2) \right) \right). \quad (\text{D.28})$$

For $D = 4 + 2\epsilon$ dimensions we obtain:

$$h_0(q^2, q_0) = \frac{3m_\pi}{16\pi} + \mathcal{O}(\epsilon), \quad (\text{D.29})$$

$$h_1(q^2, q_0) = -\frac{\sqrt{m_\pi^2 - q_0^2}}{8\pi} + \mathcal{O}(\epsilon), \quad (\text{D.30})$$

$$h_2(q^2, q_0) = \frac{1}{4\pi^2} q_0 \tilde{L} + \frac{1}{4\pi^2} \left(2\sqrt{m_\pi^2 - q_0^2} \sin^{-1} \left(\frac{q_0}{m_\pi} \right) - q_0 \right) + \mathcal{O}(\epsilon), \quad (\text{D.31})$$

$$h_3(q^2, q_0) = \frac{1}{16\pi} \left(\frac{(6m_\pi^2 q^2 - 8m_\pi^2 q_0^2 - q^4) \mathcal{I}_1 - \frac{m_\pi}{\mathbf{q}^2} \sqrt{1 - \frac{q_0^2}{m_\pi^2}} (2m_\pi^2 - q^2 + 2q_0^2)}{2\mathbf{q}^2 \sqrt{\mathbf{q}^2}} \right) + \frac{m_\pi (2m_\pi^2 + q^2)}{\mathbf{q}^2} + \mathcal{O}(\epsilon), \quad (\text{D.32})$$

$$h_4(q^2, q_0) = \frac{-1}{16\pi} \left(\frac{(-6m_\pi^2 (q^2 - 2q_0^2) + q^4 + 2q_0^4) (4m_\pi^2 (q_0^2 - q^2) + q^4) \mathcal{I}_1}{2\mathbf{q}^4 \sqrt{\mathbf{q}^2} (4m_\pi^2 \mathbf{q}^2 + q^4)} \right. \\ \left. + \frac{m_\pi (16m_\pi^4 (q^2 - q_0^2) - 2m^2 (6q^4 - 16q^2 q_0^2 + 13q_0^4) + q^2 (2q^4 - 6q^2 q_0^2 + q_0^4))}{\mathbf{q}^4 (4m_\pi^2 \mathbf{q}^2 + q^4)} \right. \\ \left. + \frac{(m_\pi (16m_\pi^4 (q_0^2 - q^2) + m_\pi^2 (10q_0^4 - 4q^2 q_0^2) + q^6 + 2q^4 q_0^2))}{\mathbf{q}^4 (4m_\pi^2 \mathbf{q}^2 + q^4)} \sqrt{1 - \frac{q_0^2}{m_\pi^2}} \right) + \mathcal{O}(\epsilon), \quad (\text{D.33})$$

$$h_5(q^2, q_0) = \frac{1}{16\pi} \left(-\frac{m_\pi q_0 (16m_\pi^4 \mathbf{q}^2 - 6m_\pi^2 q_0^2 (q^2 - 2q_0^2) + q^6 + 2q^4 q_0^2)}{\mathbf{q}^4 (4m_\pi^2 \mathbf{q}^2 + q^4)} \right. \\ \left. + \frac{q_0 (m_\pi^2 (10q_0^2 - 4q^2) + q^4 + 2q^2 q_0^2) \mathcal{I}_1}{2\mathbf{q}^4 \sqrt{\mathbf{q}^2}} \right. \\ \left. + \frac{(m_\pi q_0 (16m_\pi^4 \mathbf{q}^2 + m_\pi^2 (14q^2 q_0^2 - 8q^4) + 3q^6))}{\mathbf{q}^4 (4m_\pi^2 \mathbf{q}^2 + q^4)} \sqrt{1 - \frac{q_0^2}{m_\pi^2}} \right) + \mathcal{O}(\epsilon), \quad (\text{D.34})$$

$$h_6(q^2, q_0) = \frac{1}{16\pi} \left(-\frac{q^2 (-6m_\pi^2 (q^2 - 2q_0^2) + q^4 + 2q^2 q_0^2) \mathcal{I}_1}{2\mathbf{q}^4 \sqrt{\mathbf{q}^2}} \right. \\ \left. + \frac{m_\pi (8m_\pi^4 (q_0^4 - q^4) - 2m_\pi^2 (q^6 + 2q^4 q_0^2 - 6q^2 q_0^4) + q^8 + 2q^6 q_0^2)}{\mathbf{q}^4 (4m_\pi^2 \mathbf{q}^2 + q^4)} \right. \\ \left. + \frac{(m_\pi (8m_\pi^4 (q^4 - q_0^4) + m_\pi^2 (-6q^6 + 32q^4 q_0^2 - 48q^2 q_0^4 + 16q_0^6) + q^8 - 8q^6 q_0^2 + 4q^4 q_0^4))}{\mathbf{q}^4 (4m_\pi^2 \mathbf{q}^2 + q^4)} \right)$$

$$\sqrt{1 - \frac{q_0^2}{m_\pi^2}} + \mathcal{O}(\epsilon), \quad (\text{D.35})$$

$$h_7(q^2, q_0) = \frac{1}{16\pi} \left(\frac{(4m_\pi^2 \mathbf{q}^2 + q^4)}{2\mathbf{q}^2 \sqrt{\mathbf{q}^2}} \mathcal{I}_1 - \frac{\sqrt{1 - \frac{q_0^2}{m_\pi^2}} (m_\pi (q^2 - 2q_0^2))}{\mathbf{q}^2} - \frac{m_\pi q^2}{\mathbf{q}^2} \right) + \mathcal{O}(\epsilon), \quad (\text{D.36})$$

$$h_8(q^2, q_0) = \frac{1}{16\pi} \left(\frac{(4m_\pi^2 \mathbf{q}^2 + q^4 + 2q^2 q_0^2)}{2\mathbf{q}^4 \sqrt{\mathbf{q}^2}} \mathcal{I}_1 + \frac{3m_\pi q^2 \sqrt{1 - \frac{q_0^2}{m_\pi^2}}}{\mathbf{q}^4} - \frac{m_\pi (q^2 + 2q_0^2)}{\mathbf{q}^4} \right) + \mathcal{O}(\epsilon), \quad (\text{D.37})$$

$$h_9(q^2, q_0) = \frac{1}{16\pi} \left(\frac{(4m_\pi^2 q^2 \mathbf{q}^2 + q^6 + 2q^4 q_0^2)}{2\mathbf{q}^4 \sqrt{\mathbf{q}^2}} \mathcal{I}_1 - \frac{m_\pi (q^4 - 8q^2 q_0^2 + 4q_0^4)}{\mathbf{q}^4} \sqrt{1 - \frac{q_0^2}{m_\pi^2}} - \frac{m_\pi q^2 (q^2 + 2q_0^2)}{\mathbf{q}^4} \right) + \mathcal{O}(\epsilon), \quad (\text{D.38})$$

$$h_{10}(q^2, q_0) = \frac{1}{16\pi} \left(-\frac{q_0 (4m_\pi^2 \mathbf{q}^2 + q^2 (2q^2 + q_0^2))}{2\mathbf{q}^4 \sqrt{\mathbf{q}^2}} \mathcal{I}_1 + \frac{\sqrt{1 - \frac{q_0^2}{m_\pi^2}} (m_\pi q_0 (q_0^2 - 4q^2))}{\mathbf{q}^4} + \frac{m_\pi q_0 (2q^2 + q_0^2)}{\mathbf{q}^4} \right) + \mathcal{O}(\epsilon), \quad (\text{D.39})$$

$$h_{11}(q^2, q_0) = -\frac{1}{4\pi^2} q_0 \tilde{L} + \frac{q_0}{4\pi^2} + \frac{-1}{2\pi^2} \left(2\sqrt{\tilde{m}^2 - q_0^2 x^2} \sin^{-1} \left(\frac{q_0 x}{\sqrt{\tilde{m}^2}} \right) + q_0 x \ln \left(\frac{\tilde{m}^2}{m_\pi^2} \right) \right) + \mathcal{O}(\epsilon), \quad (\text{D.40})$$

$$h_{12}(q^2, q_0) = \frac{1}{4\pi^2} \int_0^1 dx x (1 - 2x) \frac{\sin^{-1} \left(\frac{q_0 x}{\sqrt{\tilde{m}^2}} \right)}{\sqrt{\tilde{m}^2 - q_0^2 x^2}} + \mathcal{O}(\epsilon), \quad (\text{D.41})$$

$$h_{13}(q^2, q_0) = \frac{-1}{8\pi^2} \tilde{L} - \frac{1}{8\pi^2} - \frac{1}{4\pi^2} \int_0^1 dx x \left\{ \ln \left(\frac{\tilde{m}^2}{m_\pi^2} \right) - \frac{2q_0 x \sin^{-1} \left(\frac{q_0 x}{\sqrt{\tilde{m}^2}} \right)}{\sqrt{\tilde{m}^2 - q_0^2 x^2}} \right\} + \mathcal{O}(\epsilon), \quad (\text{D.42})$$

$$h_{14}(q^2, q_0) = \frac{1}{16\pi} \frac{q^2}{(\mathbf{q}^2)^{3/2}} (2m_\pi^2 - q^2) \mathcal{I}_1 - \frac{1}{8\pi} \frac{m_\pi}{\mathbf{q}^2} (2m_\pi^2 - q^2) + \frac{1}{8\pi} \frac{m_\pi}{\mathbf{q}^2} (2m_\pi^2 + q^2 - 2q_0^2) \sqrt{1 - \frac{q_0^2}{m_\pi^2}} + \mathcal{O}(\epsilon), \quad (\text{D.43})$$

$$h_{15}(q^2, q_0) = -\frac{1}{32\pi} \frac{2m_\pi^2 - q^2}{\mathbf{q}^2 \sqrt{\mathbf{q}^2}} q_0 \mathcal{I}_1 - \frac{1}{16\pi} \frac{m_\pi}{q_0 \mathbf{q}^2} (2m_\pi^2 - q_0^2) \left(\sqrt{1 - \frac{q_0^2}{m_\pi^2}} - 1 \right) + \mathcal{O}(\epsilon), \quad (\text{D.44})$$

$$h_{16}(q^2, q_0) = \frac{1}{8\pi^2} \tilde{L} - \frac{1}{8\pi^2} + \frac{1}{4\pi^2} \int_0^1 dx \left\{ x \ln \left(\frac{\tilde{m}^2}{m_\pi^2} \right) + \frac{2}{q_0} \sqrt{\tilde{m}^2 - q_0^2 x^2} \sin^{-1} \left(\frac{q_0 x}{\sqrt{\tilde{m}^2}} \right) \right\} + \mathcal{O}(\epsilon), \quad (\text{D.45})$$

$$h_{17}(q^2, q_0) = -\frac{1}{8\pi} \frac{m_\pi^3}{q_0^2} \left(1 - \left(1 - \frac{q_0^2}{m_\pi^2} \right)^{3/2} \right) + \mathcal{O}(\epsilon), \quad (\text{D.46})$$

$$h_{18}(q^2, q_0) = \frac{3}{16\pi} \frac{m_\pi^3}{q_0^2} \left(1 - \left(1 - \frac{q_0^2}{m_\pi^2} \right)^{3/2} \right) + \mathcal{O}(\epsilon), \quad (\text{D.47})$$

$$h_{19}(q^2, q_0) = \frac{1}{16\pi} \frac{m_\pi^3}{q_0^2} \left(1 - \left(1 - \frac{q_0^2}{m_\pi^2} \right)^{3/2} \right) + \mathcal{O}(\epsilon). \quad (\text{D.48})$$

These expressions agree with Eqs. (81)-(84) of Ref. [65] when $q_0 = 0$ and $\epsilon \cdot v = 0$.

We have explicitly checked that our result is gauge invariant through the following relations between the h 's:

$$h_2(q^2, q_0) + h_{11}(q^2, q_0) + q^2 h_{12}(q^2, q_0) + q_0 (h_{13}(q^2, q_0) + h_{16}(q^2, q_0)) = 0, \quad (\text{D.49})$$

$$h_0(q^2, q_0) + h_1(q^2, q_0) + h_3(q^2, q_0) + h_7(q^2, q_0) + q_0 (h_{10}(q^2, q_0) + h_{15}(q^2, q_0)) \\ + q^2 (h_4(q^2, q_0) + h_8(q^2, q_0)) = 0, \quad (\text{D.50})$$

$$-\frac{q_0^2}{q^2} (-h_1(q^2, q_0) + h_6(q^2, q_0) + h_9(q^2, q_0) + h_{14}(q^2, q_0) + h_{17}(q^2, q_0) + h_{18}(q^2, q_0) + h_{19}(q^2, q_0)) \\ + h_0(q^2, q_0) + h_1(q^2, q_0) + h_3(q^2, q_0) + h_7(q^2, q_0) + q^2 (h_4(q^2, q_0) + h_8(q^2, q_0)) = 0. \quad (\text{D.51})$$

D.2 Pion loops which include a Δ excitation

Here we collect the amplitudes of all the diagrams contributing to the proton polarizability with a Δ particle and through a loop of pions, represented in Fig. 3.3, plus the ones with a crossed photon lines or permutations, which are assumed to be implicit in the representation. For all the diagrams here we consider the overall factor $\mathcal{A} = -\frac{8}{3} M_p \frac{g_{\pi N \Delta}^2}{F_\pi^2}$. We take a positive infinitesimal imaginary part for the propagators of $h_{14}^\Delta - h_{19}^\Delta$.

$$\mathcal{M}_{\Delta\pi 1}^{\mu\nu} = \mathcal{A} g^{\mu\nu} h_0^\Delta(q^2, q_0), \quad (\text{D.52})$$

$$\mathcal{M}_{\Delta\pi 2}^{\mu\nu} = \mathcal{A} \left\{ (g^{\mu\nu} - v^\mu v^\nu) h_1^\Delta(q^2, q_0) + i \epsilon^{\mu\nu\alpha\beta} v_\alpha S_\beta h_2^\Delta(q^2, q_0) \right\}, \quad (\text{D.53})$$

$$\mathcal{M}_{\Delta\pi 3}^{\mu\nu} = \mathcal{A} \left\{ g^{\mu\nu} h_3^\Delta(q^2, q_0) + q^\mu q^\nu h_4^\Delta(q^2, q_0) + (q^\mu v^\nu + v^\mu q^\nu) h_5^\Delta(q^2, q_0) + v^\mu v^\nu h_6^\Delta(q^2, q_0) \right\}, \quad (\text{D.54})$$

$$\mathcal{M}_{\Delta\pi 4}^{\mu\nu} = \mathcal{A} \left\{ g^{\mu\nu} h_7^\Delta(q^2, q_0) + q^\mu q^\nu h_8^\Delta(q^2, q_0) + (q^\mu v^\nu + v^\mu q^\nu) h_{10}^\Delta(q^2, q_0) + v^\mu v^\nu h_9^\Delta(q^2, q_0) \right. \\ \left. + i \epsilon^{\mu\nu\alpha\beta} v_\alpha S_\beta h_{11}^\Delta(q^2, q_0) + i v_\alpha S_\beta q_\lambda (\epsilon^{\mu\lambda\alpha\beta} q^\nu - \epsilon^{\nu\lambda\alpha\beta} q^\mu) h_{12}^\Delta(q^2, q_0) \right. \\ \left. + i v_\alpha S_\beta q_\lambda (\epsilon^{\mu\lambda\alpha\beta} v^\nu - \epsilon^{\nu\lambda\alpha\beta} v^\mu) h_{13}^\Delta(q^2, q_0) \right\}, \quad (\text{D.55})$$

$$\mathcal{M}_{\Delta\pi 5}^{\mu\nu} = \mathcal{A} \left\{ v^\mu v^\nu h_{14}^\Delta(q^2, q_0) + (q^\mu v^\nu + v^\mu q^\nu) h_{15}^\Delta(q^2, q_0) \right. \\ \left. + i v_\alpha S_\beta q_\lambda (\epsilon^{\mu\lambda\alpha\beta} v^\nu - \epsilon^{\nu\lambda\alpha\beta} v^\mu) h_{16}^\Delta(q^2, q_0) \right\}, \quad (\text{D.56})$$

$$\mathcal{M}_{\Delta\pi 6}^{\mu\nu} = \mathcal{A} \left\{ v^\mu v^\nu h_{17}^\Delta(q^2, q_0) \right\}, \quad (\text{D.57})$$

Appendix D. HBET amplitudes

$$\mathcal{M}_{\Delta\pi 7}^{\mu\nu} = \mathcal{A} \left\{ v^\mu v^\nu h_{18}^\Delta(q^2, q_0) \right\}, \quad (\text{D.58})$$

$$\mathcal{M}_{\Delta\pi 8}^{\mu\nu} = \mathcal{A} \left\{ v^\mu v^\nu h_{19}^\Delta(q^2, q_0) \right\}, \quad (\text{D.59})$$

where in terms of the master integrals:

$$h_0^\Delta(q^2, q_0) = -2(D-2)J_2'(-\Delta, m_\pi^2), \quad (\text{D.60})$$

$$h_1^\Delta(q^2, q_0) = \frac{D-2}{D-1} \left(J_0(q_0 - \Delta, m_\pi^2) + J_0(-q_0 - \Delta, m_\pi^2) \right), \quad (\text{D.61})$$

$$h_2^\Delta(q^2, q_0) = \frac{-2}{D-1} \left(J_0(q_0 - \Delta, m_\pi^2) - J_0(-q_0 - \Delta, m_\pi^2) \right), \quad (\text{D.62})$$

$$h_3^\Delta(q^2, q_0) = 4 \frac{D-2}{D-1} \int_0^1 dx (1-x) \left\{ -\mathbf{q}^2 x^2 \left(J_2''(q_0 x - \Delta, \tilde{m}^2) + J_2''(-q_0 x - \Delta, \tilde{m}^2) \right) \right. \\ \left. + (D+1) \left(J_6''(q_0 x - \Delta, \tilde{m}^2) + J_6''(-q_0 x - \Delta, \tilde{m}^2) \right) \right\}, \quad (\text{D.63})$$

$$h_4^\Delta(q^2, q_0) = \frac{D-2}{D-1} \int_0^1 dx (1-x)(2x-1) \\ \times \left\{ -\mathbf{q}^2 x^2 (2x-1) \left(J_0''(q_0 x - \Delta, \tilde{m}^2) + J_0''(-q_0 x - \Delta, \tilde{m}^2) \right) \right. \\ \left. + (4x(D+1) - (1+2x)(D-1)) \left(J_2''(q_0 x - \Delta, \tilde{m}^2) + J_2''(-q_0 x - \Delta, \tilde{m}^2) \right) \right\}, \quad (\text{D.64})$$

$$h_5^\Delta(q^2, q_0) = 2 \frac{D-2}{D-1} \int_0^1 dx \left\{ (-\mathbf{q}^2 x^2 (1-2x)) \left(J_1''(q_0 x - \Delta, \tilde{m}^2) - J_1''(-q_0 x - \Delta, \tilde{m}^2) \right) \right. \\ \left. + 2q_0 x (1-2x) \left(J_2''(q_0 x - \Delta, \tilde{m}^2) + J_2''(-q_0 x - \Delta, \tilde{m}^2) \right) \right. \\ \left. + (D-1 - 2(D+1)x) \left(J_4''(q_0 x - \Delta, \tilde{m}^2) - J_4''(-q_0 x - \Delta, \tilde{m}^2) \right) \right\}, \quad (\text{D.65})$$

$$h_6^\Delta(q^2, q_0) = 4 \frac{D-2}{D-1} \int_0^1 dx (1-x) \left\{ x \left(-\mathbf{q}^2 x \left(J_3''(q_0 x - \Delta, \tilde{m}^2) + J_3''(-q_0 x - \Delta, \tilde{m}^2) \right) \right. \right. \\ \left. \left. + 4q_0 \left(J_4''(q_0 x - \Delta, \tilde{m}^2) - J_4''(-q_0 x - \Delta, \tilde{m}^2) \right) \right) \right. \\ \left. - 2 \left(J_6''(q_0 x - \Delta, \tilde{m}^2) + J_6''(-q_0 x - \Delta, \tilde{m}^2) \right) \right\}, \quad (\text{D.66})$$

$$h_7^\Delta(q^2, q_0) = -4 \frac{D-2}{D-1} \int_0^1 dx \left\{ J_2'(q_0 x - \Delta, \tilde{m}^2) + J_2'(-q_0 x - \Delta, \tilde{m}^2) \right\}, \quad (\text{D.67})$$

$$h_8^\Delta(q^2, q_0) = 2 \frac{D-2}{D-1} \int_0^1 dx (1-2x)x \left\{ J_0'(q_0 x - \Delta, \tilde{m}^2) + J_0'(-q_0 x - \Delta, \tilde{m}^2) \right\}, \quad (\text{D.68})$$

$$h_9^\Delta(q^2, q_0) = 4 \frac{D-2}{D-1} \int_0^1 dx \left\{ J_2'(q_0 x - \Delta, \tilde{m}^2) + J_2'(-q_0 x - \Delta, \tilde{m}^2) \right. \\ \left. - q_0 x \left(J_1'(q_0 x - \Delta, \tilde{m}^2) - J_1'(-q_0 x - \Delta, \tilde{m}^2) \right) \right\}, \quad (\text{D.69})$$

$$h_{10}^\Delta(q^2, q_0) = \frac{D-2}{D-1} \int_0^1 dx x \left\{ 2 \left(J_1'(q_0 x - \Delta, \tilde{m}^2) - J_1'(-q_0 x - \Delta, \tilde{m}^2) \right) \right. \\ \left. - (1-2x)q_0 \left(J_0'(q_0 x - \Delta, \tilde{m}^2) + J_0'(-q_0 x - \Delta, \tilde{m}^2) \right) \right\}, \quad (\text{D.70})$$

$$h_{11}^\Delta(q^2, q_0) = \frac{8}{D-1} \int_0^1 dx \left\{ J_2'(q_0 x - \Delta, \tilde{m}^2) - J_2'(-q_0 x - \Delta, \tilde{m}^2) \right\}, \quad (\text{D.71})$$

$$h_{12}^\Delta(q^2, q_0) = -\frac{2}{D-1} \int_0^1 dx x(1-2x) \left\{ J_0'(q_0 x - \Delta, \tilde{m}^2) - J_0'(-q_0 x - \Delta, \tilde{m}^2) \right\}, \quad (\text{D.72})$$

$$h_{13}^\Delta(q^2, q_0) = -\frac{4}{D-1} \int_0^1 dx x \left\{ J_1'(q_0x - \Delta, \tilde{m}^2) + J_1'(-q_0x - \Delta, \tilde{m}^2) \right\}, \quad (\text{D.73})$$

$$\begin{aligned} h_{14}^\Delta(q^2, q_0) = & 4 \frac{D-2}{D-1} \frac{1}{q_0} \int_0^1 dx \left\{ (D-1) \left(J_4'(q_0x - \Delta, \tilde{m}^2) - J_4'(-q_0x - \Delta, \tilde{m}^2) \right) \right. \\ & - (1-2x)q_0 \left(J_2'(q_0x - \Delta, \tilde{m}^2) + J_2'(-q_0x - \Delta, \tilde{m}^2) \right) \\ & \left. + (1-x)x\mathbf{q}^2 \left(J_1'(q_0x - \Delta, \tilde{m}^2) - J_1'(-q_0x - \Delta, \tilde{m}^2) \right) \right\}, \end{aligned} \quad (\text{D.74})$$

$$\begin{aligned} h_{15}^\Delta(q^2, q_0) = & \frac{D-2}{D-1} \frac{1}{q_0} \int_0^1 dx (1-2x) \left\{ (D+1) \left(J_2'(q_0x - \Delta, \tilde{m}^2) + J_2'(-q_0x - \Delta, \tilde{m}^2) \right) \right. \\ & \left. + \mathbf{q}^2(1-x)x \left(J_0'(q_0x - \Delta, \tilde{m}^2) + J_0'(-q_0x - \Delta, \tilde{m}^2) \right) \right\}, \end{aligned} \quad (\text{D.75})$$

$$h_{16}^\Delta(q^2, q_0) = -\frac{2}{D-1} \frac{2}{q_0} \int_0^1 dx \left\{ J_2'(q_0x - \Delta, \tilde{m}^2) - J_2'(-q_0x - \Delta, \tilde{m}^2) \right\}, \quad (\text{D.76})$$

$$h_{17}(q^2, q_0) = -2 \frac{D-1}{4} \frac{1}{q_0^2} \left(-2J_2(0, m_\pi^2) + J_2(-q_0, m_\pi^2) + J_2(q_0, m_\pi^2) \right), \quad (\text{D.77})$$

$$\begin{aligned} h_{17}^\Delta(q^2, q_0) = & 2 \frac{D-2}{D-1} \left(\frac{1-D}{2} \frac{1}{q_0^2} \left(-2J_2(-\Delta, m_\pi^2) + J_2(-q_0 - \Delta, m_\pi^2) + J_2(q_0 - \Delta, m_\pi^2) \right) \right), \\ & (\text{D.78}) \end{aligned}$$

$$h_{18}^\Delta(q^2, q_0) = 2 \frac{D-2}{D-1} \frac{D-1}{4} \frac{3}{q_0^2} \left(J_2(q_0 - \Delta, m_\pi^2) + J_2(-q_0 - \Delta, m_\pi^2) - 2J_2(-\Delta, m_\pi^2) \right), \quad (\text{D.79})$$

$$h_{19}^\Delta(q^2, q_0) = 2 \frac{D-2}{D-1} \frac{D-1}{4} \frac{1}{q_0^2} \left(J_2(q_0 - \Delta, m_\pi^2) + J_2(-q_0 - \Delta, m_\pi^2) - 2J_2(-\Delta, m_\pi^2) \right). \quad (\text{D.80})$$

These results, in the limit $q^2 = 0$ and in the gauge where $\epsilon \cdot v = 0$, agree with Eqs. (89)-(92) of Ref. [65].

Now, expanding in $D = 4 + 2\epsilon$ we get

$$h_0^\Delta(q^2, q_0) = -\frac{1}{4\pi^2} \Delta \tilde{L} - \frac{1}{2\pi^2} m_\pi \mathcal{Z} \left(\frac{\Delta}{m_\pi} \right), \quad (\text{D.81})$$

$$h_1^\Delta(q^2, q_0) = \frac{1}{6\pi^2} \Delta \tilde{L} + \frac{1}{18\pi^2} \left(3m_\pi \left(\mathcal{Z} \left(\frac{\Delta - q_0}{m_\pi} \right) + \mathcal{Z} \left(\frac{\Delta + q_0}{m_\pi} \right) \right) - 2\Delta \right) + \mathcal{O}(\epsilon), \quad (\text{D.82})$$

$$h_2^\Delta(q^2, q_0) = \frac{1}{6\pi^2} q_0 \tilde{L} + \frac{1}{6\pi^2} \left(m_\pi \left(\mathcal{Z} \left(\frac{\Delta + q_0}{m_\pi} \right) - \mathcal{Z} \left(\frac{\Delta - q_0}{m_\pi} \right) \right) - \frac{5q_0}{3} \right) + \mathcal{O}(\epsilon), \quad (\text{D.83})$$

$$\begin{aligned} h_3^\Delta(q^2, q_0) = & \frac{5\Delta \tilde{L}}{12\pi^2} - \frac{\Delta}{9\pi^2} + \frac{1}{6\pi^2} \int_0^1 dx (1-x) \\ & \times \left\{ 5\Delta \ln \left(\frac{\tilde{m}^2}{m_\pi^2} \right) + \sqrt{\tilde{m}^2} \left(\left(5 - \frac{\mathbf{q}^2 x^2}{\tilde{m}^2 - (\Delta + q_0 x)^2} \right) \right. \right. \\ & \left. \left. \mathcal{Z} \left(\frac{\Delta + q_0 x}{\sqrt{\tilde{m}^2}} \right) + \left(5 - \frac{\mathbf{q}^2 x^2}{\tilde{m}^2 - (\Delta - q_0 x)^2} \right) \mathcal{Z} \left(\frac{\Delta - q_0 x}{\sqrt{\tilde{m}^2}} \right) \right) \right\} + \mathcal{O}(\epsilon), \end{aligned} \quad (\text{D.84})$$

$$\begin{aligned} h_4^\Delta(q^2, q_0) = & \frac{1}{24\pi^2} \int_0^1 dx (1-x)(2x-1) \\ & \times \left\{ x^2(2x-1) \frac{\mathbf{q}^2}{\tilde{m}^2} \left(\frac{\Delta + q_0 x}{\tilde{m}^2 - (\Delta + q_0 x)^2} + \frac{\Delta - q_0 x}{\tilde{m}^2 - (\Delta - q_0 x)^2} \right) \right. \\ & \left. - \frac{\sqrt{\tilde{m}^2}}{\tilde{m}^2 - (\Delta + q_0 x)^2} \left(3 \left(1 - \frac{14x}{3} \right) - \frac{\mathbf{q}^2 x^2 (2x-1)}{\tilde{m}^2 - (\Delta + q_0 x)^2} \right) \mathcal{Z} \left(\frac{\Delta + q_0 x}{\sqrt{\tilde{m}^2}} \right) \right\} \end{aligned}$$

$$- \frac{\sqrt{\tilde{m}^2}}{\tilde{m}^2 - (\Delta - q_0x)^2} \left(3 \left(1 - \frac{14x}{3} \right) - \frac{\mathbf{q}^2 x^2 (2x - 1)}{\tilde{m}^2 - (\Delta - q_0x)^2} \right) \mathcal{Z} \left(\frac{\Delta - q_0x}{\sqrt{\tilde{m}^2}} \right) \Big\} + \mathcal{O}(\epsilon), \quad (\text{D.85})$$

$$\begin{aligned} h_5^\Delta(q^2, q_0) &= \frac{1}{12\pi^2} \int_0^1 dx \left\{ (2x - 1)x^2 \left(\frac{\mathbf{q}^2}{\tilde{m}^2 - (\Delta - q_0x)^2} - \frac{\mathbf{q}^2}{\tilde{m}^2 - (\Delta + q_0x)^2} \right) \right. \\ &- \frac{\sqrt{\tilde{m}^2}}{\tilde{m}^2 - (\Delta + q_0x)^2} \left(\frac{x^2(2x - 1)\mathbf{q}^2(\Delta + q_0x)}{\tilde{m}^2 - (\Delta + q_0x)^2} - q_0x(5(1 - 2x) - 4x) \right. \\ &+ \left. \left. \Delta(4x + 3(2x - 1)) \right) \mathcal{Z} \left(\frac{\Delta + q_0x}{\sqrt{\tilde{m}^2}} \right) + \frac{\sqrt{\tilde{m}^2}}{\tilde{m}^2 - (\Delta - q_0x)^2} \left(\frac{x^2(2x - 1)\mathbf{q}^2(\Delta - q_0x)}{\tilde{m}^2 - (\Delta - q_0x)^2} \right. \right. \\ &+ \left. \left. q_0x(5(1 - 2x) - 4x) + \Delta(4x + 3(2x - 1)) \right) \mathcal{Z} \left(\frac{\Delta - q_0x}{\sqrt{\tilde{m}^2}} \right) \right\} + \mathcal{O}(\epsilon), \quad (\text{D.86}) \end{aligned}$$

$$\begin{aligned} h_6^\Delta(q^2, q_0) &= -\frac{1}{6\pi^2} \Delta \tilde{L} + \frac{\Delta}{9\pi^2} + \frac{1}{6\pi^2} \int_0^1 dx (1 - x) \left\{ -2\Delta \ln \left(\frac{\tilde{m}^2}{m_\pi^2} \right) \right. \\ &+ \mathbf{q}^2 x^2 \left(\frac{\Delta + q_0x}{\tilde{m}^2 - (\Delta + q_0x)^2} + \frac{\Delta - q_0x}{\tilde{m}^2 - (\Delta - q_0x)^2} \right) + \sqrt{\tilde{m}^2} \left(\frac{\mathbf{q}^2 x^2 (\Delta + q_0x)^2}{(\tilde{m}^2 - (\Delta + q_0x)^2)^2} \right. \\ &+ \left. \frac{4q_0x(\Delta + q_0x) + \mathbf{q}^2 x^2}{\tilde{m}^2 - (\Delta + q_0x)^2} - 2 \right) \mathcal{Z} \left(\frac{\Delta + q_0x}{\sqrt{\tilde{m}^2}} \right) + \sqrt{\tilde{m}^2} \left(\frac{\mathbf{q}^2 x^2 (\Delta - q_0x)^2}{(\tilde{m}^2 - (\Delta - q_0x)^2)^2} \right. \\ &+ \left. \frac{\mathbf{q}^2 x^2 - 4q_0x(\Delta - q_0x)}{\tilde{m}^2 - (\Delta - q_0x)^2} - 2 \right) \mathcal{Z} \left(\frac{\Delta - q_0x}{\sqrt{\tilde{m}^2}} \right) \Big\} + \mathcal{O}(\epsilon), \quad (\text{D.87}) \end{aligned}$$

$$\begin{aligned} h_7^\Delta(q^2, q_0) &= -\frac{1}{3\pi^2} \Delta \tilde{L} + \frac{2\Delta}{9\pi^2} \\ &- \frac{1}{3\pi^2} \int_0^1 dx \left\{ \Delta \ln \left(\frac{\tilde{m}^2}{m_\pi^2} \right) + \sqrt{\tilde{m}^2} \left(\mathcal{Z} \left(\frac{\Delta - q_0x}{\sqrt{\tilde{m}^2}} \right) + \mathcal{Z} \left(\frac{\Delta + q_0x}{\sqrt{\tilde{m}^2}} \right) \right) \right\} + \mathcal{O}(\epsilon), \quad (\text{D.88}) \end{aligned}$$

$$h_8^\Delta(q^2, q_0) = \frac{1}{6\pi^2} \int_0^1 dx (1 - 2x)x \sqrt{\tilde{m}^2} \left\{ \frac{\mathcal{Z} \left(\frac{\Delta + q_0x}{\sqrt{\tilde{m}^2}} \right)}{\tilde{m}^2 - (\Delta + q_0x)^2} + \frac{\mathcal{Z} \left(\frac{\Delta - q_0x}{\sqrt{\tilde{m}^2}} \right)}{\tilde{m}^2 - (\Delta - q_0x)^2} \right\} + \mathcal{O}(\epsilon), \quad (\text{D.89})$$

$$\begin{aligned} h_9^\Delta(q^2, q_0) &= \frac{1}{3\pi^2} \Delta \tilde{L} - \frac{2\Delta}{9\pi^2} + \frac{1}{3\pi^2} \int_0^1 dx \left\{ \Delta \ln \left(\frac{\tilde{m}^2}{m_\pi^2} \right) + \sqrt{\tilde{m}^2} \left(\left(1 - \frac{x(q_0(\Delta + q_0x))}{\tilde{m}^2 - (\Delta + q_0x)^2} \right) \right. \right. \\ &\mathcal{Z} \left(\frac{\Delta + q_0x}{\sqrt{\tilde{m}^2}} \right) + \left. \left. \left(\frac{x(q_0(\Delta - q_0x))}{\tilde{m}^2 - (\Delta - q_0x)^2} + 1 \right) \mathcal{Z} \left(\frac{\Delta - q_0x}{\sqrt{\tilde{m}^2}} \right) \right) \right\} + \mathcal{O}(\epsilon), \quad (\text{D.90}) \end{aligned}$$

$$\begin{aligned} h_{10}^\Delta(q^2, q_0) &= \frac{1}{12\pi^2} \int_0^1 dx \sqrt{\tilde{m}^2} x \left\{ \frac{(2\Delta + q_0(4x - 1)) \mathcal{Z} \left(\frac{\Delta + q_0x}{\sqrt{\tilde{m}^2}} \right)}{\tilde{m}^2 - (\Delta + q_0x)^2} \right. \\ &+ \left. \frac{(q_0(4x - 1) - 2\Delta) \mathcal{Z} \left(\frac{\Delta - q_0x}{\sqrt{\tilde{m}^2}} \right)}{\tilde{m}^2 - (\Delta - q_0x)^2} \right\} + \mathcal{O}(\epsilon), \quad (\text{D.91}) \end{aligned}$$

$$h_{11}^\Delta(q^2, q_0) = -\frac{q_0 \tilde{L}}{6\pi^2} + \frac{5q_0}{18\pi^2} - \frac{1}{3\pi^2} \int_0^1 dx \left\{ q_0x \ln \left(\frac{\tilde{m}^2}{m_\pi^2} \right) - \sqrt{\tilde{m}^2} \left(\mathcal{Z} \left(\frac{\Delta - q_0x}{\sqrt{\tilde{m}^2}} \right) \right. \right.$$

$$- \mathcal{Z} \left(\frac{\Delta + q_0 x}{\sqrt{\tilde{m}^2}} \right) \Big\} + \mathcal{O}(\epsilon), \quad (\text{D.92})$$

$$h_{12}^\Delta(q^2, q_0) = -\frac{1}{12\pi^2} \int_0^1 dx (1-2x)x \sqrt{\tilde{m}^2} \left\{ \frac{\mathcal{Z} \left(\frac{\Delta - q_0 x}{\sqrt{\tilde{m}^2}} \right)}{\tilde{m}^2 - (\Delta - q_0 x)^2} - \frac{\mathcal{Z} \left(\frac{\Delta + q_0 x}{\sqrt{\tilde{m}^2}} \right)}{\tilde{m}^2 - (\Delta + q_0 x)^2} \right\} + \mathcal{O}(\epsilon), \quad (\text{D.93})$$

$$h_{13}^\Delta(q^2, q_0) = -\frac{\tilde{L}}{12\pi^2} - \frac{1}{36\pi^2} - \frac{1}{6\pi^2} \int_0^1 dx x \left\{ \ln \left(\frac{\tilde{m}^2}{m_\pi^2} \right) - \sqrt{\tilde{m}^2} \left(\frac{(\Delta + q_0 x) \mathcal{Z} \left(\frac{\Delta + q_0 x}{\sqrt{\tilde{m}^2}} \right)}{\tilde{m}^2 - (\Delta + q_0 x)^2} + \frac{(\Delta - q_0 x) \mathcal{Z} \left(\frac{\Delta - q_0 x}{\sqrt{\tilde{m}^2}} \right)}{\tilde{m}^2 - (\Delta - q_0 x)^2} \right) \right\} + \mathcal{O}(\epsilon), \quad (\text{D.94})$$

$$h_{14}^\Delta(q^2, q_0) = \frac{\Delta \tilde{L}}{\pi^2} + \frac{1}{3\pi^2} \int_0^1 dx \left\{ (-1 + 8x) \Delta \ln \left(\frac{\tilde{m}^2}{m_\pi^2} \right) + \frac{\sqrt{\tilde{m}^2}}{q_0} \left(\left(3\Delta - q_0(1-5x) - \frac{\mathbf{q}^2(1-x)x(q_0x + \Delta)}{(\Delta + q_0x)^2 - \tilde{m}^2} \right) \mathcal{Z} \left(\frac{-q_0x - \Delta}{\sqrt{\tilde{m}^2}} \right) - \left(3\Delta + q_0(1-5x) - \frac{\mathbf{q}^2(1-x)x(-q_0x + \Delta)}{(\Delta - q_0x)^2 - \tilde{m}^2} \right) \mathcal{Z} \left(\frac{q_0x - \Delta}{\sqrt{\tilde{m}^2}} \right) \right) \right\} + \mathcal{O}(\epsilon), \quad (\text{D.95})$$

$$h_{15}^\Delta(q^2, q_0) = \frac{1}{24\pi^2 q_0} \int_0^1 dx (1-2x) \left\{ 10\Delta \ln \left(\frac{\tilde{m}^2}{m_\pi^2} \right) + 2\sqrt{\tilde{m}^2} \left(\left(\frac{\mathbf{q}^2(1-x)x}{\tilde{m}^2 - (\Delta + q_0x)^2} + 5 \right) \mathcal{Z} \left(\frac{\Delta + q_0x}{\sqrt{\tilde{m}^2}} \right) + \left(\frac{\mathbf{q}^2(1-x)x}{\tilde{m}^2 - (\Delta - q_0x)^2} + 5 \right) \mathcal{Z} \left(\frac{\Delta - q_0x}{\sqrt{\tilde{m}^2}} \right) \right) \right\} + \mathcal{O}(\epsilon), \quad (\text{D.96})$$

$$h_{16}^\Delta(q^2, q_0) = \frac{\tilde{L}}{12\pi^2} - \frac{5}{36\pi^2} + \frac{1}{6\pi^2} \int_0^1 dx \left\{ x \ln \left(\frac{\tilde{m}^2}{m_\pi^2} \right) + \frac{\sqrt{\tilde{m}^2}}{q_0} \left(\mathcal{Z} \left(\frac{\Delta + q_0x}{\sqrt{\tilde{m}^2}} \right) - \mathcal{Z} \left(\frac{\Delta - q_0x}{\sqrt{\tilde{m}^2}} \right) \right) \right\} + \mathcal{O}(\epsilon), \quad (\text{D.97})$$

$$h_{17}^\Delta(q^2, q_0) = \frac{-1}{6\pi^2} \left(-3\tilde{L}\Delta + 2\Delta - \frac{m_\pi}{q_0^2} \left(((q_0 + \Delta)^2 - m_\pi^2) \mathcal{Z} \left(\frac{\Delta + q_0}{m_\pi} \right) + ((q_0 - \Delta)^2 - m_\pi^2) \mathcal{Z} \left(\frac{-\Delta + q_0}{m_\pi} \right) - 2(-m_\pi^2 + \Delta^2) \mathcal{Z} \left(-\frac{\Delta}{m_\pi} \right) \right) \right) + \mathcal{O}(\epsilon), \quad (\text{D.98})$$

$$h_{18}^\Delta(q^2, q_0) = \frac{1}{4\pi^2} \left(-3\tilde{L}\Delta + 2\Delta - \frac{m_\pi}{q_0^2} \left(((q_0 + \Delta)^2 - m_\pi^2) \mathcal{Z} \left(\frac{\Delta + q_0}{m_\pi} \right) + ((q_0 - \Delta)^2 - m_\pi^2) \mathcal{Z} \left(\frac{-\Delta + q_0}{m_\pi} \right) - 2(-m_\pi^2 + \Delta^2) \mathcal{Z} \left(-\frac{\Delta}{m_\pi} \right) \right) \right) + \mathcal{O}(\epsilon), \quad (\text{D.99})$$

$$h_{19}^\Delta(q^2, q_0) = \frac{1}{12\pi^2} \left(-3\tilde{L}\Delta + 2\Delta - \frac{m_\pi}{q_0^2} \left(((q_0 + \Delta)^2 - m_\pi^2) \mathcal{Z} \left(\frac{\Delta + q_0}{m_\pi} \right) + ((q_0 - \Delta)^2 - m_\pi^2) \mathcal{Z} \left(\frac{-\Delta + q_0}{m_\pi} \right) - 2(-m_\pi^2 + \Delta^2) \mathcal{Z} \left(\frac{\Delta}{m_\pi} \right) \right) \right) + \mathcal{O}(\epsilon). \quad (\text{D.100})$$

We have explicitly checked that our result is gauge invariant through the following relations between the h^Δ 's:

$$h_2^\Delta(q^2, q_0) + h_{11}^\Delta(q^2, q_0) + q^2 h_{12}^\Delta(q^2, q_0) + q_0 (h_{13}^\Delta(q^2, q_0) + h_{16}^\Delta(q^2, q_0)) = 0, \quad (\text{D.101})$$

$$h_0^\Delta(q^2, q_0) + h_1^\Delta(q^2, q_0) + h_3^\Delta(q^2, q_0) + h_7^\Delta(q^2, q_0) + q_0 (h_{10}^\Delta(q^2, q_0) + h_{15}^\Delta(q^2, q_0))$$

$$+ q^2 \left(h_4^\Delta(q^2, q_0) + h_8^\Delta(q^2, q_0) \right) = 0, \quad (\text{D.102})$$

$$\begin{aligned} & -\frac{q_0^2}{q^2} \left(-h_1^\Delta(q^2, q_0) + h_6^\Delta(q^2, q_0) + h_9^\Delta(q^2, q_0) + h_{14}^\Delta(q^2, q_0) + h_{17}^\Delta(q^2, q_0) \right. \\ & + h_{18}^\Delta(q^2, q_0) + h_{19}^\Delta(q^2, q_0) \left. \right) + h_0^\Delta(q^2, q_0) + h_1^\Delta(q^2, q_0) + h_3^\Delta(q^2, q_0) + h_7^\Delta(q^2, q_0) \\ & + q^2 \left(h_4^\Delta(q^2, q_0) + h_8^\Delta(q^2, q_0) \right) = 0. \end{aligned} \quad (\text{D.103})$$

These relations are equivalent to:

$$h_2(q^2, q_0 - \Delta) + h_{11}(q^2, q_0 - \Delta) + q^2 h_{12}(q^2, q_0 - \Delta) + q_0 (h_{13}(q^2, q_0) + h_{16}(q^2, q_0 - \Delta)) = 0, \quad (\text{D.104})$$

$$\begin{aligned} & h_0(q^2, q_0 - \Delta) + h_1(q^2, q_0 - \Delta) + h_3(q^2, q_0 - \Delta) + h_7(q^2, q_0 - \Delta) + q_0 \left(h_{10}(q^2, q_0 - \Delta) \right. \\ & \left. + h_{15}(q^2, q_0 - \Delta) \right) + q^2 \left(h_4(q^2, q_0 - \Delta) + h_8(q^2, q_0 - \Delta) \right) = 0, \end{aligned} \quad (\text{D.105})$$

$$\begin{aligned} & -\frac{q_0^2}{q^2} \left(-h_1(q^2, q_0 - \Delta) + h_6(q^2, q_0 - \Delta) + h_9(q^2, q_0 - \Delta) + h_{14}(q^2, q_0 - \Delta) + h_{17}(q^2, q_0 - \Delta) \right. \\ & + h_{18}(q^2, q_0 - \Delta) + h_{19}(q^2, q_0 - \Delta) \left. \right) + h_0(q^2, q_0 - \Delta) + h_1(q^2, q_0 - \Delta) \\ & + h_3(q^2, q_0 - \Delta) + h_7(q^2, q_0 - \Delta) + q^2 \left(h_4(q^2, q_0 - \Delta) + h_8(q^2, q_0 - \Delta) \right) = 0, \end{aligned} \quad (\text{D.106})$$

which are also fulfilled.

Appendix E

Muonium spectrum

We profit from the results obtained in Part II of this work to give the spectrum for the muonium bound state (μe) for general quantum numbers at $\mathcal{O}(m_r \alpha^5)$. We first exchange the proton by the muon and the muon by the electron. Then, the main difference with muonic hydrogen is the lack of hadronic contributions, as well as the fact that all electron VP effects can be eliminated, in particular this implies that the static potential becomes trivial. Thus, we are only left with the relativistic corrections to the potential which come from Eqs. (4.15) and (4.16) plus the energy coming from the kinetic term and the ultrasoft effect. The ultrasoft correction to the energy only depends on the reduced mass, and so it will be the same as the one for the muonic hydrogen in Eq. (5.28). Altogether, for a given energy level we get

$$\begin{aligned}
E_{nlj_e} &= -\frac{m_r \alpha^2}{2n^2} + (\delta E_{nlj_e}^{V(2,1)} + \delta E_{nl}^{V(3,0)}) + (\delta E_{nlj_e}^{V_{\text{no-VP}}^{(2,2)}} + \delta E_{nl}^{\text{US}}) \\
&= -\frac{m_r \alpha^2}{2n^2} \\
&+ \frac{m_r \alpha^4}{n^3} \left[\frac{m_r^2}{2m_e^2} \left\{ \delta_{l0} + \frac{3}{4n} - \frac{2}{2l+1} + \frac{(1-\delta_{l0})}{l(l+1)(2l+1)} d_{j_e,l} + 2 \frac{m_e}{m_\mu} \left(\frac{5}{8n} - \frac{2+\delta_{l0}}{2l+1} \right. \right. \right. \\
&+ \left. \left. \frac{8}{3} \delta_{l0} \delta_{s1} + \frac{(1-\delta_{l0}) \delta_{s1}}{2l(l+1)(2l+1)} (c_{j,l} + 4h_{j,l}) \right\} \right. \\
&+ \left. \frac{m_e^2}{m_\mu^2} \left(\delta_{l0} + \frac{3}{4n} - \frac{2}{2l+1} + \frac{(1-\delta_{l0})}{l(l+1)(2l+1)} (2\delta_{s1} h_{j,l} - d_{j_e,l}) \right) \right] \\
&+ \frac{\alpha}{\pi} \left\{ \delta_{l,0} \left(-\frac{4}{3} (\ln R(n,l) + 2 \ln \alpha) + \frac{10}{9} \right) - (1-\delta_{l,0}) \frac{4}{3} \ln R(n,l) \right. \\
&+ \left. \frac{m_r^2}{2m_e^2} \left\{ \frac{4}{3} \left(-\frac{2}{5} + \ln \left(\frac{m_e^2}{m_r^2} \right) \right) \delta_{l,0} + \frac{1-\delta_{l,0}}{l(l+1)(2l+1)} d_{j_e,l} \right. \right. \\
&+ \left. \left. \frac{m_e^2}{m_\mu^2} \left(\frac{4}{3} \left(-\frac{2}{5} + \ln \left(\frac{m_\mu^2}{m_r^2} \right) \right) \delta_{l,0} + \frac{1-\delta_{l,0}}{l(l+1)(2l+1)} (2\delta_{s,1} h_{j,l} - d_{j_e,l}) \right) \right. \right. \\
&+ \left. \frac{m_e}{m_\mu} \left(-\frac{10}{3} \delta_{l,0} - \frac{14}{3} \frac{1-\delta_{l,0}}{l(l+1)(2l+1)} + \frac{14}{3} \delta_{l,0} \left(1 - \frac{1}{n} + 2k(n) + 2 \ln \left(\frac{2\alpha}{n} \right) \right) \right) \right. \\
&+ \left. \frac{16}{3} \delta_{s,1} \delta_{l,0} + \frac{1-\delta_{l,0}}{l(l+1)(2l+1)} (c_{j,l} + 2h_{j,l}) \right) + \frac{2m_e^2 \delta_{l,0}}{m_e^2 - m_\mu^2} \left(\frac{m_\mu}{m_e} \left(\frac{1}{3} + \ln \left(\frac{m_e^2}{m_r^2} \right) \right) \right)
\end{aligned}$$

$$+ \left. \left. \left. \frac{m_e}{m_\mu} \left(\frac{1}{3} + \ln \left(\frac{m_\mu^2}{m_r^2} \right) \right) + \ln \left(\frac{m_e^2}{m_\mu^2} \right) (3 - 4\delta_{s,1}) \right) \right\} \right\} \right], \quad (\text{E.1})$$

where $c_{j,l}$, $h_{j,l}$ and $d_{j_e,l}$ have been defined in Eqs. (5.21)-(5.23), and the first and second parenthesis in the right hand side of the first equality contain the $\mathcal{O}(m_r\alpha^4)$ and $\mathcal{O}(m_r\alpha^5)$ contributions respectively. In our notation, the ill-defined quantity $(1 - \delta_{l0})/l \rightarrow 0$ when $l \rightarrow 0$. Note that the exact mass dependence has been kept in this expression to order α^5 .

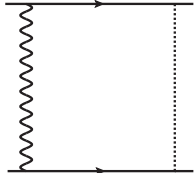
The expressions for the potential of muonium can also be found in Ref. [171]. One could be worried that the potential is different to the one we use. The reason for this difference is that they obtain the potential by matching on-shell S-matrix elements (and by a change in the renormalization scheme of the ultrasoft computation), still their potential is equivalent to ours through field redefinitions, and yields the same physical results. In particular, for spin-independent states the result for the energy shift can already be found in Eqs. (2.12) and (2.13) of that reference.

Appendix F

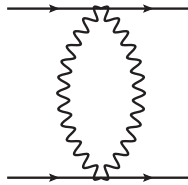
Off-shell NRQCD amplitudes for the $\mathcal{O}(\alpha^2/m^2)$ potential

Computations in the CG are usually thought of as being somehow cumbersome. We have found that this is not the case for the computation at hand. In fact, the substantially smaller number of diagrams makes the computation quite light. The minor presence of CG computations in the literature makes us think that it would be interesting to present the results for each diagram, which we do in this appendix.

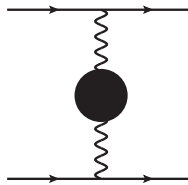
This is the result we find the following amplitudes $\Sigma^{(2)}$ for the off-shell matching of the spin-independent $\mathcal{O}(1/m^2)$ potentials:



$$= \frac{-ig_B^4}{3m_1m_2} \frac{\mathbf{k}^{2\epsilon-4}}{2^{1+8\epsilon}\pi^{1+\epsilon}} \frac{\Gamma(1-\epsilon)\Gamma(4\epsilon)}{\Gamma(2\epsilon+\frac{1}{2})\Gamma(2\epsilon+\frac{3}{2})} [C_F^2 \mathbf{k}^4(\epsilon+1)(2\epsilon+1) - \frac{C_A C_F}{2} ((\mathbf{p}'^2 - \mathbf{p}^2)^2 \epsilon(1-\epsilon) + \mathbf{k}^2(1+5\epsilon)(\mathbf{k}^2 - (\mathbf{p}'^2 + \mathbf{p}^2)))]$$



$$= \frac{-ig_B^4}{3m_1m_2} \frac{\mathbf{k}^{2\epsilon} \csc(\pi\epsilon)}{2^{4\epsilon+8}\pi^{\epsilon+\frac{1}{2}}\Gamma(\epsilon+\frac{5}{2})} (C_A C_F - C_F^2) [(\epsilon+1)(2\epsilon+3)(8\epsilon+7) - \frac{2^{6\epsilon+5}\Gamma(\epsilon+\frac{3}{2})\Gamma(2\epsilon+3)\Gamma(\epsilon+\frac{5}{2})}{\pi\Gamma(4\epsilon+3)}]$$



$$= \frac{ig_B^4}{3m_1m_2} \frac{\mathbf{k}^{2\epsilon} \csc(\pi\epsilon)}{2^{4\epsilon+6}\pi^{\epsilon+\frac{1}{2}}\Gamma(\epsilon+\frac{5}{2})} \mathcal{G} [12C_F T_F n_f (1+\epsilon) - C_A C_F \left(\epsilon(40\epsilon+89) + 45 - \frac{\Gamma^2(\epsilon+\frac{3}{2})}{\sqrt{\pi}\Gamma(2\epsilon+\frac{5}{2})} \frac{2^{2\epsilon+2}(2\epsilon+3)(5\epsilon(4\epsilon+5)+9)}{2\epsilon+1} \right)]$$

Appendix F. Off-shell NRQCD amplitudes for the $\mathcal{O}(\alpha^2/m^2)$ potential

$$\begin{aligned}
 &= \frac{ig_B^4}{m_1 m_2} \mathcal{G} C_A C_F \frac{\mathbf{k}^{2\epsilon}}{2^{4\epsilon+3} \pi^{\epsilon+\frac{3}{2}}} \frac{(\epsilon+1)\Gamma(-\epsilon)\Gamma(2\epsilon+1)}{\Gamma(2\epsilon+\frac{5}{2})} \\
 &= -\frac{ig_B^4}{3m_1^2} \frac{\mathbf{k}^{2\epsilon} \csc(\pi\epsilon)(2\epsilon+3)}{2^{4\epsilon+6} \pi^{\epsilon+\frac{1}{2}} \Gamma(\epsilon+\frac{5}{2})} C_A C_F \left[\mathcal{G} \left(-2(\epsilon(4\epsilon+7)+4) + \frac{2^{2\epsilon+3} \Gamma^2(\epsilon+\frac{3}{2})}{\sqrt{\pi} \Gamma(2\epsilon+\frac{5}{2})} (2\epsilon(\epsilon+2)+3) \right) \right. \\
 &\quad \left. + \left(\frac{\mathbf{p}'^2 + \mathbf{p}^2}{\mathbf{k}^2} - 1 \right) \left((\epsilon+1)(4\epsilon+5) - \frac{4^{\epsilon+1} \Gamma^2(\epsilon+\frac{3}{2})}{\sqrt{\pi} \Gamma(2\epsilon+\frac{5}{2})} (\epsilon+1)(2\epsilon+3) \right) \right] \\
 &= \frac{ig_B^4 c_D^{(i)}}{m_i^2} \frac{\mathbf{k}^{2\epsilon}(\epsilon+1) \csc(\pi\epsilon)}{2^{4\epsilon+9} \pi^{\epsilon+\frac{1}{2}} \Gamma(\epsilon+\frac{5}{2})} (C_A C_F (8\epsilon+11) - 4C_F T_F n_f) \\
 &= \frac{ig_B^4 c_D^{(i)}}{m_i^2} C_A C_F \frac{\mathbf{k}^{2\epsilon}(\epsilon+1)\Gamma(-\epsilon)\Gamma(\epsilon+1)\Gamma(\epsilon+\frac{3}{2})}{(4\pi)^{\epsilon+2} \Gamma(2\epsilon+\frac{5}{2})} \\
 &= -\frac{ig_B^4 c_D^{(i)}}{m_i^2} C_A C_F \frac{\mathbf{k}^{2\epsilon} \csc(\pi\epsilon)}{2^{4\epsilon+9} \pi^{\epsilon+\frac{1}{2}} \Gamma(\epsilon+\frac{5}{2})} \left((\epsilon+1)(8\epsilon+11) - \frac{2^{2\epsilon+4} \Gamma^2(\epsilon+\frac{3}{2})}{\sqrt{\pi} \Gamma(2\epsilon+\frac{5}{2})} (\epsilon+1)(2\epsilon+3) \right) \\
 &= \frac{ig_B^4 c_F^{(i)2}}{m_i^2} C_A C_F \frac{\mathbf{k}^{2\epsilon}(\epsilon+1)(4\epsilon+5) \csc(\pi\epsilon)}{2^{4\epsilon+9} \pi^{\epsilon+\frac{1}{2}} \Gamma(\epsilon+\frac{5}{2})} \\
 &= -\frac{ig_B^4 c_1^{hl(i)}}{m_i^2} C_F T_F n_f \frac{\mathbf{k}^{2\epsilon}(\epsilon+1) \csc(\pi\epsilon)}{2^{4\epsilon+7} \pi^{\epsilon+\frac{1}{2}} \Gamma(\epsilon+\frac{5}{2})}
 \end{aligned}$$

$$\begin{aligned}
&= -\frac{ig_B^4}{3} \frac{k_0^2 \mathbf{k}^{2\epsilon-4} \csc(\pi\epsilon)}{2^{4\epsilon+4} \pi^{\epsilon+\frac{1}{2}} \Gamma(\epsilon+\frac{5}{2})} [3C_F T_F n_f \epsilon(1+\epsilon) \\
&\quad - \frac{C_A C_F}{4} ((\epsilon+1)(\epsilon(56\epsilon+121)+60)) - \frac{5\Gamma(\epsilon+\frac{3}{2})^2}{\sqrt{\pi}\Gamma(2\epsilon+\frac{5}{2})} 4^{\epsilon+1} (\epsilon+1)(2\epsilon+3)(4\epsilon+3)] \\
&= -\frac{ig_B^4}{3m_i} C_A C_F \frac{\mathbf{k}^{2\epsilon-4} (\epsilon+1)(2\epsilon+1)\Gamma(1-\epsilon)\Gamma(2\epsilon)}{4^{2\epsilon+1} \pi^{\epsilon+\frac{3}{2}} \Gamma(2\epsilon+\frac{3}{2})} \\
&\quad [E_i (\mathbf{k}^2 - (\mathbf{p}'^2 - \mathbf{p}^2)^2) + E'_i (\mathbf{k}^2 + (\mathbf{p}'^2 - \mathbf{p}^2)^2)]
\end{aligned}$$

where

$$\mathcal{G} = \frac{1}{4} \left(2 \frac{\mathbf{p}'^2 + \mathbf{p}^2}{\mathbf{k}^2} - 2 - \frac{(\mathbf{p}'^2 - \mathbf{p}^2)^2}{\mathbf{k}^4} \right). \quad (\text{F.1})$$

In the above diagrams, the sum over crossed and mirrored diagrams is implicit. The black bubble represents the complete gluon self-energy correction $\Pi^{\mu\nu}$, which in FG also has non-zero off-diagonal elements Π^{0i} . Note that only the last two diagrams depend on the energies. Here E_i (E'_i) denote the incoming (outgoing) heavy quark/antiquark, respectively, $k_0 = E'_1 - E_1 = E_2 - E'_2$ is the total energy transfer from the antiquark to the quark and we have projected the quark pair onto the color singlet state.

Altogether, the sum of all the diagrams in CG is

$$\begin{aligned}
\Sigma_{\text{CG}}^{(2)} &= \frac{ig_B^4}{3m_1 m_2} \frac{2^{-4(\epsilon+2)} \pi^{-\epsilon-\frac{1}{2}} |\mathbf{k}|^{2\epsilon-4} \csc(\pi\epsilon)}{\Gamma(\epsilon+\frac{5}{2})} \left\{ \right. \\
&\quad + C_A C_F \left[(12\epsilon^2 + 27\epsilon + 15) \mathbf{k}^4 \frac{(c_F^{(2)})^2 m_1^2 + (c_F^{(1)})^2 m_2^2}{2m_1 m_2} + \frac{2^{2\epsilon+3} (2\epsilon^2 + 5\epsilon + 3) \Gamma(\epsilon+\frac{3}{2})^2}{\sqrt{\pi}\Gamma(2\epsilon+\frac{3}{2})} \times \right. \\
&\quad \times \left\{ 2[\mathbf{k}^2 + (\mathbf{p}^2 - \mathbf{p}'^2)] (E_1 m_2 + E_2 m_1) + 2[\mathbf{k}^2 - (\mathbf{p}^2 - \mathbf{p}'^2)] (E'_1 m_2 + E'_2 m_1) \right. \\
&\quad \left. \left. + [(\mathbf{p}^2 - \mathbf{p}'^2)^2 - \mathbf{k}^2 (\mathbf{p}^2 + \mathbf{p}'^2)] \frac{m_1^2 + m_2^2}{m_1 m_2} - 20k_0^2 m_1 m_2 - (\mathbf{p}^2 - \mathbf{p}'^2)^2 \right\} \right. \\
&\quad - 2(8\epsilon^3 + 26\epsilon^2 + 29\epsilon + 12) (\mathbf{p}^2 - \mathbf{p}'^2)^2 \frac{m_1^2 + m_2^2}{m_1 m_2} + 2(8\epsilon^3 + 34\epsilon^2 + 45\epsilon + 18) \mathbf{k}^4 \frac{m_1^2 + m_2^2}{m_1 m_2} \\
&\quad - 4(4\epsilon^2 + 8\epsilon + 3) \mathbf{k}^2 (\mathbf{p}^2 + \mathbf{p}'^2) \frac{m_1^2 + m_2^2}{m_1 m_2} + 4(56\epsilon^3 + 177\epsilon^2 + 181\epsilon + 60) k_0^2 m_1 m_2 \\
&\quad \left. \left. - (40\epsilon^2 + 89\epsilon + 45) [2\mathbf{k}^2 (\mathbf{p}^2 + \mathbf{p}'^2) - (\mathbf{p}^2 - \mathbf{p}'^2)^2] + 2(8\epsilon^3 + 47\epsilon^2 + 74\epsilon + 33) \mathbf{k}^4 \right] \right\} \\
&\quad + C_F n_f T_F 6(\epsilon+1) \left[-\mathbf{k}^4 \frac{(c_1^{hl(1)} + c_D^{(1)}) m_2^2 + (c_1^{hl(2)} + c_D^{(2)}) m_1^2}{m_1 m_2} - 8k_0^2 m_1 m_2 \epsilon \right. \\
&\quad \left. - 2\mathbf{k}^4 + 4\mathbf{k}^2 (\mathbf{p}^2 + \mathbf{p}'^2) - 2(\mathbf{p}^2 - \mathbf{p}'^2)^2 \right] - C_F^2 4(16\epsilon^3 + 54\epsilon^2 + 59\epsilon + 21) \mathbf{k}^4 \left. \right\}, \quad (\text{F.2})
\end{aligned}$$

On top of the previous diagrams, in the FG the diagrams in Fig. F.1 also contribute to the off-shell matching of the spin-independent $\mathcal{O}(1/m^2)$ potentials. For the sum of these diagrams

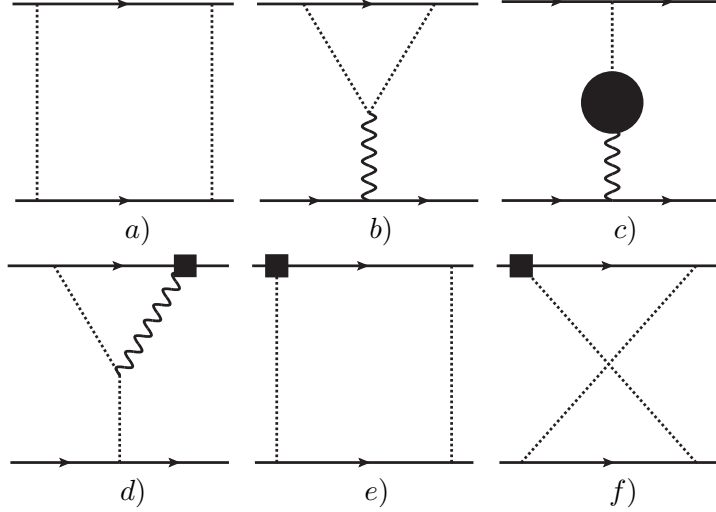


Figure F.1: *One-loop NRQCD diagrams contributing to the off-shell matching of the spin-independent $1/m^2$ potentials in FG. The square, crossed-circle and triangular vertices denote the subleading NRQCD vertices with Wilson coefficients c_D , c_F and c_1^{hl} , respectively. Mirror graphs, crossed graphs and all possible insertions of higher order kinetic corrections from quark and gluon propagators to reach the second order in the $1/m$ expansion, e.g. in diagram a, are understood.*

we obtain in FG

$$\begin{aligned}
 \Sigma_{\text{FG}}^{(2)} = & \frac{ig_B^4}{3m_1m_2} \frac{2^{-4(\epsilon+2)} \pi^{-\epsilon-\frac{1}{2}} |\mathbf{k}|^{2\epsilon-4} \csc(\pi\epsilon)}{\Gamma(\epsilon + \frac{5}{2})} \left\{ \right. \\
 & + C_A C_F \left[3(4\epsilon^2 + 9\epsilon + 5) \mathbf{k}^4 \frac{(c_F^{(2)})^2 m_1^2 + (c_F^{(1)})^2 m_2^2}{2m_1m_2} - 12(8\epsilon^3 + 5\epsilon^2 - 9\epsilon + 4) k_0^2 m_1m_2 \right. \\
 & - 2(16\epsilon^3 + 76\epsilon^2 + 109\epsilon + 48) (\mathbf{p}^2 + \mathbf{p}'^2) \mathbf{k}^2 + 2(8\epsilon^3 + 47\epsilon^2 + 74\epsilon + 33) \mathbf{k}^4 \\
 & + (32\epsilon^3 + 72\epsilon^2 + 40\epsilon + 6) \mathbf{k}^2 [m_1(E_1 + E_1') + m_2(E_2 + E_2')] \\
 & + (64\epsilon^3 + 168\epsilon^2 + 122\epsilon + 21) \mathbf{k}^2 [m_1(E_2 + E_2') + m_2(E_1 + E_1')] \\
 & + 4(8\epsilon^3 + 12\epsilon^2 - 2\epsilon - 3) (4m_1m_2(E_1^2 + E_1E_2' + E_2^2 + E_2E_1' + E_1'^2 + E_2'^2) \\
 & - (\mathbf{p}^2 + \mathbf{p}'^2) [m_1(E_1 + 2E_2 + E_1' + 2E_2') + m_2(2E_1 + E_2 + 2E_1' + E_2')]) \\
 & + (\mathbf{p}^2 + \mathbf{p}'^2)^2 \frac{m_1^2 + m_1m_2 + m_2^2}{2m_1m_2} - (64\epsilon^3 + 200\epsilon^2 + 186\epsilon + 45) (\mathbf{p}^2 + \mathbf{p}'^2) \mathbf{k}^2 \frac{m_1^2 + m_2^2}{2m_1m_2} \\
 & + 2(8\epsilon^3 + 34\epsilon^2 + 45\epsilon + 18) \mathbf{k}^4 \frac{m_1^2 + m_2^2}{m_1m_2} + (8\epsilon^2 + 10\epsilon - 3) (\mathbf{p}^2 - \mathbf{p}'^2)^2 \frac{m_1^2 + m_2^2}{m_1m_2} \\
 & \left. - (8\epsilon^2 + 19\epsilon + 9) (\mathbf{p}^2 - \mathbf{p}'^2)^2 - 6(8\epsilon^2 + 13\epsilon + 1) k_0 (\mathbf{p}^2 - \mathbf{p}'^2) (m_1 - m_2) \right] \left. \right\}
 \end{aligned}$$

$$\begin{aligned}
& + C_F n_f T_F 6(\epsilon + 1) \left[4\mathbf{k}^2(\mathbf{p}^2 + \mathbf{p}'^2) - 2(\mathbf{p}^2 - \mathbf{p}'^2)^2 - 2\mathbf{k}^4 - 8(\epsilon - 2)k_0^2 m_1 m_2 \right. \\
& \quad \left. - \mathbf{k}^4 \frac{(c_1^{hl(1)} + c_D^{(1)})m_2^2 + (c_1^{hl(2)} + c_D^{(2)})m_1^2}{m_1 m_2} - 4k_0(\mathbf{p}^2 - \mathbf{p}'^2)(m_1 - m_2) \right] \\
& + C_F^2 \left[8(16\epsilon^3 + 36\epsilon^2 + 20\epsilon + 3)\mathbf{k}^2 [(\mathbf{p}^2 + \mathbf{p}'^2) - m_1(E_1 + E'_1) - m_2(E_2 + E'_2)] \right. \\
& \quad + 8(8\epsilon^3 + 12\epsilon^2 - 2\epsilon - 3) \left(2[m_1(E_1 + E'_1) + m_2(E_2 + E'_2)](\mathbf{p}^2 + \mathbf{p}'^2) - (\mathbf{p}^2 + \mathbf{p}'^2)^2 \right. \\
& \quad \left. \left. - 4m_1 m_2 (E_1 + E'_1)(E_2 + E'_2) \right) - 4(16\epsilon^3 + 54\epsilon^2 + 59\epsilon + 21)\mathbf{k}^4 \right] \Bigg\}. \tag{F.3}
\end{aligned}$$

In the off-shell matching procedure the sum of the soft NRQCD diagrams $\Sigma^{(2)}$ is directly identified with

$$-i \left[\frac{\tilde{V}_{SI}^{(1,1)}}{m_1 m_2} + \frac{\tilde{V}_{SI}^{(2,0)}}{m_1^2} + \frac{\tilde{V}_{SI}^{(0,2)}}{m_2^2} \right]. \tag{F.4}$$

In order to obtain energy-independent potentials we have to express the energies E_i , E'_i and k_0 in $\Sigma^{(2)}$ in terms of three-momenta. We achieve this by redefining the heavy quark fields in the pNRQCD Lagrangian before projecting onto the quark-antiquark system, i.e. where the potentials are four-fermion operators (see, for instance, Eq. (42) in Ref. [103]). For an example of such a field redefinition see Eq. (B13) of Ref. [172]. At the order we are working, this can be approximated by applying the full heavy quark EOMs (and analogously for the antiquark) in the matrix elements. The EOMs read

$$\begin{aligned}
\partial_t \psi(t, \mathbf{x}_1) &= i \frac{\nabla^2}{2m_1} \psi(t, \mathbf{x}_1) - i \int d^d \mathbf{x}_2 \psi(t, \mathbf{x}_1) V^{(0)}(|\mathbf{x}_1 - \mathbf{x}_2|) \chi_c^\dagger \chi_c(t, \mathbf{x}_2) + \dots, \\
\partial_t \psi^\dagger(t, \mathbf{x}_1) &= -i \frac{\nabla^2}{2m_1} \psi^\dagger(t, \mathbf{x}_1) + i \int d^d \mathbf{x}_2 \psi^\dagger(t, \mathbf{x}_1) V^{(0)}(|\mathbf{x}_1 - \mathbf{x}_2|) \chi_c^\dagger \chi_c(t, \mathbf{x}_2) + \dots. \tag{F.5}
\end{aligned}$$

In addition to the free EOMs, they include the static potential. Higher order terms in the coupling constant g and/or in $1/m$ produce subleading effects, therefore we neglect them in Eq. (F.5) for the following discussion.

Eq. (F.5) mixes different orders in $1/m$ (and sectors with different number of heavy quarks), but still maintains the strict $1/m$ expansion in the off-shell scheme.

Replacing the heavy quark energies by means of the EOMs introduces a potential ambiguity in the determination of the $1/m^2$ potentials, since each energy E_i , E'_i can be written in terms of the others by the equality $E_1 + E_2 = E'_1 + E'_2$ (energy conservation). This can lead to different results for the individual $1/m^2$ potentials.

Consider e.g. a term proportional to

$$\begin{aligned}
& \frac{\mathbf{p}^2 - \mathbf{p}'^2}{m_1 m_2} \left[m_1(E'_1 - E_1) - m_2(E_2 - E'_2) - m_1(E_2 - E'_2) + m_2(E'_1 - E_1) \right] \\
& \rightarrow -(\mathbf{p}^2 - \mathbf{p}'^2)^2 \left(\frac{1}{2m_1^2} + \frac{1}{2m_2^2} + \frac{1}{m_1 m_2} \right) = -\frac{(\mathbf{p}^2 - \mathbf{p}'^2)^2}{2m_r^2}. \tag{F.6}
\end{aligned}$$

The first line in Eq. (F.6) is zero due to energy conservation. Therefore, we are free to add it to $\Sigma^{(2)}$. Transforming the energies E_i using Eq. (F.5) generates non-zero contributions to the off-shell terms in $V^{(2,0)}$, $V^{(0,2)}$ and $V^{(1,1)}$, as indicated by the second line in Eq. (F.6). However, using Eq. (F.5) in Eq. (F.6) also generates additional contributions to the α^3/m potentials such that physical observables, like the heavy quarkonium mass, remain unaffected by the apparent ambiguities.

In spite of this ambiguity, there are some choices that we consider more natural for the diagrams. For example, for the k_0^2 -dependent terms we use the prescription

$$\frac{k_0^2}{\mathbf{k}^4} \rightarrow -\frac{1}{4m_1m_2} \frac{(\mathbf{p}'^2 - \mathbf{p}^2)^2}{\mathbf{k}^4}. \quad (\text{F.7})$$

As shown in Appendix B of Ref. [58], this transformation does not affect the $1/m$ potential, because it is based on the continuity equation, which does not contain potential terms. It also maintains invariance under $m_1 \leftrightarrow m_2$ exchange. In CG only the last diagram contains also a dependence on the energy. In this case the energies are introduced by the gluons attached to the top line, thus we consider it more natural to remain as they are written than to use any other energy conservation on them. Applying Eq. (F.5) on this amplitude gives rise to the $1/m^2$ CG potential in Sec. 9.1. It is remarkable that this convention has exactly the same divergence scheme as the on-shell potential. It also produces an $\mathcal{O}(\alpha^3/m)$ potential coming from this diagram. Its contributions reads

$$\tilde{V}_E^{(1)} = \frac{g_B^6}{3m_r} \frac{C_F^2 C_A}{\mathbf{k}^{1-4\epsilon}} \frac{(\epsilon+1)(2\epsilon+1)(8\epsilon+1) \sin(\pi\epsilon) \Gamma\left(\frac{1}{2} - 2\epsilon\right) \Gamma(1-\epsilon) \Gamma(2\epsilon) \Gamma(4\epsilon)}{16^{3\epsilon+1} \pi^{2\epsilon+3} (1-\epsilon) \Gamma\left(2\epsilon + \frac{3}{2}\right) \Gamma(3\epsilon+1)}. \quad (\text{F.8})$$

We do not compute the $1/m$ potential explicitly in this work, but this computation would be useful for future work on this.

The energy dependence of the FG computation is more complicated. In addition to the use of Eqs. (F.5) and (F.7) we have chosen the prescriptions

$$\begin{aligned} n_f T_F k_0 (\mathbf{p}^2 - \mathbf{p}'^2) (m_1 - m_2) &\rightarrow -n_f T_F (\mathbf{p}^2 - \mathbf{p}'^2)^2, \\ C_A k_0 (\mathbf{p}^2 - \mathbf{p}'^2) (m_1 - m_2) &\rightarrow C_A \frac{3m_1^2 + 2m_1m_2 + 3m_2^2}{4m_1m_2} (\mathbf{p}^2 - \mathbf{p}'^2)^2, \end{aligned} \quad (\text{F.9})$$

for the energy dependent terms in $\Sigma_{\text{FG}}^{(2)}$ in order to obtain the concrete off-shell matching results in Eqs. (9.15)-(9.16). These prescriptions are motivated by simplicity, and the fact that the resulting off-shell potentials are finite and, therefore, do not require renormalization, see Sec. 9.4.

Finally, note that the on-shell $1/m^2$ potentials resulting from the calculation above are gauge invariant and independent of the conventions for the field redefinitions we performed.

Appendix G

The NRQCD potential

In this appendix we give some interesting expressions related to the NRQCD potential, which have been relegated from the main body of the text for reasons of compactness.

G.1 The NRQCD potential in position space

From our momentum space results we obtain the potentials in position space using Eqs. (8.59)-(8.64). For conciseness we write the coefficients in terms of the ones found in momentum space. For a given matching scheme X we have

$$D_{r,0,X}^{(1,1)}(\epsilon) = \tilde{D}_{r,0}^{(1,1)}(\epsilon) = d_{ss} + C_F d_{vs}, \quad (\text{G.1})$$

$$D_{\mathbf{p}^2,1,X}^{(2,0)}(\epsilon) = 4\pi \left(\tilde{D}_{\mathbf{p}^2,1}^{(2,0)} - 4\epsilon \tilde{D}_{\text{off},1,X}^{(2,0)} \right), \quad (\text{G.2})$$

$$D_{\mathbf{L}^2,1,X}^{(2,0)}(\epsilon) = 8\pi(1+2\epsilon)\tilde{D}_{\text{off},1,X}^{(2,0)}, \quad (\text{G.3})$$

$$D_{r,1,X}^{(2,0)}(\epsilon) = 4\pi \left(\tilde{D}_{r,1}^{(2,0)} + (1+2\epsilon)\tilde{D}_{\text{off},1,X}^{(2,0)} \right), \quad (\text{G.4})$$

$$D_{\mathbf{p}^2,1,X}^{(1,1)}(\epsilon) = 4\pi \left(\tilde{D}_{\mathbf{p}^2,1}^{(1,1)} - 4\epsilon \tilde{D}_{\text{off},1,X}^{(1,1)} \right), \quad (\text{G.5})$$

$$D_{\mathbf{L}^2,1,X}^{(1,1)}(\epsilon) = 8\pi(1+2\epsilon)\tilde{D}_{\text{off},1,X}^{(1,1)}, \quad (\text{G.6})$$

$$D_{r,1,X}^{(1,1)}(\epsilon) = 4\pi \left(\tilde{D}_{r,1}^{(1,1)} + (1+2\epsilon)\tilde{D}_{\text{off},1,X}^{(1,1)} \right), \quad (\text{G.7})$$

$$D_{\mathbf{L}^2,2,X}^{(2,0)}(\epsilon) = 8\pi \frac{1+4\epsilon}{1-\epsilon} \tilde{D}_{\text{off},2,X}^{(2,0)}, \quad (\text{G.8})$$

$$D_{\mathbf{p}^2,2,X}^{(2,0)}(\epsilon) = 4\pi \left(\tilde{D}_{\mathbf{p}^2,2}^{(2,0)} - \frac{8\epsilon}{1-\epsilon} \tilde{D}_{\text{off},2,X}^{(2,0)} \right), \quad (\text{G.9})$$

$$D_{r,2,X}^{(2,0)}(\epsilon) = 4\pi \left(\tilde{D}_{r,2}^{(2,0)} + \frac{1+3\epsilon}{1-\epsilon} \tilde{D}_{\text{off},2,X}^{(2,0)} \right), \quad (\text{G.10})$$

$$D_{\mathbf{L}^2,2,X}^{(1,1)}(\epsilon) = 8\pi \frac{1+4\epsilon}{1-\epsilon} \tilde{D}_{\text{off},2,X}^{(1,1)}, \quad (\text{G.11})$$

$$D_{\mathbf{p}^2,2,X}^{(1,1)}(\epsilon) = 4\pi \left(\tilde{D}_{\mathbf{p}^2,2}^{(1,1)} - \frac{8\epsilon}{1-\epsilon} \tilde{D}_{\text{off},2,X}^{(1,1)} \right), \quad (\text{G.12})$$

$$D_{r,2,X}^{(1,1)}(\epsilon) = 4\pi \left(\tilde{D}_{r,2}^{(1,1)} + \frac{1+3\epsilon}{1-\epsilon} \tilde{D}_{\text{off},2,X}^{(1,1)} \right), \quad (\text{G.13})$$

where X is "CG"/"FG" for the CG/FG off-shell matching scheme, "W" for the Wilson-loop scheme to be introduced in the next section, and "on-shell" for the on-shell scheme.

G.2 The static potential in momentum space

In this section we quote the values of $\tilde{D}_i^{(0)}(\epsilon)$ up to $i = 3$ in Eq. (8.35) from Ref. [37]:

$$\tilde{D}_1^{(0)}(\epsilon) = 1, \quad (\text{G.14})$$

$$\tilde{D}_2^{(0)}(\epsilon) = (4\pi)^2 (c_{11}C_A + c_{12}T_f n_f), \quad (\text{G.15})$$

$$\tilde{D}_3^{(0)}(\epsilon) = (4\pi)^4 \left(c_{21}C_A^2 + c_{22}C_A T_f n_f + c_{23}C_f T_f n_f + c_{24}T_f^2 n_f^2 \right), \quad (\text{G.16})$$

where

$$\begin{aligned} c_{11} &= -\frac{4^{-2\epsilon-3}\pi^{-\epsilon-\frac{1}{2}}(\epsilon+1)(8\epsilon+11)\csc(\pi\epsilon)}{\Gamma\left(\epsilon+\frac{5}{2}\right)}, \\ c_{12} &= \frac{2^{-4(\epsilon+1)}\pi^{-\epsilon-\frac{1}{2}}(\epsilon+1)\csc(\pi\epsilon)}{\Gamma\left(\epsilon+\frac{5}{2}\right)}, \\ c_{21} &= \frac{4^{-4\epsilon-7}\pi^{-2\epsilon}}{(1-2\epsilon)^2\Gamma(\epsilon+2)^4} \left(-\frac{16^{\epsilon+2}(2\epsilon-1)(14\epsilon^4+93\epsilon^3+144\epsilon^2+93\epsilon+33)\Gamma^2(1-\epsilon)\Gamma^8(\epsilon+2)}{\pi^4\epsilon^3(\epsilon+1)^2\Gamma^2(2\epsilon+4)} \right. \\ &\quad - \frac{16^{\epsilon+2}(4\epsilon+3)(4\epsilon+5)(4\epsilon+7)\Gamma(1-2\epsilon)\Gamma(1-\epsilon)\Gamma^2(2\epsilon+4)\Gamma^5(\epsilon+2)}{\pi^4\epsilon^3(\epsilon+1)^2(2\epsilon+1)^2(2\epsilon+3)^2\Gamma(4\epsilon+8)} \\ &\quad \times \left(16\epsilon^5 + 72\epsilon^4 + 172\epsilon^3 + 138\epsilon^2 - 4\epsilon - 11 \right) \\ &\quad + \frac{3 \cdot 2^{4\epsilon+7}\Gamma(1-2\epsilon)\Gamma^7(\epsilon+2)}{\pi^4\epsilon^3(\epsilon+1)^2(2\epsilon+1)^2(2\epsilon+3)^2\Gamma(3\epsilon+4)} \\ &\quad \times \left(864\epsilon^9 + 4272\epsilon^8 + 8032\epsilon^7 + 7128\epsilon^6 + 3374\epsilon^5 + 1899\epsilon^4 + 1549\epsilon^3 + 405\epsilon^2 - 171\epsilon - 66 \right) \\ &\quad + \frac{3 \cdot 4^{2\epsilon+5}(6\epsilon+1)(6\epsilon+5)(6\epsilon+7)(6\epsilon+11)\Gamma^3(2\epsilon+4)\Gamma(3\epsilon+6)\Gamma(1-2\epsilon)\Gamma(\epsilon+2)}{(2\epsilon+3)(2\pi\epsilon+\pi)^2\Gamma(6(\epsilon+2))} \\ &\quad \left. + \frac{4(\epsilon+1)^2(2\epsilon-1)(6\epsilon+1)\Gamma^2(2\epsilon+4)\Gamma^2(1-2\epsilon)}{(2\epsilon+1)^2(2\epsilon+3)^2\Gamma(1-\epsilon)^2} \right), \\ c_{22} &= \frac{(4\pi)^{-2(\epsilon+2)}\Gamma(\epsilon+2)}{\epsilon^3(\epsilon+1)^2} \left(\frac{8(4\epsilon^4+12\epsilon^3+9\epsilon^2+13\epsilon+6)\Gamma^2(1-\epsilon)\Gamma^3(\epsilon+2)}{\Gamma(2\epsilon+4)^2} \right. \\ &\quad - \frac{8(4\epsilon+3)(4\epsilon+5)(4\epsilon+7)(2\epsilon^2+7\epsilon+2)\Gamma(1-2\epsilon)\Gamma(1-\epsilon)\Gamma^2(2\epsilon+4)}{(4\epsilon^2+8\epsilon+3)^2\Gamma(4\epsilon+8)} \\ &\quad \left. - \frac{12\epsilon(112\epsilon^5+500\epsilon^4+864\epsilon^3+729\epsilon^2+294\epsilon+44)\Gamma(1-2\epsilon)\Gamma^2(\epsilon+2)}{(4\epsilon^2+8\epsilon+3)^2\Gamma(3\epsilon+4)} \right), \\ c_{23} &= \frac{3 \cdot 2^{-4(\epsilon+1)}\pi^{-2\epsilon-3}}{\epsilon^2\Gamma(2\epsilon+4)^2\Gamma(3\epsilon+4)} \left(2(2\epsilon+1)(\epsilon(\epsilon+2)+2)\csc(2\pi\epsilon)\Gamma^3(\epsilon+2)\Gamma(2\epsilon+4) \right. \\ &\quad \left. - \pi\epsilon(\epsilon+1)^4(2\epsilon+3)(2\epsilon^2+\epsilon+2)\csc^2(\pi\epsilon)\Gamma^2(\epsilon+1)\Gamma(3\epsilon+3) \right), \\ c_{24} &= \frac{2^{-8(\epsilon+1)}\pi^{-2\epsilon-1}(\epsilon+1)^2\csc^2(\pi\epsilon)}{\Gamma\left(\epsilon+\frac{5}{2}\right)^2}. \end{aligned}$$

(G.17)

G.3 The renormalized potential in momentum space

We can transform the expressions in Eqs. (9.77)-(9.98), back to momentum space. With the definitions in Eqs. (8.38) and (8.39) we then obtain

$$\begin{aligned} \tilde{D}_r^{(2,0),\overline{\text{MS}}}(\mathbf{k}) &= \frac{C_F \pi \alpha_s(\mathbf{k})}{2} \left\{ c_D^{(1)} + \frac{\alpha_s}{\pi} \left[\left(\frac{1}{3} + \frac{13}{36} c_F^{(1)2} \right) C_A - \frac{5}{9} \left(c_1^{hl(1)} + c_D^{(1)} \right) T_F n_f \right. \right. \\ &\quad \left. \left. + \left(-C_A \left(2 + \frac{5}{12} c_F^{(1)2} - \frac{11}{12} c_D^{(1)} \right) + \frac{1}{3} c_1^{hl(1)} T_F n_f \right) \ln \left(\frac{\mathbf{k}^2}{\nu^2} \right) \right] \right\}, \end{aligned} \quad (\text{G.18})$$

$$\tilde{D}_{\mathbf{p}^2}^{(2,0),\overline{\text{MS}}}(\mathbf{k}) = \frac{2C_F C_A \alpha_s^2}{3} \ln \left(\frac{\mathbf{k}^2}{\nu^2} \right), \quad (\text{G.19})$$

$$\begin{aligned} \tilde{D}_r^{(1,1),\overline{\text{MS}}}(\mathbf{k}) &= \pi C_F \alpha_s(\mathbf{k}) \left(1 + \frac{\alpha_s}{4\pi} \left\{ a_1 - \frac{1}{3} C_A + \frac{4}{3} C_F + \left(-\frac{11}{3} C_A + \frac{28}{3} C_F \right) \ln \left(\frac{\mathbf{k}^2}{\nu^2} \right) \right\} \right) \\ &\quad + C_F d_{vs} + d_{ss}, \end{aligned} \quad (\text{G.20})$$

$$\tilde{D}_{\mathbf{p}^2}^{(1,1),\overline{\text{MS}}}(\mathbf{k}) = -4\pi C_F \alpha_s(\mathbf{k}) \left(1 + \frac{\alpha_s}{4\pi} \left\{ a_1 - \frac{4}{3} C_A \ln \left(\frac{\mathbf{k}^2}{\nu^2} \right) \right\} \right). \quad (\text{G.21})$$

The coefficients \tilde{D}_{off} and $\tilde{D}^{(1,0)}$ depend on the matching scheme. For the cases we consider we find

$$\tilde{D}_{\text{off,CG}}^{(2,0),\overline{\text{MS}}}(\mathbf{k}) = C_F C_A \alpha_s^2 \left(\frac{1}{2} - \frac{4}{3} \ln 2 \right), \quad (\text{G.22})$$

$$\tilde{D}_{\text{off,CG}}^{(1,1),\overline{\text{MS}}}(\mathbf{k}) = C_F \pi \alpha_s(\mathbf{k}) \left(1 + \frac{\alpha_s}{4\pi} \left\{ a_1 + 4C_A + \beta_0 - \frac{32}{3} C_A \ln 2 \right\} \right), \quad (\text{G.23})$$

$$\begin{aligned} \tilde{D}_{\text{CG}}^{(1,0),\overline{\text{MS}}}(\mathbf{k}) &= -\frac{C_F C_A \alpha_s^2(\mathbf{k}) \pi^2}{2} \left\{ 1 + \frac{\alpha_s}{\pi} \left[\frac{89}{36} C_A - \frac{49}{36} T_F n_f - \frac{8}{3} \ln 2 \right. \right. \\ &\quad \left. \left. - \frac{2}{3} (C_A + 2C_F) \ln \left(\frac{\mathbf{k}^2}{\nu^2} \right) \right] \right\}, \end{aligned} \quad (\text{G.24})$$

$$\tilde{D}_{\text{off,FG}}^{(2,0),\overline{\text{MS}}}(\mathbf{k}) = \tilde{D}_{\text{off,CG}}^{(2,0),\overline{\text{MS}}}(\mathbf{k}) + \alpha_s^2 \frac{2}{3} C_F C_A \left(2 \ln 2 + \frac{35}{16} \right), \quad (\text{G.25})$$

$$\tilde{D}_{\text{off,FG}}^{(1,1),\overline{\text{MS}}}(\mathbf{k}) = \tilde{D}_{\text{off,CG}}^{(1,1),\overline{\text{MS}}}(\mathbf{k}) + \alpha_s^2 \frac{4}{3} C_F C_A \left(2 \ln 2 + \frac{35}{16} \right), \quad (\text{G.26})$$

$$\tilde{D}_{\text{FG}}^{(1,0),\overline{\text{MS}}}(\mathbf{k}) = \tilde{D}_{\text{CG}}^{(1,0),\overline{\text{MS}}}(\mathbf{k}) - \pi \alpha_s^3 \frac{2}{3} C_F^2 C_A \left(2 \ln 2 + \frac{35}{16} \right), \quad (\text{G.27})$$

$$\tilde{D}_{\text{off,W}}^{(2,0),\overline{\text{MS}}}(\mathbf{k}) = -\frac{1}{6} C_F C_A \alpha_s^2 \left(1 - 4 \ln \left(\frac{\mathbf{k}^2}{\nu^2} \right) \right), \quad (\text{G.28})$$

$$\tilde{D}_{\text{off,W}}^{(1,1),\overline{\text{MS}}}(\mathbf{k}) = C_F \alpha_s(\mathbf{k}) \pi \left\{ 1 + \frac{\alpha_s}{\pi} \left[\frac{13C_A}{9} - \frac{8T_F n_f}{9} + \frac{4}{3} C_A \ln \left(\frac{\mathbf{k}^2}{\nu^2} \right) \right] \right\}, \quad (\text{G.29})$$

$$\tilde{D}_W^{(1,0),\overline{\text{MS}}}(\mathbf{k}) = -\frac{C_F C_A \alpha_s^2(\mathbf{k}) \pi^2}{2} \left\{ 1 + \frac{\alpha_s}{\pi} \left[\frac{89}{36} C_A - \frac{49}{36} T_F n_f - \frac{2}{3} C_A \ln \left(\frac{\mathbf{k}^2}{\nu^2} \right) \right] \right\}. \quad (\text{G.30})$$

Finally, in the on-shell scheme (where obviously $\tilde{D}_{\text{off,on-shell}}^{(2,0),\overline{\text{MS}}}(\mathbf{k}) = 0$), we have

$$\begin{aligned} \frac{\tilde{D}_{\text{on-shell}}^{(1,0),\overline{\text{MS}}}(\mathbf{k})}{m_1} + \frac{\tilde{D}_{\text{on-shell}}^{(0,1),\overline{\text{MS}}}(\mathbf{k})}{m_2} &= C_F^2 \pi^2 \alpha_s^2(\mathbf{k}) \frac{m_r}{m_1 m_2} \left(1 + \frac{\alpha_s}{2\pi} (a_1 - \beta_0) \right) \\ &- \frac{C_F C_A \pi^2 \alpha_s^2(\mathbf{k})}{2m_r} \left\{ 1 + \frac{\alpha_s}{\pi} \left(\frac{89}{36} C_A - \frac{49}{36} T_F n_f - C_F - \frac{2}{3} (C_A + 2C_F) \ln \left(\frac{\mathbf{k}^2}{\nu^2} \right) \right) \right\}. \end{aligned} \quad (\text{G.31})$$

Note that this is not the result one obtains by just subtracting the $1/\epsilon$ poles in momentum space (which is what it is usually named $\overline{\text{MS}}$ scheme). This renormalization scheme would complicate the (ultrasoft part of the) bound state calculation for the spectrum. For our purposes, it is more convenient to do the subtraction in position space, and the prescription we have proposed here is particularly useful, because it avoids spurious logarithms of \mathbf{k}^2 . We will refer to it as $\overline{\text{MS}}$ scheme here. In this way we can efficiently carry out the bound state computations in four dimensions.

For completeness of the momentum space representation we quote here the results for the spin-dependent potential, which in momentum space we write as:

$$\tilde{V}_{SD}^{(2,0)} = \tilde{D}_{\Lambda_{11}}^{(2,0)} \Lambda_{11}(\mathbf{k}), \quad (\text{G.32})$$

$$\tilde{V}_{SD}^{(0,2)} = -\tilde{D}_{\Lambda_{22}}^{(0,2)} \Lambda_{22}(\mathbf{k}), \quad (\text{G.33})$$

$$\tilde{V}_{SD}^{(1,1)} = -\tilde{D}_{\Lambda_{12}}^{(1,1)} \Lambda_{12}(\mathbf{k}) + \tilde{D}_{\Lambda_{21}}^{(1,1)} \Lambda_{21}(\mathbf{k}) + \tilde{D}_T^{(1,1)} T(\mathbf{k}) + \tilde{D}_{S_1 S_2}^{(1,1)} \mathbf{S}_1 \cdot \mathbf{S}_2, \quad (\text{G.34})$$

where $\Lambda_{ij}(\mathbf{k}) \equiv -i\mathbf{S}_i \cdot \frac{\mathbf{k} \times \mathbf{p}_j}{\mathbf{k}^2}$, $T \equiv 4 \frac{\mathbf{S}_1 \cdot \mathbf{S}_2 \mathbf{k}^2 - 3(\mathbf{S}_1 \cdot \mathbf{k})(\mathbf{S}_2 \cdot \mathbf{k})}{\mathbf{k}^2}$ and the renormalized potentials read:

$$\tilde{D}_{\Lambda_{11}}^{(2,0),\overline{\text{MS}}} = -2\pi \alpha_s(\mathbf{k}) C_F \left\{ c_S^{(1)} - \frac{\alpha_s}{2\pi} \left(C_A \left(\frac{5}{18} - \ln \left(\frac{\mathbf{k}^2}{\nu^2} \right) \right) + \frac{10T_F n_f}{9} \right) \right\}, \quad (\text{G.35})$$

$$\tilde{D}_{\Lambda_{22}}^{(0,2),\overline{\text{MS}}} = \tilde{D}_{\Lambda_{11}}^{(2,0)}((1) \rightarrow (2)), \quad (\text{G.36})$$

$$\tilde{D}_{\Lambda_{12}}^{(1,1),\overline{\text{MS}}} = -4\pi \alpha_s(\mathbf{k}) C_F \left\{ c_F^{(1)} + \frac{\alpha_s}{4\pi} \left(C_A \left(\ln \left(\frac{\mathbf{k}^2}{\nu^2} \right) + \frac{13}{9} \right) - \frac{20T_F n_f}{9} \right) \right\}, \quad (\text{G.37})$$

$$\tilde{D}_{\Lambda_{21}}^{(1,1),\overline{\text{MS}}} = \tilde{D}_{\Lambda_{12}}^{(1,1)}((1) \rightarrow (2)), \quad (\text{G.38})$$

$$\tilde{D}_T^{(1,1),\overline{\text{MS}}} = \frac{\pi C_F \alpha_s(\mathbf{k})}{3} \left\{ c_F^{(1)} c_F^{(2)} + \frac{\alpha_s}{2\pi} \left(C_A \left(\ln \left(\frac{\mathbf{k}^2}{\nu^2} \right) + \frac{13}{18} \right) - \frac{10T_F n_f}{9} \right) \right\} \quad (\text{G.39})$$

$$\begin{aligned} \tilde{D}_{S_1 S_2}^{(1,1),\overline{\text{MS}}} &= -4(C_F d_{vv} + d_{sv}) \\ &+ \frac{8\pi C_F \alpha_s(\mathbf{k})}{3} \left\{ c_F^{(1)} c_F^{(2)} + \frac{\alpha_s}{2\pi} \left(\frac{7}{4} C_A \left(\ln \left(\frac{\mathbf{k}^2}{\nu^2} \right) - \frac{4}{9} \right) - \frac{10T_F n_f}{9} \right) \right\}. \end{aligned} \quad (\text{G.40})$$

Finally, the renormalized static potential is known up to three loops and, as defined in Eq. (8.35), reads:

$$\tilde{D}^{(0)}(\mathbf{k}) = 4\pi C_f \alpha_s(\mathbf{k}) \left\{ 1 + \frac{\alpha_s(\mathbf{k})}{4\pi} a_1 + \left(\frac{\alpha_s(\mathbf{k})}{4\pi} \right)^2 a_2 + \left(\frac{\alpha_s(\mathbf{k})}{4\pi} \right)^3 \left(a_3 - 8\pi^2 C_A^3 \ln \left(\frac{\mathbf{k}^2}{\nu^2} \right) \right) + \dots \right\}, \quad (\text{G.41})$$

where (from RG arguments),

$$\alpha_s(\mathbf{k}) = \alpha_s \left\{ 1 - \frac{\alpha_s}{4\pi} \beta_0 \ln \left(\frac{\mathbf{k}^2}{\nu^2} \right) - \left(\frac{\alpha_s}{4\pi} \right)^2 \left(\beta_1 - \beta_0^2 \ln \left(\frac{\mathbf{k}^2}{\nu^2} \right) \right) \ln \left(\frac{\mathbf{k}^2}{\nu^2} \right) - \left(\frac{\alpha_s}{4\pi} \right)^3 \left(\beta_2 - \frac{5}{2} \beta_0 \beta_1 \ln \left(\frac{\mathbf{k}^2}{\nu^2} \right) + \beta_0^3 \ln^2 \left(\frac{\mathbf{k}^2}{\nu^2} \right) \right) \ln \left(\frac{\mathbf{k}^2}{\nu^2} \right) + \dots \right\}. \quad (\text{G.42})$$

Appendix H

Expectation values

H.1 List of expectation values of single potential insertions

Throughout this chapter we display the results for a system bounded by QCD. In order to obtain the equivalent QED results one should exchange $\alpha_s \rightarrow \alpha$ and set $C_F = 1$. For the computation of the spectrum we have used the following expectation values of the relevant operators:

$$\langle n l | \mathbf{p}^4 | n l \rangle = \frac{(m_r C_F \alpha_s)^4}{n^4} \left(\frac{8n}{2l+1} - 3 \right), \quad (\text{H.1})$$

$$\langle n l | \left\{ \frac{1}{2r}, \mathbf{p}^2 \right\} | n l \rangle = -(m_r C_F \alpha_s)^3 \left(\frac{1}{n^4} - \frac{4}{(2l+1)n^3} \right), \quad (\text{H.2})$$

$$\begin{aligned} \langle n l | \left\{ \frac{\ln(re^{\gamma_E})}{2r}, \mathbf{p}^2 \right\} | n l \rangle &= -\frac{(m_r C_F \alpha_s)^3}{n^4(2l+1)} \left[(2l+1-4n) \ln \frac{na}{2} \right. \\ &\quad \left. + (2l+1+4n)S_1(n+l) - 4n(S_1(2l+1) + S_1(2l)) \right], \end{aligned} \quad (\text{H.3})$$

$$\langle n l | \frac{1}{r^3} \mathbf{L}^2 | n l \rangle = (m_r C_F \alpha_s)^3 \frac{2}{(2l+1)n^3} (1 - \delta_{l0}), \quad (\text{H.4})$$

$$\begin{aligned} \langle n l | \frac{\ln(re^{\gamma_E})}{r^3} \mathbf{L}^2 | n l \rangle &= \frac{2(m_r C_F \alpha_s)^3}{n^3(2l+1)} (1 - \delta_{l0}) \left[\ln \frac{na}{2} \right. \\ &\quad \left. - S_1(n+l) + S_1(2l+2) + S_1(2l-1) - \frac{n-l-1/2}{n} \right], \end{aligned} \quad (\text{H.5})$$

$$\langle n l | \delta^{(3)}(\mathbf{r}) | n l \rangle = \frac{(m_r C_F \alpha_s)^3}{\pi n^3} \delta_{l0}, \quad (\text{H.6})$$

$$\begin{aligned} \langle n l | \text{reg} \frac{1}{r^3} | n l \rangle &= \frac{2(m_r C_F \alpha_s)^3}{n^3} \left[\left(\ln \frac{na}{2} - S_1(n) - \frac{n-1}{2n} \right) 2\delta_{l0} \right. \\ &\quad \left. + \frac{1 - \delta_{l0}}{l(l+1)(2l+1)} \right], \end{aligned} \quad (\text{H.7})$$

$$\langle n l | \frac{1}{r} | n l \rangle = \frac{m_r C_F \alpha_s}{n^2}, \quad (\text{H.8})$$

$$\langle n l | \frac{\ln(re^{\gamma_E})}{r} | n l \rangle = \frac{m_r C_F \alpha_s}{n^2} \left(\ln \frac{na}{2} + S_1(n+l) \right), \quad (\text{H.9})$$

$$\langle n l | \frac{1}{r^2} | n l \rangle = \frac{2(m_r C_F \alpha_s)^2}{n^3(2l+1)}, \quad (\text{H.10})$$

$$\langle n l | \frac{\ln(re^{\gamma E})}{r^2} | n l \rangle = \frac{2(m_r C_F \alpha_s)^2}{n^3(2l+1)} \left[\ln \frac{na}{2} - S_1(n+l) + S_1(2l+1) + S_1(2l) \right], \quad (\text{H.11})$$

$$\langle n l | \frac{1}{r^3} | n l \rangle = \frac{2(m_r C_F \alpha_s)^3}{n^3 l(2l+1)(l+1)} (1 - \delta_{l0}), \quad (\text{H.12})$$

$$\begin{aligned} \langle n l | \frac{\ln(re^{\gamma E})}{r^3} | n l \rangle &= \frac{2(m_r C_F \alpha_s)^3 (1 - \delta_{l0})}{n^3 l(2l+1)(l+1)} \left[\ln \frac{na}{2} \right. \\ &\quad \left. - S_1(n+l) + S_1(2l+2) + S_1(2l-1) - \frac{n-l-1/2}{n} \right], \end{aligned} \quad (\text{H.13})$$

$$\langle n l | \delta^{(3)}(\mathbf{r}) \mathbf{S}^2 | n l \rangle = s(s+1) \frac{(m_r C_F \alpha_s)^3}{\pi n^3} \delta_{l0}, \quad (\text{H.14})$$

$$\begin{aligned} \langle n l | \text{reg} \frac{1}{r^3} \mathbf{S}^2 | n l \rangle &= \\ s(s+1) \frac{2(m_r C_F \alpha_s)^3}{n^3} &\left[\left(\ln \frac{na}{2} - S_1(n) - \frac{n-1}{2n} \right) 2\delta_{l0} + \frac{(1-\delta_{l0})}{l(l+1)(2l+1)} \right], \end{aligned} \quad (\text{H.15})$$

$$\langle n l | \delta^{(3)}(\mathbf{r}) \mathbf{S}_1 \cdot \mathbf{S}_2 | n l \rangle = \mathcal{S}_{12} \frac{(m_r C_F \alpha_s)^3}{\pi n^3} \delta_{l0}, \quad (\text{H.16})$$

$$\begin{aligned} \langle n l | \text{reg} \frac{1}{r^3} \mathbf{S}_1 \cdot \mathbf{S}_2 | n l \rangle &= \\ \mathcal{S}_{12} \frac{2(m_r C_F \alpha_s)^3}{n^3} &\left[\left(\ln \frac{na}{2} - S_1(n) - \frac{n-1}{2n} \right) 2\delta_{l0} + \frac{(1-\delta_{l0})}{l(l+1)(2l+1)} \right], \end{aligned} \quad (\text{H.17})$$

$$\langle n l | \frac{1}{r^3} \mathbf{L} \cdot \mathbf{S} | n l \rangle = X_{LS} \frac{2(m_r C_F \alpha_s)^3}{l(l+1)(2l+1)n^3} (1 - \delta_{l0}), \quad (\text{H.18})$$

$$\langle n l | \frac{1}{r^3} \mathbf{L} \cdot \mathbf{S}_1 | n l \rangle = X_{LS_1} \frac{2(m_r C_F \alpha_s)^3}{l(l+1)(2l+1)n^3} (1 - \delta_{l0}), \quad (\text{H.19})$$

$$\langle n l | \frac{1}{r^3} \mathbf{L} \cdot \mathbf{S}_2 | n l \rangle = X_{LS_2} \frac{2(m_r C_F \alpha_s)^3}{l(l+1)(2l+1)n^3} (1 - \delta_{l0}), \quad (\text{H.20})$$

$$\begin{aligned} \langle n l | \frac{\ln(re^{\gamma E})}{r^3} \mathbf{L} \cdot \mathbf{S} | n l \rangle &= X_{LS} \frac{2(m_r C_F \alpha_s)^3 (1 - \delta_{l0})}{n^3 l(2l+1)(l+1)} \\ &\times \left(\ln \frac{na}{2} - S_1(n+l) + S_1(2l+2) + S_1(2l-1) - \frac{n-l-1/2}{n} \right), \end{aligned} \quad (\text{H.21})$$

$$\begin{aligned} \langle n l | \frac{\ln(re^{\gamma E})}{r^3} \mathbf{L} \cdot \mathbf{S}_1 | n l \rangle &= X_{LS_1} \frac{2(m_r C_F \alpha_s)^3 (1 - \delta_{l0})}{n^3 l(2l+1)(l+1)} \\ &\times \left(\ln \frac{na}{2} - S_1(n+l) + S_1(2l+2) + S_1(2l-1) - \frac{n-l-1/2}{n} \right), \end{aligned} \quad (\text{H.22})$$

$$\begin{aligned} \langle n l | \frac{\ln(re^{\gamma E})}{r^3} \mathbf{L} \cdot \mathbf{S}_2 | n l \rangle &= X_{LS_2} \frac{2(m_r C_F \alpha_s)^3 (1 - \delta_{l0})}{n^3 l(2l+1)(l+1)} \\ &\times \left(\ln \frac{na}{2} - S_1(n+l) + S_1(2l+2) + S_1(2l-1) - \frac{n-l-1/2}{n} \right), \end{aligned} \quad (\text{H.23})$$

$$\langle n l | \frac{S_{12}(\mathbf{r})}{r^3} | n l \rangle = D_S \frac{4(m_r C_F \alpha_s)^3}{n^3 l(2l+1)(l+1)} (1 - \delta_{l0}), \quad (\text{H.24})$$

$$\begin{aligned} \langle n l | \frac{S_{12}(\mathbf{r}) \ln(re^{\gamma E})}{r^3} | n l \rangle &= D_S \frac{4(m_r C_F \alpha_s)^3 (1 - \delta_{l0})}{n^3 l(2l+1)(l+1)} \\ &\times \left(\ln \frac{na}{2} - S_1(n+l) + S_1(2l+2) + S_1(2l-1) - \frac{n-l-1/2}{n} \right), \end{aligned} \quad (\text{H.25})$$

with

$$\mathcal{S}_{12} \equiv \langle \mathbf{S}_1 \cdot \mathbf{S}_2 \rangle = \frac{1}{2} (s(s+1) - s_1(s_1+1) - s_2(s_2+1)), \quad (\text{H.26})$$

$$D_S \equiv \frac{1}{2} \langle S_{12}(\mathbf{r}) \rangle = \frac{2l(l+1)s(s+1) - 3X_{LS} - 6X_{LS}^2}{(2l-1)(2l+3)}, \quad (\text{H.27})$$

$$X_{LS} \equiv \langle \mathbf{L} \cdot \mathbf{S} \rangle = \frac{1}{2} [j(j+1) - l(l+1) - s(s+1)], \quad (\text{H.28})$$

$$X_{LS_i} \equiv \langle \mathbf{L} \cdot \mathbf{S}_i \rangle = \frac{1}{2} [j_i(j_i+1) - l(l+1) - s_i(s_i+1)], \quad (\text{H.29})$$

and where $a = 1/(m_r C_F \alpha_s)$, $\mathbf{S} = \mathbf{S}_1 + \mathbf{S}_2$, $\mathbf{J} = \mathbf{L} + \mathbf{S}$, $\mathbf{J}_i = \mathbf{L} + \mathbf{S}_i$. In our notation, the ill-defined quantity $(1 - \delta_{l0})/l \rightarrow 0$ when $l \rightarrow 0$.

H.2 List of expectation values of double potential insertions

Here we list the expectation values of the double potential insertions relevant for our computation:

$$\langle n l | \frac{1}{r} \frac{1}{(E_n^C - h)'} \frac{1}{r} | n l \rangle = -\frac{m_r}{2n^2}, \quad (\text{H.30})$$

$$\langle n l | \frac{1}{r} \frac{1}{(E_n^C - h)'} \frac{1}{r^2} | n l \rangle = -\frac{2\alpha_s C_F m_r^2}{(2l+1)n^3}, \quad (\text{H.31})$$

$$\langle n l | \frac{1}{r} \frac{1}{(E_n^C - h)'} \frac{1}{r^3} | n l \rangle = -\frac{3\alpha_s^2 C_F^2 m_r^3 (1 - \delta_{l0})}{l(l+1)(2l+1)n^3}, \quad (\text{H.32})$$

$$\langle n l | \frac{1}{r} \frac{1}{(E_n^C - h)'} \delta^3(\mathbf{r}) | n l \rangle = -\frac{3\alpha_s^2 C_F^2 m_r^3}{2\pi n^3} \delta_{l0}, \quad (\text{H.33})$$

$$\langle n l | \frac{\ln(re^{\gamma_E})}{r} \frac{1}{(E_n^C - h)'} \frac{1}{r} | n l \rangle = -\frac{m_r}{2n^2} \left(\ln \frac{na}{2} + S_1(n+l) - 1 \right), \quad (\text{H.34})$$

$$\begin{aligned} \langle n l | \frac{\ln(re^{\gamma_E})}{r} \frac{1}{(E_n^C - h)'} \frac{1}{r^2} | n l \rangle &= \frac{2\alpha_s C_F m_r^2}{(2l+1)n^3} \left[\frac{1}{2} + n \left(\frac{\pi^2}{6} - \Sigma_2^{(k)}(n, l) - \Sigma_2^{(m)}(n, l) \right) \right. \\ &\quad \left. - \ln \frac{na}{2} - S_1(n+l) \right], \end{aligned} \quad (\text{H.35})$$

$$\begin{aligned} \langle n l | \frac{\ln(re^{\gamma_E})}{r} \frac{1}{(E_n^C - h)'} \frac{1}{r^3} | n l \rangle &= \frac{2\alpha_s^2 C_F^2 m_r^3 (1 - \delta_{l0})}{l(l+1)(2l+1)n^3} \left[\frac{1}{2} - \frac{3}{2} \ln \frac{na}{2} - \frac{3}{2} S_1(n+l) \right. \\ &\quad \left. + \Sigma_1^{(m)}(n, l) + l \left(\Sigma_1^{(m)}(n, l) + \Sigma_1^{(k)}(n, l) \right) + \frac{n\pi^2}{6} - n \left(\Sigma_2^{(m)}(n, l) + \Sigma_2^{(k)}(n, l) \right) \right], \end{aligned} \quad (\text{H.36})$$

$$\begin{aligned} \langle n l | \frac{\ln(re^{\gamma_E})}{r} \frac{1}{(E_n^C - h)'} \delta^3(\mathbf{r}) | n l \rangle &= \\ &= \frac{\alpha_s^2 C_F^2 m_r^3 \delta_{l0}}{\pi n^3} \left[\frac{1}{2} + \frac{n\pi^2}{6} - n \Sigma_2^{(k)}(n, 0) - \frac{3}{2} \ln \frac{na}{2} - \frac{3}{2} S_1(n) \right]. \end{aligned} \quad (\text{H.37})$$

Bibliography

- [1] M. Gell-Mann, “A Schematic Model of Baryons and Mesons,” *Phys. Lett.*, vol. 8, pp. 214–215, 1964.
- [2] G. Zweig, “An SU(3) model for strong interaction symmetry and its breaking. Version 2,” in *Developments in the quark theory of hadrons. Vol. 1. 1964 - 1978* (D. Lichtenberg and S. P. Rosen, eds.), pp. 22–101, 1964.
- [3] D. J. Gross and F. Wilczek, “Ultraviolet Behavior of Nonabelian Gauge Theories,” *Phys. Rev. Lett.*, vol. 30, pp. 1343–1346, 1973.
- [4] H. D. Politzer, “Reliable Perturbative Results for Strong Interactions?,” *Phys. Rev. Lett.*, vol. 30, pp. 1346–1349, 1973.
- [5] S. Weinberg, “Phenomenological Lagrangians,” *Physica*, vol. A96, p. 327, 1979.
- [6] J. Gasser and H. Leutwyler, “Chiral Perturbation Theory to One Loop,” *Annals Phys.*, vol. 158, p. 142, 1984.
- [7] E. E. Jenkins and A. V. Manohar, “Baryon chiral perturbation theory using a heavy fermion Lagrangian,” *Phys. Lett.*, vol. B255, pp. 558–562, 1991.
- [8] V. Bernard, N. Kaiser, J. Kambor, and U. G. Meissner, “Chiral structure of the nucleon,” *Nucl. Phys.*, vol. B388, pp. 315–345, 1992.
- [9] R. F. Dashen, E. E. Jenkins, and A. V. Manohar, “The $1/N(c)$ expansion for baryons,” *Phys. Rev.*, vol. D49, p. 4713, 1994. [Erratum: *Phys. Rev.*D51,2489(1995)].
- [10] N. Isgur and M. B. Wise, “Weak Decays of Heavy Mesons in the Static Quark Approximation,” *Phys. Lett.*, vol. B232, pp. 113–117, 1989.
- [11] E. Eichten and B. R. Hill, “An Effective Field Theory for the Calculation of Matrix Elements Involving Heavy Quarks,” *Phys. Lett.*, vol. B234, p. 511, 1990.
- [12] H. Georgi, “An Effective Field Theory for Heavy Quarks at Low-energies,” *Phys. Lett.*, vol. B240, pp. 447–450, 1990.
- [13] B. Grinstein, R. P. Springer, and M. B. Wise, “Strong Interaction Effects in Weak Radiative B Meson Decay,” *Nucl. Phys.*, vol. B339, pp. 269–309, 1990.
- [14] W. E. Caswell and G. P. Lepage, “Effective Lagrangians for Bound State Problems in QED, QCD, and Other Field Theories,” *Phys. Lett.*, vol. B167, p. 437, 1986.

- [15] A. Pineda and J. Soto, “Effective field theory for ultrasoft momenta in NRQCD and NRQED,” *Nucl. Phys. Proc. Suppl.*, vol. 64, pp. 428–432, 1998.
- [16] E. E. Chambers and R. Hofstadter, “Structure of the Proton,” *Phys. Rev.*, vol. 103, pp. 1454–1463, 1956.
- [17] J. C. Bernauer *et al.*, “Electric and magnetic form factors of the proton,” *Phys. Rev.*, vol. C90, no. 1, p. 015206, 2014.
- [18] P. J. Mohr, B. N. Taylor, and D. B. Newell, “CODATA Recommended Values of the Fundamental Physical Constants: 2010,” *Rev. Mod. Phys.*, vol. 84, pp. 1527–1605, 2012.
- [19] T. Lyman, “The Spectrum of Hydrogen in the Region of Extremely Short Wave-Lengths,” *Astrophysical J.*, vol. 23, p. 181, 1906.
- [20] A. Antognini *et al.*, “Proton Structure from the Measurement of $2S - 2P$ Transition Frequencies of Muonic Hydrogen,” *Science*, vol. 339, pp. 417–420, 2013.
- [21] J. E. Augustin *et al.*, “Discovery of a Narrow Resonance in $e^+ e^-$ Annihilation,” *Phys. Rev. Lett.*, vol. 33, pp. 1406–1408, 1974. [Adv. Exp. Phys.5,141(1976)].
- [22] J. J. Aubert *et al.*, “Experimental Observation of a Heavy Particle J,” *Phys. Rev. Lett.*, vol. 33, pp. 1404–1406, 1974.
- [23] S. W. Herb *et al.*, “Observation of a Dimuon Resonance at 9.5-GeV in 400-GeV Proton-Nucleus Collisions,” *Phys. Rev. Lett.*, vol. 39, pp. 252–255, 1977.
- [24] F. Abe *et al.*, “Observation of top quark production in $\bar{p}p$ collisions,” *Phys. Rev. Lett.*, vol. 74, pp. 2626–2631, 1995.
- [25] N. Brambilla *et al.*, “QCD and Strongly Coupled Gauge Theories: Challenges and Perspectives,” *Eur. Phys. J.*, vol. C74, no. 10, p. 2981, 2014.
- [26] N. Brambilla *et al.*, “Heavy quarkonium: progress, puzzles, and opportunities,” *Eur. Phys. J.*, vol. C71, p. 1534, 2011.
- [27] N. Brambilla *et al.*, “Heavy quarkonium physics,” 2004.
- [28] S. Weinberg, “Nonlinear realizations of chiral symmetry,” *Phys. Rev.*, vol. 166, pp. 1568–1577, 1968.
- [29] E. E. Jenkins and A. V. Manohar, “Chiral corrections to the baryon axial currents,” *Phys. Lett.*, vol. B259, pp. 353–358, 1991.
- [30] T. R. Hemmert, B. R. Holstein, and J. Kambor, “Systematic $1/M$ expansion for spin $3/2$ particles in baryon chiral perturbation theory,” *Phys. Lett.*, vol. B395, pp. 89–95, 1997.
- [31] T. R. Hemmert, B. R. Holstein, and J. Kambor, “Chiral Lagrangians and $\delta(1232)$ interactions: Formalism,” *J. Phys.*, vol. G24, pp. 1831–1859, 1998.
- [32] R. F. Dashen and A. V. Manohar, “ $1/N(c)$ corrections to the baryon axial currents in QCD,” *Phys. Lett.*, vol. B315, pp. 438–440, 1993.

-
- [33] E. E. Salpeter and H. A. Bethe, “A Relativistic equation for bound state problems,” *Phys. Rev.*, vol. 84, pp. 1232–1242, 1951.
- [34] C. Itzykson and J. B. Zuber, *Quantum Field Theory*. International Series In Pure and Applied Physics, New York: McGraw-Hill, 1980.
- [35] L. Susskind, “Coarse Grained Quantum Chromodynamics,” 1976.
- [36] W. Fischler, “Quark - anti-Quark Potential in QCD,” *Nucl. Phys.*, vol. B129, pp. 157–174, 1977.
- [37] Y. Schroder, “The Static potential in QCD to two loops,” *Phys. Lett.*, vol. B447, pp. 321–326, 1999.
- [38] N. Brambilla, A. Pineda, J. Soto, and A. Vairo, “The Infrared behavior of the static potential in perturbative QCD,” *Phys. Rev.*, vol. D60, p. 091502, 1999.
- [39] B. A. Kniehl and A. A. Penin, “Ultrasoft effects in heavy quarkonium physics,” *Nucl. Phys.*, vol. B563, pp. 200–210, 1999.
- [40] C. Anzai, Y. Kiyo, and Y. Sumino, “Static QCD potential at three-loop order,” *Phys. Rev. Lett.*, vol. 104, p. 112003, 2010.
- [41] A. V. Smirnov, V. A. Smirnov, and M. Steinhauser, “Three-loop static potential,” *Phys. Rev. Lett.*, vol. 104, p. 112002, 2010.
- [42] N. Brambilla, A. Pineda, J. Soto, and A. Vairo, “The QCD potential at $O(1/m)$,” *Phys. Rev.*, vol. D63, p. 014023, 2001.
- [43] A. Pineda and A. Vairo, “The QCD potential at $O(1/m^2)$: Complete spin dependent and spin independent result,” *Phys. Rev.*, vol. D63, p. 054007, 2001. [Erratum: *Phys. Rev.*D64,039902(2001)].
- [44] C. Peset and A. Pineda, “Model-independent determination of the Lamb shift in muonic hydrogen and the proton radius,” *Eur. Phys. J.*, vol. A51, no. 3, p. 32, 2015.
- [45] C. Peset and A. Pineda, “The two-photon exchange contribution to muonic hydrogen from chiral perturbation theory,” *Nucl. Phys.*, vol. B887, pp. 69–111, 2014.
- [46] C. Peset and A. Pineda, “The Lamb shift in muonic hydrogen and the proton radius from effective field theories,” 2015.
- [47] R. Pohl *et al.*, “The size of the proton,” *Nature*, vol. 466, pp. 213–216, 2010.
- [48] C. E. Carlson, “The Proton Radius Puzzle,” *Prog. Part. Nucl. Phys.*, vol. 82, pp. 59–77, 2015.
- [49] A. Antognini *et al.*, “The proton radius puzzle,” *J. Phys. Conf. Ser.*, vol. 312, p. 032002, 2011.
- [50] I. T. Lorenz and U.-G. Meißner, “Reduction of the proton radius discrepancy by $3\tilde{C}$,” *Phys. Lett.*, vol. B737, pp. 57–59, 2014.

- [51] I. T. Lorenz, U.-G. Meißner, H. W. Hammer, and Y. B. Dong, “Theoretical Constraints and Systematic Effects in the Determination of the Proton Form Factors,” *Phys. Rev.*, vol. D91, no. 1, p. 014023, 2015.
- [52] A. Antognini *et al.*, “Experiments towards resolving the proton charge radius puzzle,” 2015.
- [53] O. Tomalak and M. Vanderhaeghen, “Subtracted dispersion relation formalism for the two-photon exchange correction to elastic electron-proton scattering: comparison with data,” *Eur. Phys. J.*, vol. A51, no. 2, p. 24, 2015.
- [54] I. Akushevich, H. Gao, A. Ilyichev, and M. Meziane, “Radiative corrections beyond the ultra relativistic limit in unpolarized ep elastic and Møller scatterings for the PRad Experiment at Jefferson Laboratory,” *Eur. Phys. J.*, vol. A51, no. 1, p. 1, 2015.
- [55] Z. Epstein, G. Paz, and J. Roy, “Model independent extraction of the proton magnetic radius from electron scattering,” *Phys. Rev.*, vol. D90, no. 7, p. 074027, 2014.
- [56] O. Tomalak and M. Vanderhaeghen, “Two-photon exchange correction in elastic unpolarized electron-proton scattering at small momentum transfer,” 2015.
- [57] A. Pineda and J. Soto, “The Lamb shift in dimensional regularization,” *Phys. Lett.*, vol. B420, pp. 391–396, 1998.
- [58] A. Pineda and J. Soto, “Potential NRQED: The Positronium case,” *Phys. Rev.*, vol. D59, p. 016005, 1999.
- [59] A. Pineda, “Leading chiral logs to the hyperfine splitting of the hydrogen and muonic hydrogen,” *Phys. Rev.*, vol. C67, p. 025201, 2003.
- [60] A. Pineda, “The Chiral structure of the Lamb shift and the definition of the proton radius,” *Phys. Rev.*, vol. C71, p. 065205, 2005.
- [61] D. Nevado and A. Pineda, “Forward virtual Compton scattering and the Lamb shift in chiral perturbation theory,” *Phys. Rev.*, vol. C77, p. 035202, 2008.
- [62] A. Pineda, “Brief Review of the Theory of the Muonic Hydrogen Lamb Shift and the Proton Radius,” in *Proceedings, 14th International Conference on Hadron spectroscopy (Hadron 2011)*, 2011.
- [63] X.-D. Ji and J. Osborne, “Generalized sum rules for spin dependent structure functions of the nucleon,” *J. Phys.*, vol. G27, p. 127, 2001.
- [64] V. Bernard, N. Kaiser, and U.-G. Meißner, “Chiral dynamics in nucleons and nuclei,” *Int. J. Mod. Phys.*, vol. E4, pp. 193–346, 1995.
- [65] T. R. Hemmert, B. R. Holstein, and J. Kambor, “Delta (1232) and the polarizabilities of the nucleon,” *Phys. Rev.*, vol. D55, pp. 5598–5612, 1997.
- [66] F. Jegerlehner, “Hadronic vacuum polarization contribution to $g-2$ of the leptons and $\alpha(M(Z))$,” *Nucl. Phys. Proc. Suppl.*, vol. 51C, pp. 131–141, 1996.
- [67] A. V. Manohar, “The HQET / NRQCD Lagrangian to order α / m^3 ,” *Phys. Rev.*, vol. D56, pp. 230–237, 1997.

-
- [68] R. Barbieri, M. Caffo, and E. Remiddi, “Fourth-order charge radius of the muon and its contribution to the lamb shift,” *Lett. Nuovo Cim.*, vol. 7S2, pp. 60–62, 1973. [*Lett. Nuovo Cim.*7,60(1973)].
- [69] R. Barbieri, J. A. Mignaco, and E. Remiddi, “Electron form-factors up to fourth order. 1.,” *Nuovo Cim.*, vol. A11, pp. 824–864, 1972.
- [70] K. A. Olive *et al.*, “Review of Particle Physics,” *Chin. Phys.*, vol. C38, p. 090001, 2014.
- [71] A. Pineda and J. Soto, “Matching at one loop for the four quark operators in NRQCD,” *Phys. Rev.*, vol. D58, p. 114011, 1998.
- [72] J. M. Alarcon, V. Lensky, and V. Pascalutsa, “Chiral perturbation theory of muonic hydrogen Lamb shift: polarizability contribution,” *Eur. Phys. J.*, vol. C74, no. 4, p. 2852, 2014.
- [73] M. C. Birse and J. A. McGovern, “Proton polarisability contribution to the Lamb shift in muonic hydrogen at fourth order in chiral perturbation theory,” *Eur. Phys. J.*, vol. A48, p. 120, 2012.
- [74] H. W. Fearing, R. Lewis, N. Mobed, and S. Scherer, “Muon capture by a proton in heavy baryon chiral perturbation theory,” *Phys. Rev.*, vol. D56, pp. 1783–1791, 1997.
- [75] V. Bernard, H. W. Fearing, T. R. Hemmert, and U. G. Meissner, “The form-factors of the nucleon at small momentum transfer,” *Nucl. Phys.*, vol. A635, pp. 121–145, 1998. [Erratum: *Nucl. Phys.*A642,563(1998)].
- [76] S. Scherer, A. Yu. Korchin, and J. H. Koch, “Virtual Compton scattering off the nucleon at low-energies,” *Phys. Rev.*, vol. C54, pp. 904–919, 1996.
- [77] H. W. Fearing and S. Scherer, “Virtual Compton scattering off spin zero particles at low-energies,” *Few Body Syst.*, vol. 23, pp. 111–126, 1998.
- [78] J. Bernabeu and C. Jarlskog, “Polarizability contribution to the energy levels of the muonic helium (μ He-4)+,” *Nucl. Phys.*, vol. B75, p. 59, 1974.
- [79] T. Janssens, R. Hofstadter, E. B. Hughes, and M. R. Yearian, “Proton form factors from elastic electron-proton scattering,” *Phys. Rev.*, vol. 142, pp. 922–931, 1966.
- [80] J. J. Kelly, “Simple parametrization of nucleon form factors,” *Phys. Rev.*, vol. C70, p. 068202, 2004.
- [81] M. O. Distler, J. C. Bernauer, and T. Walcher, “The RMS Charge Radius of the Proton and Zemach Moments,” *Phys. Lett.*, vol. B696, pp. 343–347, 2011.
- [82] J. L. Friar and I. Sick, “Muonic hydrogen and the third Zemach moment,” *Phys. Rev.*, vol. A72, p. 040502, 2005.
- [83] G. S. Bali, C. Bauer, A. Pineda, and C. Torrero, “Perturbative expansion of the energy of static sources at large orders in four-dimensional SU(3) gauge theory,” *Phys. Rev.*, vol. D87, p. 094517, 2013.

- [84] J. C. Bernauer *et al.*, “High-precision determination of the electric and magnetic form factors of the proton,” *Phys. Rev. Lett.*, vol. 105, p. 242001, 2010.
- [85] I. T. Lorenz, H. W. Hammer, and U.-G. Meissner, “The size of the proton - closing in on the radius puzzle,” *Eur. Phys. J.*, vol. A48, p. 151, 2012.
- [86] J. L. Friar and G. L. Payne, “Higher order nuclear polarizability corrections in atomic hydrogen,” *Phys. Rev.*, vol. C56, pp. 619–630, 1997.
- [87] I. B. Khriplovich and R. A. Sen’kov, “Nucleon polarizability contribution to the hydrogen Lamb shift and hydrogen-deuterium isotope shift,” *Phys. Lett.*, vol. A249, pp. 474,, 1998.
- [88] T. R. Hemmert, B. R. Holstein, G. Knochlein, and D. Drechsel, “Generalized polarizabilities of the nucleon in chiral effective theories,” *Phys. Rev.*, vol. D62, p. 014013, 2000.
- [89] J. Beringer *et al.*, “Review of Particle Physics (RPP),” *Phys. Rev.*, vol. D86, p. 010001, 2012.
- [90] R. J. Hill and G. Paz, “Model independent analysis of proton structure for hydrogenic bound states,” *Phys. Rev. Lett.*, vol. 107, p. 160402, 2011.
- [91] S. D. Drell and J. D. Sullivan, “Polarizability contribution to the hydrogen hyperfine structure,” *Phys. Rev.*, vol. 154, pp. 1477–1498, 1967.
- [92] A. C. Zemach, “Proton Structure and the Hyperfine Shift in Hydrogen,” *Phys. Rev.*, vol. 104, pp. 1771–1781, 1956.
- [93] E. De Rafael, “The hydrogen hyperfine structure and inelastic electron proton scattering experiments,” *Phys. Lett.*, vol. B37, pp. 201–203, 1971.
- [94] R. N. Faustov, E. V. Cherednikova, and A. P. Martynenko, “Proton polarizability contribution to the hyperfine splitting in muonic hydrogen,” *Nucl. Phys.*, vol. A703, pp. 365–377, 2002.
- [95] C. E. Carlson, V. Nazaryan, and K. Griffioen, “Proton structure corrections to electronic and muonic hydrogen hyperfine splitting,” *Phys. Rev.*, vol. A78, p. 022517, 2008.
- [96] G. Karl and J. E. Paton, “Naive Quark Model for an Arbitrary Number of Colors,” *Phys. Rev.*, vol. D30, p. 238, 1984.
- [97] A. Dupays, A. Beswick, B. Lepetit, C. Rizzo, and D. Bakalov, “Proton Zemach radius from measurements of the hyperfine splitting of hydrogen and muonic hydrogen,” *Phys. Rev.*, vol. A68, p. 052503, 2003.
- [98] A. V. Volotka, V. M. Shabaev, G. Plunien, and G. Soff, “Zemach and magnetic radius of the proton from the hyperfine splitting in hydrogen,” *Eur. Phys. J.*, vol. D33, pp. 23–27, 2005.
- [99] A. O. G. Kallen and A. Sabry, “Fourth order vacuum polarization,” *Kong. Dan. Vid. Sel. Mat. Fys. Med.*, vol. 29, no. 17, pp. 1–20, 1955. [555(1955)].
- [100] T. Kinoshita and W. B. Lindquist, “Parametric Formula for the Sixth Order Vacuum Polarization Contribution in Quantum Electrodynamics,” *Phys. Rev.*, vol. D27, p. 853, 1983.

-
- [101] T. Kinoshita and M. Nio, “Sixth order vacuum polarization contribution to the Lamb shift of the muonic hydrogen,” *Phys. Rev. Lett.*, vol. 82, p. 3240, 1999. [Erratum: *Phys. Rev. Lett.*103,079901(2009)].
- [102] S. G. Karshenboim, E. Yu. Korzinin, V. G. Ivanov, and V. A. Shelyuto, “Contribution of Light-by-Light Scattering to Energy Levels of Light Muonic Atoms,” *JETP Lett.*, vol. 92, pp. 8–14, 2010.
- [103] A. Pineda, “Review of Heavy Quarkonium at weak coupling,” *Prog. Part. Nucl. Phys.*, vol. 67, pp. 735–785, 2012.
- [104] U. D. Jentschura, “Relativistic Reduced-Mass and Recoil Corrections to Vacuum Polarization in Muonic Hydrogen, Muonic Deuterium and Muonic Helium Ions,” *Phys. Rev.*, vol. A84, p. 012505, 2011.
- [105] K. Pachucki, “Theory of the Lamb shift in muonic hydrogen,” *Phys. Rev.*, vol. A53, pp. 2092–2100, 1996.
- [106] A. H. Hoang, “Bottom quark mass from Upsilon mesons: Charm mass effects,” 2000.
- [107] U. D. Jentschura and B. J. Wundt, “Semi-Analytic Approach to Higher-Order Corrections in Simple Muonic Bound Systems: Vacuum Polarization, Self-Energy and Radiative-Recoil,” *Eur. Phys. J.*, vol. D65, pp. 357–366, 2011.
- [108] V. G. Ivanov, E. Yu. Korzinin, and S. G. Karshenboim, “Comment on ‘Sixth-Order Vacuum-Polarization Contribution to the Lamb Shift of Muonic Hydrogen’ by T. Kinoshita and M. Nio, *Phys.Rev. Lett.*82,3240 (1999),” 2009.
- [109] K. Pachucki, “Proton structure effects in muonic hydrogen,” *Phys. Rev.*, vol. A60, pp. 3593–3598, 1999.
- [110] C. E. Carlson and M. Vanderhaeghen, “Higher order proton structure corrections to the Lamb shift in muonic hydrogen,” *Phys. Rev.*, vol. A84, p. 020102, 2011.
- [111] A. P. Martynenko, “Proton polarizability effect in the Lamb shift of the hydrogen atom,” *Phys. Atom. Nucl.*, vol. 69, pp. 1309–1316, 2006.
- [112] M. Gorchtein, F. J. Llanes-Estrada, and A. P. Szczepaniak, “Muonic-hydrogen Lamb shift: Dispersing the nucleon-excitation uncertainty with a finite-energy sum rule,” *Phys. Rev.*, vol. A87, no. 5, p. 052501, 2013.
- [113] A. Veitia and K. Pachucki, “Nuclear recoil effects in antiprotonic and muonic atoms,” *Phys. Rev.*, vol. A69, p. 042501, 2004.
- [114] E. Borie, “Lamb shift in light muonic atoms: Revisited,” *Annals Phys.*, vol. 327, pp. 733–763, 2012.
- [115] S. G. Karshenboim, V. G. Ivanov, and E. Yu. Korzinin, “Relativistic recoil corrections to the electron-vacuum-polarization contribution in light muonic atoms,” *Phys. Rev.*, vol. A85, p. 032509, 2012.
- [116] I. B. Khriplovich, A. I. Milstein, and A. S. Yelkhovsky, “Logarithmic corrections in the two-body QED problem,” *Phys. Scr.*, vol. T46, p. 252, 1993.

- [117] A. Pineda, “Renormalization group improvement of the spectrum of hydrogen - like atoms with massless fermions,” *Phys. Rev.*, vol. A66, p. 062108, 2002.
- [118] E. Yu. Korzinin, V. G. Ivanov, and S. G. Karshenboim, “ $\hat{\mathbb{I}}\hat{\mathbb{S}}^2(Z\hat{\mathbb{I}}\hat{\mathbb{S}})^4m$ contributions to the Lamb shift and the fine structure in light muonic atoms,” *Phys. Rev.*, vol. D88, no. 12, p. 125019, 2013.
- [119] J. L. Friar, “Nuclear Finite Size Effects in Light Muonic Atoms,” *Annals Phys.*, vol. 122, p. 151, 1979.
- [120] A. Antognini, F. Kottmann, F. Biraben, P. Indelicato, F. Nez, and R. Pohl, “Theory of the 2S-2P Lamb shift and 2S hyperfine splitting in muonic hydrogen,” *Annals Phys.*, vol. 331, pp. 127–145, 2013.
- [121] M. Mihovilovic, H. Merkel, and A. Weber, “The initial state radiation experiment at MAMI,” *PoS*, vol. Bormio2014, p. 051, 2014.
- [122] A. Gasparian, “The PRad experiment and the proton radius puzzle,” *EPJ Web Conf.*, vol. 73, p. 07006, 2014.
- [123] M. Kohl, “The Muon Scattering Experiment (MUSE) at PSI and the proton radius puzzle,” *EPJ Web Conf.*, vol. 81, p. 02008, 2014.
- [124] A. Beyer, C. G. Parthey, N. Kolachevsky, J. Alnis, K. Khabarova, R. Pohl, E. Peters, D. C. Yost, A. Matveev, K. Predehl, S. Droste, T. Wilken, R. Holzwarth, T. W. Hänsch, M. Abgrall, D. Rovera, C. Salomon, P. Laurent, and T. Udem, “Precision spectroscopy of atomic hydrogen,” *Journal of Physics: Conference Series*, vol. 467, no. 1, p. 012003, 2013.
- [125] A. Beyer, J. Alnis, K. Khabarova, A. Matveev, C. G. Parthey, D. C. Yost, R. Pohl, T. Udem, T. W. Hänsch, and N. Kolachevsky, “Precision spectroscopy of the 2S-4P transition in atomic hydrogen on a cryogenic beam of optically excited 2S atoms,” *Annalen Phys.*, vol. 525, no. 8-9, pp. 671–679, 2013.
- [126] A. V. et al., “Progress towards a new microwave measurement of the hydrogen n=2 lamb shift: a measurement of the proton charge radius,” *Talk: BAPS.2012.DAMOP.D1.138, 2012.*, 2012.
- [127] S. Galtier, F. Nez, L. Julien, and F. Biraben, “Ultraviolet continuous-wave laser source at 205 nm for hydrogen spectroscopy,” *Optics Communications*, vol. 324, pp. 34–37, 2014.
- [128] C. Peset, A. Pineda, and M. Stahlhofen, “Potential NRQCD for unequal masses and the B_c spectrum at NNNLO,” 2015.
- [129] N. Brambilla, A. Pineda, J. Soto, and A. Vairo, “Potential NRQCD: An Effective theory for heavy quarkonium,” *Nucl. Phys.*, vol. B566, p. 275, 2000.
- [130] N. Brambilla, A. Pineda, J. Soto, and A. Vairo, “Effective field theories for heavy quarkonium,” *Rev. Mod. Phys.*, vol. 77, p. 1423, 2005.
- [131] G. T. Bodwin, E. Braaten, and G. P. Lepage, “Rigorous QCD analysis of inclusive annihilation and production of heavy quarkonium,” *Phys. Rev.*, vol. D51, pp. 1125–1171, 1995. [Erratum: *Phys. Rev.*D55,5853(1997)].

-
- [132] K. G. Wilson, “Confinement of Quarks,” *Phys. Rev.*, vol. D10, pp. 2445–2459, 1974.
- [133] B. A. Kniehl, A. A. Penin, V. A. Smirnov, and M. Steinhauser, “Potential NRQCD and heavy quarkonium spectrum at next-to-next-to-next-to-leading order,” *Nucl. Phys.*, vol. B635, pp. 357–383, 2002.
- [134] R. Aaij *et al.*, “First observation of the decay $B_c^+ \rightarrow J/\psi\pi^+\pi^-\pi^+$,” *Phys. Rev. Lett.*, vol. 108, p. 251802, 2012.
- [135] F. Abe *et al.*, “Measurement of the branching fraction $B(B_u^+ \rightarrow J/\psi\pi^+)$ and search for $B_c^+ \rightarrow J/\psi\pi^+$,” *Phys. Rev. Lett.*, vol. 77, pp. 5176–5181, 1996.
- [136] G. Aad *et al.*, “Observation of an excited B_c^\pm meson state with the atlas detector,” *Phys. Rev. Lett.*, vol. 113, p. 212004, Nov 2014.
- [137] C. W. Bauer and A. V. Manohar, “Renormalization group scaling of the $1/m^{**2}$ HQET Lagrangian,” *Phys. Rev.*, vol. D57, pp. 337–343, 1998.
- [138] E. Eichten and B. R. Hill, “STATIC EFFECTIVE FIELD THEORY: $1/m$ CORRECTIONS,” *Phys. Lett.*, vol. B243, pp. 427–431, 1990.
- [139] A. Pineda, “Renormalization group improvement of the NRQCD Lagrangian and heavy quarkonium spectrum,” *Phys. Rev.*, vol. D65, p. 074007, 2002.
- [140] B. A. Kniehl, A. A. Penin, M. Steinhauser, and V. A. Smirnov, “NonAbelian $\alpha^{**3}(s) / (m(q)r^{**2})$ heavy quark anti-quark potential,” *Phys. Rev.*, vol. D65, p. 091503, 2002.
- [141] S. N. Gupta and S. F. Radford, “Quark Quark and Quark - Anti-quark Potentials,” *Phys. Rev.*, vol. D24, pp. 2309–2323, 1981.
- [142] M. Beneke, Y. Kiyo, and K. Schuller, “Third-order correction to top-quark pair production near threshold I. Effective theory set-up and matching coefficients,” 2013.
- [143] J. T. Pantaleone, S. H. H. Tye, and Y. J. Ng, “Spin Splittings in Heavy Quarkonia,” *Phys. Rev.*, vol. D33, p. 777, 1986.
- [144] S. Titard and F. J. Yndurain, “Rigorous QCD evaluation of spectrum and ground state properties of heavy q anti-q systems: With a precision determination of $m(b)$ $M(\eta(b))$,” *Phys. Rev.*, vol. D49, pp. 6007–6025, 1994.
- [145] A. V. Manohar and I. W. Stewart, “The QCD heavy quark potential to order v^{**2} : One loop matching conditions,” *Phys. Rev.*, vol. D62, p. 074015, 2000.
- [146] M. E. Luke, A. V. Manohar, and I. Z. Rothstein, “Renormalization group scaling in non-relativistic QCD,” *Phys. Rev.*, vol. D61, p. 074025, 2000.
- [147] E. Eichten and F. Feinberg, “Spin Dependent Forces in QCD,” *Phys. Rev.*, vol. D23, p. 2724, 1981.
- [148] A. Barchielli, E. Montaldi, and G. M. Prosperi, “On a Systematic Derivation of the Quark - Anti-quark Potential,” *Nucl. Phys.*, vol. B296, p. 625, 1988. [Erratum: *Nucl. Phys.*B303,752(1988)].

- [149] A. Barchielli, N. Brambilla, and G. M. Prosperi, “Relativistic Corrections to the Quark - anti-Quark Potential and the Quarkonium Spectrum,” *Nuovo Cim.*, vol. A103, p. 59, 1990.
- [150] Y.-Q. Chen, Y.-P. Kuang, and R. J. Oakes, “On the spin dependent potential between heavy quark and anti-quark,” *Phys. Rev.*, vol. D52, pp. 264–270, 1995.
- [151] Y. Schroder, *The Static potential in QCD*. PhD thesis, Hamburg U., 1999.
- [152] M. Beneke, A. Signer, and V. A. Smirnov, “Top quark production near threshold and the top quark mass,” *Phys. Lett.*, vol. B454, pp. 137–146, 1999.
- [153] M. Beneke, Y. Kiyo, P. Marquard, A. Penin, J. Piclum, D. Seidel, and M. Steinhauser, “Leptonic decay of the $\Upsilon(1S)$ meson at third order in QCD,” *Phys. Rev. Lett.*, vol. 112, no. 15, p. 151801, 2014.
- [154] N. Brambilla, D. Eiras, A. Pineda, J. Soto, and A. Vairo, “Inclusive decays of heavy quarkonium to light particles,” *Phys. Rev.*, vol. D67, p. 034018, 2003.
- [155] A. Pineda and J. Soto, “The Renormalization group improvement of the QCD static potentials,” *Phys. Lett.*, vol. B495, pp. 323–328, 2000.
- [156] W. Buchmuller, Y. J. Ng, and S. H. H. Tye, “Hyperfine Splittings in Heavy Quark Systems,” *Phys. Rev.*, vol. D24, p. 3003, 1981.
- [157] N. Brambilla, D. Gromes, and A. Vairo, “Poincare invariance and the heavy quark potential,” *Phys. Rev.*, vol. D64, p. 076010, 2001.
- [158] N. Brambilla, D. Gromes, and A. Vairo, “Poincare invariance constraints on NRQCD and potential NRQCD,” *Phys. Lett.*, vol. B576, pp. 314–327, 2003.
- [159] N. Brambilla, A. Pineda, J. Soto, and A. Vairo, “The Heavy quarkonium spectrum at order $m \alpha^5(s) \ln \alpha(s)$,” *Phys. Lett.*, vol. B470, p. 215, 1999.
- [160] Y. Kiyo and Y. Sumino, “Full Formula for Heavy Quarkonium Energy Levels at Next-to-next-to-next-to-leading Order,” *Nucl. Phys.*, vol. B889, pp. 156–191, 2014.
- [161] A. A. Penin and M. Steinhauser, “Heavy quarkonium spectrum at $O(\alpha^5(s) m(q))$ and bottom / top quark mass determination,” *Phys. Lett.*, vol. B538, pp. 335–345, 2002.
- [162] A. A. Penin, V. A. Smirnov, and M. Steinhauser, “Heavy quarkonium spectrum and production/annihilation rates to order $\beta^3(0) \alpha^3(s)$,” *Nucl. Phys.*, vol. B716, pp. 303–318, 2005.
- [163] M. Beneke, Y. Kiyo, and K. Schuller, “Third-order Coulomb corrections to the S-wave Green function, energy levels and wave functions at the origin,” *Nucl. Phys.*, vol. B714, pp. 67–90, 2005.
- [164] N. Brambilla and A. Vairo, “The B_c mass up to order $\alpha(s)^4$,” *Phys. Rev.*, vol. D62, p. 094019, 2000.
- [165] N. Brambilla, Y. Sumino, and A. Vairo, “Quarkonium spectroscopy and perturbative QCD: Massive quark loop effects,” *Phys. Rev.*, vol. D65, p. 034001, 2002.

-
- [166] A. Pineda and F. J. Yndurain, “Calculation of quarkonium spectrum and $m(b)$, $m(c)$ to order α_s^4 ,” *Phys. Rev.*, vol. D58, p. 094022, 1998.
- [167] Y. Kiyo and Y. Sumino, “Perturbative heavy quarkonium spectrum at next-to-next-to-next-to-leading order,” *Phys. Lett.*, vol. B730, pp. 76–80, 2014.
- [168] G. S. Bali, K. Schilling, and A. Wachter, “Complete $O(v^2)$ corrections to the static interquark potential from $SU(3)$ gauge theory,” *Phys. Rev.*, vol. D56, pp. 2566–2589, 1997.
- [169] Y. Koma, M. Koma, and H. Wittig, “Relativistic corrections to the static potential at $O(1/m)$ and $O(1/m^2)$,” *PoS*, vol. LAT2007, p. 111, 2007.
- [170] Y. Koma and M. Koma, “Scaling study of the relativistic corrections to the static potential,” *PoS*, vol. LAT2009, p. 122, 2009.
- [171] S. N. Gupta, C. J. Suchyta, and W. W. Repko, “Nonsingular Potential Model for Heavy Quarkonia,” *Phys. Rev.*, vol. D40, p. 4100, 1989.
- [172] A. V. Manohar and I. W. Stewart, “Running of the heavy quark production current and $1/v$ potential in QCD,” *Phys. Rev.*, vol. D63, p. 054004, 2001.

